DC trolleygrids as sustainable, multi-functional, and multi-stakeholder electrical infrastructures

Thinking outside of the bus

Diab, I.

DOI
10.4233/uuid:6103d9e9-5c2e-487a-b77c-ae0ce9cb12f1

Publication date
2023

Document Version
Final published version

Citation (APA)
Diab, I. (2023). *DC trolleygrids as sustainable, multi-functional, and multi-stakeholder electrical infrastructures: Thinking outside of the bus.* [Dissertation (TU Delft), Delft University of Technology]. https://doi.org/10.4233/uuid:6103d9e9-5c2e-487a-b77c-ae0ce9cb12f1

Important note
To cite this publication, please use the final published version (if applicable).
Please check the document version above.

DC TROLLEYGRIDS AS SUSTAINABLE, MULTI-FUNCTIONAL, AND MULTI-STAKEHOLDER ELECTRICAL INFRASTRUCTURES

Thinking outside of the bus

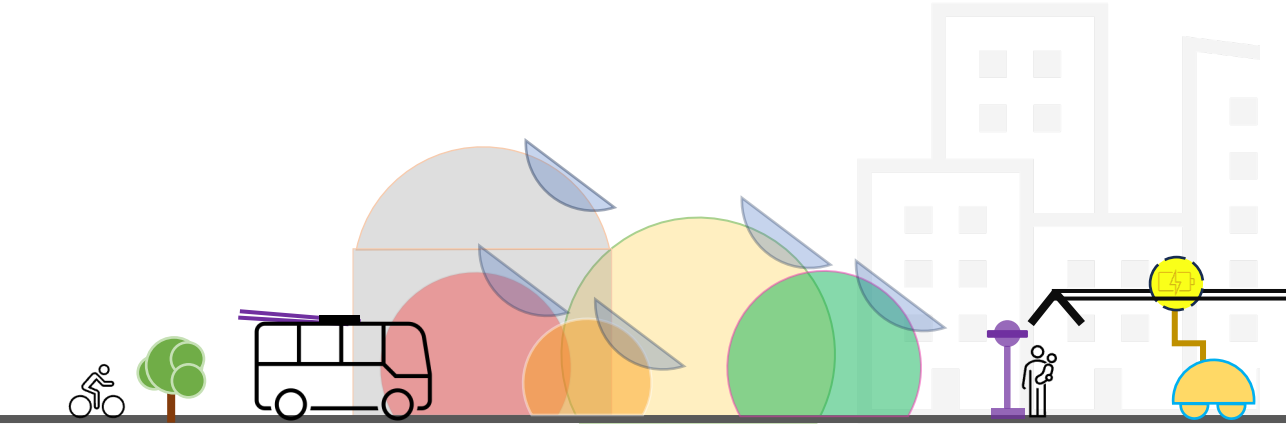

IBRAHIM DIAB

DC Trolleygrids as Sustainable, Multi-functional, and Multi-stakeholder Electrical Infrastructures

Thinking Outside of the Bus

DC Trolleygrids as Sustainable, Multi-functional, and Multi-stakeholder Electrical Infrastructures

Thinking Outside of the Bus

Dissertation

for the purpose of obtaining the degree of doctor
at Delft University of Technology
by the authority of the RectorMagnificus Prof. dr. ir. T.H.J.J. van der Hagen,
chair of the Board for Doctorates,
to be defended publicly on
Monday 2 October 2023 at 10:00 o'clock

by

Ibrahim DIAB

Master of Science in Sustainable Energy Technology, Delft University of Technology,
The Netherlands
born in Jenneta, Lebanon

The dissertation has been approved by the promotors.

Composition of the doctoral committee:

Rector Magnificus	chairperson
Prof. Dr. Ir. P. Bauer	Delft University of Technology, promotor
Dr. Ir. G.R. Chandra Mouli	Delft University of Technology, copromotor
Independent members:	
Prof. Dr. J.L. Hurink	Universiteit Twente
Prof. Dr. Ir. D. Iannuzzi	Università degli Studi di Napoli Federico II, Italy
Prof. Dr. Ir. L.A. Tavasszy	Delft University of Technology
Dr. Hab. Inz. M. Bartłomiejczyk	Gdansk University of Technology, Poland
Dr. R.A.C.M.M. van Swaaij	Delft University of Technology
Prof. Dr. Ir. M. Popov	Delft University of Technology, reserve member

Printed by: Ridderprint, on 100% recycled paper

Cover design: Ibrahim Diab

ISBN 978-94-6384-481-9

An electronic version of this dissertation is available at
http://repository.tudelft.nl/.

To the other immigrants of the world who,
unlike the randomly lucky ones of us,
lost their lives trying to reach and build better ones

CONTENTS

SUMMARY

Electricity grids are increasingly congested as the world moves toward a sustainable, electrified future. Expanding and upgrading these infrastructures is costly and challenging on a technical and administrative level and even redundant when considering that some sub-parts of these grids, such as electric transportation networks, are massively underutilized.
This thesis investigates, in four parts, the potential of one of these high-power infrastructures, the trolleybus grid, to become a sustainable, multi-functional, and multi-stakeholder backbone to urban power grids by integrating renewables, storage, and EV chargers, all while remaining ready for their next generation of sophisticated, high-power transport fleets such as In-Motion-Charging buses.

Part I looks at the opportunities, challenges, and tools needed for designing and assessing these trolleygrids of the future.
It is clear that most research in the literature focuses mainly on case studies of relatively small solar PV systems or EV chargers of unjustified sizing decisions and should start investigating the extent of the potential of these elements in the trolleygrids and methods to increase this integration potential. On the other hand, surveying typical storage technologies showed that those other than Li-ion, Supercapacitors, and Flywheels do not seem practical for implementation in transport grids. Furthermore, the research on storage should move beyond the recuperation of braking energy and focus instead on preparing future trolleygrids with capacity-building power management schemes that would avoid infrastructure expansions, as well as comparing placement scenarios (on-board or stationary). Finally, many non-technical challenges face the trolleygrids of the future, not the least of which is the legal bottleneck to EV charger integration of not allowing transport networks to sell energy to third-party users.
To investigate these research directions, comprehensive trolleygrid models and grid state estimators need to be developed that move beyond the simplistic and/or energy approach to modeling trolley networks. These were offered in Chapter 3 and Chapter 4, respectively.

Part II of the thesis investigated the outlook for renewables integration in present-day urban trolleygrids.
In the absence of a base load, no more than 40% direct utilization could be secured by a substation-connected PV system, meaning more than 60% of the generated energy needs to be stored, curtailed, or sent to the AC grid. In low-traffic substations, these numbers were as low as 13%. A hybrid wind-PV system could be optimized for 54% utilization but only came with a centralized AC-grid placement, which has technical and administrative challenges and is, in general, not a preferred or scalable solution.
A simple, third-degree polynomial method to estimate the performance of a PV system

of any size connected to any trolley traction substation was developed from simulations of both the Dutch Arnhem and Polish Gdynia grids. Trolleygrid operators could use this to quickly and efficiently assess the techno-economic feasibility of their planned system and better guide their research and consultancy efforts. This method also exposed how the absence of the base load at higher PV system sizes is paralleled by an absence in trolleygrid load coverage when looking at smaller system sizes.
Investigating on-board and off-board storage solutions in tandem with PV systems showed that there is a benefit to be obtained in the load demand (translated to a smaller PV system), but the PV Utilization was not improved much.
In conclusion for Part II, the concern about the absence of a base load is even more concrete: The Integration of smart base loads such as EV chargers is not only an opportunity but a necessity for the sustainable trolleygrid.

Part III looked at how the integration of smart non-traction loads and grid components be maximized to improve the techno-economic feasibility of the future sustainable, multifunctional trolleygrid. This looks at three options for base loads: Storage system placements (without the PV systems), EV chargers, and residential loads.
In comparing storage placement options, stationary storage -especially at the middle of the section- was superior to on-board storage in terms of the combined benefit of reducing the energy demand, overhead voltage drops, and creating spare capacity for the integration of other smart loads. A Hybrid placement (half on-board and half stationary) proved more beneficial as well than the on-board storage. Consequently, there should be no fears of redundant investment if a trolleygrid with on-board storage fleets decides to expand with stationary storage systems to create more spare grid capacity.
This grid capacity is already large enough to charge over 200 EVs per day from just one section (out of 40) of the Arnhem trolleygrid. This capacity is pushed from a baseline of almost half its volume by investigating smart grid methods such as bilateral connections and fleet-aware smart charging. The integration of EV chargers is a more efficient and lucrative option than using storage systems, as EV charging is a service with direct use rather than a simple buffering of the energy (with energy losses), like in the case of storage.
Finally, beyond the base load problem, a valid concern is the availability of physical installation space in the urban environment for PV systems connected to traction substations. Meanwhile, residential dwellings have both the base load and rooftop space as well as the need for the traction demand peaks and investment funds. Indeed, a multi-stakeholder PV system that is shared between traction substations and nearby residential loads has shown to be synergetic at any PV system size or number of households in terms of the benefits of generation-load matching. The consequence of this is less need for storage, curtailment, and exchange with the medium voltage AC grid.

Finally, Part IV looks at suitable power management and synergetic design schemes for the trolleybuses and the trolleygrids of the future.
When including other loads into the grid, such as EV chargers, care should be taken so as not to compete with the capacity needed for the integration of the next generation of high-power In-Motion-Charging trolleybuses. For this aim, two new IMC-battery

charging schemes were developed and studied, namely, Adaptive Charging and Valley-Charging, that allow for the successful electrification of new bus fleets without breaking the grid limitations.
Finally, the final chapter of this thesis looks at the integration combinations of all the previous elements into a single trolleygrid. It is found that EV chargers provide enough base load to render storage or residential loads redundant from an energy efficiency and PV utilization point of view. However, there are still the other above-mentioned benefits to be had from a multi-stakeholder system. The high-power demanding IMC buses are also feasible even with the integration of high-power EV chargers in both low and high-traffic scenarios, and both or either one of them provides a boost for the techno-economic feasibility of a connected PV system.

SAMENVATTING

De wereld gaat steeds meer naar een duurzame, geëlektrificeerde toekomst maar elektriciteitsnetten kampen met schaarste aan capaciteit. Het uitbreiden en verbeteren van deze infrastructuren is kostbaar en uitdagend op technisch en administratief niveau en zelfs overbodig omdat sommige subonderdelen van deze netwerken, zoals de elektrische openbaar vervoer netwerken, massaal onderbenut worden.
Dit proefschrift onderzoekt, in vier delen, het potentieel van een van deze hoog-vermogen infrastructuren, het trolleybusnet, om een duurzame, multifunctionele en meerdere belanghebbenden ondersteuner te worden voor stedelijke elektriciteitsnetten door hernieuwbare energiebronnen, energieopslag, en EV-opladers te integreren, terwijl ze voorbereid blijven op een volgende generatie van hoog-vermogen transportvloten. Deel I kijkt naar de mogelijkheden , uitdagingen en de middelen die nodig zijn voor het ontwerpen en beoordelen van deze trolleybusnetten van de toekomst zoals In-Motion-Charging.

Het is duidelijk dat het meeste onderzoek in de literatuur zich voornamelijk richt op gevalstudies van relatief kleine fotovoltaïsche zonne-energiesystemen of EV-opladers van ongerechtvaardigde dimensioneringsbeslissingen en zou moeten beginnen met het onderzoeken van de omvang van het potentieel van deze elementen in de trolleybusnetten en methoden om dit integratiepotentieel te vergroten. Aan de andere kant toonde het onderzoeken van typische opslagtechnologieën aan dat technologieën anders dan Li-ion, Supercondensatoren en Vliegwielen niet praktisch lijken voor implementatie in transportnetwerken. Bovendien zou het onderzoek naar opslag verder moeten gaan dan het recupereren van remenergie en zich in plaats daarvan moeten richten op het voorbereiden van toekomstige trolleybusnetten met energiebeheerschema's voor capaciteitsopbouw die infrastructuuruitbreidingen zouden voorkomen, evenals het vergelijken van plaatsingsscenario's (aan boord of stationair). Ten slotte staan de trolleybusnetten van de toekomst voor veel niet-technische uitdagingen, zoals het juridische knelpunt over de integratie van EV-opladers waarbij transportnetwerken geen energie mogen verkopen aan externe gebruikers.
Om deze onderzoeksrichtingen te kunnen nagaan, moeten uitgebreide trolleybusnetmodellen en schatters van de nettoestand worden ontwikkeld die verder gaan dan de simplistische modelen en/of energiebenadering van het modelleren van trolleynetwerken. Deze werden respectievelijk aangeboden in hoofdstuk 3 en hoofdstuk 4.

Deel II van het proefschrift onderzocht de vooruitzichten voor de integratie van duurzame energie in hedendaagse stedelijke trolleybusnetten .
Zonder basisbelasting kan niet meer dan 40% direct gebruikt worden gegarandeerd van een onderstation aangesloten PV-systeem, wat betekent dat meer dan 60% van de opgewekte energie moet worden opgeslagen, verspild, of naar het AC-net moet worden gestuurd. In onderstations met weinig verkeer waren deze aantallen slechts 13%. Een

hybride wind-PV systeem kon worden geoptimaliseerd voor een gebruik van 54%, maar dat kan alleen met een gecentraliseerde plaatsing van het wisselstroomnet, wat technische en administratieve uitdagingen met zich meebrengt en over het algemeen geen voorkeurs- of schaalbare oplossing is.
Op basis van simulaties van zowel het Arnhemse net als het Poolse Gdynia net is een eenvoudige derdegraads polynoommethode ontwikkeld om de prestaties te schatten van een PV-systeem, van elke grootte, dat is aangesloten op een willekeurig trolleybus tractieonderstation. Trolleynet-beheerders zouden dit kunnen gebruiken om snel en efficiënt de technisch-economische haalbaarheid van hun geplande systeem te beoordelen en hun onderzoeks- en adviesinspanningen beter te begeleiden. Deze methode legde ook bloot hoe de afwezigheid van de basisbelasting bij grotere PV-systemen gepaard gaat met een afwezigheid van de trolleynet-belastingsdekking bij het kijken naar kleinere systemen. Onderzoek naar ingebouwde en externe opslagoplossingen in combinatie met PV-systemen toonde aan dat er een voordeel te behalen valt in de vraag naar belasting (dus een kleiner PV-systeem), maar het PV-gebruik was niet veel verbeterd. Concluderend voor deel II is de zorg over het ontbreken van een basisbelasting nog concreter: de integratie van een slimme basisbelastingen zoals EV-laders is niet alleen een kans, maar een noodzaak voor het duurzame van het trolleybusnet.

In deel III werd gekeken naar hoe de integratie van slimme niet-tractiebelastingen en netwerkcomponenten kan worden gemaximaliseerd om de technisch-economische haalbaarheid te verbeteren van het toekomstige duurzame, multifunctionele trolleynet. Dit kijkt naar drie opties voor basisbelastingen: de plaatsing van opslagsystemen (zonder de PV-systemen), EV-laders en residentiële belastingen. Bij het vergelijken van de opslagplaatsingsopties was de stationaire opslag - vooral in het midden van de sectie – beter dan de opslag aan boord, in termen van het gecombineerde voordeel van vermindering van de vraag naar energie, spanningsdalingen bovengronds en het creëren van reservecapaciteit voor de integratie van andere slimme belastingen. Ook een hybride plaatsing (half aan boord en half stationair) bleek voordeliger dan de complete opslag aan boord. Daarnaast, hoeft er niet te worden gevreesd voor overbodige investeringen als een trolleynet met opslagvloten aan boord besluit om uit te breiden met stationaire opslagsystemen om meer reservecapaciteit op het net te creëren.
Deze netcapaciteit is al groot genoeg om meer dan 200 EV's per dag op te laden vanaf slechts één deel (van de 40) van het Arnhemse trolleynet. Deze capaciteit is verdubbeld vanaf het basisscenario door het onderzoeken van slimme netwerkmethoden zoals bilaterale verbindingen en wagenparkbewust slim laden. De integratie van EV-laders is een efficiëntere en lucratievere optie dan het gebruik van opslagsystemen, aangezien EV-laden een dienst is met direct gebruik in plaats van een simpele buffering van de energie (met energieverliezen), zoals in het geval van opslag.
Tot slot, afgezien van het probleem van de basisbelasting, is een terechte zorg de beschikbaarheid van fysieke installatieruimte in de stedelijke omgeving voor PV-systemen die zijn aangesloten op tractieonderstations. Onderwijl hebben woonhuizen zowel de basisbelasting als de dakruimte, evenals de behoefte aan vermogen-pieken van de tractienetten en hun investeringsfondsen. Inderdaad, een meerdere belanghebbende PV-systeem dat wordt gedeeld tussen tractie-onderstations en nabijgelegen residentiële be-

lastingen is synergetisch gebleken, bij elke PV-systeemgrootte of elk aantal huishoudens, in termen van de voordelen van het afstemmen van de opwekking en de belasting. Het gevolg hiervan is minder behoefte aan opslag, inperking en uitwisseling met het middenspannings-wisselstroomnet.

Ten slotte kijkt deel IV naar geschikte energiebeheer- en ontwerpschema's voor de trolleybussen en de trolleynetten van de toekomst.
Bij het opnemen van andere belastingen in het net, zoals EV-laders, moet ervoor worden gezorgd dat er niet wordt geconcurreerd met de capaciteit die nodig is voor de integratie van de volgende generatie hoog-vermogen In-Motion-Charging trolleybussen. Voor dit doel zijn twee nieuwe IMC-laadschema's ontwikkeld en bestudeerd, namelijk Adaptive Charging en Valley-Charging, die de succesvolle elektrificatie van nieuwe bus vloten mogelijk maken zonder de netlimieten te doorbreken.
Ten slotte wordt in het laatste hoofdstuk van dit proefschrift gekeken naar de integratiecombinaties van alle voorgaande elementen in één trolleygrid. Het is gebleken dat EV-laders voldoende basisbelasting bieden om opslag of residentiële belastingen overbodig te maken vanuit het oogpunt van energie-efficiëntie en PV-gebruik. Er zijn echter nog andere voordelen van een systeem met meerdere belanghebbenden. De veeleisende IMC-bussen met hoog vermogen zijn ook haalbaar, zelfs met de integratie van krachtige EV-laders in scenario's met zowel weinig als veel verkeer, en beide of een van beide bieden een toename voor de technisch-economische haalbaarheid van een aangesloten PV-systeem.

1

INTRODUCTION

"Aspetti signorina
Le dirò con due parole
Chi son? chi son!
E che faccio?
Come vivo? .. Vuole?

Che Gelida Manina - Act I, La Bohème (Puccini)

```
                    Wait, miss,
May I tell you in two words,
        who I am?  Who I am!
              And what I do?
and how I live?...  May I?
```

1

Transport grids, like trolleygrids, are oversized and underutilized as they are designed for the worst-case scenario of unpredicted traffic. In these times when electricity grids are too congested for the integration of intermittent generation like solar PV and smart loads like EV chargers, the attention is turning toward the high-power infrastructures of urban electric transport grids.
Indeed, as this thesis investigates, trolleygrids have the potential to successfully integrate renewables, storage, and EV chargers into their infrastructures, all while still catering to the demand of their present vehicles and to the future generation of trolleybus fleets: The In-Motion-Charging trolleybus.

1.1. URBAN CATENARY BUSES

1.1.1. TROLLEYBUSES AND TROLLEYGRIDS

Trolleybuses are a type of electric bus that dates as far back as 1882 with the "Elektromote" of Ernst Siemens in a suburb of Berlin [1]. They operate, in a similar way to how trams do, by drawing power from overhead wires through a device called a pantograph located on the roof of the vehicle (Figure 1.1). This power supply method allows the trolleybus to operate without using an onboard generator or fuel.
One of the main advantages of trolleybuses then, is that they are powered by electricity,

Figure 1.1: A trolleybus and its pantograph in Bucharest, Romania. Here, the overhead cables can be seen connected to the public lighting poles (Photo by author).

which can be obtained from a clean and renewable source of energy. This also means that trolleybuses produce zero emissions at the point of use, which helps to reduce air pollution and improve air quality in urban areas. Trolleybuses are also quieter than diesel buses, consequently reducing noise pollution inside and outside of the vehicle [2]. The electrical infrastructure that is used to power trolleybuses is called a trolley-

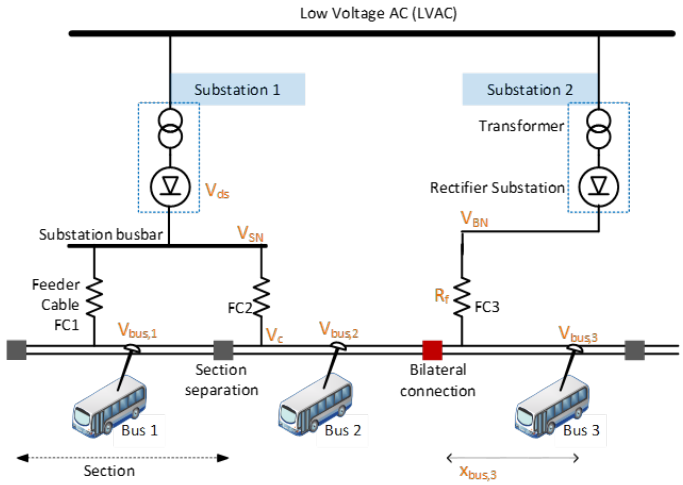

Figure 1.2: The Trolleygrid and its components.

grid. Trolleygrids consist of overhead wires that run along the bus route. The wires are suspended from poles or other structures (like the public lighting poles in Figure 1.1) and connected to a power source, such as a traction substation. A trolleygrid infrastructure is typically divided into low voltage substations that feed one or more galvanically isolated sections, as shown in Figure 1.2. From the Low Voltage AC (LVAC), a traction substation, which houses a step-down transformer and a rectifier, supplies the buses on its sections via feeder cables (e.g. FC1 in Figure 1.2), at 600-750Vdc (V_{SN}), depending on the substation and the trolleybus city. The minimum bus voltage for operation is 400V [2]–[4]. Consequently, the trolleybus lines are divided into isolated sections of a few hundred meters up to 2 km in length, depending on the trolleygrid city, to limit the resistive voltage drops in the catenary and transmission losses and for reasons such as fault protection. This last motive is especially important with catenary systems as their electric supply cables are very exposed (unlike a metro third rail), and can be easily damaged by, at the very least, weather conditions.

Trolleybuses consume about 40 kW of traction power during regular driving but can reach power peaks above 300 kW while accelerating. When a trolleybus brakes, the available regenerative braking power can be as high as 200 kW. If the braking trolleybus has an on-board storage system (also known as a dual-source trolleybus [5]–[8]), it can harvest this braking energy to be later used while accelerating. In the absence of on-board storage, this power can be fed to buses on the same section, on a connected section under the same substation busbar (trolleybus1 and trolleybus2 in Figure 1.2), or wasted in

on-board braking resistors [4], [6], [7]. The braking energy cannot be sent back to the LVAC grid because of the unidirectional rectifiers at the substation. Some bidirectional substations have been considered [9], [10], but they are not technically and economically favorable.
This elaborate infrastructure ensures another advantage of trolleybuses in that they can draw power from an available source (catenary) at all times, even when stopped at a bus stop or stuck in traffic. This means that they can have a consistent and reliable power supply on their route, which can help to improve their performance and reduce the refuelling delays common to diesel and even battery-electric buses (re-charging). Trolleybuses can even share the braking-energy recuperation advantage of battery-electric buses as mentioned earlier, when they are equipped with a relatively small, yet sufficient, onboard battery of as little as 1kWh [4], [11]. This is an important advantage as research has found that electric buses are able to recover up to 30% of their kinetic energy when braking, which reduces their overall energy consumption and improves their environmental performance [4], [12].
Finally, trolleybuses can reduce congestion on the roads and improve public transportation capacity, as they carry a relatively larger number of passengers and along more challenging terrains than what is possible with other types of buses by virtue of their electric traction and supply systems [13]. Trolleybuses are typically able to carry between 80 and 120 passengers, depending on the size of the vehicle and the configuration of the seating, which is significantly more than the average capacity of a diesel bus, which stands at about 60 seats. Finally, they are also able to operate on a wide range of routes, including those with steep gradients and high traffic, which can make them a good choice for cities with challenging terrain and repeated acceleration demands. This is thanks to the traction provided by the overhead wires, which allows them to operate on routes that would be difficult or impossible for other types of buses.

1.1.2. THE LIMITATIONS OF TROLLEYBUSES AND TROLLEYGRIDS

Despite their benefits, trolleygrids have seen waves of both expansion and contraction during the last few decades. Some challenges associated with trolleybuses have limited their use in many cities around the world, and the diesel frenzy of the mid-twentieth century saw many cities decommission their catenary networks.
One of the main challenges of trolleybuses is the infrastructure required to support them. In order to operate, trolleybuses need to have overhead wires installed along the route, which can be expensive and time-consuming to install. This infrastructure is also subject to damage and disruption, which can affect the reliability of trolleybus services. The social acceptance of catenary systems is also hostile, as the hanging overhead cables, like those in Figure 1.3 are sometimes dismissed as visual pollution. Another challenge is the limited route flexibility of trolleybuses. Because they rely on overhead wires for power, trolleybuses are not able to operate outside of their designated routes. This means that they are not as flexible as other forms of public transportation, and they cannot easily be rerouted to serve new areas or respond to changes in demand. Trolleybuses are also vulnerable to bad weather. Heavy rain or snow can interfere with the electrical connection between the overhead wires and the vehicle, causing disruptions to service. In addition, strong winds can blow the overhead wires out of alignment, resulting in power outages.

Unfortunately, trolleygrids also come at a much higher infrastructure cost than an electric bus, with one kilometer of catenary costing about 10 times as much as a 300kW opportunity charger [14].

1.1.3. THE FUTURE OF URBAN ELECTRIC PUBLIC TRANSPORT NETWORKS LIKE TROLLEYGRIDS

Urban electric public transport networks have tremendous potential for providing more smart loads by integrating these into their infrastructures [3], [11], [14]–[18]. This is because the traction substations of these grids are historically sized for the worst-case scenarios of power demand and can be better utilized by smart loads together with proper power management. One such vision is suggested in Figure 1.4.

First, since the accelerating vehicles (tram, trolleybus, etc) can consume up to 3-5 times the load of a driving vehicle [3], [4], [17]–[21], the rectifier traction substations are oversized to cater to the rare possibility of a few unscheduled vehicles accelerating together under one supply zone. In that regard, integrating renewable energy sources (RES) into the supply of transport grids would not only make the supply more sustainable but would help alleviate some of the expected power peaks from future timetabling scenarios that are more frequent in traffic and more demanding in their newer and larger types of vehicles.
One such example is the In-Motion-Charging trolleybus or IMC bus, which is a hybrid between a battery-electric bus and a trolleybus. The IMC bus differs from the trolleybus with an on-board energy storage system (OESS) in that the OESS is a passive storage component that is only used to store excess braking energy, while the IMC battery is

Figure 1.3: A complex mesh of trolleygrid overhead cables at a street intersection in Naples, Italy (Photo by author).

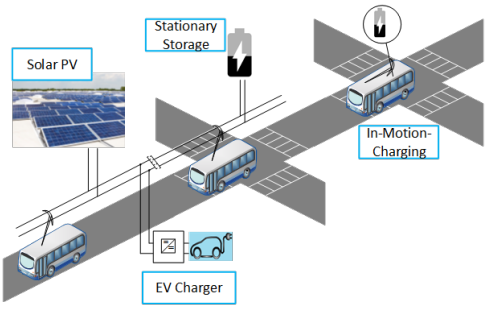

Figure 1.4: A vision of the trolleygrid of the future with integrated PV, EV chargers, storage, and IMC buses.

actively charged from sections of the trolleygrid called the charging corridors. The trolleybus typically consumes 1.5kWh/km for traction and up to an additional 1kWh/km for auxiliary systems such as heating and air conditioning. Thanks to the inherent presence of a battery, the IMC bus can recuperate most of its regenerative braking energy, typically worth a third of the average traction demand (1.5kWh/km) [3], [4], [14]. Therefore, the IMC bus requires around 2kWh/km in cold winter conditions for its traction and auxiliaries.
However, the battery of the IMC bus has a demanding load on the trolleygrid that far outweighs its braking energy recuperation benefit. This is because the IMC bus needs to pick up enough energy from the charging corridor length to cover the battery-mode route, typically at a length ratio of 1:2 or 1:3. For example, in the case 1:3, the corridor is 25% of the total route and thereby the IMC bus would consume a minimum of 4 times its average power under the catenary.

Second, vehicle timetabling creates infrequent vehicle traffic under each traction substation, leaving large amounts of unused reserved grid capacity. This would only be worse when intermittent RES are integrated into the traction power supply mix and would call for large RES storage systems, exchange with the AC grid, and/or the curtailment of excess generation energy. These solutions could easily render the RES systems technically or economically infeasible.
Many works are already rethinking these transport networks as multi-functional, active grids by integrating into them renewable energy sources (RES), storage systems, EV chargers, more sophisticated vehicle fleets (like In-Motion-Charging trolleybuses), and other smart loads [7], [10], [11], [14]–[16], [19], [21]–[39].
However, designing a sustainable, multi-functional transportation grid requires a thorough understanding and study of its stochastic power demand and a comprehensive analysis of the constructive or destructive effect of the different smart grid loads that can be integrated. The trolleygrid modeling is not a straightforward task as the vehicles move with the unpredictable city traffic and with unpredictable driver behavior, [3], [4], [40]. The consequence is that the load power and location are hard to predict. For example, Bus 2 in Figure 1.2 can be delayed enough that it is present with Bus 3 under Substation 2, creating an unpredicted high load demand. Additionally, the Heating, Ventilating, and

Air Conditioning (HVAC) demand of a trolleybus in a cold environment can be as much as its traction demand, adding to the complexity of the load prediction [3], [4], [11], [40]–[42].

1.1.4. ADDRESSED RESEARCH GAPS

The multi-functional approach to transportation grids has a growing momentum in research and applications across the catenary and rail sectors. However, there is a lack of consensus on the design and feasibility of these future grids. In that regard, this thesis addresses four research gaps:

1) Inadequacy of the present modeling and power management tools for investigating the multi-functional DC catenary grids: DC transportation grids are low-voltage, unidirectional, sectionized grids with stochastic loads both in time and location. The lumped-energy approaches and approximations of conventional rail and catenary grids are no longer fit for the detailed power, voltage, and current analysis of, for example, smart loads integration and their power management schemes.

2) Lack of understanding of the prospects of renewables integration in catenary grids: Very little research exists on the integration of renewables directly into catenary grids and is typically concerned with relatively small PV systems with storage devices. So far, there is no comprehensive study on wind and solar systems in catenary grids and no consensus on an assessment methodology or sizing and placement approaches.

3) Lack of understanding of the potential of multi-functional and multi-stakeholder catenary grids: While a few works exist on the integration of loads such as electric vehicle chargers and storage devices into these grids, they are usually confined to relatively small systems in the former case, or focused only on braking energy recuperation in the latter case. No work looks at assessing the potential of catenary networks to host these components and/or manage them with the objective of ensuring the techno-economic feasibility of the multi-functional grids (for example, keeping a certain minimum line voltage even during grid congestion episodes). Furthermore, while works in the literature look at the multi-functional grid, no work looks at multi-stakeholder grids in and out of the transport sector (for example, residential dwellings).

4) Understanding and managing the constructive and destructive effects of the multi-functional catenary grid of the future: While a number of works look at different added functionalities to the grids and at more sophisticated and power-demanding bus fleets, no work looks at the expected constructive and destructive effects of adding simultaneously some of the components together. Most critically, there is a need for managing the power demand of the buses and their (expected) on-board storage devices and quantifying the additional usefulness of stationary storage devices when other smart loads are connected to the grid.

1

1.2. RESEARCH OBJECTIVE AND QUESTIONS

The goal of this thesis is to investigate

> ***How can the existing trolleybus grid infrastructures be re-designed as sustainable and multi-functional smart DC grids?***

This investigation is carried out in four parts, each addressing one of the four research gaps introduced above.
The structure of this thesis and its chapters is a reflection of this division into 4 main research questions/gaps and their subquestions.

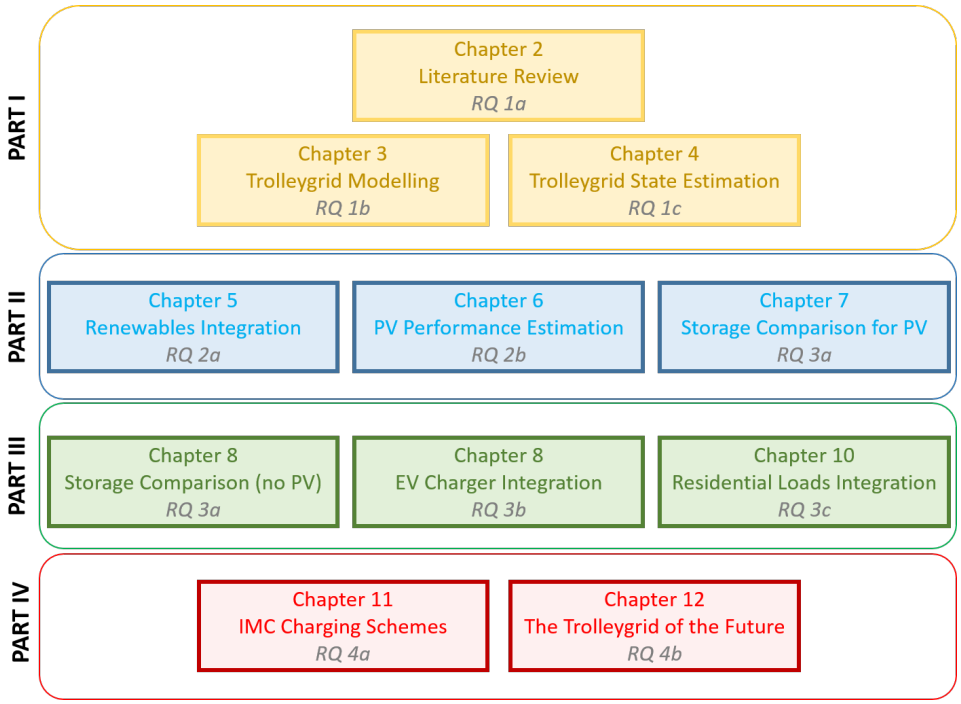

The proposed research questions are:

1. **What are the opportunities, challenges, and tools needed for designing and assessing the transformation of present-day trolleygrid infrastructures into sustainable, multi-functional grids?**

   (a) What are the main technical and non-technical challenges facing the decarbonization and the multi-functionality goals envisioned for conventional trolleygrids, and what attempts have already been made to tackle them?

(b) What are the suitable modeling methodologies, practices, and tools that are necessary to design and assess the sustainable, multi-functional trolleygrids of the future?

(c) What modeling and estimation tools can achieve suitable power management schemes for the sustainable, multi-functional trolleygrids of the future?

2. **What is the outlook for renewables integration in present-day urban trolleygrids?**

   (a) What are the favorable placement (centralized or decentralized) and sizing options of renewables in trolleygrids for better performance in terms of increasing traction load coverage and independence from AC-side storage, the main AC grid, and curtailment?

   (b) What parameters, methods, and tools can be used to estimate the performance of a PV system connected to a traction substation?

   (c) What are the favorable placement (on-board or stationary), sizing, and technology options for DC-side storage systems in terms of improving the PV system performance?

3. **How can the integration of smart non-traction loads and grid components be maximized to improve the techno-economic feasibility of the future sustainable, multi-functional trolleygrid?**

   (a) What are the favorable type, placement (on-board or stationary), and size of the storage systems to improve the trolleygrid performance w.r.t. increasing the braking energy recovery, reducing the line transmission losses, decreasing the line voltage drops, and increasing the available spare traction substation capacity?

   (b) What active grid management schemes and passive grid infrastructure updates can increase the Electric Vehicle (EV) chargers integration potential in the trolleygrid?

   (c) How can a multi-stakeholder PV-rooftop infrastructure shared by residential households and nearby traction substations improve the PV system performance in terms of increasing traction load coverage and independence from storage, the main AC grid, and curtailment?

4. **What are suitable power management and design schemes for the trolleybus fleets and the trolleygrids of the future?**

   (a) What are appropriate battery-charging schemes for the intercity and intracity In-Motion-Charging trolleybuses in the increasingly congested multi-functional trolleygrids of the future?

   (b) What synergy (or dysergy) is there for the trolleygrid and its connected PV systems in implementing the above grid components and strategies simultaneously (RES, EV chargers, storage, IMC, etc.)?

1

1.3. THESIS CONTRIBUTIONS

The contributions of this thesis are summarized below:

- A comprehensive review of the grid components, trends, results, and both technical and non-technical challenges for the electrification of urban bus fleets **(Chapter 2)**
- A comprehensive and verified trolleygrid state model that does not use the six commonly made assumptions in modeling trolleygrids (substation voltage, bilateral connections, feeder cables, bus auxiliaries demand, regenerative braking, and parallel lines) and quantifies the effect of these assumptions, and validates a seventh one (modeling of overhead cables as purely resistive cables) **(Chapter 3)**
- An original trolleygrid state estimator to predict, without additional sensors or wireless communication, the instantaneous trolleygrid states and that can be used as the basis for power-management schemes for, among others, DC-side storage and IMC buses **(Chapter 4)**
- An in-depth study of the performance of PV systems and the only study for Wind systems for different centralized and decentralized placement and sizing options at the AC side of trolleygrids **(Chapter 5)**
- A simplified and computationally efficient method for trolleygrid stakeholders to estimate the performance of a PV system of any size connected to one or more traction substations of any size **(Chapter 6)**
- The detailed, comparative study of different on-board and stationary storage system technologies and sizes in PV-augmented trolleygrids **(Chapter 7)**
- The detailed, comparative study of on-board, stationary, and hybrid-placement storage systems in trolleygrids for increasing the braking energy recovery, reducing the transmission losses, decreasing the line voltage drops, and increasing the spare traction substation capacity **(Chapter 8)**
- The detailed study of active and passive infrastructure methods for increasing the EV charger integration potential in trolleygrids while considering power, voltage, and current limitations **(Chapter 9)**
- The detailed study of a multi-stakeholder PV system shared by traction substations and their nearby residential loads to increase the available installation space and enhance the techno-economic feasibility of the PV system integration **(Chapter 10)**
- Two novel battery-charging schemes for the feasible electrification of bus fleets as In-Motion-Charging trolleybuses while maneuvering the strict power and voltage states of the multi-functional trolleygrid **(Chapter 11)**
- The detailed study of the synergetic and non-synergetic effects of implementing multiple components of the trolleygrids of the future and suggestions on the most favorable combinations **(Chapter 12)**

1.4. RESEARCH PUBLICATIONS

Journal Papers:

1. The Next Generation of Sustainable, Multi-functional Trolleybus Grids: A Review of Trends, Research, and Challenges. I Diab, K Giitsidis, M Bistřický, K vd Horst, GR Chandra-Mouli, P Bauer, *Submitted*, (Chapter 2, Research Question 1.a)

2. "A Complete DC Trolleybus Grid Model With Bilateral Connections, Feeder Cables, and Bus Auxiliaries," I Diab, A Saffirio, GR Chandra Mouli, AS Tomar and P Bauer, in **IEEE Transactions on Intelligent Transportation Systems**, vol. 23, no. 10, pp. 19030-19041, Oct. 2022 (Chapter 3, Research Question 1.b)

3. A Traction Substation State Estimator for Integrating Smart Loads in Transport Grids Without Additional Sensors: Theory and Case Studies. I Diab, GR Chandra-Mouli, P Bauer, in **IEEE Transactions on Intelligent Transportation Systems**, (Chapter 4, Research Question 1.c)

4. "Placement and Sizing of Solar PV and Wind Systems in Trolleybus Grids", I Diab, B Scheurwater, A Saffirio, GR Chandra-Mouli, P Bauer **Journal of Cleaner Production** 352, 131533, (Chapter 5, Research Question 2.a)

5. "A Simple Method for Sizing and Estimating the Performance of PV Systems in Trolleybus Grids", I Diab, A Saffirio, GR Chandra-Mouli, P Bauer, **Journal of Cleaner Production** 384, 135623, (Chapter 6, Research Question 2.b)

6. Comparison of On-board and Stationary Storage Solutions for Trolleygrids with PV Systems. I Diab, K Giitsidis, GR Chandra-Mouli, P Bauer, *Submitted*, (Chapter 7, Research Question 2.c)

7. Comparison of On-board, Stationary, and Hybrid Storage Solutions in Trolleygrids. I Diab, GR Chandra-Mouli, P Bauer, *Submitted*, (Chapter 8, Research Question 3.a)

8. "Methods for Increasing the Potential of Integration of EV Chargers into the DC Catenary of Electric Transport Grids: A Trolleygrid Case Study," K vd Horst, I Diab, GR Chandra-Mouli, P Bauer, in **eTransportation**, 2023, p.100271, (Chapter 9, Research Question 3.b)

9. A Shared PV System for Transportation and Residential Loads to Reduce Storage and Curtailment: Two Trolleygrid Case Studies. I Diab, N Damianakis, GR Chandra-Mouli, P Bauer, *Submitted*, (Chapter 10, Research Question 3.c)

10. "An Adaptive Battery Charging Method for the Electrification of Diesel or CNG Buses as In-Motion-Charging Trolleybuses," I Diab, R Eggermont, GR Chandra Mouli and P Bauer, in **IEEE Transactions on Transportation Electrification**, (Chapter 11, Research Question 4.a)

11. A Valley-Charging Method for the Electrification of Buses as IMC Trolleybuses in Congested Grid Areas. M Bistřický, I Diab, GR Chandra-Mouli, P Bauer, *Submitted*, (Chapter 11, Research Question 4.a)

12. Designing and Assessing the Sustainable, Multi-Functional, and Multi-Stakeholder Trolleygrids of the Future. I Diab, GR Chandra-Mouli, P Bauer, *Submitted*, (Chapter 12, Research Question 4.b)

Conference Papers:

1. "Toward a better estimation of the charging corridor length of in-motion-charging trolleybuses," I. Diab, G. R. Chandra Mouli, and P. Bauer, in 2022 IEEE Transportation Electrification Conference & Expo (ITEC), 2022, pp.557–562

2. "Increasing the integration potential of EV chargers in DC trolleygrids: A bilateral substation-voltage tuning approach," I. Diab, G. R. C. Mouli, and P. Bauer, in 2022 International Symposium on Power Electronics, Electrical Drives, Automation and Motion (SPEEDAM), 2022, pp.264–269.

3. "A Review of the Key Technical and Non-Technical Challenges for Sustainable Transportation Electrification: A Case for Urban Catenary Buses," I. Diab, G. R. Chandra Mouli, and P. Bauer, in Proceedings of the 20th IEEE International Power Electronics and Motion Control Conference (IEEE-PEMC 2022), September 2022

PART I

THE TROLLEYGRID OF THE FUTURE: DESIGN TRENDS AND MODELING METHODOLOGIES

This first part of the thesis presents the fundamental point of departure for the research. First, Chapter 2 surveys the available literature on the future of transport grid infrastructures and identifies the research gaps that motivate the research directions in the other chapter.

Then, the numerical and analytical models of the trolleybus power demand, trolleygrid power flow, and power management schemes are detailed in Chapters 3 and 4.

2

SUSTAINABLE AND MULTI-FUNCTIONAL TROLLEYBUS GRIDS: A REVIEW OF TRENDS, RESEARCH, AND CHALLENGES

"Madamina, il catalogo è questo [..]
In Italia seicento e quaranta;
In Almagna duecento e trentuna;
Cento in Francia, in Turchia novantuna;
Ma in Ispagna son già mille e tre.

Madamina Il Catalogo è Questo - Act I, Don Giovanni (Mozart)

Little lady, here's the list,[..]
In Italy, six hundred and forty;
In Germany, two hundred and thirty-one;
A hundred in France, In Turkey, ninety-one;
But in Spain, they're already a thousand and three

This chapter is based on The Next Generation of Sustainable, Multi-functional Trolleybus Grids: A Review of Trends, Research, and Challenges. I Diab, K Giitsidis, M Bistřický, K vd Horst, GR Chandra-Mouli, P Bauer *(Submitted)* **and** "A Review of the Key Technical and Non-Technical Challenges for Sustainable Transportation Electrification: A Case for Urban Catenary Buses," I. Diab, G. R. Chandra Mouli, and P. Bauer, in Proceedings of the 20th IEEE International Power Electronics and Motion Control Conference (IEEE-PEMC 2022), September 2022

Trolleybus grids are being redesigned as sustainable and multi-functional infrastructures by integrating renewables, storage, EV chargers, and new and sophisticated bus fleets. This chapter offers a review of the trends, research, and challenges facing this vision and identifies the research gaps and directions that must be adopted by researchers and stakeholders in investigating these networks.

2

2.1. INTRODUCTION

Changing attitudes toward diesel buses are bringing trolleybuses back into the transportation landscape as a key player in transportation electrification [1]. Even more, the oversized and underutilized high-power infrastructure of trolleygrids is being reconsidered as a sustainable and multi-functional backbone to the AC grid by integrating renewables, storage, EV chargers, and new bus fleets as shown in Figure 1.4.
This chapter looks at trends, research, and challenges in the investigation of these future grids, addressing namely:

- The modeling of trolleygrids
- Renewable energy sources (RES) integration
- Energy storage systems integration
- Smart loads integration such as EV chargers
- The new generation of trolleybus fleets (In-Motion-Charging)
- The non-technical challenges, such as policy limitations

2.1.1. COMPARISON OF TRANSPORTATION GRIDS

Before investigating the literature available on trolleygrids, it is important to justify why the literature available on metro and train networks is excluded. The key distinctions can be seen in Table 2.1 where the differences in traffic behavior, power demand, and voltage drops make research in train and metro networks untranslatable to trolleygrids. Furthermore, trolleygrids are introducing new fleets of In-Motion-Charging trolleybuses that create a different power demand profile than what could be expected from tram networks. This makes research in tram networks obsolete in the near future for application on trolley systems.

2.2. THE NEED FOR COMPREHENSIVE MODELS FOR TROLLEYBUS NETWORKS

Figure1.2 shows the typical layout of a trolleygrid. For reasons such as faults and transmission losses, the trolleybus lines are divided into isolated sections of a few hundred meters, up to 1 or 2 km, depending on the trolleygrid city. The power comes from the Low or Medium Voltage AC grid (LVAC or MVAC) depending on the trolleygrid, and a

Table 2.1: Comparison of Transportation Grids as the Subject of Transport Research [14], [43]–[47]/

	Trams and Trolleybuses	**Metros and Trains**
Traffic Behavior	Stochastic, rides with the city traffic	Predictable, goes from Station A to Station B
Order of Magnitude of Electric Power Demand	hundreds of kWs	few MWs
Potential for PV Integration	Short sections with relatively low energy demand and infrequent timetabling (no base load)	Relatively high energy demand that can justify AC-grid contracts such as Power Purchase Agreements. Also, the passenger stations themselves are large and can constitute a base load
Potential for Storage Integration	Placement and sizing are complex as the vehicle power profile is as stochastic as the traffic conditions and driver behavior	Placement and sizing are more straightforward, as the vehicles brake and accelerate predominately at the same location (station)
Potential for EV chargers Integration	Complex as the catenary is subject to severe voltage drops due to relatively low nominal voltages (600-750V) and high overhead cable resistance. The stochastic traction load can interfere with the Quality-of-Service of the EV charging session	Catenary is less subject to severe voltage drops due to relatively high nominal voltages (from 800 up to 3000V typically) and low third rail resistance. Also, the predictable traction load helps better plan the EV charging sessions even a day ahead

transformer steps down the voltage. Then, a rectifier converts into DC, as the buses run at a nominal voltage of 600-700V. The minimum voltage, due to transmission voltage drops and current limitations, that the bus runs on is 400V. The transformer-rectifier system is housed in a "substation". One substation can feed one or more sections, to which it is connected via the section feeder cables (FC). In Figure 1.2, substation 1 feeds two sections, while substation 2 feeds one.

The substations are unidirectional because of the rectifier. Consequently, a braking bus cannot send its energy back to the MVAC grid, but rather to other buses on the same section, or on a connected section.

The first possibility for two sections to be connected is when they are supplied by the same substation: Bus 1 of Figure 1.2, for example, can supply Bus 2 via the route FC1-substation busbar-FC2. The second possibility is when the sections are bilaterally connected. A bilateral connection is a controllable connection between two sections that are under different substations. The connection can be controlled as closed (connected) or open (isolated). Bus 2 can send power through the overhead lines to bus 3 as if sections 2 and 3 are one long section. Bus 1 can also share power with bus 3 via the route FC1-busbar-FC2-bilateral.

Finally, it is noticeable that each bus is connected to two lines in Figure 1.2. In trolley-grids, an overhead return path for the current is also needed as the bus runs on wheels, unlike the tram, which uses the rails as a return.

To reduce the transmission losses on the section, an element found commonly in transport networks is the parallel connection between the overhead lines of the different bus lines available in a section, i.e., the going and the returning traffic lines. Within the same section, the feed (positive) and the return (negative) lines are connected in pairs to offer a lower impedance path from the substation (or a braking bus) to the buses. These lines are introduced periodically at a distance in the order of hundreds of meters (100-300m).

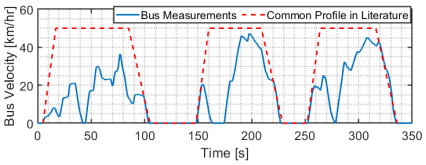

Figure 2.1: Bus velocity measurements in Arnhem compared to the trapezoidal velocity profile commonly found in the literature. The latter assumes a constant acceleration phase from the bus stop, followed by a constant-velocity cruising at 50 km/hr, and then a constant deceleration toward the next bus stop.

2.2.1. MODELING OF TROLLEYGRIDS IN LITERATURE

Modeling transportation networks has been a powerful tool in designing, analyzing, and optimizing electrical transit grids. Simulators, both commercial and academic [5]–[7], [9], [10], [12], [17], [19], [21], [36], [37], [41], [42], [48]–[64], use different solver methods and modeling techniques to investigate these networks. Generally, these simulators are used to calculate substation-level parameters such as the substation power demand and the substation component design ratings.

Nevertheless, many studies look more in-depth into variables such as the voltage drops over the transmission lines for the introduction of larger buses on the lines, for example, or the available braking energy for recuperation by storage devices.

Unfortunately, these models are limited both in the modeling of the bus load and of the grid elements. Trolleygrid studies tend to limit themselves to a single section, with an ideal trapezoidal traction power load [17], [21], [36], [48], [50], [54], [55]. A trapezoidal profile assumes a constant acceleration phase from the bus stop, followed by a constant-velocity cruising at 50 km/hr, and then a deceleration toward the next bus stop. As Figure 2.1 shows, this is not a fair representation of the actual velocity profile of the trolleybuses. The traffic conditions can seriously affect bus consumption as explained in [65].

While some sources use a more sophisticated bus traction power model [7], [49], [51], [64], they still neglect the seasonal variation of the bus demand brought by the auxiliaries, namely the HVAC (heating, ventilation, and air conditioning)[12], [17], [19], [21], [36], [48], [50], [51], [54], [55], [59]–[61], [64].

During winter conditions, this demand can be as high as the traction load (about 1.5 kWh/km each) as measurements have shown in [3] where the total HVAC demand of 17.95kWh accounts for half of the bus total demand of 36.11 kWh during the 11.60 km trip. This value is in accordance with those previously reported in literature [4].

Ignoring this HVAC power would have two consequences. First, it would remove a considerable portion of the substation load, making substation calculation inaccurate. Second, it removes a receiver of the bus regenerative braking which would result in inaccurate calculations of the shared energy between buses and of the energy wasted in the onboard braking resistors. This underestimates the substation demand brought by lower loads and higher power sharing between buses.

The regenerative braking can also feed other buses that are under the same supply zone,

relieving the two bilaterally connected substations from a fraction of the bus load. Measurements made on the trolleybuses in Arnhem ([3]) have shown that around 30% of the bus load is available for recuperation (12.00 of the 36.11kWh). This value is in line with what is reported in other trolley cities [9], [17], [42], [66]. Without a bilateral connection correctly modeled, this available energy would be assumed wasted in the on-board braking resistors and causing an overestimation of the substation energy demand.
Finally, the feeder cables can affect the regenerative braking and the bilateral connection by contributing to a sizeable voltage drop on the section, altering the supplied power share by the substations and the braking buses. This can happen when the voltage of one node, for example, becomes too low relative to the other supplying nodes and is therefore unable to push power into the circuit.
Other than the simplistic bus models, the trolleygrid itself is frequently modeled with some major assumptions.
For example, some works consider the parallel/equipotential lines ([57], [60], [62]) while others, such as [21], [63], ignore them. Feeder cables are also ignored, except in a few works ([5], [12], [19], [52], [57], [59], [61]).
The need for a complete bus power representation and trolleygrid model is more pressing nowadays. This is because DC trolleygrids are ushering in a new era of active, urban transportation grids as they look at integrating solar PV [36], [50], on-board and/or off-board storage [6], [7], [21], [37], electric-vehicle (EV) chargers [36], [67], [68], and In-Motion-Charging (IMC) buses [2], [69] into their network.
To highlight an example of the future grid, IMC buses are the new generation of trolleys that combine the advantage of a catenary operation, with the flexibility of an electric battery bus. The IMC bus is equipped with a battery that is charged while the bus is under the catenary (the charging corridor) and discharged later when the trolleybus is driving in areas outside the trolleygrid. The main urban advantages of such a system can be, for example, in operating these buses in historic city centers without the visual intrusion of lines, or in operating over new lines without the need for building a new infrastructure. With a battery charging at the order of hundreds of kWs, these buses constitute a challenge in the expansion of the trolleygrid.
A detailed model for the power consumption and the voltage drop at the substation level is needed to make sure that the introduction of IMC does not violate the operational limits. As the analysis in [3] shows, simplified grid models found in literature can lead to incorrect results in the calculation of the minimum voltage and load demand on a substation.
It is then particularly important for this subgroup of transportation grids to study in detail the line voltage, current ratings, and the in-line transmission losses of their subsystems, using specific, representative models.
In particular, six parameters that are often incorrectly ignored and/or approximated in these models are:

- The parallel lines (equipotential lines) connecting the overhead lines,
- The bus auxiliaries power (predominately the HVAC),
- The bus regenerative braking,

- The section feeder cables,
- The bilateral connections between sections,
- The real nominal voltage of the substation

2.2.2. CONCLUSIONS ON MODELING OF TROLLEYBUS GRIDS

The study of the future trolleygrid requires more specific models with a proper and accurate representation of the bus traction and auxiliary load and the trolleygrid elements. Many works in the literature do not include some or all of these key elements for a proper power flow calculation as explained above and tabulated in Table 2.2, and this should be addressed in future simulation research, especially as pilot and validation projects are difficult to conduct in trolleygrids.

Table 2.2: Summary of the comparison between common assumptions in literature as to be detailed later in Chapter 3.

Trolleygrid Parameter	Typical Modeling Assumptions Made in Literature	Effect of Assumption (case study analysis in Chapter 3)
Overhead Line Impedance	Assumed purely resistive, except in works such as [37] where it is taken as resistive-inductive	Can indeed be considered purely resistive for steady-state models
Overhead Parallel Lines	Ignored in works such as [21], [63], included in works such as [57], [60], [62]	If ignored, the line impedance could be as much as double its actual value (100% error)
Bus Auxiliaries Power	Ignored in works such as [17], [21], [36], [48], [50], [51], [54], [55], [60], [64], included in works such as [41], [42]	If ignored, errors up to 55% in substation energy calculations
Bus Regenerative Braking	Ideally, implied that it is modeled but it is not correct to include it while simultaneously ignoring the auxiliaries demand such as in [17], [21], [36], [48], [50], [51], [54], [55], [60], [64]	If ignored, errors as high as 34% in the substation power calculations
Section Feeder Cable	Only mentioned in works such as [5], [52], [57]	If ignored, errors are expected in extreme cases above 15% in the substation power calculations and 50V for the minimum line voltage
Bilateral Connections	Only mentioned in works such as [56], [62], [70]	If ignored, errors up to 25% in the substation power calculations
Substation Nominal Voltage	Typically assumed at a rounded-up nominal value of 650 or 700V such as in [21], [70], [71]	Particularly important for bilaterally connected substations because of the effect on the load-sharing ratio between them

2.3. RES INTEGRATION IN TROLLEYBUS GRIDS

2.3.1. CHALLENGES FOR RES INTEGRATION

The load profile of light rail traction networks is particular in two aspects. First, the load is stochastic and unpredictable both in time and location since the vehicles are moving with the city traffic. Second, when the vehicle exits the supply zone of one substation and enters another, the load demand suddenly disappears from the first substation. In that sense, traction grids are particular grids with no base loads and with high, unpredictable power peaks caused by vehicle acceleration (about five times that of cruising traction).

Further concerns are those of land use, mainly when considering a decentralized placement. However, a centralized placement on the AC side has its own challenges in the

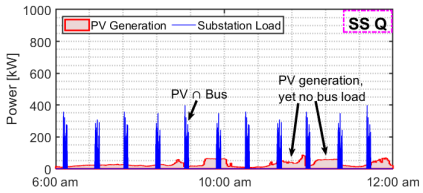

Figure 2.2: Mismatch in simulated PV generation and the bus load for a low traffic substation in the city of Arnhem, The Netherlands (detailed in Chapter 5).

reliability of the grid, the future grid capacity, and the fluctuation in pricing, as well as the administrative and legislative difficulties that come along. Policy calls already warn that to achieve the energy transition, transport operators cannot rely on the pace of national ambitions in the energy sector [72].

2.3.2. PROJECTS AND RESEARCH OF RES INTEGRATION IN TROLLEYBUS GRIDS

The major hurdle to the integration of RES in transportation grids is the intermittent nature of vehicle scheduling. This leaves areas of the grid with low or no load for hours of the day when the RES is generating (Figure 5.1(b)). In the case of PV, for example, a seasonal mismatch is very pronounced as well between the dense schedules and high heating demand of the winter months (with low PV generation) and the reduced scheduling and low cooling demands of the summer months (with high PV generation).

While some works exist in the field of PV in train and metro networks (e.g., [44], [45], [47], [73]), these rail systems are different than trolleygrids in terms of higher power levels, higher line voltages, more segmented electrical infrastructure, and less stochastic traffic conditions as shown in Table 2.1. Meanwhile, tram studies [46], [74]–[76] are mostly occupied with studies on power management and storage sizing rather than assessing the potential for RES integration in transport grids. This motivates the separate study of RES integration into trolleygrids.

As mentioned earlier, the trolleygrid substations are unidirectional because of their rectifiers. This creates a major hurdle for the implementation of PV without storage on the DC side, as all the PV energy that is not consumed by the buses or the line losses (excess) should be curtailed. One possible solution is to place the PV on the AC side of the substation to allow a path for the PV system to use the LVAC as a storage as in [11]. The PV power is first inverted to AC (either single stage or DC/DC and then DC/AC stages), allowing any excess energy to return to the AC grid and any trolleygrid power demand to be rectified again and sent to the trolleybuses. Another possibility is to connect the PV after its first DC stage to the trolleygrid. This, however, requires a separate study on the optimal feeding point location with respect to transmission losses and overhead line voltage drops, unless the PV is placed at the substation bus-bar as in some literature works [77]. Nevertheless, this placement choice could only indirectly reduce the losses in the grid by increasing the feed-in voltage and would impose a lot of curtailment on the PV system, reducing thereby its utilization. Another approach in literature places the PV systems on all the substations based on the maximum allowable line impedance that

is derived from the voltage drop limitations of the grid [78]. This method is therefore more concerned with reducing line losses rather than increasing the sustainability of the grid and the utilization of the PV system. Furthermore, the PV model consists of an ideal curve multiplied by a randomized cloud factor, neglecting the modeling of environmental variations in the PV output power.

To the best knowledge of the authors, the only work that proposes a different PV size for trolleygrids substations based on their energy demand is [77]. However, this work only suggests an estimated PV system size. Namely, that paper suggests placing 400-500kWp at large traction substations and 100-150kWp at small traffic ones. In comparison, the work presented here in this paper offers a systematic and specific sizing and placement approach as a function of the substation yearly energy demand.

Other works in the literature [11], [79], [80] have proven that the direct utilization of an energy-neutral sized, traction-substation-connected PV system can be as low as 13% in low-traffic substations, and quickly reaches a plateau of about 38% with busier substations in a study of the Dutch city of Arnhem and the Polish city of Gdynia. This means that if the excess generation is curtailed, less than 40% of the PV energy is used from a system that was sized to feed 100% of the load. The effective energy cost is thereby more than 2.5 times higher than that of the installed capacity. If the system is undersized to reduce the absolute amount of energy wasted, less of the traction load is covered. Other works have also shown the sizing limitation of a traction-grid-connected PV system because of the load and generation mismatch [81].

One way to better match the renewable generation with the trolleygrid demand is a combination of wind and PV systems that can better follow the load seasonally and daily, respectively. This was investigated in the Dutch city of Arnhem [11] in an AC-side aggregated generation. The results provided a 54.1% utilization at an optimal system share of 53% PV and 47% Wind. This still means that almost half of the renewable energy generated is not used by the trolleygrid, but since the system is connected to the Medium Voltage AC grid directly, the excess power can be utilized by other loads. However, such contractual purchasing agreements have their economic and policy limitations, and are subject to grid reliability constraints and risky fluctuations in energy pricing, and are still not preferred over a distributed generation system.

Other research on renewable integration in trolleygrids is on the trolleygrid of the German city of Solingen. In [82], the model for power flow calculations is derived and presented, although no PV analysis is conducted. In [83] a 100 kWp PV system is analyzed, claiming a 90% PV utilization with 5% in losses. The methodology for the results is not clear enough to justify these numbers, but it is understood from the work that the PV system is shared by multiple interconnected substations. Finally, in other works for the city, 10kW and 50kW converters are designed for direct implementation of PV and batteries [84], [85].

In other forms of renewables, the work on the Portuguese city of Coimbra in [86] studied a hydro plant connection to its trolleygrid. As expected, the hydro-power generation is orders of magnitude higher than the trolleybus demand even for the small investigated plant, producing 2 to 11 times the energy demand of the maximum trolleybus demand projections which stand at less than 1000MWh/year.

Finally, it can be mentioned that the work in [87] has referenced the PV integration into

trolleygrids but without investigating it.

2.3.3. CONCLUSIONS ON RES IN TROLLEYBUS GRIDS

RES integration into traction grids has been investigated in some works in the literature. Some key gaps and worrying trends can be highlighted:

1. Despite their techno-economic shortcomings, decentralized PV systems remain the preferred choice for the sustainable supply of trolleygrids and must be further investigated in terms of AC and DC side placement and sizing

2. The integration of more base loads, such as EV chargers, into traction networks is a necessity for the techno-economic feasibility of the projects of renewables integration

3. There is no work in the literature yet that addresses the physical installation concern for PV panels in the urban environment (scarcity of the hundreds of square meters of needed installation space)

4. There is no work in the literature yet that investigates the PV system performance when trolleygrids roll out their more power-demanding fleets of IMC buses

2.4. ENERGY STORAGE SYSTEMS IN TROLLEYBUS GRIDS

Energy storage can be made via a variety of technologies, whether chemical such as batteries, or mechanical such as flywheels, that have advantages and disadvantages according to the application.
In the specific case of transport grids, storage can be placed on-board the vehicle and/or off-board (wayside) at the traction substation, for example.
In both placement options, there is a need for a fast response time in the order of seconds to respond to the dynamics of moving vehicles. Furthermore, the constant deceleration (battery charging) and acceleration (battery discharging) of transport vehicles at their stops create a need for a high cycle life of the implemented storage; for example, 10 stops per hour can easily count over 10000 cycles per year for relatively small battery sizes. Also of importance is the round-trip efficiency of the storage system.
Beyond this, each placement option has its particular requirements. For on-board placement, Power density and Specific power are important as the storage is implemented to recuperate the quick bursts of regenerative braking, without needing a lot of space and adding to the weight of the vehicle. Energy and self-discharge are less of a requirement as the storage on-board is mostly designed to store relatively small amounts of energy for a relatively short duration. For example, charging when the bus pulls up at a bus stop to discharging when it accelerates a few moments later when driving away. This is, of course, not the case with IMC trolleybuses that have high requirements for both energy and power densities. Finally, safety is a big concern.
In stationary applications, specific power and energy are not a limitation since weight is not an issue. The occupied space, however, necessitates high values of power and energy densities. Self-discharge is also of importance as the energy in stationary applications tends to be stored for longer periods of time as these storage applications go beyond a

simple recuperation of braking energy. Safety is always a concern, but housing the storage at the substation rather than on the vehicle with passengers allows for a bit more leniency (for example, in accepting the possible debris release from a flywheel).

2.4.1. COMPARING STORAGE TECHNOLOGIES FOR USE IN TRANSPORT GRIDS

In light of these requirements, Table 2.3 presents a comprehensive list of common storage technologies and their key characteristics. The cells highlighted in red conflict directly with the requirements described here above for storage in transport grids. Meanwhile, the yellow-colored cells flag limitations for the highlighted technology for a particular placement scenario.

First to be eliminated are the compressed air or liquid air energy storage systems (CAES or LAES) and thermal energy storage, as their response time goes beyond seconds, and their efficiency is well below that of other technologies.

On the other hand, while superconducting magnetic energy storage boasts high efficiency, its cost and extremely poor energy density and specific energy make it an unsuitable choice.

Flow batteries (Redox) such as Vanadium Redox, Zinc Bromine, and Polysulfide Bromine also have enough reasons to be disqualified, with one or more of low-efficiency performance, power density, safety, and cycle life. These same reasons also disqualify Nickel Cadmium and Lead-acid batteries, with added concerns of maintenance and toxicity that are quickly disqualifying them from any previous share of the transport storage market. While Nickel metal hydrate (NiMH) does not have the toxic Cadmium component, its charging scheme is very complex. Another battery technology to be disqualified over operational requirements is the sodium-sulfur battery which requires temperatures above 300C.

While capacitors bring disqualifying energy density, safety, efficiency, and self-discharge concerns, Supercapacitors (or Ultracapacitors) are good energy candidates in transport grids, especially as an On-board storage as their power density is much better than that of any studied candidate at over 100000W/L. Their self-discharge is lower than that of capacitors but still relatively high. However, as mentioned earlier, this is of less importance in on-board applications when the discharge comes often in the order of seconds after the charge (acceleration after a stop).

Li-ion technologies are also excellent candidates. While NMC and LFP batteries have been used in transport grids, LTO batteries are excellent candidates for both on-board and off-board applications, with a cycle lifetime more than 5 times above that of their counterparts. This makes them also perfect candidates for IMC trolleybuses as they can deliver both the C-rates and large energy requirements. The self-discharge of all mentioned Li-ion batteries is attractively low as well, at below 0.1% per day.

Table 2.3: Comparison of the characteristics of various energy storage technologies for use in transportation networks (yellow and red highlights are for minor and critical disadvantages, respectively).

Technology	Energy density (Wh/L)	Power density (W/L)	Specific energy (Wh/kg)	Specific power (W/kg)	Roundtrip efficiency (%)	Self-discharge (%/day)	Life-time (cycles)	Life-time (years)	Particular Characteristic
Nickel Manganese Cobalt (NMC, Li-ion)	250-545[88]	1,000-3,000 [89]	~190-275 [88], [90]	~340[88]	~90-97 [88]	<0.1[88]	1,000-1,500 [88]	5-10 [88]	High in Minerals [91]
Lithium Iron Phosphate (LFP, Li-ion)	220-375 [88]	1,000-2,500 [89]	90-160 [90] 200 [92]	~ 200[88]	>95[93]	<0.1 [88]	~3,000-5,000[94]	10-15 [88]	flat cell voltage (SOC and balancing) [91]
Lithium-Titanate-oxide battery (LTO)	~84 [95] 128 [96]	>6,000 [95]	45-100 [97] 50-80 [98] 70 [96]	420 [96] >1,000 [99]	>95 [100], [101]	~0.1 [100], [102]	2,000-6,800 [97] >10,000 [99]	10-25 [101]	Cost and lower nominal voltage [103]
Nickel Metal Hydrate battery (NiMH)	<350 [104] 150 [105] 250 [106]	500-3,000 [104]	60-120 [104] 65 [105], [107] 72 [108]	70-756 [104] 200 [105], [107]	80 [109] 65-85 [110]	0.4-1.2 [104] 0.6 [107]	300-500 [104] 500 [109]	15 [109]	Complex Charging [107]
Nickel Cadmium battery (NiCd)	60-150 [88] 80 [105]	80-600 [89]	50-75 [88] 45-80 [111]	150-300 [88] 160 [112] 150 [105]	60-70 [88] 60-83 [91]	0.2-0.6 [88] 0.3 [113]	2,000-2,500 [88]	10-20 [88] 15-20 [113]	memory effect and toxic Cadmium[91]
Lead-acid battery (Pb-acid)	50-80 [88] 50-90 [105]	80-600 [89]	30-50 [88] 25-50 [114]	75-300 [88] 250 [105] 180 [113]	70-80 [88] 75-80 [115]	0.1-0.3 [88] <0.1 [113] 0.2 [116]	500-1,000 [88] 200-1,800 [112]	5-15 [88], [113] 13 [116]	Maintenance and Limited DoD [117], [118]
Sodium Sulfur battery (NaS)	150-250 [88] 150-300 [89]	140-180 [89]	150-240 [88] 174 [106]	150-230 [88] 90-230 [119] 115 [112]	~75-90 [88] 75 [120] 75-85 [115]	negligible [112], [121]	2,500 [88] 3,000 [120]	10-15 [88] 15 [116] 12-20 [122]	High operating temp. and limited commercialization [122], [123]
Vanadium Redox battery (VRB)	16-33 [88] 25-35 [124]	~<2 [89]	10-30 [88]	166 [125]	75-85 [88] 65-75 [93]	negligible [88], [112]	>12,000 [88] ~13,000 [116]	5-10 [88] 20 [126]	Rare minerals [91]
Zinc Bromine battery (ZnBr)	30-60 [88] ~55-65 [89]	~<25 [89]	30-50 [88] 80 [108]	100 [108]	65-75 [88] 66-80 [91] 66 [117]	negligible [88], [127]	2,000 [88] 1,500 [116]	5-10 [88] 10 [116] 8-10 [128]	Material corrosion and dendrite formation [129]
Polysulfide Bromine battery (PSB)	~20-30 [130]	~<2 [89]	10-15 [110]	~<2 *	~60-75 [88], [131] 60-65 [110]	negligible [88], [126]	9,000-10,000 [110]	10-15 [88] 15 [131]	Limited Commercial Availability[132]
Capacitor	2-10 [88]	>100,000 [88]	0.05-5 [88] ~0.05 [133]	100,000 [88]	60-70 [88]	40 [88] 50 [134]	>50,000 [88]	~5 [88] ~1-10 [134]	Safety concerns [91]
Supercapacitor (SC)	10-30 [88]	>100,000 [88]	2.5-15 [88]	500-5,000 [88]	~90-97 [88] 84-95 [135]	11.3 [136]–[138] 20-40 [88]	>50,000 [88]	10-30 [88] 10-12 [135]	Relatively lower operating voltage [117]
Superconducting magnetic energy storage (SMES)	0.2-2.5 [88]	1,000-4,000 [88] ~2,500 [89]	0.5-5 [88]	500-2,000 [88]	~95-97 [88] 95-98 [135]	10-15 [88]	>100,000 [88]	>20 [88] 30 [117]	Cost of refrigeration and superconducting coil [139]
Compressed air energy storage (CAES)	3-6 [88] 2-6 [89]	0.5-2 [88] ~1 [89]	30-60 [88]	2.2-24 [94]	42-54 [88]	negligible [88], [122]	8,000-12,000 [91]	20-40 [88] 30 [105] >20 [116], [130]	Response time in minutes [117]
Liquid air energy storage (LAES)	80-120 [94] 50-200 [140]	-	214 [130]	-	55-80 [141]	negligible [141]	22,000-33,000 [142]	20-40 [140] >25 [141]	Response time in minutes [140], [143]
Flywheel energy storage (FES)	20-80 [88], [89]	1,000-5,000 [88]	10-30 [88] 5-80 [144]	400-1,500 [88]	~80-90 [88], [105]	11.6 [145] 100 [88]	>20,000 [88] >21,000 [116]	~15 [88] >15 [116] 20 [117]	Possible release of debris, and high cost [130]
Thermal energy storage (TES)	80-500 [88]	60-180 *	80-250 [88]	10-30 [88]	30-60 [146]	0.05-1 [88]	2,000-14,600 [146]	10-20 [88] 5-15 [88]	hours [130]

*Calculated from data

2.4.2. ON-BOARD ENERGY STORAGE IN TROLLEYGRIDS

The on-board energy storage systems, due to their small capacity size, have the advantage of being more affordable than the stationary energy storage systems, which translates to lower capital costs [147], [148]. They are also easier to implement as they do not usually require any modifications to the catenary grid. Existent vehicles, such as trolleybuses or trams, can be modified and retrofitted with those rather easily [149]. Thus, their implementation can provide many benefits with a rather low initial capital cost of installation [147], [148].

Academic research in storage on-board vehicles for trolleybuses is mainly preoccupied with the field of In-Motion-Charging. However, a few works do look at OESS applications.

In [150], the installation of a supercapacitor in the trolleybus with an induction motor traction drive allowed for the efficient recuperation of the braking energy independently of the presence of other overhead-connected consumers. Moreover, the storage provided the bus with an autonomous traction period with a maximum speed of 45 km/h.

Other works on on-board storage [5]–[8], [151], [152] are not focused on sizing or comparisons but are primarily concerned with power flow modeling and distributed control strategies. These cited works are all investigating the dual-source trolleybuses of Beijing, which are equipped with supercapacitors. It would be then interesting to revisit these works as power management schemes when the trolleygrid is equipped with EV chargers and solar panels.

One more work [153] looks at replacing the emergency internal combustion engine (ICE) of the trolleybus with a battery system. The work is proven feasible and validates the use of Li-ion batteries in trolleybus applications. This work is then concerned with one case study and does not look at any aspect of the sustainable and multi-functional trolleygrid.

2.4.3. STATIONARY ENERGY STORAGE IN TROLLEYGRIDS

Stationary energy storage systems offer a wider range of functionalities than on-board ones and are typically implemented with bigger energy capacities as they have lower weight and volume requirements [154]. This is rather important, especially, for the integration of RES and PV systems in the electric transport grids. They provide the opportunity for the intermittent energy provided by the PV systems to be stored to a great extent and to be used by the vehicles in the catenary grid when needed [155]. This renders them a future-proof investment, which will be able to cope with the increasing power demand of the trolleygrid of the future.

Again, most existing works in the literature look at the storage implementation solely from the perspective of energy recuperation and not in capacity building in power and voltage in preparation for the multi-functional trolleygrid.

The works in [2], [17], [147], [156] examine the energy recovery effectiveness of stationary storage applications and prove that over 20% of the trolleybus energy can be recuperated. An interesting conclusion of [156] is the claim that the need for storage systems decreases with increasing traffic. However, the examined storage in that paper is placed at the DC busbar of the substation, rendering it effectively operational as an on-board energy storage. This claim requires then further investigation.

A few works do examine the effect of storage in multi-functional trolleygrids. The work in

[11] examines coupling storage systems with PV systems on the AC side of traction substations. The storage system did not prove beneficial within reasonable sizes as seasonal storage was required. At the conclusion of the work, a call was renewed for the integration of loads, such as EV chargers, to provide the proper base load for the PV system.
Finally, the work in [12] looked at storage implementation in trolleygrids with IMC buses. The line voltage drops were reduced by over 5%, and the minimum line voltage was up by 19%.

2.4.4. CONCLUSIONS ON STORAGE INTEGRATION IN TROLLEYGRIDS

While many works look at storage in transport networks such as trolleygrids, three missing research aspects can be pointed out:

- The existing works are predominately pre-occupied with the harvesting of braking energy, and very few works look at preparing the voltage and power performance of traction networks for the new generation of trolleygrids with integrated solar, EV chargers, and IMC buses
- The existing works examine on-board and stationary storage separately, and no work exists yet that compares both placement options (or a hybrid thereof) in the context of the new generation of trolleygrids with integrated solar, EV chargers, and IMC buses
- The viable technologies for future research in trolleygrids are possibly limited to LTO batteries, Supercapacitors, and Flywheels

2.5. SMART LOADS AND CONVERTERS INTEGRATION IN TROLLEYGRIDS

2.5.1. PROJECTS AND RESEARCH OF EV CHARGER INTEGRATION IN TROLLEYBUS GRIDS

Today, EV charging infrastructures are a critical bottleneck for the diffusion of electric vehicles (EVs). The barrier is the unavailability of spare charging capacity in the increasingly congested electricity grids that are not designed for more of such high, variable, and inconsistent power demands [157]–[160].
For this, urban electric public transport networks are being researched to host smart grid loads, like EV chargers, by integrating them into their infrastructures [3], [11], [15], [16], [67], [161]. This is because these grids are historically sized for the worst-case scenarios of power demand, and can be better utilized by smart grid loads and appropriate power management. There is also a benefit for the transport grids as this creates a base load on their substations in the moments of no vehicle traffic. This can reduce the need for expensive storage systems for the recuperation of braking energy or for when a solar PV system is connected to the traction substation. This can be illustrated by the example of Figure 5.1(b) of the trolleybus grid of Arnhem, the Netherlands, where the lack of a base load jeopardized the techno-economic feasibility of the integration of renewables [11], [80].
The integration of EV chargers directly into transport infrastructures is an emerging topic,

Table 2.4: Overview of the projects with the integration of EV chargers into traction networks powering trolleybuses and trams.

Location	Traction network	Description/objective
Solingen, Germany [35], [36], [83], [162], [163]	Trolleybus	Investigating the potential of integrating decentralized renewable power generation (e.g., photovoltaics), charging stations for EVs, and stationary battery storage into the existing DC trolleybus infrastructure.
Gdynia, Poland [32]–[34], [164], [165]	Trolleybus	Analyzing the available capacity of the traction grid of Gdynia to charge electric cars. Furthermore, Smart Grid solutions for urban traction supply systems are introduced to improve the efficiency and stability of the traction network.
Edinburgh, Scotland [29], [30], [166]	Tram	Electrical capacity for EV charging systems based on four different charging control strategies are assessed and tested on the public tram system. The various connection topology, earthing methods, and stability criteria are considered.
Lisbon, Portugal [28]	Tram	Integration of bidirectional EV chargers into a DC catenary grid for trams. The authors looked into the concept V4G with an associated fuzzy control method. Furthermore, the benefits of an energy storage system in a catenary grid are demonstrated.
Sheffield, UK [26], [27]	Tram	Method to improve the energy efficiency of trams with the use of static energy storage systems and EV batteries in the public tram network. Current flow measurements and tram GPS data were used to simulate the energy flow in the catenary grid using a MATLAB/Simulink model.

although it is still mostly confined to metro and tram networks. As explained in Table 2.1, since tram networks are similar enough to trolleybus networks, this section will also look at EV chargers in tram grids. While a number of studies exist on this theme, they mostly deal with simplified grid models and/or a lumped-energy methodology that does not consider the operational violations on the DC side of the transportation grid that an extra charging load could bring. Unfortunately, this is often overlooked in the literature, and while some works already tackle the integration of EV chargers in transport grids such as trams and trolleybuses (Table 9.1), they deal mostly with:

- Simplified grid models that do not calculate and/or consider the resulting grid power, voltage, and current violations, and/or
- An analysis of measurements that offer insight only into one case of a relatively small charger, and does not quantify the potential of the grid beyond it, and/or
- A focus on harvesting the baseline spare capacity of a specific EV charger case study, but without offering insights on how to increase this capacity and/or optimize the EV charger placement
- A focus on a local case study without an analysis that could serve the extrapolation of the results beyond the local studied grid

To start with the first point: As mentioned, transportation grids are oversized to account for rare occurrences of high power demands. These moments should still be considered when integrating EV chargers so as not to violate the substation power rating. However, same as with the maximum power limit, there are maximum line current and minimum line voltage limitations dictated by the overhead cable temperature limit and the vehicle current collector, respectively. It is then important for any transport grid study to consider all three violations simultaneously. Meanwhile, none of the studied cities reported in Table 9.1 account for this.

For example, the work in Gdynia [165] starts with historical measurements of the minimum line voltage and adds to them an estimated voltage drop based on the superposition principle. This approach has three limitations: First, the transport grid deals with (mechanical) power-source loads whose power flow cannot be accurately computed linearly by the superposition principle. Second, the superposition principle would ignore the combined voltage drop effect of all the load currents at the substation feeder cable (additional non-linearity in the solution). Third, the moments of maximum power, current, and voltage do not necessarily occur at the same moment; hence, a historical maximum/minimum of each parameter cannot be studied independently. For example, a high load near the substation would not necessarily create a large voltage drop. This is why *instantaneous* measurements or simulations of the current, voltage, and power must be *simultaneously* studied. Beyond this work, other studies either ignore studying the voltage drop, such as the works in Edinburgh [29] or Sheffield [26], or look only at averaged values of the voltage drops and not in absolute terms such as the work in Solingen [163], or overlook the reported line voltages as low as 350V such as the Lisbon study [28].

Regarding the second point, on the vehicle charger size, the study of Gdynia [165] and Lisbon [28] look at one fast charger up to 50kW, while the study in Solingen [163] goes up to 132kW in steps of 22kW. Meanwhile, the study in Sheffield [26] only mentions the advantages of EV charging, and the study in Edinburgh [29] finds an energy equivalent of the available EV charging power from the spare energy capacity afforded by historical substation measurements.

Regarding the third point, only the Edinburgh [29] study looks at the maximal achievable EV potential from the grid, while the other studies suffice themselves with integrating one, relatively small charger, and do not look at the achievable potential in trolleygrids.
Finally, all of the studies limit themselves to investigating their local case study, without any analysis that could serve as lessons-learned and extrapolation to other transport grids based on their local traffic intensity, section lengths, and desired EV charger location along the line.

2.5.2. SUBSTATION POWER INVERTERS FOR BRAKING ENERGY RECUPERATION

One idea that is seldom researched in light rail grids is the integration of inverters at the traction substation to allow a path for the excess braking energy to return to the AC grid. While the works in [9], [10], [167], [168] examine this possibility, they agree that the return of unused recuperation energy into the AC low voltage network is not an economical choice, and would be limited to the local needs of the trolleygrid operator, for example in administration buildings located within the area covered by the overhead contact line. The economic feasibility of these projects is also hindered by price fluctuations in the AC grid and the fact that energy comes typically to trolleygrid operators at a subsidized cost. Furthermore, not many commercially available solutions exist for this technical task [168].

2.5.3. CONCLUSIONS ON SMART LOADS AND CONVERTERS INTEGRATION IN TROLLEYGRIDS

The integration of EV chargers in trolley infrastructures is not studied enough despite their great potential for relieving the congested city grid of this charging burden by tapping into the reserve capacity of the trolley network.
Furthermore, EV charging can create the necessary base load for both the connected renewable generation sources and the recuperation of braking energy, where competing substation inverters are not performing in a commercial, technical, or economical way.
Research on EV charger integration should move away from simple sizing and placement approaches of relatively small chargers and investigate the full potential of the trolleygrid and methods to increase its EV charging potential.

2.6. IN-MOTION CHARGING TROLLEYBUSES

Trolleybuses have a few advantages over battery electric buses. First, trolleybuses do not need a heavy on-board battery to complete their routes. This charging from the catenary also means that trolleybuses are more flexible in terms of scheduling and delays, while battery buses need to complete their charging sessions, which leads to accumulated delays throughout the day, and/or requires the use of a larger fleet than their diesel counterpart [169], [170]. On the other hand, battery electric buses are independent of the catenary, which gives them route flexibility. Trolleygrids are also often criticized for their expensive overhead catenary and the visual impact of its wires [87], [170].
The benefits of both e-buses and trolleybuses can be accomplished by the new generation of trolleybuses IMC (sometimes also referred to as dynamic charging or Slide-In system). In such a system, part of the route is covered with overhead lines (charging corridor), whereas the rest has no contact points with the trolleygrid at all [14], [171], [172]. In the charging corridor, the overhead lines are used as the power source for traction and also for charging the on-board storage. Outside the corridor, the vehicle uses this battery (battery-mode operation). Therefore, IMC buses allow the electrification of bus routes with shorter catenary lengths and smaller on-board batteries, while maintaining route flexibility.
Even though the IMC technology seems promising as a replacement for diesel buses, researchers tend to leave it out of their electric public transport feasibility studies and focus instead on conventional battery bus charging schemes such as depot, and end-stop opportunity charging such as in [87], [173], [174].

2.6.1. IN-MOTION CHARGING MAIN CHALLENGE: CHARGING POWER DEMAND

The problem with IMC buses is the initial investment costs in a catenary system which can be over 1-1.2 million euros per km. Still, the costs can be justified as IMC systems have the highest infrastructure utilization rate (75%) when compared to Overnight (19%) or Opportunity Charging (38%) [175]. It is interesting to note that there are more than 300 existing trolleybus networks in the world [170] that can directly make use of this IMC technology.
However, utilizing existing infrastructures to this extent does bring a charging demand

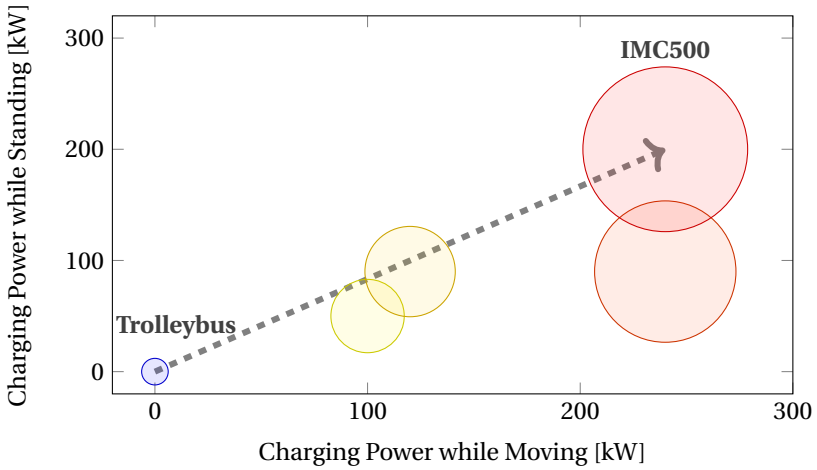

Figure 2.3: Growth in energy demand of a trolleybus (bubble size), as the newer IMC buses go for higher charging powers (even while standing) and consume more than 6 times the energy demand per km of a regular trolleybus (Adapted from [80] and [22]).

in the order of 100-200kW on top of the vehicle demand for the traction power substations.
The trolleybus typically consumes 1.5kWh/km for traction, and up to an additional 1kWh/km for auxiliary systems such as heating and air conditioning. Thanks to the inherent presence of a battery, the IMC bus is able to recuperate most of its regenerative braking energy, worth typically a third of the average traction demand (1.5kWh/km) [3], [4], [14]. Therefore, the IMC bus requires around 2kWh/km in harsh weather conditions for its traction and auxiliaries.
However, as IMC bus projects move toward a vision of only a third of the catenary length requirement, this means their average power consumption in the charging corridor is over 3 times that of a trolleybus.
Figure 2.3 quantifies this requirement for a number of IMC bus powers, including the latest IMC500 by Kiepe Electric [176] which charges 240kW while in motion, and 200kW while standing still (at traffic lights, stops, etc.) The lower charging power is usually curtailed to a third at a standstill so as to not overheat the connection to the catenary [177] but the IMC technology is clearly advancing faster than the electric current-collector technologies.

2.6.2. TRENDS IN EXISTING IMC PROJECTS

Polish trolleygrids are rapidly moving toward IMC fleets. In 2014, the IMC share in trolleygrids stood at 19 to 71% of the trolley fleet, and by 2019 had risen to 55-78% with more than double the installed battery capacity [81]. There was also a marked shift from NiCd batteries toward Li-ion technologies in these fleets.
The German cities of Eberswalde, Esslingen, and Solingen are looking at the IMC500 technology with coverage length of the charging corridor between 67 and 80% [175],

[178], [179].
Other examples are the Swiss town of Montreux which has extended its trolleygrid with IMC capabilities (2.8km of battery mode of a 12.7km route). The Czech city of Prague has an interesting IMC/Opportunity charging combination where the IMC bus only sees 10% of the road as an uphill catenary system (16% if both ways) which charging powers as low as 50kW [175].
Finally, the Dutch city of Arnhem is looking at electrifying its Bus Line 352 as In-Motion-Charging buses that utilize the existing catenary in the city and then continue in battery mode to the nearby city of Wageningen. This project has an impressive battery mode length of 17km each way, requiring a 90 kWh battery to be charged at 240 kW from under the catenary. Unfortunately, to realize this project, the trolleygrid operator has chosen to re-route trolleybus Line 1 to clear the catenary and substation capacity for the IMC fleet alone [180]

2.6.3. ADDRESSING THE IMC CHARGING POWER CHALLENGE

As detailed above, IMC projects tend to be either cautiously sized or still coupled with stationary chargers, or even designed to run alone by re-routing all other trolleybus lines. While the motivating benefits and implementation challenges of IMC buses are clear, little work exists that attempts to address them.
One work [181] looked at how the minimal coverage rate is also affected by traffic speed. In two charging power studies, with the average speed in Gdynia of 14 - 18 km/h, it was found that 30 - 35% of the route needs to be covered at 120 kW or only 20% if charging at 250 kW. This paper used the yearly average energy consumption of the vehicle to calculate the minimal coverage rate. However, the energy consumption can be much larger, especially in harsh weather conditions.
The work in [87] also neglected the HVAC system for the case study of the IMC system of Quito, Ecuador. An impressively low coverage rate of around 5% was reached, yet this was unfortunately compensated by a massive depot charging power of 1.4 MW.
One suggestion to adjust to the power demand of IMC buses from a study in Poland is to use a bilateral trolleygrid where two substations power the section, thus reducing the distance of the vehicle from the feed-in point (transmission losses) and sharing the IMC power across multiple substations [182].
One other work [12] looks at storage implementation in the Bologna trolleygrid as a preparation to keep the minimum line voltage high enough for successfully integrating IMC fleets.
Finally, the work in [183] looks at both the power and voltage limitations and suggests a new charging method for IMC, namely the Adaptive Charging Method, to electrify four bus lines in Arnhem. The charging scheme adapts the battery power under each substation according to historical spare capacity data rather than fixing one, conservative charging value for the whole route as is the case currently with IMC buses.

2.6.4. CONCLUSIONS ON STORAGE INTEGRATION IN TROLLEYGRIDS

While IMC fleets have an indisputable potential, especially when utilizing existing trolleybus infrastructures, little work exists on preparing trolleygrids for the power and voltage effects of their integration.

The existing work in the literature is mostly concerned with the sizing of batteries and charging corridors to fit IMC fleets into existing, congested infrastructures, rather than investigating storage and more sophisticated IMC battery charging methods that would increase this potential.
Finally, no work has looked in detail at IMC in trolleygrids with integrated renewables.

2.7. NON-TECHNICAL CHALLENGES FOR THE MULTI-FUNCTIONAL TROLLEYGRID

2.7.1. HESITATION TOWARD CATENARY INFRASTRUCTURE SOLUTIONS (COSTS AND PUBLIC OPINION)

The trolleybus comes at a much higher infrastructure cost than an electric bus, with one kilometer of catenary costing about 10 times as much as a 300kW opportunity charger [14]. Additionally, an electric bus can be about 10% higher in operational costs. Furthermore, the lack of battery data and understanding of battery aging and behavior leaves the trolleybus operators overestimating the costs in their tenders as a financial risk management strategy. Recent examples of unforeseen and inexplicable battery behavioral problems are the electric buses breaking down in Berlin and Trier in cold conditions, while those in Scandinavian countries have been operating normally in harsh winter conditions [184], [185].
To overcome this, data sharing between international transport network operators should be facilitated by international bodies, and explicitly incentivized in tendering documents to allow operators and researchers a faster understanding of battery aging and operational lessons learned in the context of transportation grids.
Funding should also be made more available for sustainable electrification projects. In Europe, the predominant long-term funding bodies are the European Investment Bank (EIB) and local banks, as well as EU research agendas (e.g. ELIPTIC, EfficienCE, ASSURED, Trolley 2.0, H2ME). On the other hand, the yearly operations are funded by local and national sources (e.g. Barcelona, Budapest) or federal funding (USA), but in both cases limited in resources and project-specific. Otherwise, tax and subsidies are offered as is the case in China (with its city of Shenzhen operating the world's largest electric bus fleet) and India [184], [186]–[190].
Finally, it is worth noting that there is general hostility from the public toward catenary systems. The infrastructure is seen as unattractive and intrusive, although some work is being actively pursued to change this public opinion [14], [81]. This again makes a case for IMC systems as they can retain the benefits of a trolleygrid with minimal catenary lengths.

2.7.2. THE DIESEL MENTALITY

Another non-technical challenge is the Diesel-oriented point of view of the stakeholders; a concept that can be suitably referred to as the "Diesel Mentality".
If the electrification of diesel buses is seen as a mere replacement of the bus traction energy source, the potential of the possibilities of an active, smart grid backbone to the local grid as discussed in the introduction of this thesis would be lost. In other terms, there should not be a reductive view of the transport network as a mono-functional grid

inherited from diesel networks.
Beyond missing out on the synergetic potential of these electrified networks and their active role, two dangerous consequences of the diesel mentality are already observable in the contracting and organization of the tenders for the buses and charging infrastructures and of daily bus operations.
The first problem is a lack of a centralized body and approach to tendering and contracting. This is the most problematic in locations where the fleet ownership and maintenance are privately owned (e.g., the UK and The Netherlands). In these locations, strong coordination and harmonization is needed among the tenders to avoid a heterogeneous charging infrastructure throughout the city that can cause problems for both future bus operating companies and the operation of the electric network. [191] The city of Munich, for example, tendered the charging infrastructure and the buses separately. An interesting example is from Hamburg where the electric network provider is a partner in managing the transport network, to better integrate the electricity demand in the city demand and share the operational expertise. [190], [191].
These sorts of models are the most important for the integration of RES and storage in the future transport grids as not all stakeholders can handle alone the technical expertise and financial costs of running such complex systems [14], [190]. The local authority should take over or at least delegate the division of roles and be more involved in the (faster) licensing and permit processes. It is also important as the lifetime of the charging infrastructure (15+ years) does not match that of the typical bus operating tenders (4-10 years) or that of the batteries (6-8 years). This leaves a lot of uncertainties and risks for the involved parties while preparing tenders [190], [191].
The other problem is the legal barrier for trolleygrid operators to sell their (subsidized) energy to third parties. This creates a major hurdle for the integration of EV chargers for private car charging. While the solution is as simple as a net metering of the demand of the trolleygrid, the contractual limitation needs to be addressed in future tenders before EV chargers can be implemented. An example to highlight is the trolleygrid of Arnhem, The Netherlands, where EV chargers are used to charge the battery mini-buses of the transportation company itself [16], [67].

2.7.3. THE IMPRACTICALITY OF PILOT PROJECTS

Finally, it is worth acknowledging the difficulty of implementing pilot projects on a public transportation service as that could severely disrupt operations, especially when the DSO/TSO is not involved. This is again why the Hamburg model, where the electric network provider is included in the process, is interesting.
In the face of limited pilots, bus operators and stakeholders should be urged and incentivized to intensify their cooperation with researchers and academic institutions who have the skills to conduct in-depth and accurate theoretical studies.

2.7.4. CONCLUSIONS ON THE NON-TECHNICAL CHALLENGES

In conclusion, the sustainable, multi-functional urban bus grid of the future faces many technical and non-technical problems. The feasible vision of this grid is a catenary grid running IMC trolleybuses, with integrated PV, EV chargers, and stationary storage systems. Their operation should involve an array of partners from key operational stake-

holders to the DSO/TSO and research/academic institutions to share both the operational expertise as well as the financial loads while being guided and connected via a coordinating body. Transport system stakeholders are urged to open up to the possibilities of an active, multi-functional smart transport grid that can act as a backbone to the city grid, and reduce all legal and financial hurdles facing it.

2.8. CONCLUSIONS

In conclusion, the next generation of trolleygrids is a feasible vision for a sustainable and multi-functional infrastructure with integrated renewables, storage, EV chargers, and IMC bus fleets that come from new electrification projects. However, serious research gaps need to be addressed.

In the modeling techniques, the lumped-sum energy approach must be abandoned and researchers must take into account the sensitivity of trolleygrids to voltage dips and power surges by accurately considering the braking energy, heating/cooling demand, feeder cables, bilateral connections, parallel lines, and the nominal substation voltages.

In the field of renewables, there is a severe, proven mismatch between generation and load that should be addressed. Researchers should focus on synergetic methods of creating base loads; for example, EV chargers or connections to nearby residential loads. Research is also needed in finding the urban space for PV integration, especially as the upcoming IMC fleets predict much higher energy demands.

Energy storage systems must meet safety, weight, size, self-discharge, and efficiency criteria on top of high cycling endurance to be implemented in trolleygrids. This leaves the few options of supercapacitors, Li-ion technologies (preferably LTO), and flywheels. There is a lack of comparison of storage placement methods in trolleygrids, as no consensus exists yet on this matter. This should also be investigated for trolleygrids with PV and/or EV chargers and/or IMC buses. Research on storage should then move away from the recuperation of braking energy and focus on preparing the trolleygrid for the vision of the next generation of trolleygrids.

EV chargers and IMC buses both face the same conservative approach of being undersized to fit into the existing grids with their congestion issues. On the contrary, research should focus on methods of increasing this integration potential and quantifying their benefit on the sustainability of trolleygrids as they provide a larger load base.

Finally, the non-technical challenges of trolleygrids should also be addressed as the vision of the future grid is bottlenecked by a hesitation toward catenary systems and a lack of coordinating bodies among different stakeholders. The implementation of pilot projects is also difficult from a logistic and administrative point of view, and so research institutes need to partner with local grid operators to design and validate the projects of the next generation of trolleygrids.

This thesis aims to address these research gaps, at least at the technical level. For this, the first step is a suitable and reliable modeling methodology for the trolleybuses and the trolleygrid. This model is the subject of the next chapter.

3

A Comprehensive Model of Trolleybuses and Trolleygrids

"Straniero! Non tentar la fortuna!
Gli enigmi sono tre, la morte è una!"

In Questa Reggia - Act II, Turandot (Puccini)

```
Stranger!  Do not try your luck!
The riddles are three, death is one!
```

This chapter is based on [3]: I. Diab, A. Saffirio, G. R. Chandra Mouli, A. S. Tomar, and P. Bauer, "A Complete DC Trolleybus Grid Model with Bilateral Connections, Feeder Cables, and Bus Auxiliaries," IEEE Transactions on Intelligent Transportation Systems, vol. 23, no. 10, pp. 19 030–19 041, 2022

This chapter offers a comprehensive and verified model of DC trolleybus grids and examines the effect of the common modeling assumptions made in the literature by using simulations, as well as bus and substation measurements from the grid of Arnhem, the Netherlands.

Section 3.1 starts with an introduction and presents the contributions of this chapter. Section 3.2 offers a detailed description of trolleybuses and trolleygrids. This serves as a technical background to Section 3.3 which details how these grids are typically modeled in the literature and the common simplifying assumptions made in those models. In contrast, Section 3.4 presents the comprehensive model developed in this thesis which forms the basis of the analysis of all the upcoming chapters. This model is then compared to the simplified assumptions of the available literature in Section 3.5. Finally, Section 3.6 concludes this chapter.

3.1. INTRODUCTION

The modeling of transportation systems such as trolleygrids is complex on two levels. On the first level, the vehicles are in motion with traffic and with varying mass and temperature every time their doors open. This makes it difficult to estimate their velocity profile, as well as their traction and heating demands. On the other hand, as will be elaborated on in Section 3.2, the transport grid architecture is the complex result of a number of measures aimed at reducing the effect of faults, the equivalent impedance between the substations and the vehicles, and reducing voltage drops and transmission line losses. Consequently, many assumptions in the literature are made when analyzing these grids that aim to simplify the bus demand and/or the equivalent circuit of the grid. However, transport grids are moving toward including non-traction loads and renewables in their networks and larger and more sophisticated fleets such as IMC buses. This requires a detailed approach to modeling these networks, as is presented in this chapter.

CHAPTER CONTRIBUTIONS

This chapter offers the following contributions:

1. A complete and experimentally verified trolleybus grid model that includes typically overlooked system elements and can be used for unilateral and bilateral substations.

2. A new modeling method for bilaterally connected substations as an equivalent stationary, regenerating bus

3. An equivalent-impedance model for the overhead lines taking into account the line impedance and parallel connections between the lines

4. A quantification of the effect of the non-traction components of the bus power profile (regenerative braking and auxiliaries) and of the trolleygrid architecture

(feeder cables and presence of bilateral connections) on the trolleygrid energy demand using measured and simulated bus traction, heating, and velocity profiles

3.2. RECAP: THE COMPONENTS AND CHARACTERISTICS OF TROLLEYGRIDS

Figure 1.2 shows the typical layout of a part of a trolleygrid. For reasons such as faults and transmission losses, the trolleybus lines are divided into isolated sections of a few hundred meters, up to 1 or 2 km, depending on the trolleygrid city. The power comes from the Low Voltage AC grid LVAC, and a transformer steps down the voltage, then a rectifier converts into DC, as the buses run at a nominal voltage of 600-700V. The transformer-rectifier system is housed in a "substation." One substation can feed one or more sections, to which it is connected via the section feeder cables (FC). For example, in Figure 1.2, substation 1 feeds two sections, while substation 2 feeds one.

The substations are unidirectional because of the rectifier. Consequently, a braking bus cannot send its energy back to the LVAC grid but only to other buses on the same section or on a connected section. The first possibility for two sections to be connected is when they are supplied by the same substation: Bus 1 of Figure 1.2, for example, can supply Bus 2 via the route FC1-substation busbar-FC2. The second possibility is when the sections are bilaterally connected. A bilateral connection is a controllable connection between two sections that are under different substations. The connection can be controlled as closed (connected) or open (isolated). Bus 2 can send power through the overhead lines to bus 3 as if sections 2 and 3 are one long section. Bus 1 can also share power with bus 3 via the route FC1-busbar-FC2-bilateral.
Finally, it is noticeable that each bus is connected to two lines in Figure 1.2. In trolleygrids, an overhead return path for the current is also needed as the bus runs on wheels, unlike the tram, which uses the rails as a return.

This thesis defines the "supply zone" as the electrically connected zone in which a bus can send and receive power. Thanks to the bilateral connection, all the elements shown in Figure 1.2 are part of one supply zone.
The bus is supplied with the power to feed its traction and non-traction demands (Figure 3.1). When a bus is braking, in the absence of a receiving bus on the same supply zone or if the braking energy is excessive, the excess braking energy is wasted on-board in the braking resistors. The amount of energy wasted is controlled by a chopper circuit that controls the on-time of the resistors to keep the grid voltage below the allowable upper limit (around 780V, depending on the city). At values of around 720-740V, also depending on the trolleygrid, the braking resistor is fully engaged to prevent any over-voltages (see Figure 3.2).

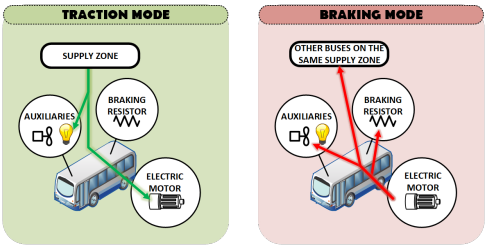

Figure 3.1: The bus power flow: In traction mode, the power from the supply zone (substation(s) and/or regenerating bus(es)) feeds the motor and auxiliaries. In braking mode, the power is used to supply the auxiliaries and any other bus on the same supply zone. Excess energy is wasted in the braking resistor.

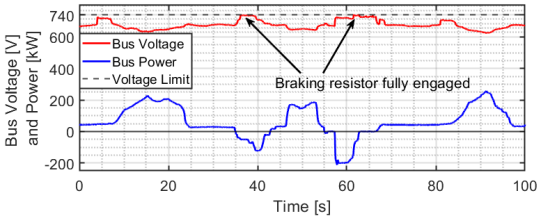

Figure 3.2: Bus voltage and power measurements from the trolleygrid in Arnhem, the Netherlands. The braking resistor is fully engaged when the generating bus voltage rises to the upper voltage limit of the grid (740V in Arnhem).

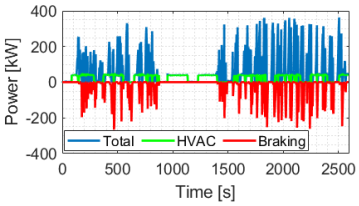

Figure 3.3: Total, HVAC, and braking bus power measurements for an exemplary drive on trolleybus line 1 in Arnhem, the Netherlands on 22 January 2019.

The impedance of the overhead cables causes the bus to see a voltage drop from the nominal voltage and increases the temperature of the cable by resistive losses. This is not desired as the buses start curtailing their power demand at values below 500V, and the overheating of the cables could permanently damage the material. To reduce the impedance between the bus and the substation on the section, an element found commonly in transport networks is the parallel connection between the overhead lines of the different bus lines available in a section, i.e., the going and the returning traffic lines. Within the same section, the feed (positive) and the return (negative) lines are connected in pairs to offer a lower impedance path from the substation (or a braking bus) to the buses. These lines are introduced periodically at a distance in the order of hundreds of meters (100-300m). This chapter looks at Arnhem, the Netherlands, as a case study. In Arnhem, for example, these parallel lines are currently being changed from a frequency of 150m to one of 100m.

3.3. MODELING OF TROLLEYGRIDS IN THE LITERATURE

Modeling transportation networks has been a powerful tool in designing, analyzing, and optimizing electrical transit grids. Academic and Commercial simulators, such as [5]–[7], [9], [10], [17], [21], [36], [37], [41], [42], [48]–[58], [60], [62]–[64], use different solver methods and modeling techniques to investigate these networks. Generally, these simulators are used to calculate substation-level parameters such as the substation power demand and the substation component design ratings. Some look more in-depth into variables such as the voltage drops over the transmission lines for the introduction of larger buses on the lines, for example, or the available braking energy for recuperation by storage devices.
Unfortunately, these models are limited in modeling the busload and the grid elements. Transport grid studies such as the ones in [17], [21], [36], [48], [50], [54], [55] tend to limit themselves to a single section with an ideal trapezoidal profile.
A trapezoidal velocity profile assumes a constant acceleration phase from the bus stop, followed by a constant-velocity cruising at 50 km/hr, and then a deceleration toward the next bus stop. As Figure 2.1 showed earlier, this is not a fair representation of the actual velocity profile of the trolleybuses. The traffic conditions directly affect the bus power profile and total energy consumption by causing multiple accelerations (power peak) and decelerations (partial or complete waste of traction power).

While some research uses a more sophisticated bus traction power model [7], [49], [51], [64], they still neglect the seasonal variation of the bus demand brought by the auxiliaries, namely the HVAC (heating, ventilation, and air conditioning) such is the case in [17], [21], [36], [48], [50], [51], [54], [55], [60], [64]. During winter conditions, this demand can be as high as the traction load at about 1-1.5 kWh/km each.
Figure 3.3 shows an example of bus measurements to validate this claim. Here, the total HVAC demand of 17.95 kWh accounts for half of the bus total demand of 36.11 kWh during the 11.60 km trip. This share of the total power consumption is in accordance with those previously reported in literature [4], [192].
Ignoring this HVAC power would have two consequences. First, it would remove a con-

siderable portion of the substation load, making substation calculation inaccurate. Second, it removes a receiver of the bus regenerative braking (see Figure 3.1), which would result in inaccurate calculations of the shared energy between buses and of the energy wasted in the on-board braking resistors. This underestimates the substation demand brought by expectations of lower load demands from higher power sharing between buses.

The regenerative braking can also feed other buses that are under the same supply zone, relieving the two bilaterally connected substations from a fraction of the bus load. Measurements made on the trolleybuses in Arnhem (Figure 3.3) have shown that around 30% of the bus load is available for recuperation (12.00 of the 36.11kWh). This value is in line with what is reported in other trolley cities [9], [17], [42], [66]. Without a bilateral connection correctly modeled, this available energy would be assumed to be wasted in the on-board braking resistors, causing an overestimation of the substation energy demand. Finally, the feeder cables can affect the regenerative braking and the bilateral connection by contributing to a sizeable voltage drop on the section, altering the supplied power share by the substations and the braking buses. This can happen when the voltage of one node, for example, becomes too low relative to the other supplying nodes and is unable to push power into the circuit.

Other than the simplistic bus models, the trolleygrid itself is frequently modeled with some major assumptions. For example, some works consider the parallel lines ([57], [60], [62]) while others, such as [21], [63], ignore them. Feeder cables are also ignored, except in a few works ([5], [52], [57]).

The need for a complete bus power representation and trolleygrid model is more pressing nowadays. This is because DC trolleygrids are ushering in a new era of active, urban transportation grids as they look at integrating solar PV [36], [50], on-board and/or off-board storage [6], [7], [21], [37], electric-vehicle (EV) chargers [36], [67], [68], and In-Motion-Charging (IMC) buses [2], [69] into their network. To highlight an example of the future grid, IMC buses are the new generation of trolleys that combine the advantage of a catenary operation with the flexibility of an electric battery bus. The IMC bus is equipped with a battery that is charged while the bus is under the catenary (the charging corridor) and discharged later when the trolleybus is driving in areas outside the trolleygrid. The main urban advantages of such a system can be, for example, in operating these buses in historic city centers without the visual intrusion of lines or in operating over new lines without the need for building new infrastructure. With a battery charging at the order of hundreds of kWs, these buses constitute a challenge in the expansion of the trolleygrid. A detailed model for the power consumption and the voltage drop at the substation level is needed to ensure that the introduction of IMC does not violate the operational limits. As sections III-E and III-F show, the simplified grid models found in the literature can lead to incorrect results in calculating the minimum voltage and load demand on a substation.

It is then particularly important for this subgroup of transportation grids to study in detail the line voltage, current ratings, and the in-line transmission losses of their subsystems using specific, representative models.

In particular, seven parameters that are often ignored and/or approximated in these models are:

- The inductive component of the overhead line impedance,
- The parallel lines connecting the overhead lines,
- The bus auxiliaries power (predominately the HVAC),
- The bus regenerative braking,
- The section feeder cables,
- The bilateral connections between sections,
- The nominal voltage of the substation

In brief, the study of the future trolleygrid requires more specific models with proper representation of the bus load and grid elements. While many works in the literature include some of these elements, to the knowledge of the authors, no work has included all of them, as presented in this chapter. The effects and errors from excluding these elements are also studied in this work and summarized in Table 3.1.

Table 3.1: Summary of the comparison between common assumptions in literature and the trolleybus model in this thesis.

Trolleygrid Parameter	Typical Modeling Assumptions Made in Literature	Effect of Assumption (case study analysis in this chapter)	Detailed Explanation
Overhead Line Impedance	Assumed purely resistive, expect in works such as [37] where it is taken as resistive-inductive	Can indeed be considered purely resistive for steady-state models	section 3.5.1
Overhead Parallel Lines	Ignored in works such as [21], [63], included in works such as [57], [60], [62]	If ignored, the line impedance could be as much as double its actual value (100% error)	section 3.5.2
Bus Auxiliaries Power	Ignored in works such as [17], [21], [36], [48], [50], [51], [54], [55], [60], [64], included in works such as [41], [42]	If ignored, errors up to 55% in substation energy calculations	section 3.5.3
Bus Regenerative Braking	Ideally, implied that it is modeled but it is not correct to include it while simultaneously ignoring the auxiliaries demand such as in [17], [21], [36], [48], [50], [51], [54], [55], [60], [64]	If ignored, errors as high as 34% in the substation power calculations	section 3.5.4
Section Feeder Cable	Only mentioned in works such as [5], [52], [57]	If ignored, errors are expected in extreme cases above 15% in the substation power calculations and 50V for the minimum line voltage. However, equations 3.19 and 3.20 offer an easy way to estimate where these cables can still be ignored	section 3.5.5
Bilateral Connections	Only mentioned in works such as [56], [62], [70]	If ignored, errors up to 25% in the substation power calculations	section 3.5.6
Substation Nominal Voltage	Typically assumed at a rounded-up nominal value of 650 or 700V such as in [21], [70], [71]	Particularly important for bilaterally connected substations because of the effect on the load-sharing ratio between them	section 3.5.7

3.4. THE TROLLEYGRID AND TROLLEYBUS MODEL

This section offers the analytical equations and logic flowcharts for the trolleybus and trolleygrid models developed for this thesis and which constitute the basis of the analysis of all the upcoming chapters. The general flowchart is offered in Figure 3.4.

3.4.1. THE BUS POWER MODEL

TROLLEYBUS TOTAL POWER

The trolleygrid model begins with the creation of bus demand from measured velocity and power cycles and randomized traffic and stoplight probability data.
The bus powers are given by Eq.3.1. During braking, the bus power, P_{bus}, is the auxiliaries power P_{aux} plus the net exchanged with the grid P_{net} (by iteration), and the excess power P_{BR} that is wasted in the braking resistors (see Figure 3.5 and Eq.3.1). While in traction mode, the bus power is simply the traction P_{tr} and the auxiliaries demand, P_{aux}.

$$P_{\text{bus},j} = \begin{cases} P_{\text{net},j} + P_{\text{aux},j} + P_{\text{BR},j} & \text{if braking} \\ P_{\text{tr},j} + P_{\text{aux},j} & \text{if traction} \end{cases} \quad j = 1..N_{\text{bus}} \tag{3.1}$$

TROLLEYBUS HVAC POWER MODEL

The auxiliaries are -predominately- the HVAC load plus other base loads such as the on-board lights, screens, door motors, the control systems, etc.:

$$P_{\text{aux}} = P_{\text{HVAC}} + P_{\text{base}} \tag{3.2}$$

The HVAC requirement is calculated by a thermodynamic heat exchange model between the trolleybus and the surrounding environment and is a function of:

- Q_c: Conductive and convective heat transfer load
  The heat exchange through the vehicle body due to the difference in temperature between the cabin and the external environment.
- Q_v: Ventilation heat
  The heat exchange due to the forced air ventilation and air circulation (air quality requirement). This heat component is determined by the inside-outside temperature difference and humidity difference.
- Q_d: Door-opening air ventilation
  The air ventilation due to the opening of the doors for passenger transit. This heat component is determined by the inside-outside temperature difference and humidity difference.
- Q_s: Solar heat load
  The solar heat gain due to direct, diffuse, and reflected radiation.
- Q_m: Metabolic heat load
  The metabolic heat gain from the passenger bodies. This heat component depends on the number of passengers, and on the characteristics of the passengers,

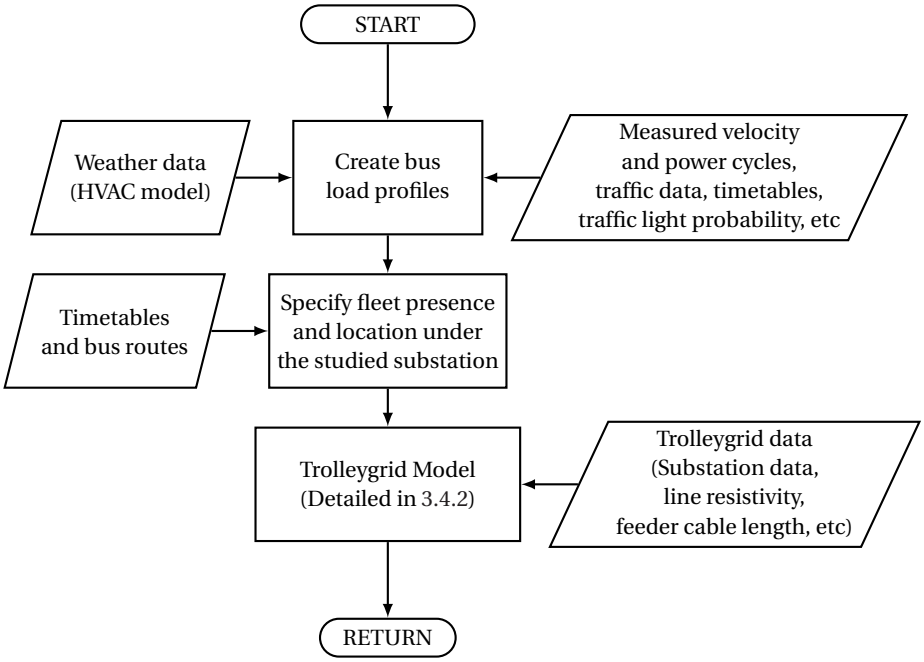

Figure 3.4: Flowchart of the trolleygrid model logic.

and their standing/seating status. The number of passengers was assumed to be constant in the Arnhem simulations, but the model can be extended with passenger traffic estimations (e.g., [193], [194]).

For the Arnhem bus types, the HVAC system is controlled with a duty cycle (t_{cycle}) of 300 seconds, or 5 minutes. The on-time, t_{on}, of the HVAC system for each period is dictated by the average HVAC power requirement of the bus during that cycle:

$$t_{on} = t_{cycle} \frac{\overline{P_{HVAC}}}{P_{rated}} \tag{3.3}$$

where $\overline{P_{HVAC}}$ is the average power requirement in the 5 minutes, and P_{rated} is the nominal HVAC power, namely 36.5 kW for the Arnhem system. Finally, P_{base} is taken as 5 kW. Once the bus power is computed, the location of the bus is obtained from the local timetables and bus routes. The load demands and the positions of the buses are input to the grid model.

3.4.2. THE TROLLEYGRID MODEL LOGIC

The grid model is based on the backward-forward sweep method [195]. A flowchart of the full model is presented in Figure 3.5. The substation is taken as a slack node (SN), with a fixed nominal voltage at the rectifier output (i.e., before the feeder cable voltage drop) that delivers the total power demand on the supply zone (bus loads minus the regenerating bus exchanges).

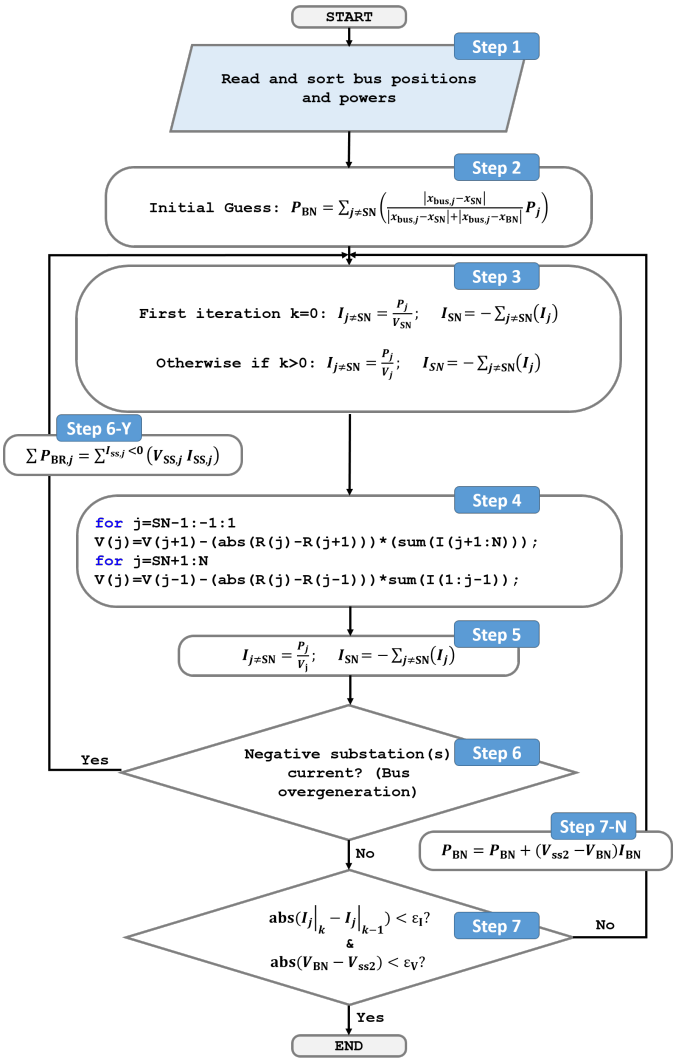

Figure 3.5: Flowchart of the grid model logic for node voltage and branch current calculations.

However, when two sections are connected bilaterally, there are two slack nodes, adding complexity to the model in estimating the power delivered by each substation (the load share of each substation). If there is one bus on the supply zone, and the two substations are at the same nominal voltage, then the power share ratio of each substation is trivially the ratio of the impedances between each substation and the bus. However, this is generally not the case, as there are multiple buses on the section, and the two substations have different nominal voltages. The solution requires then an iterative process. An original method suggested in this chapter (steps 2, 7, and 7-N in Figure 3.5) allows the same unilateral model to be extended for this bilateral case by modeling the second

substation (the bilateral node, BN) as a trolleybus in regenerative braking mode with a variable power, P_{BN}. At each iteration, the power of this virtual bus node is updated until its voltage V_{BN} converges to the known voltage of the bilateral substation, V_{ss2}.
The algorithm is described in Figure 3.5 and proceeds as follows:

- *Step 1*: The model starts by reading and sorting the positions and powers of all the nodes on the supply zone
- *Step 2*: An initial guess is then made for P_{BN} by an impedance-weighted sum of the bus nodes on the supply zone
- *Step 3*: At the first iteration step, the voltage at each node is assumed to be the voltage of the SN, and therefore the current at each node is the power of the node divided by V_{BN}. At later iterations, with a voltage assigned to each node (from step 4 of the previous iteration), the current is obtained by dividing the power of each node by its voltage
- *Step 4*: The model starts from SN and sweeps across all nodes. Each node voltage is the voltage of its adjacent node minus the resistive voltage drop between them (see also Eq.3.4)
- *Step 5*: The algorithm sweeps back across all the nodes and updates their currents. The slack node is then set to deliver the sum of all the node currents
- *Step 6*: As the model is concerned with non-reversible substations, I_{SN} in step 5 is checked if negative (oversharing of braking energy)
- *Step 6-Y*: If I_{SN} is negative, step 6-Y reduces the power of the generating buses by the amount that is being sent into the substation. In practical terms, this means the buses are wasting this energy on their on-board braking resistors
- *Step 7*: If I_{SN} is not negative, the model checks for convergence and exits if it is achieved. A tolerance is defined for the current at each node (here, 0.2A) and for the voltage of the BN (here, 0.5V)
- *Step 7-N*: If the voltage of the virtual bus at BN is found to be below (or above) V_{ss2}, this means that P_{BN} is lower (or higher, respectively) than it should be, and it is updated

The total impedance between two nodes n and n-1, $R_{n,n-1}$, is obtained from the equivalent impedance model considering the impedance of the supply and return lines and the effect of the parallel connections between them, as explained in the section III-A and III-B.

$$R_{n,n-1} = \rho \cdot |x_n - x_{n-1}| \tag{3.4}$$

$$V_{\mathrm{c},n} = \begin{cases} V_{\mathrm{s},n} - R_{\mathrm{f},n} \cdot i_{\mathrm{s},n} & i_{\mathrm{s},n} > 0 \\ V_{\mathrm{s},n} + V_{\mathrm{ds},n} & i_{\mathrm{s},n} = 0 \quad n = \mathrm{SN,\ BN} \end{cases} \tag{3.5}$$

It is important to note that the voltage at the connection point of each substation to the section, V_{c}, is given by Eq.3.5. If the substation is supplying power, this voltage is equal to

the substation voltage, V_s, minus the voltage drop across the feeder cable resistance R_f. If the substation is not supplying power, the voltage is equal to the substation nominal voltage plus any voltage blocked by the rectifier diodes, V_{ds}.

3.4.3. MODEL VERIFICATION

The model is peer-reviewed and was verified by comparing it to the substation measurements (2019) that were generously provided by the trolleygrid operator under a confidentiality agreement. The error, calculated by Eq.3.6, was below 4%. This equation is used to calculate the percentage errors throughout this chapter.

$$\text{Error} = \frac{\text{Value} - \text{Simulated/Estimated Value}}{\text{Value}} \cdot 100[\%] \tag{3.6}$$

3.5. COMPARISON OF THE MODEL TO OTHER MODELS IN THE LITERATURE

As explained earlier, trolleygrid models in the available literature make one or more of seven key assumptions. This section, in the seven following subsections, looks at the effect of each of these simplifying assumptions on the trolley model output by comparing the results of simulations made with and without them.

3.5.1. THE OVERHEAD LINES IMPEDANCE

This subsection looks into the error caused by ignoring the inductive component of the overhead line impedance.

The impedance of the overhead lines that provide power to the trolleybuses is largely modeled as purely resistive. Few papers look into a resistive-inductive line, especially when matters of system stability or control are studied as the capacitance of the added converters forces a study of the dynamic conditions [37].

The voltage drop across the overhead feeding (or return) line, ΔV_{fd}, is due to its resistance and inductance. As the bus is in motion, the drop across one line (feeding or return) can be written as:

$$\Delta V_{fd} = \frac{d(Li)}{dt} + Ri \tag{3.7}$$

$$= \lambda x_{bus} \frac{di}{dt} + \frac{d(\lambda x_{bus})}{dt} i + \rho x_{bus} i \tag{3.8}$$

$$= \lambda x_{bus} \frac{di}{dt} + v_{bus} \lambda i + \rho x_{bus} i \tag{3.9}$$

Where λ is the inductance per meter (H/m) of the transmission lines (order of 10^{-7} [196]), x_{bus} is the bus distance from the substation in m, v_{bus} is the bus velocity in m/s, ρ is the resistance per m (Ω/m) of the transmission lines (order of 10^{-4}), and i is the current drawn by the bus.

The measured bus current and its derivative in Arnhem (Figure 3.6) shows that they are

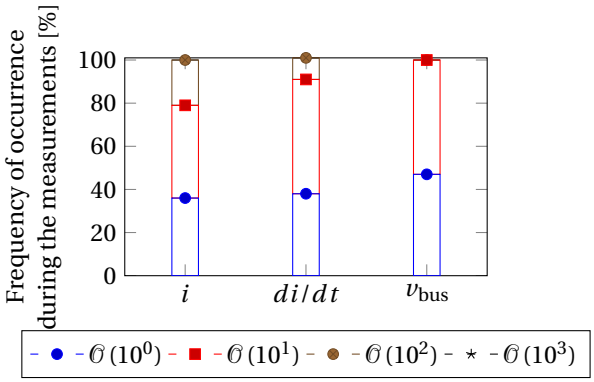

Figure 3.6: Analysis of the trolleybus measurement data across the different Arnhem bus lines for the estimation in Eq.3.10. The order of magnitude of the current i and its derivative di/dt is consistently at or below $\mathcal{O}(10^2)$. The bus velocity, v_{bus},is always at or below $\mathcal{O}(10^1)$.

consistently at the order of 10^2 or below. The measurements also show that the bus velocity, v_{bus}, is always at or below values of the order of $\mathcal{O}(10^1)$.
Consequently,

$$\begin{aligned}\mathcal{O}(\Delta V_{\text{fd}}) = \mathcal{O}(10^{-7})\cdot\mathcal{O}(10^3)\cdot\mathcal{O}(10^2)\\ +\mathcal{O}(10^1)\cdot\mathcal{O}(10^{-7})\cdot\mathcal{O}(10^2)\\ +\mathcal{O}(10^{-4})\cdot\mathcal{O}(10^3)\cdot\mathcal{O}(10^2)\\ =\mathcal{O}(10^{-2})+\mathcal{O}(10^{-4})+\mathcal{O}(10^1)\end{aligned} \tag{3.10}$$

As the bus voltage itself is at the order of $\mathcal{O}(10^2)$, Eq.3.10 shows that the assumption of neglecting the line inductance (first two terms of Eq.3.9) is a valid one for the calculation of the voltage drop across the overhead line. In other terms:

$$\therefore \Delta V_{\text{fd}} \approx Ri \quad \text{(feed or return line)} \tag{3.11}$$

The conclusion is to model the line impedance as resistive in a steady-state model, offering the possibility of a simpler simulator without any significant error in the output. An inductance component is, however, needed in any dynamic model that looks, for example, at the stability of the grid after the addition of the PV and/or EV chargers and/or storage especially as the added converters will introduce a significant capacitance to be seen by the substation and the line inductance.

3.5.2. THE OVERHEAD PARALLEL LINES

This section looks into the error caused by different approximation methods of the overhead line total impedance.
The parallel lines, as introduced earlier, contribute to a lower equivalent impedance in the circuit.

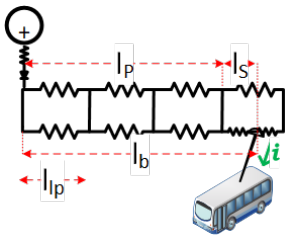

Figure 3.7: Circuit representation and nomenclature of the parallel lines connection between (here shown) two feed/positive overhead lines. For simplicity, the return overhead lines (also paralleled) are omitted from the figure.

The total voltage drop between the substation and the bus can be given by the expression:

$$\Delta V_{tr} = 2 \cdot (\frac{\rho}{2} l_p + \rho l_s (1 - \frac{l_s}{2 l_{lp}})) i \tag{3.12}$$

Where the term '2' accounts for lumping the feeder and the return lines, and Figure 3.7 shows the other key parameters. The parallel lines are separated (on average) by a distance of l_{lp}. The bus distance from the substation, l_b, is composed of a fully paralleled distance, l_p, that is the highest integer multiple of l_{lp} lower than or equal to l_b, and a single distance l_s.
This equation requires precise knowledge of the position of the parallel line, and the distance in between them. This information is not readily available as the ultimate position of the parallel lines is subject to changes between the design stage and the actual implementation by the contractors. The voltage drop can either be approximated by ignoring the current path division in the last single section, and assuming that all the current passes through the shortest path to the bus after l_p, the highest integer multiple of the parallel lines (Approximation 1):

$$\Delta V_{tr} = 2 \cdot (\frac{\rho}{2} l_p + \rho l_s) i \tag{3.13}$$

or by lumping the total resistance, R, as an equivalent parallel resistance of R/2 (Approximation 2):

$$\Delta V_{tr} = 2 \cdot (\frac{\rho}{2} l_b) i \tag{3.14}$$

Figure 5.11 shows the total voltage drop between the substation (700V nominal, 100 mm^2 Cu lines) and the bus as a function of the bus power and distance. The current is obtained iteratively from the bus power by:

$$i = \frac{P_{bus}}{V_{bus}} = \frac{P_{bus}}{V_s - \Delta V_{tr}} \tag{3.15}$$

As expected, Approximation 1 overestimates the voltage drops (up to 40V) while Approximation 2 underestimates them (within 10V). However, the former introduces more serious errors, especially when the bus is getting close to the end of a parallel connection. This is because as the bus comes closer to the parallel connection, Approximation 1

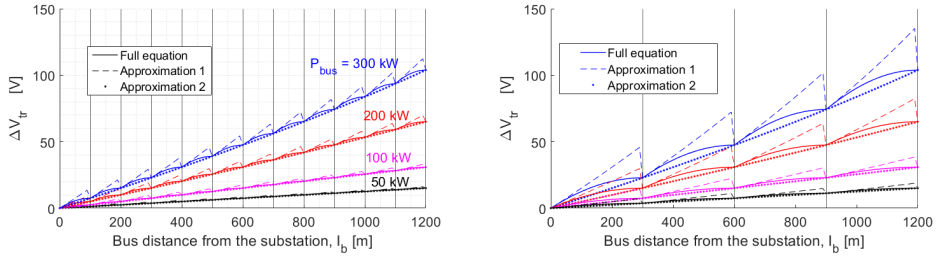

((a)) Parallel lines at 100m distance.

((b)) Parallel lines at 300m distance.

Figure 3.8: The voltage drop between the substation and the bus as a function of the bus power (P_{bus}) and distance from the substation (l_{b}) The parallel lines in (a) are at every 100m and in (b) at 300m, and shown with vertical lines. Approximation 1 always overestimates the voltage drop (up to 40V), while Approximation 2 always underestimates it (but errors under 10V).

counts it as a full impedance, while it is in reality nearing an equivalent half-impedance. Approximation 2 is also an attractive solution as it does not require knowledge of the location of the parallel connections or the spacing between them.

3.5.3. THE BUS AUXILIARIES POWER

This section looks into the error caused by ignoring the HVAC power demand of the trolleybuses.

Recent measurements in Arnhem have revealed that the bus auxiliaries demand, mainly the HVAC, is as significant as its traction load demand [4]. This order of magnitude is in line with previous values reported in literature [192].

This motivates the inclusion of HVAC in the study of a trolleygrid, as is done in [41], [42]. It is worth noting, however, that the different climate conditions and thermal comfort standards between trolley cities require a location-specific HVAC load to be simulated, rather than the addition of a constant load.

Figure 3.9 shows the Arnhem total supplied energy measurements at the substations for the January and May months of 2016 till 2019.

January and May run the same schedule in Arnhem but differ only in the ambient temperature (2-4 degrees and 13-18 degrees Celsius, respectively). This translates into a heavy HVAC heating demand in January, while the May weather does not trigger as much heating or air conditioning.

The measurements show that while the HVAC is expected to effectively double the demand of the substation, the actual substation load increases only by about 55%. This reflects the effective use of regenerative braking and the importance of modeling these two components together for an accurate model of the trolleygrid.

3.5.4. THE BUS REGENERATIVE BRAKING

This section looks into the error caused by ignoring the regenerative power of trolleybuses. For the remaining case studies, six exemplary days (Table 3.2) are chosen to highlight the key operating modes of the Arnhem trolleygrid. The days were chosen to also represent different HVAC demands throughout the year.

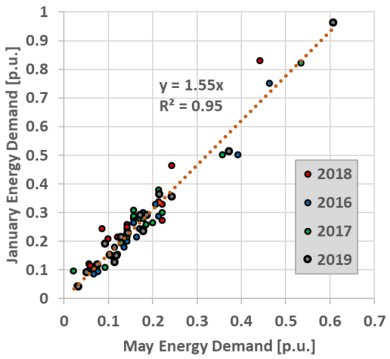

Figure 3.9: Per-unit measurements of the January and May energy demand for the Arnhem substations over 4 years (normalized for data sensitivity concerns).

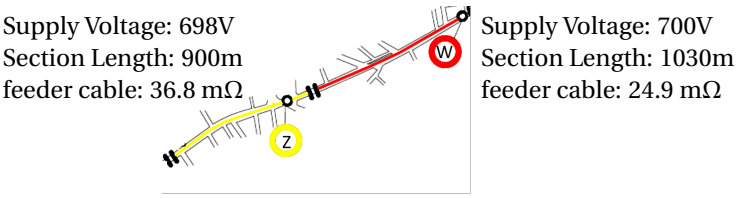

Figure 3.10: Regenerative braking: Layout of the investigated sections Z and W in Arnhem and their parameters.

The bilaterally connected sections Z and W in Arnhem (Figure 3.10) are simulated with and without regenerative braking by removing the negative power from the created bus load (before adding the HVAC). The results are summarized in Table 3.3. Errors as high as 34.4% can be expected in the power calculations in high traffic/high HVAC scenarios (Days 1 and 268) between the actual scenario (with) and the assumption (without) as per Eq.3.6. This is expected as the regenerative braking on those days is efficiently recuperated by the HVAC and neighboring buses, while it is, in this new case, being supplied by the substations. In low-traffic scenarios (Day 200), the error is still above 5%.

3.5.5. THE SECTION FEEDER CABLES

This section looks into the error caused by ignoring the section feeder cable. First, a case study is presented, then a method to approximate when the feeder cable can indeed be ignored without significant errors.

THE FEEDER CABLE CASE STUDY

As explained earlier, the section feeder cables connect the substations to the sections they supply. These lines are thicker than the overhead lines on the sections as they need to carry the current to multiple sections. The consequence of this is that the feeder cables

Table 3.2: Characteristics of the six days of the year (out of 365) chosen for the grid case study in this chapter representing different traffic and auxiliaries conditions in the Arnhem trolleygrid.

Day	Schedule Category	Traffic	Auxiliaries (HVAC)
1	School holiday week	High	High (winter)
117	Sunday & special holiday	Low	Low (spring)
197	Summer weekday	Low	Medium (summer)
200	Summer Saturday	Low	Medium (summer)
268	Regular weekday	High	High (winter)
305	Regular Saturday	Low	High (winter)

Table 3.3: Daily energy demand for sections Z and W of Arnhem when simulated with and without (w/o) considering regenerative braking.

	Substation Z [kWh]			Substation W [kWh]		
Day	with	w/o	Error%	with	w/o	Error
1	270	298	10.4 %	262	352	34.4 %
117	130	138	6.2 %	122	138	13.1 %
197	272	286	5.1 %	171	181	5.8 %
200	241	254	5.4 %	163	172	5.5 %
268	328	357	8.8 %	290	340	17.2 %
305	321	347	8.1 %	255	283	11.0 %

have lower resistance than that of the overhead line and tend to be ignored in trolleybus simulations. Parallel line connections, however, effectively halve the impedance of the overhead lines, making the feeder cables a modeling necessity, especially when they are long. In Arnhem, for example, some feeder cables go beyond 1 kilometer in length. In dense urban environments, it is expected that feeder cables can be of such lengths as there is no space in city centers for bulky rectifier stations. To highlight the effect of including the feeder cables, a feasibility study is performed on a substation in Arnhem on the introduction of 100kW In-Motion-Charging (IMC) buses. The IMC battery is modeled by adding 100 kW to the bus load before running the grid model, i.e., in the "Create Bus Load Profile" step in the flowchart of Figure 3.4. This method assumes that the IMC battery is never at the maximum battery SOC while under the section, and therefore is always charging. The studied section has the following parameters: substation nominal voltage of 698V, 630 mm^2 Cu feeder cables of 1000 meters. Table 3.4 summarizes the results of the study. Ignoring the feeder cable gives the green light to the introduction of IMC buses with a minimum line voltage well above the 400V operational limit of the buses. On the other hand, including the feeder cable shows the voltage dipping below

Table 3.4: Example of a study resulting in false results by ignoring the feeder cable on a sample section in Arnhem during a Summer Saturday schedule (Day 200).

Minimum line voltage during the day			
Present case: No IMC operation		**Study: With 100kW IMC buses**	
Feeder Cable	Ignore Feeder	Feeder Cable	Ignore Feeder
520V	569V	**396V** (Not ok)	514V (ok)

the minimum grid operational threshold, which would cause the bus to shut down, and disturb the daily operation.

ESTIMATING THE EXPECTED ERROR

The effect of the section feeder cable, however, is a function of its length and the power that it delivers. Short lines and/or low-traffic sections can still have their feeder cables ignored. The below set of equations offers an estimation of the error incurred. For a substation seeing a total energy demand ΣP_s, the total power demand can be approximated as:

$$P_{\text{s, tot}} = \alpha \Sigma P_{\text{s}} \tag{3.16}$$

Where the factor α accounts for the average losses on that section (e.g., for 6% transmission losses, α=1.06). The current supplied from the substation, I_{s}, can be written from Eq.3.16 in terms of the substation voltage V_{s} as:

$$I_{\text{s}} = \alpha \frac{\Sigma P_{\text{s}}}{V_{\text{s}}}, \tag{3.17}$$

allowing the losses in the feeder cable (of resistance R_{f}) to be calculated by:

$$P_{\text{loss, f}} = R_{\text{f}} (\alpha \frac{\Sigma P_{\text{s}}}{V_{\text{s}}})^2, \tag{3.18}$$

Finally, the portion of the power lost in the feeder cable to the total power in the section can be approximated from Eq.3.18 by:

$$\frac{P_{\text{loss, f}}}{\Sigma P_{\text{s}}} = R_{\text{f}} \alpha^2 \frac{\Sigma P_{\text{s}}}{V_{\text{s}}^2}, \tag{3.19}$$

Using 3.17, the voltage drop in the feeder cable can also be estimated by:

$$\Delta V_{\text{f}} = R_{\text{f}} \alpha \frac{\Sigma P_{\text{s}}}{V_{\text{s}}}. \tag{3.20}$$

To highlight the significance of these equations, figures 3.11(a) and 3.11(b) show the expected errors as a function of the substation feeder cable length and the power delivered. Typical values from the Arnhem grid are also shown in the figure. The error is defined between the actual case (with the feeder cable), and the assumption made not to model the feeder cable. Some substations would see less than 1% error in the power calculations and less than 5V in the voltage calculations if the section feeder cables are ignored.

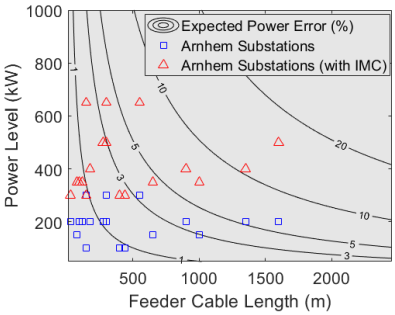

((a)) Error expected in the power calculation (Eq.3.19).

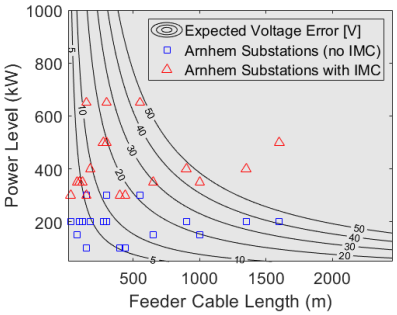

((b)) Error expected in the voltage calculation (Eq.3.20).

Figure 3.11: Error expected in the power (left) and voltage (right) calculations as a function of the feeder cable length and section power levels when the section feeder cable is ignored. Values of each Arnhem substation with and without IMC fleets are marked in blue and red, respectively.

However, some see more than 5% error and 30V in the power and voltage computations, respectively. This validates the idea that the feeder cable assumption can be made case-by-case.
Important to notice as well how IMC substations see greater errors. This shows again that while the current trolleygrids can sometimes be modeled with certain assumptions, the trolleygrid of the future requires more sophisticated models such as the one presented in this chapter.

3.5.6. THE BILATERAL CONNECTIONS

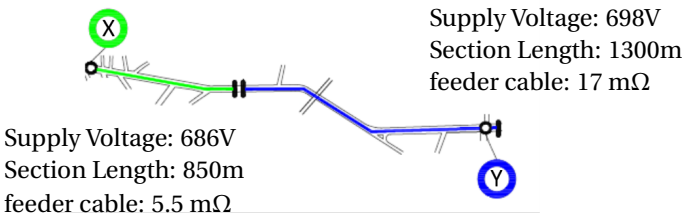

Figure 3.12: Bilateral Connection: Layout of the investigated sections X and Y in Arnhem and their parameters.

This section looks into the error caused by not considering bilateral connections in a trolleygrid.
A straightforward (and computationally light) option is to model two bilaterally connected sections as isolated, unilateral sections. Measurements and simulations [56], [62], however, indicate that this assumption would not be valid as there could be significant errors in the voltage and power levels.
As a case study, Figure 3.12 shows the two bilaterally connected sections X and Y in Arnhem. Tables 3.5 and 3.6 show the expected error in simulating X and Y as bilateral or

Table 3.5: Daily energy demand for substations X and Y in Arnhem when simulated with the assumption of being unilateral (Uni), and when correctly modeled as bilateral (Bi) substations.

	Substation X [kWh]			Substation Y [kWh]			Sum X & Y [kWh]		
Day	Uni	Bi	Error%	Uni	Bi	Error%	Uni	Bi	Error%
1	164	146	12%	347	359	-3.3%	511	505	1.2 %
117	71	64	11%	155	149	4.0%	226	213	6.1 %
197	95	86	11%	147	157	-6.4%	242	243	-0.4%
200	96	83	16%	141	151	-6.6%	237	235	0.9 %
268	195	156	25%	237	272	-13%	432	428	0.9 %
305	146	126	16%	228	244	-6.6%	374	369	1.4 %

Table 3.6: Minimum line voltage in a day for substations X and Y in Arnhem when simulated with the assumption of being unilateral (Uni), and when correctly modeled as bilateral (Bi) substations.

	Substation X (686V)			Substation Y (698V)		
Day	Uni [V]	Bi [V]	Error [V]	Uni [V]	Bi [V]	Error [V]
1	627	646	19	607	646	39
117	645	642	-3	599	642	43
197	627	648	21	598	648	50
200	627	648	21	569	648	79
268	652	642	-10	603	642	39
305	617	622	5	490	622	132

unilateral sections. While the errors in the sum of the loading of the two sections are mostly insignificant, the individual loading of each substation sees errors as high as 25%. Under-loading of the station (as far as -13%) is also reported. Additionally, the voltage drops can be over 100V. The bilaterally connected sections do not see a voltage below 622V, while the unilateral sections sometimes dip into the range of 500 and 400V. This could lead to large errors in the design and control of, for example, EV chargers and storage control algorithms on a particular section.

3.5.7. THE SUBSTATION VOLTAGE

This section looks into the error of assuming a theoretical value for the substation voltage in case studies (commonly 700V) instead of using the actual substation nominal voltage. Running sections X and Y as unilateral sections with their actual voltage versus 700V did not produce significant errors (less than 1kWh per day from the values reported in

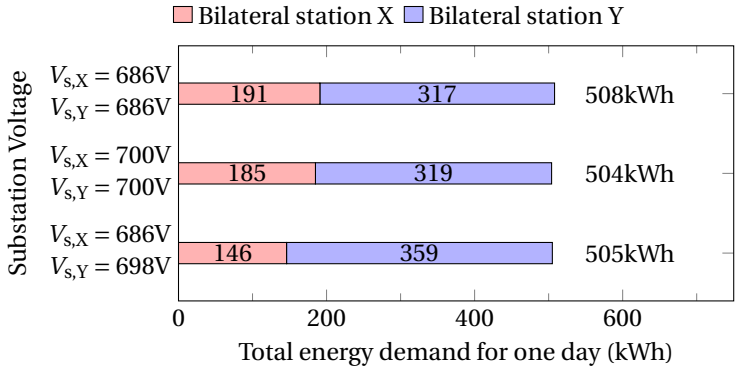

Figure 3.13: The different total energy supply by two bilaterally connected sections (X and Y) in Arnhem for different substation voltages for the same one-day load (Day 1).

Table 3.5). However, Figure 3.13 shows an interesting behavior when the energy demand for substations X and Y is simulated with their nominal voltages or with the common 700V assumption. It can be observed that while the sum of the daily energy supplied by the two substations has an error of only a few kWh, the individual energy share of the load by the substations is shifted. This means that the nominal voltages of the bilateral substations play a role in the power sharing between them. Therefore, any study of the individual demand of a bilaterally-connected substation requires an accurate input of the substation voltages, otherwise it could lead to large errors in the design and control of EV chargers and storage control algorithms, for example.

3.5.8. SUMMARY OF THE ANALYSIS OF THE COMMON MODELING ASSUMPTIONS

This chapter proposed a comprehensive model for a trolleybus grid, including six elements that are often ignored in literature (bullet points below.) Another point, point A, was found to be indeed negligible. To quantify the influence of these elements on the modeling of the grid, case studies were conducted using a verified simulation model, as well as four years of substation energy measurements and over 70 hours of trolleybus measurements in the trolleygrid of Arnhem, The Netherlands. The results are summarized below:

- The overhead wire impedance: The impedance can be assumed as purely resistive for a steady state model. The inductive component of the lines causes a voltage drop at the order of 10^{-2} for a bus, while the resistive drop is at the order of 10^{1}.
- The parallel lines: The impedance seen between two nodes can be assumed as half the impedance of the line connecting them.
- The bus auxiliaries load: The auxiliaries have to be included in the modeling of the trolleybus load; otherwise, an average error of 55% is expected in the substation demand calculations.

- Regenerative braking: The regenerative braking must be included in a trolleygrid model. Errors as high as 34% in the energy demand have been reported otherwise.
- The section feeder cable: This line has to be included in a trolleygrid model, depending on its length and the power it typically carries. A set of equations is presented in this chapter to make the judgment.
- Bilateral connection: Modeling two bilaterally connected sections as two isolated, unilateral sections is not recommended, except for total grid consumption calculations. The loading of individual substations and line voltages included serious errors (maximum of 25% and 132V, respectively).
- Substation nominal voltage: The exact substation voltage is crucial when modeling bilaterally connected substation as it alters the load share of each substation. For unilateral substations, the difference is not significant.

3.6. CONCLUSIONS

Transport grids like the trolleygrid are expanding and adapting to the advancements in smart grid technologies and energy savings. This requires of them more sophisticated models, and this chapter set out to examine seven commonly made assumptions in the analysis of light rail transport grids. Four of these assumptions were not acceptable: Ignoring the bus auxiliaries power demand, ignoring regenerative braking, modeling bilateral substations as two unilateral substations, and not taking the exact substation nominal voltage into account. Furthermore, one suggestion was made to simplify the parallel line impedance. Interestingly, ignoring the feeder cable was found to be acceptable for some low power levels and cable lengths, according to the defined acceptable errors a modeler would choose. However, it is still not advised for most cases. Finally, the assumption of modeling the overhead cable impedance as purely resistive is indeed acceptable for steady-state studies.

Any future research into trolleygrids, especially on the line voltage and power levels (for integration of PV or IMC, for example,) needs to consider the full specifics of the trolleygrid as mentioned here.

This chapter presented a comprehensive numerical (iterative) model that highlights the complexity of analyzing trolleygrids and their loads. It is interesting to investigate in the upcoming chapter if a rather analytical (mathematical) approach to the modeling could provide lessons that allow for the development of power management schemes for trolley networks.

4

A Traction Substation State Estimator for Integrating Smart Loads Without Additional Sensors

"Freunde! Seht!
Fühlt und seht ihr's nicht?
Höre ich nur diese Weise,
die so wundervoll und leise,
Wonne klagend,
alles sagend,
mild versöhnend
aus ihm tönend[..]?

Isoldes Liebestod - Act III, Tristan und Isolde (Wagner)

Friends! Look!
Don't you feel and see it?
Do I alone hear this melody,
which wonderfully and softly,
lamenting delight,
telling it all,
mildly reconciling
sounds out of him[..]?

This chapter is based on A Traction Substation State Estimator for Integrating Smart Loads in Transport Grids Without Additional Sensors: Theory and Case Studies. I Diab, GR Chandra-Mouli, P Bauer in IEEE Transactions on Intelligent Transportation Systems

The integration and power management of smart loads in transport networks like trolley-grids is a complex task as the loads are stochastic both in time and space. The extremes of the variations are also the vehicles can go from an acceleration peak that is about 5 times their typical traction demand to regenerative braking dips that can supply also the equivalent of a few orders of magnitude of their traction power. The loads can also suddenly appear and disappear from the supply zones of some traction substations when the sections are galvanically separated.
For this aim, this chapter proposes a traction substation state estimator that makes use of already existing measurements at the power node of interest, such as an EV charger or an IMC trolleybus, to help it estimate the local traffic density and the spare traction substation power capacity.

This chapter starts with a more detailed motivation for the need for the proposed traction grid state estimator in Section 4.1. Section 4.2 explains the methodology used for testing and validating the sets of equations and conditions that make up this estimator. The first of these sets of equations is presented in section 4.3 with the V-sigma (V_σ) condition that detects the presence of more than one power-consuming node on the studied supply zone. Section 4.4 presents the N2-front used to detect the presence of more than two nodes. Section 4.5 presents the N3 Region, which can be used to detect the presence of more than three nodes, and to reason out some insights on the node order in terms of distance from the traction substation. Then, Section 4.6 details the method for estimating the traction grid spare capacity. The proposed equations in this chapter are then validated in Section 4.7 by a series of 100000 stochastic simulations. Section 4.8 suggests some extensions for this estimator, while Section 4.9 proposes a number of power management applications of this estimator in smart load integration, as will be applied later in this thesis. Finally, Section 4.10 closes with conclusions.

4.1. INTRODUCTION

4.1.1. THE NEED FOR A GRID STATE ESTIMATOR

Despite having an underutilized spare energy capacity, traction grids can frequently have short periods of power congestion problems. These moments should be considered when integrating smart loads such as EV chargers so as not to violate the traction substation power rating, maximum line current, or minimum line voltage limitations. Consequently, tapping into the unused capacity of these grids requires intelligent power management schemes and ample information on the traction grid state. These systems are even more complex because the loads constantly vary not only in power demand but also in location, which can affect the line voltage, transmission power losses, and line currents. Therefore, gathering the necessary grid state information requires a large array of wireless communication sensors communicating between themselves, with the traction substation, and with a local data processor for each grid supply zone.

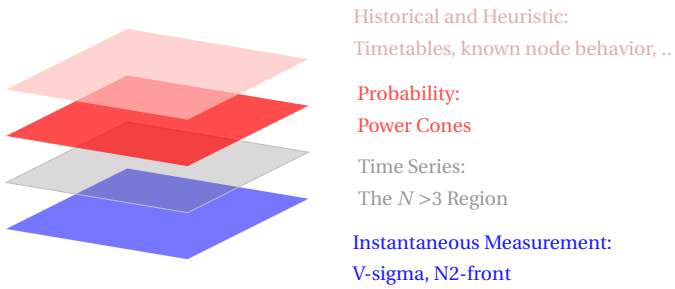

Figure 4.1: The layers of the grid state estimator presented in this chapter. Both the computational complexity and yet also the grid state information increase as the user decides to include more layers from bottom to top.

4.1.2. THE PROPOSED GRID STATE ESTIMATOR

Conveniently, some information is already available at each node (vehicle or smart load) because of the smart protection systems (e.g., measurements of overhead connection point voltage, current, and node power) and of vehicle live position sensing (GPS tracking for user apps, for example).
This chapter aims to use only the already available local data at a power node to estimate the traction substation's state and the number of other nodes present on the same traction grid section. This state estimation can be then used to better manage and integrate smart loads and renewables into traction networks and render them more sustainable, better utilized, and multi-functional.
Figure 4.1 explains the layers of the grid state estimator presented in this chapter. Both the computational complexity and yet also the grid state information increase as the user decides to include more layers from bottom to top.

4.1.3. CHAPTER CONTRIBUTIONS

The chapter offers the following contributions:

1. A traction grid state estimator able to estimate the number of nodes (traffic) present on a traction grid supply zone without the need for additional sensors or wireless communication among them

2. A traction grid state estimator to estimate the instantaneous power load demand on a traction substation to find the spare grid capacity for the power management of smart grid components in transport grids, without the need for additional sensors and wireless communication among them

3. A proposed methodology for estimating the node order on a traction grid supply zone to detect the presence of a node between the node of interest and the substation without the need for additional sensors and wireless communication among them

4. A list of proposed applications of the proposed traction grid state estimator for the power management of smart loads in traction grids

4.2. DESIGNED TEST CONDITIONS FOR THE STOCHASTIC SIMULATIONS IN THIS CHAPTER: DTC

While the estimator offered in this chapter can be extended to any traction network, the examples and validations given to the developed theory here will study trolleygrid scenarios for the sake of an example.
Unless otherwise stated, the examples and validation cases in this chapter use the here-defined Designed Test Conditions (DTC) based on the trolleygrid of Arnhem, the Netherlands (explained in [3]). These conditions are:

- A constant traction substation of 700V nominal voltage, V_s with a rated power capacity, P_r, of 800kW and a negligible length of the substation feeder cable, connected at the start of the section
- A standard overhead line of 0.172Ω/km, paralleled (also known as *equipotential lines*) in sets of 2 [3], [4], [19]
- A section of 1200m with nodes (bus, storage, etc.) always in load mode, between 0 and 300kW
- The maximum operating conditions are defined as a node drawing 500A and moving at a speed of 15m/s [3], [4], [14]

Furthermore, the scenarios studied in this chapter are presented with line diagrams, of which the legend is in Figure 4.2:

- A (green) substation node of known nominal voltage and position at the start of a traction section
- A node of interest (orange) at a known distance and operating conditions. This is the node that is assumed to be using the estimator and has measurements of voltage, power, current, and position
- Other possibly present nodes (dashed circles with a question mark) at an unknown distance(s). These nodes can either be at unknown operating conditions (white) or assumed to be operating at maximum operating conditions (purple). If a node is already known to be present on the section, regardless of the information on its operational condition, it does not have a question mark in its representation

4.3. THE $N>1$ CONDITION

4.3.1. CASE OF A SINGLE NODE ON THE SECTION (N=1)

Assume a node of interest alone on the section, at a known distance from the substation, that can be expressed by an overhead impedance of R_σ (Figure 4.3). The substation voltage is V_s. Since the work in [3] has already verified that the line impedance can be assumed as purely resistive in steady-state calculations, it can be said that:

$$V_\sigma = V_s - R_\sigma I_\sigma = V_s - R_\sigma \frac{P_\sigma}{V_\sigma} \tag{4.1}$$

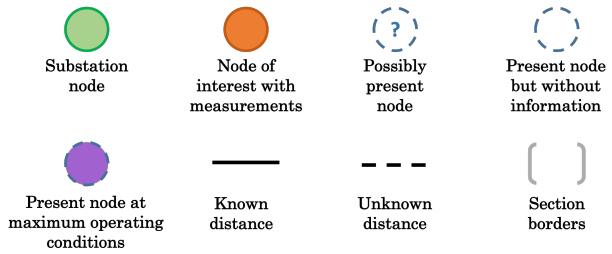

Figure 4.2: Legend for the diagrams of the designed scenarios.

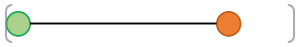

Figure 4.3: The case of a single node at a known distance from the substation.

Where V_σ, I_σ, and P_σ are the voltage, current, and power of the single node, respectively. Which, when multiplied by V_σ, produces a quadratic equation, the solution of which is

$$V_\sigma = \frac{V_s + \sqrt{V_s^2 - 4R_\sigma P_\sigma}}{2} \tag{4.2}$$

This equation serves as a general definition of V_σ as the voltage at a node of interest when it is -or would have been- alone on a section. This definition can also be written as

$$V_\sigma \triangleq \frac{V_s + \sqrt{V_s^2 - 4\Gamma_\sigma}}{2} \tag{4.3}$$

Where Γ_σ is defined as

$$\Gamma_\sigma \triangleq R_\sigma P_\sigma \tag{4.4}$$

This alternative form is useful for later derivations in this chapter when re-arranging Eq.4.3 so that Γ_σ can be written in terms of the grid parameters as:

$$\Gamma_\sigma = V_\sigma (V_s - V_\sigma) \tag{4.5}$$

4.3.2. THE NODAL VOLTAGE ESTIMATION ERROR CAUSED BY THE EQUIVALENT IMPEDANCE APPROACH TO PARALLEL LINES

It is important at this stage to re-visit an implicit assumption made at the beginning in calculating the equivalent overhead line impedance, R_σ, by using a lumped impedance of the overhead feed and return line and the parallel overhead lines. The parallel lines (also called equipotential lines) are the paralleling of the sets of overhead feed and return cables to reduce the overall impedance by creating more paths for the current. The work in [3] flags the potential error from the lumped calculation approach and invites further investigation of it here.

Assume a trolleygrid section with p parallel lines, connected every λ_p meter (see Figure 4.4). The line resistance per unit length is ρ in Ω/m. A power-consuming node is alone

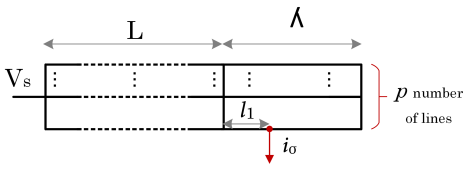

Figure 4.4: Nomenclature of the variables used in the analysis of the error caused in the voltage calculation by the equivalent parallel impedance assumption.

on the section and at a position l_1 between two consecutive parallel lines after a distance L of an integer multiple of paralleled portions. In simpler words, the node is at $L + l_1$ meters from the substation. The substation is at voltage V_s, and the node is drawing a current I_σ.
For better readability in the following derivations, define the normalized bus position within a paralleled section, ϕ, as:

$$\phi \triangleq \frac{l_1}{\lambda_p} \tag{4.6}$$

Without the lumped equivalent-impedance assumption, the real voltage drop, ΔV_{real}, between the substation and the node is

$$\Delta V_{real} = 2\rho \left[\phi\lambda_p \left(\frac{p-\phi(p-1)}{p} \right) + \frac{L}{p} \right] \cdot I_\sigma \tag{4.7}$$

And the actual equivalent resistance between the node and the station, defined here as $\mathscr{R}_\sigma$, is given accurately by the term:

$$\mathscr{R}_\sigma = 2\rho \left[\phi\lambda_p \left(\frac{p-\phi(p-1)}{p} \right) + \frac{L}{p} \right] \tag{4.8}$$

Meanwhile, the simplified equivalent resistance between the station and the node, R_σ, is given by:

$$R_\sigma \approx 2\rho \left(\frac{L+l_1}{p} \right) = 2\rho \left(\frac{L+\phi\lambda_p}{p} \right) \tag{4.9}$$

The error in the resistance value, ϵ_R, caused by the simplification in the resistance can be therefore quantified as:

$$\epsilon_R \triangleq \mathscr{R}_\sigma - R_\sigma = 2\rho \left(\frac{p-1}{p} \right) \phi(1-\phi)\lambda_p \tag{4.10}$$

Moreover, the sensitivity of the nodal voltage to the node impedance value is given by the partial derivative

$$\frac{\partial V_\sigma}{\partial R} = \frac{-P_\sigma}{\sqrt{V_s^2 - 4\mathscr{R}_\sigma P_\sigma}} \tag{4.11}$$

Thereby, the error, ϵ_p, inflicted on V_σ by an error in the line resistance calculation can be quantified by the Propagation of Errors method [197] as:

$$\epsilon_p = \left| \frac{\partial V_\sigma}{\partial R} \right| \cdot \epsilon_R = 2 \left(\frac{p-1}{p} \right) \frac{\rho\lambda_p\phi(1-\phi)P_\sigma}{\sqrt{V_s^2 - 4\mathscr{R}_\sigma P_\sigma}} \tag{4.12}$$

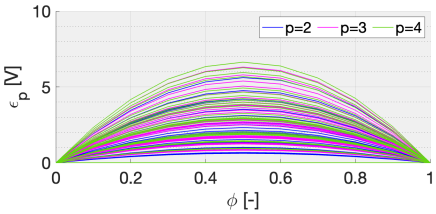

Figure 4.5: The voltage computation error, ϵ_p, as a function of the normalized bus position within a paralleled section, ϕ, for a different number of paralleled lines, p. Each curve looks at a different scenario with L going from 0 to 1200m, λ_p from 100 to 300m, and the remaining variables at DTC.

The above Eq.4.12 provides an estimate of the calculated voltage error expected as a function of P_σ as most of the terms in the equation are constant and known for a grid. Of course, the built infrastructure can sporadically differ from the design parameters because of constraints such as intersections and power pole positioning. Consequently, the precise value of λ_p - and thereby of ϕ and L- cannot always be guaranteed and would be an estimation. Luckily, considering the array of possible combinations of all the Eq.4.12 parameters (Figure 4.5), the error is predominately contained and under 6V. This allows the proposition of the "V-sigma condition" presented in the coming subsection.

4.3.3. APPLICATION OF THE RESULTS: THE V-SIGMA CONDITION

A key grid state can be derived from the calculation of V_σ. Per definition, The V-sigma voltage is the voltage expected when a node is *alone* on a section. This value can be calculated, as shown previously, to an accuracy of ϵ_p. It follows logically then, that if a measured nodal voltage, V_M, were to be outside of this range, the studied node is not alone on the section, and there is *at least* one other node.
However, because of the welcomed sharing of braking energy between nodes, it is advised to shy away from assuming that a measured nodal voltage, V_M, that is (almost) equal to V_σ implies that the node is alone on the section. This mathematical coincidence can arise from the fact that some nodes are supplying power, and thereby masking some of the expected voltage drop effects of other nodes. Also, a vehicle/node could be momentarily not drawing power, or close enough to the section feed-in point that it is not causing an observable voltage drop. This is again a motivation to not interpret $V_M \approx V_\sigma$ as a sign that a node is indeed alone on the section -that is to say:

$$\begin{cases} N > 1 & \text{, if } V_M \notin [V_\sigma - \epsilon_p, V_\sigma[\\ \text{No information} & \text{, if otherwise} \end{cases} \tag{4.13}$$

4.4. THE $N > 2$ FRONT

4.4.1. STUDY OF TWO NODES ON A SECTION (N=2)

Consider a node of interest at an impedance R_M from the substation and drawing a power P_M (or, say, current I_M), such as in Figure 4.6. Notice that the subscript σ is not used as this no longer concerns the case of a single node and is replaced by M as an abbreviation for Measurement Node. Additionally, one node at an impedance R is drawing

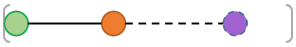

Figure 4.6: The case of a node of interest as the first node and at a known position with only one other node, which is at an unknown position, but at the maximum operating conditions.

the maximum allowed node current of $\hat{I}$. For example, for a trolleybus, $\hat{I} = 500$A, and for a metro, the value is about 3900A. This is the limit imposed by the overhead current collector [3], [14].
It follows then from Kirchhoff's voltage law that:

$$V_M = \begin{cases} V_s - R\hat{I} - R_M I_M & \text{, if } R \leq R_M \\ V_s - R_M(\hat{I} + I_M) & \text{, if } R \geq R_M \end{cases} \tag{4.14}$$

From this, it is trivial that the second situation would produce a more severe voltage drop at the node n, which would be the maximum deviation from the substation voltage, V_s, since the current drawn by the other node is its maximal allowable current. In mathematical terms:

$$V_{M,min}\Big|_{N=2} = (V_s - R_M\hat{I}) - R_M I_M \tag{4.15}$$

Which is analogous to Eq.4.1 and leads then to

$$V_{M,min}\Big|_{N=2} = \frac{(V_s - R_M\hat{I}) + \sqrt{(V_s - R_M\hat{I})^2 - 4R_M P_M}}{2} \tag{4.16}$$

4.4.2. APPLICATION OF RESULTS: THE N2-FRONT

An important consequence of Eq.4.16 is that it quantifies the lowest measured node voltage that can be observed when a power-demanding node is present on the section with another power-demanding node that is at its maximal operational point. It follows logically then that any observed voltage beyond this threshold signals the presence of *at least* three nodes on the section. This value defines the N2-front or threshold, V_{N2F}, as

$$V_{N2F} \triangleq V_{M,min}\Big|_{N=2} \tag{4.17}$$

In other terms:

$$\begin{cases} N > 2 & \text{, if } V_M < V_{N2F} - \epsilon_p \\ \text{No information} & \text{, if otherwise} \end{cases} \tag{4.18}$$

Since, under extreme conditions, the N2-front can already be more than 100V away from V_σ, it is not practical to extend this methodology to estimate the presence of more than 3 nodes, as that could unhelpfully contain most of the operating voltage range. The following section presents a new methodology for that purpose.

4.5. THE $N > 3$ REGION

Now, assuming there are N load nodes on the section, like in Figure 4.7. The nodal voltages and currents can be expressed by:

$$\mathbf{V} = -\mathbf{RI} + \mathbf{V_s} \tag{4.19}$$

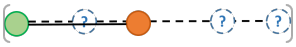

Figure 4.7: The case of a node of interest is at a known distance from the substation, and no other information is known about the possible other node(s).

Where **V** and **I** are the Nx1 vectors of voltages and currents, respectively, and **R** is the NxN branch resistance matrix, similar to the concept of an admittance matrix, and built by applying Kirchhoff's voltage law. $\mathbf{V}_s$ is an Nx1 vector holding the substation voltage value. An example of a 3x3 (i.e., N=3) system is:

$$\begin{bmatrix} V_1 \\ V_2 \\ V_3 \end{bmatrix} = - \begin{bmatrix} R_1 & R_1 & R_1 \\ R_1 & R_1 + R_2 & R_1 + R_2 \\ R_1 & R_1 + R_2 & R_1 + R_2 + R_3 \end{bmatrix} \begin{bmatrix} I_1 \\ I_2 \\ I_3 \end{bmatrix} + \begin{bmatrix} V_s \\ V_s \\ V_s \end{bmatrix} \tag{4.20}$$

The branch resistance can be understood as the line resistance per SI unit length, ρ, multiplied by the branch length **X**.

$$\mathbf{V} = -\rho \mathbf{X} \mathbf{I} + \mathbf{V}_s \tag{4.21}$$

For the sake of an example in this chapter, assume a constant velocity profile, with a vector velocity **v** and initial position $\mathbf{X_0}$, the branch length vector can be rewritten so that:

$$\mathbf{V} = -\rho(\mathbf{v}t + \mathbf{X_0})\mathbf{I} + \mathbf{V}_s \tag{4.22}$$

Taking the derivative with respect to time,

$$\frac{\partial \mathbf{V}}{\partial t} = \frac{\partial}{\partial t}\left(-\rho \mathbf{v} \mathbf{I} t - \rho \mathbf{X_0} \mathbf{I} + \mathbf{V}_s\right) \tag{4.23}$$

Which can be developed into:

$$\frac{\partial \mathbf{V}}{\partial t} = -\rho \mathbf{v} \mathbf{I} - \rho \mathbf{v} t \frac{\partial}{\partial t}\mathbf{I} - \rho \mathbf{X_0} \frac{\partial}{\partial t}\mathbf{I} + 0 \tag{4.24}$$

4.5.1. THE CASE OF $\forall k \neq n$ AT EXTREME OPERATIONAL CONDITIONS

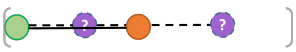

Figure 4.8: The case of a node of interest at a known distance from the substation together with two other nodes on the section at unknown position and at maximum operating conditions.

Let the interest be now focused on a specific node, n, to study the maximum effect on its voltage variation brought by the extreme velocity and power operational conditions of all nodes k other than n (i.e., $\forall k \neq n$). This is represented in Figure 4.8. For the short studied duration, assume that the power demand, velocity, and node order of node n do not change significantly during the evaluation period. This complete set of conditions

and assumptions can be summarized as follows:

$$\begin{cases} \frac{\partial}{\partial t}P_n \approx 0 & \text{, for the studied duration} \\ \frac{\partial}{\partial t}v_n \approx 0 & \text{, for the studied duration} \\ V_k(t=0) \stackrel{\Delta}{=} V_{k,0} & \text{,Initial voltage } \forall k \\ i_k = \hat{I} & \text{, } \forall k \neq n \\ v_k = \hat{v} & \text{, } \forall k \neq n \end{cases} \tag{4.25}$$

For the sake of example, below follows a detailed derivation of Eq. 4.24 for the case of n=1.

$$\frac{\partial}{\partial t}V_1 = -\rho(v_1 i_1 + 2v_1\hat{I}) - \rho[v_1 v_1 v_1]\begin{bmatrix}\frac{\partial}{\partial t}i_1\\0\\0\end{bmatrix}t - \rho[X_{1,0}X_{1,0}X_{1,0}]\begin{bmatrix}\frac{\partial}{\partial t}i_1\\0\\0\end{bmatrix} \tag{4.26}$$

Leading to:

$$\frac{\partial}{\partial t}V_1 = -\rho v_1\frac{P_1}{V_1} - 2\rho v_1\hat{I} + \rho v_1 t\frac{\partial}{\partial t}(\frac{P_1}{V_1}) + \rho X_{1,0}\frac{\partial}{\partial t}(\frac{P_1}{V_1}) \tag{4.27}$$

Finally:

$$\frac{\partial}{\partial t}V_1 = \underbrace{-\rho v_1 P_1}_{\alpha}\frac{1}{V_1}\underbrace{-2\rho v_1}_{\beta}\hat{I} - (\underbrace{-\rho v_1 P_1}_{\alpha}\underbrace{t - \rho X_{1,0}P_1}_{\gamma})\frac{1}{V_1^2}\frac{\partial V_1}{\partial t} \tag{4.28}$$

This same derivation can be repeated for any other position of the node n between 1 and N, giving a differential equation of the form

$$\frac{\partial}{\partial t}V_n = \alpha\frac{1}{V_n} + \beta - (\alpha t + \gamma)\frac{1}{V_n^2}\frac{\partial V_n}{\partial t} \tag{4.29}$$

For which the general solution for any n is

$$V_n(t) = (-\frac{\gamma_n}{2V_{n,0}} + \frac{V_{n,0}}{2}) + \frac{\beta_n t}{2} + \frac{\sqrt{4(\alpha_n t + \gamma_n) + (\frac{\gamma_n - V_{n,0}(\beta_n t + V_{n,0})}{V_{n,0}})^2}}{2} \tag{4.30}$$

Where the terms α_n, β_n, and γ_n are given by:

$$\alpha_n = -\rho\left(\sum_{k=1}^{n} v_k\right)\cdot P_n \tag{4.31}$$

$$\beta_n = -\rho\hat{I}\left(\sum_{k=1}^{n}(N-k)v_k\right) \tag{4.32}$$

$$\gamma_n = -\rho\left(\sum_{k=1}^{n} X_{k,0}\right)\cdot P_n \tag{4.33}$$

Yet a more interesting insight is offered by the derivative of V_n with respect to time:

$$\frac{\partial V_n}{\partial t} = \frac{\beta_n}{2} + \frac{\partial}{\partial t}\left(\frac{\sqrt{4(\alpha_n t + \gamma_n) + \left(\frac{\gamma_n - V_{n,0}(\beta_n t + V_{n,0})}{V_{n,0}}\right)^2}}{2} \right) \tag{4.34}$$

Which leads to:

$$\frac{\partial V_n}{\partial t} = \frac{\beta_n}{2} + \frac{4\alpha_n + 2\beta_n^2 t - 2\beta_n(\frac{\gamma_n - V_{n,0}^2}{V_{n,0}})}{4\sqrt{4(\alpha_n t + \gamma_n) + \left(\frac{\gamma_n - V_{n,0}^2}{V_{n,0}}\right)^2 + \beta_n^2 t^2 - 2\beta_n(\frac{\gamma_n - V_{n,0}^2}{V_{n,0}})t}} \tag{4.35}$$

Some simplifications can be made regardless of the transport system in the study as the values of line resistance per unit length are at the order of $\mathcal{O}(10^{-4})$ (in SI units), the line current at, or higher than, $\mathcal{O}(10^2)$, the vehicle velocity at the order of $\mathcal{O}(10^1)$, the section lengths at the order of $\mathcal{O}(10^3)$, and the power at the order of $\mathcal{O}(10^5)$ or even higher [3], [14]. Consequently, $\mathcal{O}(\alpha_n) = \mathcal{O}(10^2)$, $\mathcal{O}(\beta_n) = \mathcal{O}(10^0)$, and $\mathcal{O}(\gamma_n) = \mathcal{O}(10^4)$ or $\mathcal{O}(10^5)$ depending on n . The important consequence is that the derivative can be thereby simplified to:

$$\frac{\partial V_n}{\partial t} \approx \frac{\beta_n}{2} + \frac{4\alpha_n - 2\beta_n(\frac{\gamma_n - V_{n,0}^2}{V_{n,0}})}{4\sqrt{4\gamma_n + \left(\frac{\gamma_n - V_{n,0}^2}{V_{n,0}}\right)^2}} \tag{4.36}$$

Where the denominator can be simplified to allow writing

$$\frac{\partial V_n}{\partial t} = \frac{\beta_n}{2} + \frac{4\alpha_n - 2\beta_n(\frac{\gamma_n - V_{n,0}^2}{V_{n,0}})}{4\sqrt{\left(\frac{\gamma_n + V_{n,0}^2}{V_{n,0}}\right)^2}} \tag{4.37}$$

Leading to

$$\frac{\partial V_n}{\partial t} = \frac{1}{2}\beta_n\left(1 - \frac{\gamma_n - V_{n,0}^2}{\gamma_n + V_{n,0}^2}\right) + \frac{\alpha_n V_{n,0}}{\gamma_n + V_{n,0}^2} \tag{4.38}$$

Or ultimately to:

$$\frac{\partial V_n}{\partial t} = \frac{\beta_n V_{n,0}^2 + \alpha_n V_{n,0}}{\gamma_n + V_{n,0}^2} = \text{constant!} \tag{4.39}$$

The benefit of this equation is that it offers a constant value benchmark for the rate of change in voltage over a short period of time at the node of interest n, allowing to re-write the partial differential as a constant slope equation:

$$\frac{\Delta V_n}{\Delta t} = \frac{\beta_n V_{n,0}^2 + \alpha_n V_{n,0}}{\gamma_n + V_{n,0}^2} \quad (\text{for } \Delta t \leq 10s) \tag{4.40}$$

4.5.2. A COMMENT ON THE COMPUTATION OF γ_n

A concern that can be raised is that the parameter γ_n requires knowledge of the original positions of the other load nodes on the section. While this information is not known, it is still reassuring that the sensitivity of the multi-variable Eq.4.40 with respect to the variable γ_n, given by

$$\frac{\partial}{\partial \gamma_n}\frac{\Delta V_n}{\Delta t} = -\frac{\beta_n V_{n,0}^2 + \alpha_n V_{n,0}}{(\gamma_n + V_{n,0}^2)^2} \tag{4.41}$$

is at the order of $\mathcal{O}(10^{-5})$. Consequently, the propagation of error from the $\sum_{k=1}^{n} X_{k,0}$ term, whose elements are the order of $\mathcal{O}(10^3)$, into Eq. 4.40, is at the order of $\mathcal{O}(10^{-2})$ or $\mathcal{O}(10^{-1})$.

Fortunately, the error in assuming the original position of the other nodes $\forall k \neq n$ can be easily compensated for. One possible suggestion is to use an averaged approach around the known $X_{n,0}$ term, suggested as

$$\gamma_n = -\rho\left(\sum_{k=1}^{n} X_{k,0}\right)\cdot P_n \approx -\rho(\frac{n+1}{2})X_{n,0}\cdot P_n \tag{4.42}$$

It is perhaps worth mentioning again that this is not an argument against the influence of γ_n on Eq.4.40, but rather on the sensitivity of ΔV_n to an error in the approximation of the initial positions of all nodes k other than n. Indeed, Eq.4.42 is not to be understood then as an invitation to ignore the term γ_n in Eq.4.40, but as a validation of the offered simplification.

4.5.3. APPLICATION OF RESULTS: THE N >3 REGION

The derivations presented in this section allow, for any studied node position, velocity, and power, to delimit the n-lines and the N >3 region of this node.

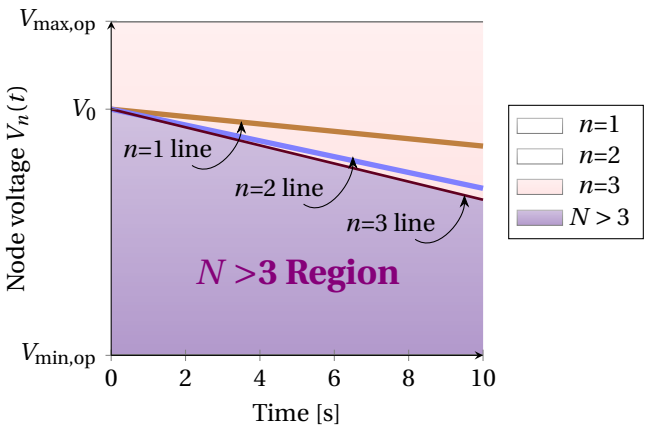

Figure 4.9: Visual Representation of the N >3 Region for the example in Section 4.5.3. At any time t, a measured node voltage $V_n(t)$ that falls in the purple N >3 region indicates that more than three buses are on the studied section.

To explain the meaning and utility of these lines, an example is presented in Figure 4.9 for a bus moving from X=1000m from the substation, away at 10m/s, and drawing 100kW. Since the presented equations in this section of the chapter consider the worst-case scenarios for the two other nodes on the studied grid section, any measured node voltage $V_n(t)$ that falls in the purple $N>3$ region would signal the presence of more than 3 nodes on this grid section. The $N>3$ region is described mathematically as the region between the minimum operating voltage of the grid, $V_{\text{min,op}}$, and the $V_3(t)$ node voltage described in this section when setting n=3. The latter is presented in the figure as the "n=3 line". However, the other nodes could be operating at conditions more favorable than the worst-case conditions, even up to regenerative mode. Consequently, the zone between the maximum operating voltage of the grid, $V_{\text{max,op}}$, and the "n=3 line" does not offer reliable information on the number of nodes on the section, and should not be used for this purpose.

In the event that reliable information is available for a particular grid zone (e.g., historically knowing that there would never be more than 3 nodes on this section), then the n-lines could offer information on the position of the studied node with respect to the two other nodes. For example, consider that the studied node is that of stationary storage, and historical information guarantees the presence of only two vehicles on this section at this time. It can follow that a measured node voltage falling between lines n=1 and n=2 signals to the storage system that there is at least one of the vehicles between it and the substation. This information is very useful when estimating the load demand on the section, as explained in the coming section of this chapter.

4.6. APPROXIMATION OF THE SPARE TRACTION SUBSTATION POWER CAPACITY

Revisiting the equation for a single bus, an approximation can be extended for the case of two or more buses by lumping the effect of other loads on the section and their position into a grid Γ factor, namely Γ_G, and introducing it as a disturbance to the bus Γ_σ factor as follows:

$$V_M = \frac{V_s + \sqrt{V_s^2 - 4(\Gamma_\sigma + \Gamma_G)}}{2} \tag{4.43}$$

Where V_M is the measured node voltage. Re-arranging the above equation,

$$\Gamma_G = V_M(V_s - V_M) - \Gamma_\sigma \tag{4.44}$$

Or finally

$$\Gamma_G = (V_\sigma - V_M)(V_\sigma + V_M - V_s) \tag{4.45}$$

Equation 4.45 can then be extended to allow an approximation of the grid support (from a storage system, for example) to be added, Γ_a, to reach the voltage level of V_σ:

$$V_M = \frac{V_s + \sqrt{V_s^2 - 4(\Gamma_\sigma + \overbrace{\Gamma_G + \Gamma_a}^{\text{aim is} \approx 0})}}{2} \tag{4.46}$$

Yet more generally, this approach can offer insight into the spare grid capacity or the needed grid support to reach a desired voltage V^* which is not necessarily V_σ. This is useful if, for example, a traction-grid-connected EV charger needs to estimate the available power it can draw while staying above a minimum voltage threshold.

$$V_\mathrm{M} = \frac{V_\mathrm{s} + \sqrt{V_\mathrm{s}^2 - 4(\Gamma_\sigma + \Gamma_\mathrm{G} + \Gamma_\mathrm{a})}}{2} \tag{4.47}$$

Whereby Γ_a can be expressed as:

$$\Gamma_\mathrm{a} = -(V^* - V_\mathrm{M})(V^* + V_\mathrm{M} - V_\mathrm{s}) \tag{4.48}$$

A powerful application of this derivation is the ability to estimate the total power demand on a traction substation. While this seems like a straightforward solution, it is important to remember that the Γ parameter is a product of power and impedance, and further work is required to attempt to decouple the power information from the Γ variable. This decoupling work is presented in the following subsections, looking at the three possible scenarios of the position of the studied node n in relation to the substation and the other power nodes.

4.6.1. THE CASE OF n=1

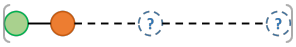

Figure 4.10: The case when the node of interest (orange) is the first load node and at a known, close distance to the substation (green). No other information is known about the other node(s).

For the case when the node of interest is the closest to the substation, an accurate estimation of the substation demand is obtained by setting V^* to the value of V_s. In such a scenario, the voltage drop between the substation and the first node is 0 (=$V_\mathrm{s} - V_\mathrm{s}$), meaning that no current flows between the substation and node 1, as if the node itself is supplying all the loads on the section had its voltage been V_s.
The effectiveness of this method can be validated by recognizing the similarity between this case and the mere presence of an equivalent feeder cable before node 1. Indeed, node 1 has all the information needed about the substation current demand caused by the other nodes as it experiences a voltage drop caused by this aggregated demand.
It can be said of this system that the state of every node is not *separately observable* by node 1; however, their lumped effect is perfectly observed. This allows the reader to avoid the approximation of Eq.4.45 and to return to an extension of Eq. 4.1 for calculating the spare substation capacity as:

$$P_\mathrm{r} = P_\mathrm{spare}\Big|_{n=1} + V_\mathrm{s} \cdot I_\mathrm{s}\Big|_{n=1} \tag{4.49}$$

Or, ultimately:

$$P_\mathrm{spare}\Big|_{n=1} = P_\mathrm{r} - V_\mathrm{s}\frac{(V_\mathrm{s} - V_\mathrm{M})}{R_\sigma} \tag{4.50}$$

Since it follows logically from Ohm's law that if n=1, then the substation current, I_s, is observed fully through the voltage drop between the substation voltage and the measured voltage of the first node over the resistance that separates them.
This is particularly interesting when, for example, the storage is placed near the traction substation or when a bus with on-board storage sees that it is *sufficiently* close to the substation. The threshold for this closeness is a design question of a statistical nature, which is a function of the total section length and the average section traffic. This is then an application-specific design decision to be made by the stakeholders.

4.6.2. THE CASE OF $n \neq 1$

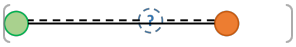

Figure 4.11: The case when one node possibly exists between the node of interest (orange) and the substation (green).

The case $n \neq 1$ means at least one node exists on the section between the substation and the node of interest. Thereby, setting V^* to the value of V_s would not produce the same "blocking out" effect as previously attained.
It could be worth mentioning for the interested reader that this case becomes synonymous with the case of a bilaterally connected substation described in [16] (the case of two traction substations feeding one section), with our interest node being a *virtual* bilateral substation.
In any case, it can be argued then that if V^* is set to the value of V_s, the power share between the substations is obtained from simple circuit analysis as the ratio of the branch impedances between the load node and the two substations. Unfortunately, the position of the load node is unknown, and as a consequence, neither is this ratio of impedances. This brings the analysis back to a Γ value where, at best, an estimate can be offered for the product of the branch resistance and power of a node, but the information cannot be decoupled into the two parameters. However, some information can be inferred from a stochastic analysis. Figure 4.12 shows the stochastic distribution of the spare trolleybus traction substation capacity ($= P_r - V_s \cdot I_s$) as a function of the measured node voltage for 100000 stochastic grid simulations. Figure 4.12(a) shows the case of 2 load nodes, while Figure 4.12(b) studies 4 load nodes. Both figures look at simulations under the DTC of this chapter. In both figures, the measured node is at the end of the line, at 1200m, to look at the worst-case scenario in terms of grid state observability (previously addressed in section 4.4). The measured node power demand is randomly selected between 0 and 200 kW. The first observation from Figure 4.12 is the existence of a linear upper envelope. The slope of this line can be shown in fact to be described by Eq.4.50. This follows logically, as the linear Eq.4.50 describes the least-conservative, most-observant state estimation, and all other possible grid states would in reality have a lower spare grid capacity.

4.6.3. APPLICATION: POWER CONES

This section proposes one possible methodology for estimating the grid spare capacity using the spare-capacity cones introduced above. The derivations are conducted for a

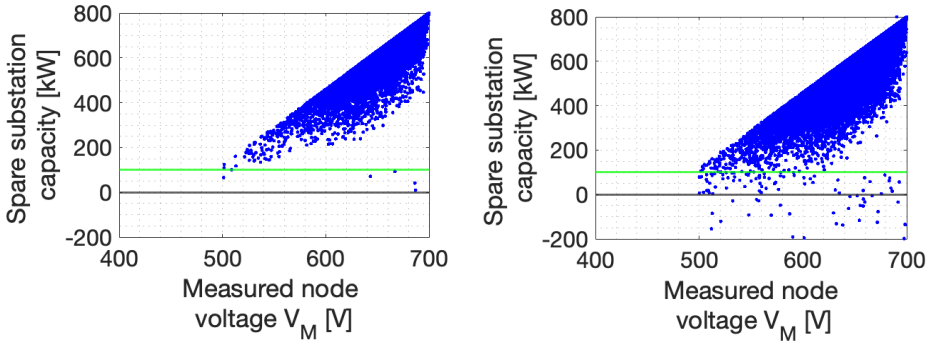

((a)) Case of N=2.

((b)) Case of N=4.

Figure 4.12: Stochastic distribution of the spare trolleybus traction substation capacity as a function of the measured node voltage for 100000 grid simulations of (a) 2 load nodes and (b) 4 load nodes. The two plots have the same upper-envelope slope and are mostly populated by data above the (green) 100 kW line.

full-cone geometry but should be adapted to the specific total node number, N, expected at a section.

The cones of Figure 4.12 can be approximated by Figure 4.13, for a measured node voltage V_{M} that is bound by an upper limit V_{U} and a lower limit V_{L}. These limits are a case-specific design choice and particularly useful when the estimation is not done continuously, for example, by a traction-grid-connected EV charger that only estimates the grid state every 5 seconds. Such limits would thereby consider the possible zone of voltages that the estimator can see when it "wakes up" at the next estimation step. The cone crosses the zero spare capacity line at the voltage V_{ZP}, defined by setting Eq.4.50 equal to zero:

$$V_{\mathrm{ZP}} \triangleq V_{\mathrm{s}} - \frac{P_{\mathrm{r}} R_{\sigma}}{V_{\mathrm{s}}} \tag{4.51}$$

This is the most conservative voltage level at which there is no spare capacity left as it translates to the scenario where the measured node and its caused line transmission losses to consume the substation capacity completely. The simulations of Figure 4.12 show that this extreme scenario is never reached in practice, as most values are above the 100kW (green) line.

Consider now a desired spare capacity level, P^*. Define C_{TZ} as the number of possibilities (blue dots of Figure 4.12) in the trapezoid formed by the V_{L} line, V_{U} line, the upper envelope, and the P^* line (blue trapezoid in Figure 4.13). C_{R} is defined as the number of dots in the rectangle formed by the V_{L} line, V_{U} line, the P^* line, and the zero spare capacity line (pink rectangle in Figure 4.13). In case the voltage associated with P^*, namely V_{P^*}, is higher than V_{L}, then it is more accurate to speak of a C_{TR} count of the cases inside the triangle formed by the V_{P^*} line, V_{U} line, the upper-envelope of the cone, and the P^* line, together with $C_{\mathrm{R,VP}^*}$ as the number of cases in the rectangle formed with V_{P^*}.

It can be proposed then that the probability of having *at least* a P^* amount of spare trac-

tion substation capacity when seeing a node voltage of V_M is

$$p(P \geq P^*) = \begin{cases} \dfrac{C_{TZ}}{C_{TZ} + C_R} & \text{, if } V_{P^*} < V_L \\ \dfrac{C_{TR}}{C_{TR} + C_{R,VP^*}} & \text{, if } V_{P^*} \geq V_L \end{cases} \tag{4.52}$$

The difference between figures 4.12(a) and 4.12(b) shows how the higher traffic substations tend to populate their cones more evenly, while the lower traffic substations have a more dense distribution. If preferred then, for the high-traffic substations, the probability can be easily (albeit less accurately) by a ratio of areas of the geometric entities previously defined. If A_{TZ} is the area of the blue trapezoid,

$$A_{TZ} = \left[P_r - \frac{V_s^2}{R_\sigma} + \frac{V_s}{2R_\sigma}(V_U + V_L) - P^* \right] (V_U - V_L) \tag{4.53}$$

and A_{TR} is the area of the V_{P^*} triangle,

$$A_{TR} = \frac{1}{2} \left[P_r - \frac{V_s}{R_\sigma}(V_s - V_U) - P^* \right] (V_U - V_{P^*}) \tag{4.54}$$

and A_R is the area of the pink rectangle,

$$A_R = P^* \cdot (V_U - V_L) \tag{4.55}$$

and A_{R,VP^*} is the area of the V_{P^*} rectangle,

$$A_{R,VP^*} = P^* \cdot (V_U - V_{P^*}) \tag{4.56}$$

Then it can be said that, for high-traffic substations,

$$p(P \geq P^*)\Big|_{N>>1} \approx \begin{cases} \dfrac{A_{TZ}}{A_{TZ} + A_R} & \text{, if } V_{P^*} < V_L \\ \dfrac{A_{TR}}{A_{TR} + A_{R,VP^*}} & \text{, if } V_{P^*} \geq V_L \end{cases} \tag{4.57}$$

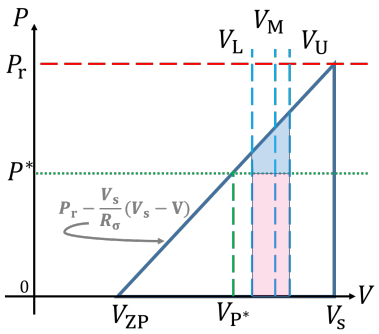

Figure 4.13: The cone suggested in this chapter.

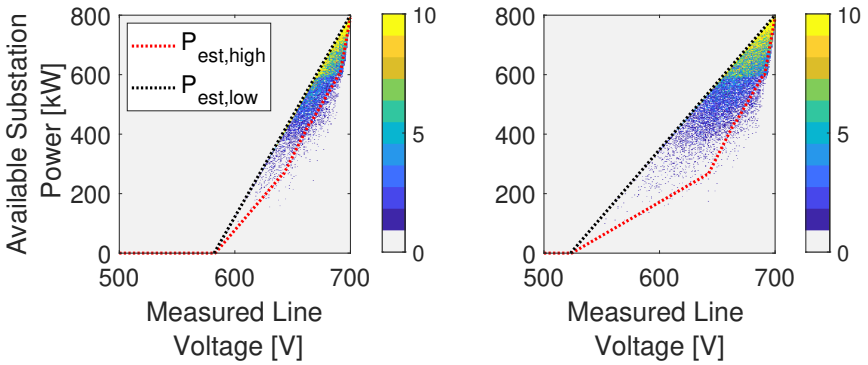

Figure 4.14: Heatmap of the stochastic distribution of the available spare traction substation capacity as a function of the measured line voltage by the storage system in 100000 stochastic grid simulations. The storage is placed at 600m (left) and 900m (right) from the substation feed-in point and the black and red linear traces are given by Eq.4.50 and Eq.4.58, respectively.

One final approach to the cone can be done through a heatmap. Figure 4.14 shows the stochastic distribution of the spare trolleybus traction substation capacity with the node placed at 600m (left figure) and 900m (right figure) from the substation feed-in point.

The first observation is the existence of a linear upper envelope to the cloud of possible points. The slope of this line is described by Eq.4.50. This follows logically, as the linear Eq.4.50 describes the least-conservative, most-observant state estimation, and all other possible grid states would, in reality, have a lower spare grid capacity due to "unobservable" loads such as a bus very close to the feed-in point.

Meanwhile, a more conservative estimation of a higher load demand (lower spare capacity) can be offered by the here-defined red trace in Figure 4.14. This empirically-defined red line of the high estimated power (low spare), $P_{\text{est, high}}$, can be described by

linear interpolations among the following voltage points:

$$P_{\text{est, high}} \begin{cases} 0 & \text{, at } V_{\text{M}} = V_{\text{ZP}} \\ \frac{1}{3}P_{\text{r}} & \text{, at } V_{\text{M}} = V_{\text{ZPm}} \\ \frac{5}{3}P_{\text{r}} & \text{, at } V_{\text{M}} = 0.95V_{\text{s}} \\ \frac{3}{4}P_{\text{r}} & \text{, at } V_{\text{M}} = V_{\text{s}} - 10 \\ \frac{99}{100}P_{\text{r}} & \text{, at } V_{\text{M}} = V_{\text{s}} \\ P_{\text{r}} & \text{, if } V_{\text{M}} > V_{\text{s}} \end{cases} \tag{4.58}$$

Where V_{ZPm} is defined as the midpoint between V_{ZP} and V_{s}:

$$V_{\text{ZPm}} \triangleq \frac{V_{\text{ZP}} - V_{\text{s}}}{2} \tag{4.59}$$

The high estimation (red) curve would remain under the low estimation (black) curve as long as $V_{\text{ZPm}} < 0.95V_{\text{s}}$, which, by using Eq.4.51 and Eq. 4.59 leads to:

$$V_{\text{ZPm}} < 0.95V_{\text{s}} \iff R_{\sigma} > \frac{V_{\text{s}}^2}{10P_{\text{r}}} \tag{4.60}$$

Otherwise, it is advised to drop the V_{ZPm} point from the red curve trace and interpolate directly between V_{ZP} and $0.95V_{\text{s}}$.

4.7. VALIDATION OF THE PROPOSED METHODS THROUGH STOCHASTIC SIMULATIONS

4.7.1. V-SIGMA CONCEPT

Figure 4.15 shows the results of 10000 stochastic simulation tests of the V_{σ} condition introduced in Eq.4.13 with up to N=4 nodes. The simulation parameters are according to the DTC of this chapter, with ϵ_{p} set as 6V according to the outcome of Figure 4.5.
As expected, every $V_{\text{M}} \notin [V_{\sigma} - \epsilon_{\text{p}}, V_{\sigma}[$ correctly signals the presence of more than 1 node, as there are no cases when this occurs while N=1. Meanwhile, $V_{\text{M}} \in [V_{\sigma} - \epsilon_{\text{p}}, V_{\sigma}[$ does not offer information on the number of nodes as there are times when it is flagged for any N between 1 and 4.
The performance of this method (desired number of flags over total cases) is then 74%, with no false flags (false positive).

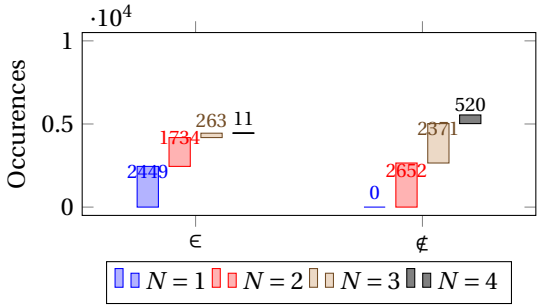

Figure 4.15: Results of 10000 stochastic simulation tests of the V_σ condition introduced in Eq.4.13 with up to N=4 nodes. As expected, triggering $V_M \notin [V_\sigma - \epsilon_p, V_\sigma[$ always correctly notifies of the presence of more than 1 node, while $V_M \in [V_\sigma - \epsilon_p, V_\sigma[$ does not offer information.

4

4.7.2. N2-FRONT

Figure 4.16 shows the results of 10000 stochastic simulation tests of the V_{N2F} condition introduced in Eq.4.18 with up to N=4 nodes. The simulation parameters are according to the DTC of this chapter, with ϵ_p set as 6V according to the outcome of Figure 4.5.
As expected, triggering $V_M < V_{N2F} - \epsilon_p$ always correctly notifies of the presence of more than 2 nodes, while otherwise, no information can be deduced The performance of this method (desired number of flags over total cases) is then 37%, with no false positives.

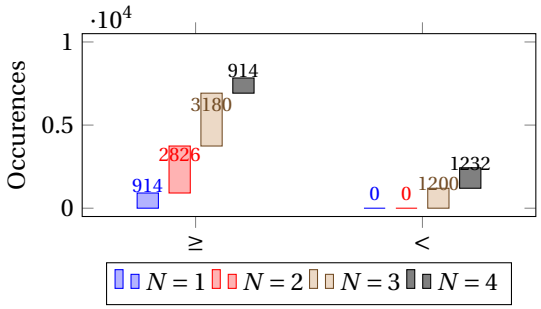

Figure 4.16: Results of 10000 stochastic simulation tests of the V_σ condition introduced in Eq.4.18 with up to N=4 nodes. As expected, triggering $V_M < V_{N2F} - \epsilon_p$ always correctly notifies of the presence of more than 2 nodes, while otherwise, no information can be deduced.

4.7.3. N3-REGION

To test the N3-region hypothesis, 10000 stochastic simulations of 10 seconds were run with up to N=5 nodes placed on a section under the DTC of this chapter. The power ramp-up is taken as a random number between 0 and 25kW, with an upper cap per node at 300kW. The parallel line error adopted, ϵ_p, is again of 6V. The greatly simplified Eq. 4.39 detects 76% of the cases of the presence of more than three nodes, at the cost of 2% in false positives.

Table 4.1: Results of 10000 Stochastic simulation tests of the N>3 Region introduced in Figure 4.9 and Eq.4.39. The greatly simplified Eq.4.39 detects 76% of the cases of the presence of more than three nodes, at the cost of 2% in false positives.

	$N>3$	$N=3$	$N<3$
Flagged	1649	228	0
Unflagged	535	3327	4261
Total cases	2814	3555	4261
Performance*	**76%**	**98%**	**100%**

*Desired behavior (green) over total cases

4.8. SUGGESTED EXTENSIONS OF THE GRID ESTIMATOR

4.8.1. ADDRESSING OTHER TRACTION SECTION ARCHITECTURES: TIMETABLES

The derivations in this chapter were presented for the most common cases of a substation feed-in at the start of the section, rather than the cases when a feed-in point can be connected somewhere along the section. Having all the nodes on the same *side* of the section offers the necessary observability to the node of interest through the voltage drops and the non-linearity in the current demand, which is key for these derivations. Another possibility is that one substation could be feeding 2 sections (or rarely, more). One suggestion is to include the vehicle timetable -and expected delays- in the estimation of the spare power capacity. In future work, this estimator can be extended to use the grid dynamics as input to new estimation methods.

4.8.2. ADDRESSING OTHER UNCERTAINTIES: HEURISTICS

Another extension of the estimator can rely on heuristic approaches to the grid behavior. Heuristics are calculated guesses derived from previous experiences. Examples of such methods could be:

- Expecting a low spare power capacity in the moments after a sharp rise in line voltage: An acceleration will be coming after this regenerative braking
- Expecting that the node count has gone from N to N-1 after a step rise in voltage: A node has left the section (and from N to N+1 after a step drop)
- Expecting a lower certainty in the cones calculations as the line voltage rises slowly: A node is moving closer to the substation and the effect of its presence will soon be masked from other nodes

4.9. EXAMPLES OF APPLICATIONS OF THE THEORY

- Stationary Storage Systems: Can benefit from the estimator spare capacity calculations to know when to charge/discharge
- Stationary Storage Systems with distributed renewables: As above, but can also better plan the charge/discharge to increase the direct utilization of AC-side con-

nected renewable energy systems. When renewables are on the DC side, the estimator can already pick-up on the excess energy via the voltage rises.

- Overhead-line-connected EV chargers: Can benefit from the estimator spare capacity calculations to know when to charge -or discharge if with V2G
- In-Motion-Charging buses: IMC buses typically move under the catenary while charging with a fixed value of up to 240 kW, depending on the city, but most cities only charge conservatively as low as 100 kW. IMC buses can benefit from the estimator spare capacity calculations to know how much is available for it to charge at *any given moment* rather than a fixed value per year per city. It can also use the node number estimation to hold back if it detects the presence of another IMC bus on the section. This can significantly support the electrification of bus lines without the need for additional grid infrastructure by better utilizing the spare grid capacity.

4.10. CONCLUSIONS

This chapter presented an extensive set of equations and conditions to help estimate the number of load nodes and spare grid capacity in traction substations. The methods do not require any additional sensors to be installed, which would be otherwise expensive and required to communicate reliably with each other. Up to 76% of the monitored cases were detected when validating the results with 10000 to 100000 stochastic test simulations of a verified and validated trolleygrid model, with all but one case accurately showing zero false positives (2% in the other case). Finally, some application examples were offered for the implementation of this estimator for the integration of smart grid components into traction grids, making them more sustainable, efficient, and able to electrify more fleets without the need for additional infrastructure.

This chapter will form the basis of the power management scheme to be used in the upcoming chapters to control the storage systems whether stationary or on-board the IMC buses as in Chapters 7, 8, 11, and 12. This estimator can also be investigated as an alternative to the Fleet-Aware-Smart-Charging that will be introduced in the EV Charger analysis of Chapter 9.

PART II

OUTLOOK FOR RENEWABLES INTEGRATION IN PRESENT-DAY URBAN TROLLEYGRIDS

Part I presented the research gaps, directions, and methodology for this thesis.

This part is focused on the sustainability of the trolleygrid from an energy source perspective.

First, Chapter 5 studies solar PV and wind systems in a variety of sizing and placement methodologies on the AC side of the Arnhem grid, with and without AC-side storage. The choice for AC-side placement is to provide a path for the excess renewable energy back to the main grid. However, this option seems to be used too often, effectively rendering the city grid a storage for the trolleygrid, which is against the initial goal of providing the trolleygrid with sustainable and independent power sourcing.

Chapter 6 then attempts to answer two questions. First, is the question if this problem is unique to the Arnhem trolleygrid. In studying the Polish trolleygrid of Gdynia, the problem seems universal, and an upper plateau of about 38% in direct PV utilization is exposed, meaning at least 62% of the PV energy at a trolleygrid will need to be curtailed, stored, or sent to the AC grid. To avoid PV projects that are not techno-economically feasible, the second question to answer is if there exists a trend that could allow a quick and simple estimation of the performance of a PV system in a trolleygrid without the need for complex modeling. The answer is yes, and the mathematical trend is detailed in the chapter, proving a simple way of estimating the performance of a PV system of any size connected to one or more traction substations of any size.

Finally, Chapter 7 re-looks at the question of storage with PV systems but from the DC side where the storage could offer more functionalities. A comparison of the storage between on-board and off-board the vehicle (stationary) and across technologies found that the benefit of storage is still not enough for the techno-economic feasibility of PV systems in trolleygrids. While on-board storage seemed best at reducing the PV system size, they did not provide a noticeable change in PV direct utilization. Meanwhile, stationary storage is beneficial yet its DC side placement did not offer much advantage over its AC side benefit -which, as Chapter 5 pointed out was insufficient.

This motivates the work of Part III where base loads are introduced to the trolleygrid to tackle the mismatch between intermittent solar generation and no-base-load traction demand. This starts first by re-examining storage technologies in Chapter 8 but using power schemes that are not designed to harvest the AC solar energy from the DC side.

5

PLACEMENT AND SIZING OF SOLAR PV AND WIND SYSTEMS IN TROLLEYGRIDS

"Diedi gioielli della Madonna al manto,
e diedi il canto agli astri, al ciel,
che ne ridean più belli.
Nell'ora del dolor
perchè, perchè, Signor,
ah, perchè me ne rimuneri così..?"

Vissi D'Arte - Act II, Tosca (Puccini)

I gave jewels to the Madonna's mantle,
and gave my song to the stars, to the heaven,
which then shined more beautifully.
In the hour of need
Why? Why, Lord?
Oh, why do you reward me like this..?

This chapter is based on [11]: I. Diab, B. Scheurwater, A. Saffirio, G. R. Chandra-Mouli, and P. Bauer, "Placement and Sizing of Solar PV and Sind Systems in Trolleybus Grids," Journal of Cleaner Production, p. 131 533, 2022

This chapter looks at the placement and sizing of solar PV and wind systems in trolleygrids to offer a dedicated, sustainable energy supply to the trolleygrid.

Section 5.1 starts by an introduction to the main challenges and research gaps that motivate the listed chapter contributions. Section 5.3 then details the modeling methodology and the key definitions used in the study of solar and wind energy systems.
The remaining sections, Section 5.4 to 5.9, suggest and investigate six different sizing and placement options for RES in the trolleygrid: Decentralized energy-neutral PV without storage, decentralized PV of different sizes without storage, Decentralized PV sized for 50% utilization and without storage, Decentralized PV system of different sizes and with storage, decentralized PV system of different sizes and with storage and AC exchange limitations (PV curtailing), and centralized PV and/or Wind systems with/without storage.
Finally, Section 5.10 offers conclusions and future work recommendations.

5.1. INTRODUCTION

Transport accounts for about 24% of the global CO_2 emissions, and transportation electrification is a necessary step toward the sustainability of this sector [198], [199]. Fortunately, the electrification of urban public transport is already growing in momentum, and current trends predict a market penetration of up to 75% by 2030 [200]. However, this is counter-productive if the transportation system is still fed with electricity from fossil fuel sources.
Integrating RES into the grid could alleviate some of the energy demand from the AC grid and increase the capacity of the future DC trolleygrid. PV systems, for example, are DC, scalable, and urban-friendly. This makes them an attractive solution for the sustainable powering of urban transport networks. However, one main challenge is that the trolleybuses, like any transportation system, run on a schedule with some time intervals between vehicles. This results in sections of the grid experiencing long periods of zero bus demand while the PV system is generating power, as seen in the simulations of Figure 5.1 of the city of Arnhem. Moreover, the PV system does not generate power at night while the buses are still operational.
This calls for a storage system, an exchange with the AC grid for later use (storing in the grid), or even curtailing (wasting) the excess generation. These modes are explained in Figure 5.2. Moreover, in northern climates such as the Netherlands, the PV generation peaks in the summer while the trolleygrid is at its lowest demand requirements. This is because in the summer, the buses run on lower-traffic schedules and without the significant bus load of HVAC which constitutes half of the demand of the winter months [4].
This mismatch has also made wind energy an attractive RES option. Figure 5.3 shows that the wind generation trend matches the trolleybus demand better than the PV on a yearly scale. Additionally, wind power is available after sunset, so it can cover the power demand of nighttime buses. However, the simulations of the whole trolleygrid of Arnhem in Figure 5.4, show that the PV is still an interesting option as it better matches the bus demand on a daily basis. This makes a hybrid Wind/PV solution an attractive option.

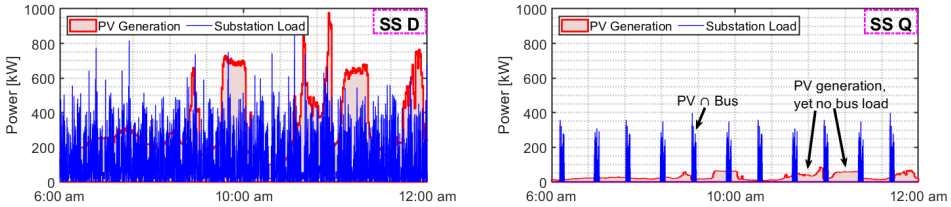

((a)) Substation D (high traffic substation).

((b)) Substation Q (low traffic substation).

Figure 5.1: Mismatch in simulated PV generation and the bus load for two Arnhem substations.

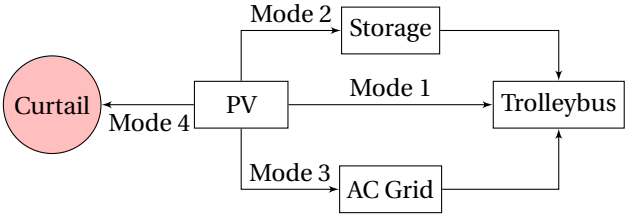

Figure 5.2: The PV power flow: Generated energy can be used directly by the trolleybus (mode 1, most desirable), kept in the storage for later use by the trolleybus (mode2), sent to the main AC Grid -if local policy allows it- to be used later by the trolleybus (mode 3, net metering), or curtailed (mode 4, wasted).

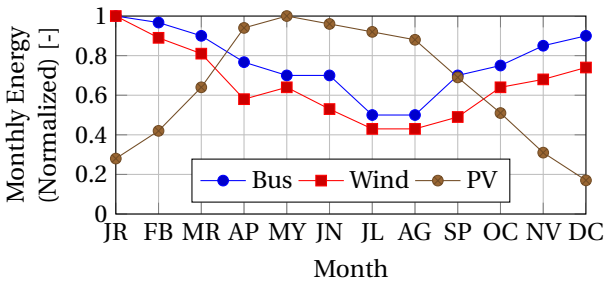

Figure 5.3: Yearly simulated bus demand, wind generation, and PV generation trends by month for the entire Arnhem grid. Each variable is normalized with respect to the highest monthly value it reports. It is observable that the wind generation better follows the bus demand trend on a yearly basis.

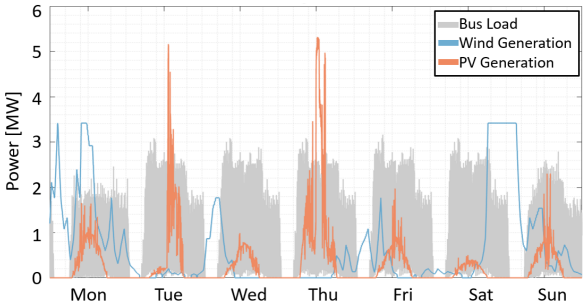

Figure 5.4: Exemplary week number 9 of the per-second simulated bus demand, wind generation, and PV generation trends for the entire Arnhem grid. The PV and Wind systems are both sized to cover the whole grid demand for comparison reasons. The PV generation better follows the bus demand trend on a daily basis.

CHAPTER CONTRIBUTIONS

The research has the following contributions:

1. The first sizing and placement study of wind and wind/PV hybrid systems as a renewable energy source for a trolleygrid system, both with and without storage, using detailed and verified trolleybus, trolleygrid, PV, and wind models
2. Six RES sizing and placement approaches that can cater for any trolleygrid substations by distinguishing them based on their demand size, presence of storage systems, and allowable exchange with the LVAC grid, using detailed and verified trolleybus, trolleygrid, PV, and wind models
3. A simple, original expression to find the performance limits of the PV system at a trolleygrid substation: the maximum achievable direct utilization and the highest direct load coverage (without storage systems)
4. A new decision factor (the PV traffic-view-factor) that assesses quickly which trolleygrid substations should have PV systems and which should not

5.2. RENEWABLES IN TROLLEYBUS GRIDS

The major hurdle to the integration of RES in transportation grids is the intermittent nature of vehicle scheduling. This leaves areas of the grid with low or no load for hours of the day when the RES generates.
There is also a seasonal mismatch. In the case of a PV in the grid of Arnhem, for example, a seasonal mismatch is very pronounced as well between the dense schedules and high heating demand of the winter months (with low PV generation) and the reduced scheduling and low cooling demands of the summer months (with high PV generation).

Some works exist on PV integration in train, metro, and tram networks (e.g., [44]–[47], [73]–[76]). However, these rail systems are different than trolleygrids in terms of their higher power levels, higher line voltages, and less stochastic traffic conditions. This motivates the separate study of RES integration into trolleygrids. As mentioned earlier, the

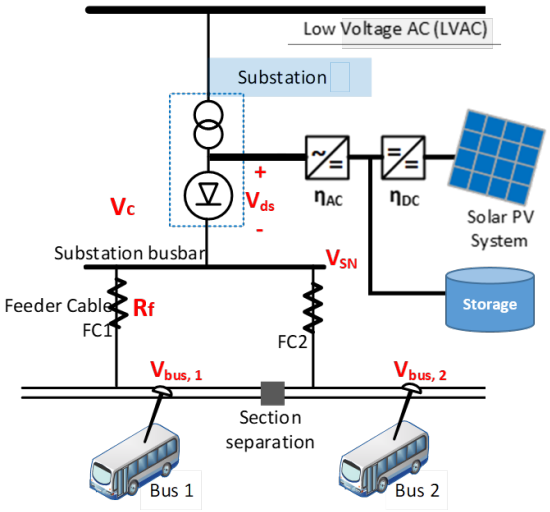

Figure 5.5: The trolleygrid and its components with the solar PV system installed on the AC side.

trolleygrid substations are unidirectional because of their rectifiers. This creates a major hurdle for the implementation of PV without storage on the DC side, as all the PV energy that is not consumed by the buses or the line losses (excess) should be curtailed.
One possible solution is to place the PV on the AC side of the substation to allow a path for the PV system to use the LVAC as storage as in Figure 5.5. The PV power is first inverted to AC (either single stage or DC/DC and then DC/AC stages), allowing any excess energy to return to the AC grid and any trolleygrid power demand to be rectified again and sent to the trolleybuses (see Figure 5.5). This is the first approach to placement on the AC side.
Another possibility is to connect the PV after its first DC stage to the trolleygrid. However, this requires a separate study on the optimal feeding point location concerning transmission losses and overhead line voltage drops unless the PV is placed at the substation bus-bar as in some literature works [77]. Nevertheless, this placement choice could only indirectly reduce the losses in the grid by increasing the feed-in voltage. It would impose a lot of curtailment on the PV system, thereby increasing its utilization.
Another approach in literature places the PV systems on all the substations based on the maximum allowable line impedance that is derived from the voltage drop limitations of the grid [78]. Therefore, this method is more concerned with reducing line losses rather than increasing the sustainability of the grid and the utilization of the PV system. Furthermore, the PV model consists of an ideal curve multiplied by a randomized cloud factor, neglecting the modeling of environmental variations in the PV output power.
To the authors' best knowledge, the only work that proposes a different PV size for trolleygrids substations based on their energy demand is [77].
However, that work only suggests an estimated PV system size: Placing 400-500kW at traction substations with relatively high energy demand, and 100-150kW at the smaller ones. In comparison, the work presented here in this chapter offers a systematic and

specific sizing and placement approach as a function of the substation yearly energy demand.
Finally, trolleygrid networks have only been studied in tandem with PV systems. This chapter offers the first Wind approach to trolleygrids.

In conclusion, for this chapter, all RES placement would be done on the AC side, using detailed and verified RES and trolleygrid models. The systems will be studied in decentralized and centralized configurations. The former, local and scaled for each substation demand, is to allow for a more distributed installment with lower space requirements and lower transmission losses. The latter, aggregated and scaled for the whole grid demand, is a way of benefiting from a less intermittent base load. Different and specific sizing, storage, and placement conclusions are drawn based on the size of the yearly demand of different substations of the trolleygrid, allowing for better RES system performance.

5.3. RES MODELING METHODOLOGY

5.3.1. MODELING THE SOLAR PV OUTPUT

The PV model is a per-second simulation of the energy output of the solar panels. The model takes into accounts parameters such as: solar altitude (a_S), solar azimuth (A_S), global horizontal irradiance (GHI), diffuse horizontal irradiance (DHI), ambient temperature, ground temperature, and wind speed, to name a few. These values were obtained from Meteonorm [201]. The shading from clouds is considered. However, enough distance is assumed between panels to allow for panel-on-panel shading to be neglected.
The optimal azimuth angle and the tilt angle of the PV module are identified through an iteration in which the yearly irradiance per square meter on the module is calculated for each possible combination of azimuth and tilt. At these positions, the global irradiance on the model, G_M, is:

$$G_M = G_{M,dir} + G_{M,diff} + G_{M,refl} \tag{5.1}$$

Where the terms on the right-hand side are the direct, diffuse, and reflected irradiance on the tilted module, respectively. The detailed equations for these terms are described in [202]. The PV module efficiency is a function of the module's temperature. This temperature is estimated as a function of meteorological parameters using a fluid dynamic model (energy balance between the PV module and the external surroundings). The model presented is based on reference [202]. Two main assumptions are steady state conditions, and that the whole PV module is at a single temperature. The second assumption is justified since the thickness of the solar cells (item of interest) is much smaller than that of the module and so is its heat capacity. The module's temperature, T_M, can be described as:

$$T_M = \frac{(1-R)(1-\eta)G_M + h_c T_a + h_{r,sky} T_{sky} + h_{r,gr} T_{gr}}{h_c + h_{r,sky} + h_{r,gr}} \tag{5.2}$$

Where R is the module reflectivity, η is the module's efficiency, h_c is the overall convective heat transfer coefficient (considering both top and back of the module), and T_a, T_{sky}, and T_{gr}, are the ambient, sky, and ground temperature, respectively. Finally, $h_{r,sky}$ and $h_{r,gr}$ are the linearized radiation heat transfer coefficient between the module and the sky and

between the module and the ground, respectively. The linearization of $h_{r,sky}$ and $h_{r,gr}$ has the value of T_M in its expression, and hence Eq.5.2 is solved iteratively.

The PV module's data sheet provided by the manufacturer show the effect on the efficiency by the deviation of the solar cell temperature from 25°C (STC). The power at the maximum power point of the module, P_{MPP}, at T_M and STC irradiance G_{STC} can be calculated as:

$$P_{MPP}(T_M, G_{STC}) = P_{MPP} + \frac{\partial P_{MPP}}{\partial T}(\text{STC})(T_M - T_{STC}) \tag{5.3}$$

with $\frac{\partial P_{MPP}}{\partial T}(\text{STC})$ as the power temperature coefficient from data sheets. From this, the efficiency at any irradiance and temperature can be calculated as:

$$\eta(T_M, G_{STC}) = \frac{P_{mpp}(T_M, G_{STC})}{G_{STC} A_M} \tag{5.4}$$

where A_M is the module area. Rearranging equation 5.4, the efficiency temperature coefficient $\frac{\partial \eta}{\partial T}(\text{STC})$ can be obtained:

$$\eta(T_M, G_{STC}) = \eta(\text{STC}) + \frac{\partial \eta}{\partial T}(\text{STC})\left(T_M - 25°\text{C}\right) \tag{5.5}$$

Quantifying the effect of irradiance variation on solar cell performance is less straightforward than for the effect of temperature due to a lack of data from manufacturers. According to [202], the overall module efficiency can be approximated as:

$$\eta(T_M, G_M) = \eta\left(25°\text{C}, G_M\right)\left[1 + \kappa\left(T_M - 25°\text{C}\right)\right] \tag{5.6}$$

where the first term represents the effect of irradiance and the second that of temperature, with κ computed as:

$$\kappa = \frac{1}{\eta(\text{STC})}\frac{\partial \eta}{\partial T} \tag{5.7}$$

representing the temperature effect on the performance relative to the STC conditions efficiency. The selected module is the 'AstroSemi 365W' mono-crystalline panels from Astroenergy. The solar modules have a 365 Wp rated power and a 19.7% efficiency.

5.3.2. MODELING THE WIND TURBINE

The wind turbine model uses the same weather data as the PV model and assumes that the turbine will be placed onshore (near Arnhem). The selected turbine is a 3.5MW turbine from NREL, based on their 5MW model, and the key parameters are presented in Table 5.1. The wind speed data is only available at 10 meters above ground level. The scaling to hub height is done in two steps. First, from 10 to 60 meters to account for the surface roughness in the atmospheric boundary layer using the semi-empirical *log wind profile* fit described in Eq.5.8. Second, from 60m to the hub height of 90m using the *power profile* expression represented in Eq.5.9[204].

$$u(z_2) = u(z_1)\frac{\ln((z_2 - d)/z_0)}{\ln((z_1 - d)/z_0)} \tag{5.8}$$

Table 5.1: Parameters for the wind model [203].

Hub height	90 m
Rotor radius, r	53 m
Cut-in wind speed, $v_{\text{cut-in}}$	3 m/s
Cut-out wind speed, $v_{\text{cut-out}}$	25 m/s
Rated wind speed, v_{rated}	11.4 m/s
Rated output power, P_{rated}	3.5 MW

$$u(z_3) = u(z_2)\left(\frac{z_3}{z_2}\right)^{\alpha} \tag{5.9}$$

Here z_1, z_2 and z_3 are the heights at which the wind speeds u_1, u_2, and u_3 are measured or calculated i.e. at 10, 60, and 90 m, respectively. z_0 is the surface roughness factor (0.3 m for wind turbines on land), and α is the power factor which depends on the atmospheric conditions. It is common practice to assume that the atmosphere has on average neutral stability (α=1) [204].

Once the wind velocity at hub height is known, the power delivered by the wind turbine is given by:

$$P_{\text{w}} = \begin{cases} \frac{1}{2}\rho_{\text{air}}\pi r^2 v_{\text{w}}^3 c_{\text{p}} & , v_{\text{cut-in}} < v_{\text{w}} < v_{\text{rated}} \\ P_{\text{rated}} & , v_{\text{rated}} \leq v_{\text{w}} < v_{\text{cut-out}} \\ 0 & , \text{otherwise} \end{cases} \tag{5.10}$$

$$c_{\text{p}} = \frac{P_{\text{rated}}}{\frac{1}{2}\rho_{\text{air}}\pi r^2 v_{\text{rated}}^3} = 0.45 \tag{5.11}$$

Where ρ_{air} is the air density.

5.3.3. DEFINITION OF SYSTEM PERFORMANCE VARIABLES

The indicators defined and used to analyze the variation of the potential of integrating a PV system in a specific substation are:

PV Utilization, U_{PV}: This factor represents the independence from the LVAC grid as the percentage of solar power that is directly used to cover the load of the trolleygrid without being exchanged with the LVAC (Modes 1 and 3 in Figure 5.2):

$$U_{\text{PV}} \triangleq \frac{\int_{\text{year}} (P_{\text{load}} - P_{\text{grid}})\,\text{d}t}{\int_{\text{year}} P_{\text{PV}}\,\text{d}t} \tag{5.12}$$

with P_{load} the total load power demand of the trolleybuses, P_{grid} the power delivered from the AC grid, and P_{PV} the PV generated power.

Direct Load Coverage, Λ: This factor is the fraction of the load that can be directly supplied by the output of the PV system, and it can be calculated by

$$\Lambda \triangleq \frac{\int_{\text{year}} (P_{\text{load}} - P_{\text{grid}})\,\text{d}t}{\int_{\text{year}} P_{\text{load}}\,\text{d}t} \tag{5.13}$$

It is possible to combine Eq.5.12 and 5.13 as

$$\Lambda = \zeta \cdot U_{\text{PV}} \quad \text{(ignoring all converter losses)} \tag{5.14}$$

By defining the **Energy-Neutrality Ratio,** ζ, as:

$$\zeta \triangleq \frac{\int_{\text{year}} P_{\text{PV}}\,\mathrm{d}t}{\int_{\text{year}} P_{\text{load}}\,\mathrm{d}t} \tag{5.15}$$

Which becomes a normalized indication of the size of the PV system installed at a particular substation. For example, a PV system sized to yield the entire bus load demand in a year is said to have ζ=1.
However, accounting for the converter losses, the energy delivered to the buses is found by:

$$\begin{aligned} \text{PV generation} &= \text{PV energy directly used} \\ &\quad + \text{PV energy sent} \\ &\quad \text{to the AC grid and re-used later} \end{aligned} \tag{5.16}$$

$$\begin{aligned} \rightarrow \zeta \cdot \int_{\text{year}} P_{\text{load}}\,\mathrm{d}t = U_{\text{PV}} \cdot \int_{\text{year}} P_{\text{PV}}\,\mathrm{d}t \cdot \eta_{\text{DC}} \cdot \eta_{\text{AC}} \cdot \eta_{\text{r}} \\ + (1 - U_{\text{PV}}) \cdot \int_{\text{year}} P_{\text{PV}}\,\mathrm{d}t \cdot \eta_{\text{DC}} \cdot \eta_{\text{AC}} \cdot {\eta_{\text{ts}}}^2 \cdot \eta_{\text{r}} \end{aligned}$$

Where η_{AC}, η_{DC}, η_{r}, and η_{ts} are respectively the efficiencies of the inverter, DC/DC converter, substation rectifier, and substation transformer (see Figure 5.5).
Re-arranging Eq.5.16:

$$\int_{\text{year}} P_{\text{PV}}\,\mathrm{d}t = \frac{\zeta \cdot \int_{\text{year}} P_{\text{load}}\,\mathrm{d}t}{\eta_{\text{DC}} \cdot \eta_{\text{AC}} \cdot \eta_{\text{r}} \cdot (U_{\text{PV}} \cdot (1 - {\eta_{\text{ts}}}^2) + {\eta_{\text{ts}}}^2)} \tag{5.17}$$

Finally, combining Eq.5.14 and 5.17:

$$\Lambda = \frac{\zeta}{\eta^*} \cdot U_{\text{PV}} \quad \text{(considering converter losses)} \tag{5.18}$$

Where η^* is the denominator term in Eq.5.17. For the study in this chapter, an optimistic efficiency of 99% is assumed for each conversion step (Figure 5.5), and the trolleygrid weighted average of scenario I of 31% for U_{PV}. Ultimately:

$$\therefore \quad \eta^* \approx 0.957 \qquad \text{(this thesis)} \tag{5.19}$$

5.3.4. CASE STUDY DEFINITION

This chapter looks at the 18 substations of the city of Arnhem, The Netherlands.
For all the studied scenarios, the aim is to send the PV power to the buses to increase the sustainability of the grid in the most efficient manner. This is mode 1 of Figure 5.2. In the scenarios with storage, any excess PV energy is sent to the storage first (mode 2), and any further power is sent to the AC grid (mode 3). In scenarios where the AC grid has limits on the AC power it can receive, such as in scenario V, the remaining PV energy is curtailed (mode 4).

Table 5.2: The characteristics of the Arnhem trolleygrid.

Number of Bus Lines	6
Number of buses	42
Number of sections	43
Number of Substations	18
Average section length [km]	1.1
Average daily sunshine duration [h]	4.0
Average yearly irradiance [kWh/m^2]	1165
Average trolleybus energy demand [kWh/km]	2.5
Peak trolleybus power demand [kW]	300
Average trolleybus power demand [kW]	70

Table 5.3: Summary of the characteristics of the six placement and sizing scenarios.

Scenario	RES Type	RES Placement	ζ	Storage	LVAC Exchange
I	PV	Decentralized	1.0	No	Allowed
II	PV	Decentralized	Varying	No	Allowed
III	PV	Decentralized	Varying	No	Allowed
IV	PV	Decentralized	Varying	Yes	Allowed
V	PV	Decentralized	Varying	Yes	Limited
VI	PV and Wind	Centralized	1.0	Yes	N/A

5.4. SCENARIO I: THE DECENTRALIZED ENERGY-NEUTRAL APPROACH WITHOUT STORAGE (ζ=1)

The first approach is to place the PV in a decentralized manner (at each SS), with a size that covers the yearly demand of the substation (energy neutral), and using the AC grid as storage. The sizing results for the different substations in KW peak (kWp) are presented in Table 5.4, and U_{PV} is shown in Figure 5.6.
It is worth defining for the unfamiliar reader that a KWp is a unit of installed PV panel capacity, defined as its nominal output under the standard test conditions of 1000W/m^2, 25^{o}C, and an AM1.5 solar spectrum.

The values of U_{PV} lie between 13% and 38.7%, with a weighted average for the grid at 31.0%. This means that 69.0% of the PV power is sent into the AC grid to be used at a later stage. More specifically, power is sent to the grid in the summer to be recalled in the winter. On the other hand, only 32.4% of the load is covered (Eq.5.18). In this manner, the AC grid still practically provides the trolleygrid load during the largest part of the year.
The results are unsatisfactory because the resulting PV system is too large for the urban environment (over 5 MWp) for only a 32.4% direct load coverage and a significant dependency on the AC grid. It is not, therefore, advisable to size the PV in a fully decentralized, energy-neutral manner without storage.

Table 5.4: Size of the PV system in kW peak (kWp) at each substation for an energy neutral approach without storage (ζ=1).

SS	Size (kWp)	SS	Size (kWp)	SS	Size (kWp)
A	152	G	188	M	244
B	372	H	142	N	305
C	761	I	238	O	231
D	789	J	195	P	158
E	188	K	192	Q	73
F	213	L	376	R	276
				Total	**5093**
				Average	283

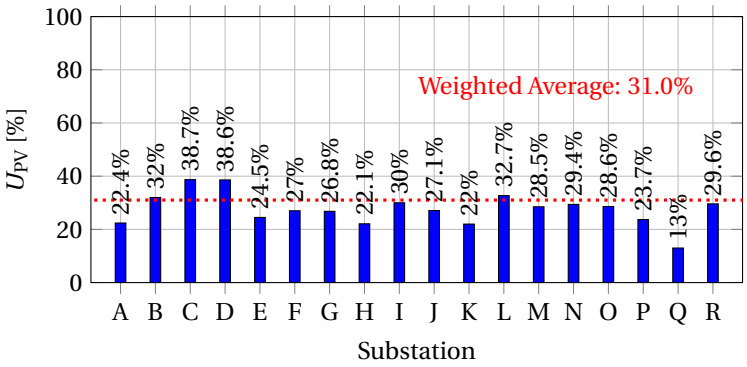

Figure 5.6: PV Utilization (U_{PV}) at each substation in Arnhem for scenario 1: the decentralized energy-neutral approach without storage.

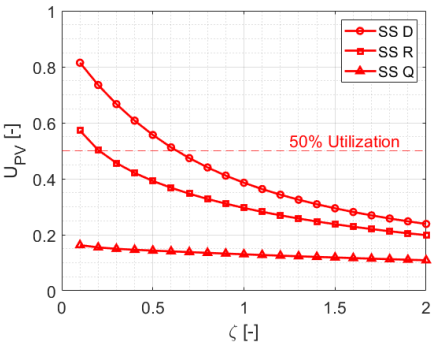

((a)) PV Utilization, U_{PV}, for three substations in Arnhem: Largest (SS-D), average (SS-R), and smallest (SS-Q).

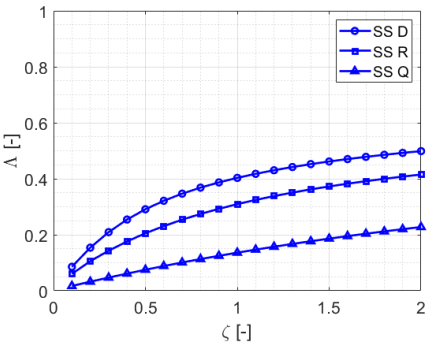

((b)) direct load coverage, Λ, for three substations in Arnhem: Largest (SS-D), average (SS-R), and smallest (SS-Q).

Figure 5.7: PV Utilization and Load Coverage at the three studied substations in Arnhem.

5

5.5. SCENARIO II: VARYING THE PV SYSTEM SIZE WITHOUT STORAGE

The decentralized energy-neutral approach without storage results were not satisfactory because the low PV utilization meant a strong dependence on the grid. This section looks at varying the PV size from ζ=0.1 to 2.0 as another method for avoiding using storage. The motivation is that undersized PV systems ($\zeta < 1$) are interesting because they have a high U_{PV} since they do not generate a lot and therefore do not need to dump a lot. Consequently, however, they do not offer a lot of direct load coverage. On the other hand, oversized PV systems (ζ>1) would offer a high direct load coverage and their excessive energy can be curtailed. The motive is that this procedure is cheaper than installing storage systems as these systems cost more than PV systems. Figures 5.7(a) and 5.7(b) show the results of three substations in Arnhem: The highest (SS-D), average (SS-R), and lowest (SS-Q) substation demand size. Over-sizing the system does not seem to produce interesting direct load coverage results. By doubling the PV system size from ζ=1 to ζ=2, the direct load coverage increases only by 10 percentage points (40% to 50%), 12 points (30% to 42%), and 9 points (14% to 23%) for SS-D, SS-R, and SS-Q, respectively.
On the other hand, under-sizing the PV system to increase its utilization rapidly decreases its direct load coverage. While the U_{PV} can go beyond 80% for SS-D, for example, the direct load coverage, Λ, at that system size is merely 9%.
Undersizing PV systems, without storage, at small substations does not produce promising results. On the other hand, there is a potential for small PV systems at large substations, even if the absence of storage limits them to system sizes that would not offer a lot of load coverage.

5.6. SCENARIO III: MARGINAL UTILIZATION SIZING APPROACH (U_{PV}=50%) WITHOUT STORAGE

5.6.1. SIZING THE PV SYSTEM

It was concluded that the PV Utilization drops rapidly for large systems with increasing system size. Another approach is to size using the marginal utilization, i.e. the difference in utilization brought on by an increment in the system size. In this method, the system size is increased until the point where adding 1 kWp of PV would result in more of its yearly yield $E_{y/kWp}$ being dumped than utilized. In Arnhem, this value is 1155.7 kWh/kWp. In simpler terms, this is equivalent to sizing the system at each substation for U_{PV}=50%.

The method is explained by the flowchart in Figure 5.8, and the results are presented in Figure 5.9.

For 4 out of the 18 substations in Arnhem, namely substations A, E, K, and Q, the suggested PV system size is zero. This is already expected from Figure 5.7(a) as SS-Q does not reach the 50% utilization line even for very small PV system sizes. Figure 5.9 also echoes the results found for SS-D and SS-R in Figure 5.7(a) looking at the system sizes at the 50% utilization line.

5.6.2. TRAFFIC VIEW FACTOR

The wide difference between the suggested PV system sizing for the substations in Figure 5.9 can be traced again back to Figure 5.1. The bus traffic under some substations is so infrequent that the PV system would not *see* a bus for long periods of time. To further explain this difference, define the parameter "bus traffic view factor of the PV" for a substation as the fraction of the PV generation time where the PV system sees *at least* one

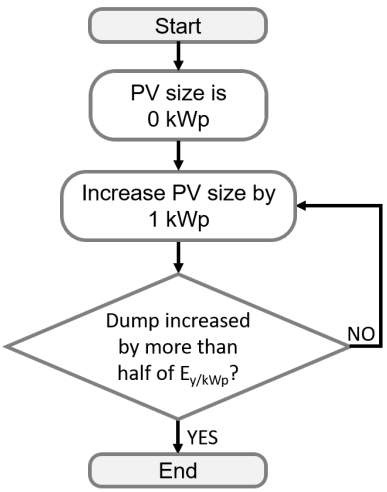

Figure 5.8: Flowchart for the PV system sizing in the Marginal Utilization Sizing approach (U_{PV}=50%) without storage (scenario III).

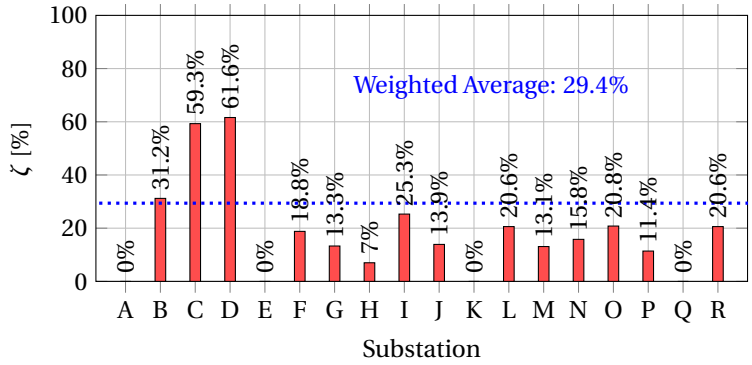

Figure 5.9: Attainable fraction of energy neutral sizing for each substation using the Marginal Utilization sizing approach. For substations A, E, K, and Q, no PV is advised.

5

bus under the substation. Mathematically, it can be expressed as:

$$\Phi_{B/PV} \triangleq \frac{\Sigma\text{time}(PV \cap \text{Bus})}{\Sigma\text{time}(PV)} \tag{5.20}$$

The $\Phi_{B/PV}$ in Arnhem varies between 0.17 and 0.89, with an average of 0.62. This means that, on average, a PV system in Arnhem does not see a bus for 38% of the sunshine hours. It follows then that even an infinitely small PV system is not able to power the buses without storing a considerable part of its energy in the AC grid. In mathematical terms:

$$\lim_{\text{PV Size}\to 0} U_{PV} = \Phi_{B/PV} \tag{5.21}$$

As for the direct load coverage, Λ, the maximum attainable value, even for an infinitely large system, would be the fraction of the trolleybus demand that occurs during the sun hours. With no storage system in place, the PV system cannot power the bus traffic before sunrise and after sunset. Assuming an average consumption by the buses throughout the year, the ratio of energy consumption can be approximated by the ratio of time duration as expressed by:

$$\lim_{\text{PV Size}\to\infty} \Lambda = \frac{\Sigma^{\text{time}(PV\cap\text{Bus})} P_{\text{Bus}}}{\Sigma^{\text{year}} P_{\text{Bus}}} \approx \frac{\Sigma\text{time}(PV \cap \text{Bus})}{\Sigma\text{time}(\text{Bus})} \tag{5.22}$$

The estimate offered by Eq.5.22 can be made even more accurate by averaging the limit for each month of the year rather than for the whole year. This is because in the winter months, the sun hours are shorter and the bus load is higher, while in the summer months, the opposite is true. Figure 5.10 shows a trend between the traffic view factor of the PV system and the system size for 50% PV Utilization. The four substations A, E, K, and Q that have a suggested PV size of 0 kWp by this method can be traced to having a $\Phi_{B/PV}$<50%. This means that the PV system at these locations does not see the bus for more than half of the sun hours, consequently, no PV system size will reach a U_{PV}>50%. An increasing trend is reported in the same Figure between $\Phi_{B/PV}$ and the system size

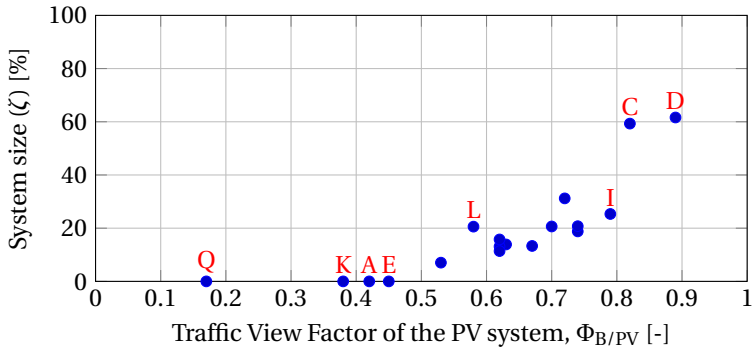

Figure 5.10: PV system size as a fraction of the Energy Neutral size for each substation versus the traffic view factor of the PV system $\Phi_{B/PV}$.

for 50% PV Utilization. This motivates the placement of PV systems at high $\Phi_{B/PV}$ locations. However, some trends are not fully explained by only looking at this parameter alone. For example, substations I and L have about the same system size recommendation (25.3% and 20.6%, respectively) despite SS-I seeing about 20 percentage points higher in traffic than SS-L. Additionally, SS-I and SS-C have about the same $\Phi_{B/PV}$, yet the recommendation for SS-C is a system size of about 2.5 times that of SS-I (ζ=59.3%). One explanation of this behavior is that the $\Phi_{B/PV}$ only takes into account the presence of a load, not its magnitude. SS-C has, in fact, 3.2 times the load demand of SS-I. Figure 5.7(a) already predicted that larger substations see a better PV Utilization.
The Marginal Utilization Approach offers a ζ=29.4% as a weighted grid average, which translates to only a 15.4% direct load coverage, Λ, according to Eq. 5.18. This method is superior in performance if compared to the first scenario of the decentralized energy-neutral approach. In the earlier method, an energy-neutral system (ζ=100%) offered 31% direct load coverage, while this method offers half of this direct load coverage (Λ=15.4%) by installing less than a third of the former system size (ζ=29.4%), meaning far less exchange with the grid and a much lower cost per kWp installed. However, the disadvantage of the marginal utility method, is that it leaves out some substations completely to be powered by the grid (here, SS-A, E, K, and Q).

5.7. SCENARIO IV: THE DECENTRALIZED GENERATION WITH STORAGE APPROACH

This method looks at storage as a way to increase the utilization of the PV system and its load coverage. Figures 5.11(a) and 5.11(b) summarize the results of the direct load coverage, Λ, for different PV system sizes, ζ, and storage sizes for substations D and Q, respectively.
Storage does not seem to benefit the direct load coverage for a large substation such as SS-D, until a steep increase in direct load coverage at the order of hundreds of kWh. This is because high load/traffic substations already have the advantage of a steady load base (see Figure 5.1) that directly utilizes more of the daily PV generation. An advantage is

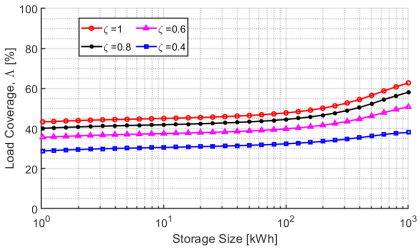

((a)) Direct load coverage, Λ, for different ζ values and storage sizes for the large substation D.

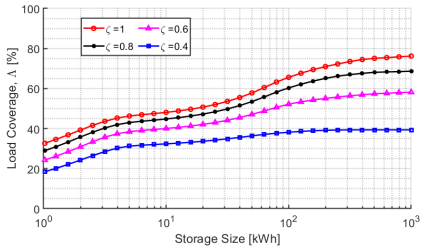

((b)) Direct load coverage, Λ, for different ζ values and storage sizes for the small substation Q.

Figure 5.11: Approximation 2 always underestimates it (but errors under 10V).

only observed when stepping into systems at the order of seasonal storage, where these large storage systems can gather the PV energy in the summer to be used in the winter. However, a storage system as large as 1 MWh, has only increased the direct load coverage of SS-D from 44% to 63% for the ζ=1 case.

Meanwhile, for a small substation such as SS-Q, storage benefits the direct load coverage through a steep increase in the direct load coverage even for relatively small storage system sizes. This can again be traced back to Figure 5.1, where it is clear that a mismatch is far more pronounced between the PV and the load in low-traffic substations. Small storage systems can help carry the PV energy generated in the short no-load periods between buses on the trolleygrid section. Storage systems of the order of seconds/minutes ($<10^1$kWh) affect all the ζ cases by 12 to 17 percentage points higher in direct load coverage.
Storage on the daily level (between 10^1 and 10^2 kWh) has also benefited the direct load coverage. However, while the increase is still steep in the cases of ζ=0.8 or 1.0, with another 16 percentage points, it is less pronounced in the cases of ζ=0.6 and 0.4, where the direct load coverage increased only by 12 and 5 percentage points, respectively. This is because, at large PV system sizes (high generation), the mismatch in generation versus load becomes more important than the temporal mismatch between the presence of a load and the PV generation (more important role at low generation levels). In simpler terms, there is more to store with larger PV systems on a daily level. In contrast, smaller systems start to behave sooner on the storage scale like a seasonal storage scenario because their small daily generation is already stored completely by any system between 10^1 and 10^2 kWh. In conclusion, for large substations, storage is not recommended, and smaller PV systems seem more attractive. Meanwhile, a larger PV system size (high ζ) and a storage system are recommended for smaller substations.

5.8. SCENARIO V: THE LVAC GRID EXCHANGE LIMIT APPROACH (PV CURTAILMENT)

So far, the sizing strategies have taken the grid as a fully available sink to the PV excess energy without considering power quality issues or local policy restrictions. The sizing of

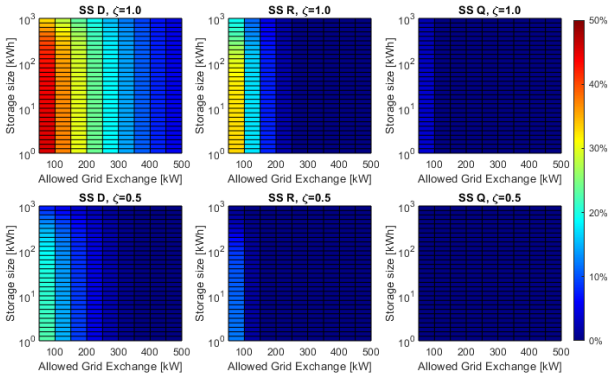

Figure 5.12: Percentage of curtailed PV energy as a function of the storage system size and the allowed exchange with the AC grid for different PV system sizes at substations D (trolleygrid highest load demand), R (average demand), and Q (lowest demand).

the PV and storage systems in this section considers the maximum allowable exchange with the AC grid, and curtails (wastes) the remaining PV generation (Mode 4 of Figure 5.2). Figure 5.12 shows the percentage of the PV generation that is curtailed at ζ=1 and 0.5 and various storage sizes and allowable power exchange levels with the AC grid, for substations D, R and Q, respectively.

The busy substation D needs a large PV system and is, therefore, more prone to sending higher surges of power, and more frequently, to the AC grid. The curtailment can be as high as 45.5% and 22.7% for ζ=1 and ζ=0.5, respectively. For the average substation R, the values can be as high as 33.1% and 12.1% for ζ=1 and ζ=0.5.

The smaller substation Q, on the other hand, requires a small PV system. For a size of only ζ=0.5, the PV output can be used entirely (maximum curtailment of 0.0%). For ζ=1, the curtailment is only 3.9% in the most restrictive cases, but is 0.0% if an exchange of 100kW is permitted.

Small substations, therefore, offer a more feasible implementation of PV systems with minimal storage and grid interference. Interesting to note that the curtailment value is not affected much by the storage size when strict dumping levels are imposed. This is again a consequence of the seasonal variation of PV and the bus load and the necessity for seasonal storage and imposes a hurdle on the implementation of PV systems for the trolleygrid energy-neutrality. The same trend is observed for the larger substations, where the curtailment is considerable. This reconfirms the suggestion of scenario IV that small substations should have large PV systems and vice-versa.

5.9. SCENARIO VI: THE CENTRALIZED ENERGY-NEUTRAL WIND AND PV APPROACH (AGGREGATED APPROACH)

The final approach is to size the PV system or the Wind system in an aggregated manner for the whole grid. This can be done by contracting a PV or Wind energy supplier, for example, the way the Dutch railways operate. The advantage of this method from the

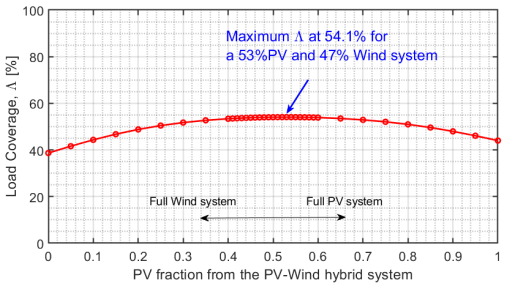

Figure 5.13: Direct Load coverage as a function of the RES system composition (PV and Wind, no storage).

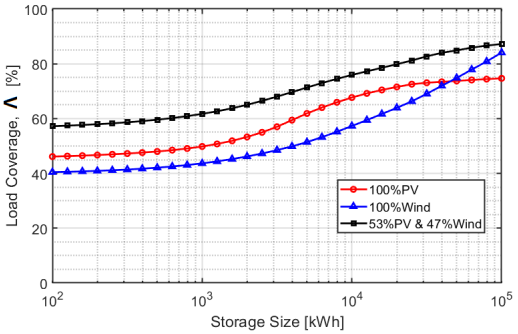

Figure 5.14: Direct Load coverage as a function of the hybrid RES system composition (PV and Wind, with storage).

point of view of utilization is that on the grid level, there are loads present at all times, unlike at the fragmented substation level.

Figure 5.13 shows the direct load coverage, Λ, of the aggregated approach from a full wind system to a full PV system. The full wind system achieves a Λ of 39% while the full PV system reaches 45%. The highest Λ value of 54.1% is obtained for a hybrid system of 53% PV and 47% wind. The superior outcome of the hybrid approach is an expected result as it has been explained earlier in figures 5.3 and 5.4 that while the PV generation matches the bus profile better on a daily basis, the wind generation matches it better on a yearly basis. A hybrid solution would therefore have a lower need for storage systems. Figure 5.14 shows the increase in direct load coverage by including storage. The aggregated grid behaves like a large substation, which explains why the PV system equipped with storage does not see much of an increase in load coverage, as seen earlier in Figure 5.11(a) when studying a single, high-traffic substation. However, the wind system equipped with storage overtakes the PV system and becomes almost equal in performance to the hybrid system from storage systems at the order of daily storage (10^4 kWh at this system size). This is because the wind system benefits more from the daily storage systems, while the PV needs storage systems at the seasonal level to finally start yielding advantages.

5.10. CONCLUSIONS

This chapter looked into a nuanced approach to the placement and sizing of RES systems at different trolleygrid substations based on the expected bus power demand.

Six different approaches were simulated and assessed based on the direct RES utilization and the direct load coverage of their suggested RES systems. These are: Decentralized energy-neutral PV without storage (Section 5.4), decentralized PV of different sizes without storage (Section 5.5), Decentralized PV sized for 50% utilization and without storage (Section 5.6), Decentralized PV system of different sizes and with storage (Section 5.7), decentralized PV system of different sizes and with storage and AC exchange limitations (PV curtailing) (Section 5.8), and centralized PV and/or Wind systems with/without storage (Section 5.9).

In summary, the best recommendation for the sustainable powering of the trolleygrid from the AC side is to aggregate the generation for the whole grid. A hybrid PV/Wind system proved superior to a full wind or full PV option. Still, the system had a direct utilization of 54.1%, which means that almost half of the generated energy needs to be stored or curtailed if the AC grid imposes limitations on the accepted power. Furthermore, this is not a favorable solution in terms of sizing and placement as it is simply a contractual workaround to the trolleygrid sustainability problem, and the local grid might be too congested or too weak to accept such a scenario. As a decentralized system is still preferred for sizing or location limitations, the recommendation is to undersize the PV systems for large substations (aiming for U_{PV}=50%) and without storage. In contrast, the smaller substations could be sized for full energy neutrality and would benefit greatly from storage systems, even at relatively small sizes. Yet, in both cases, the techno-economic feasibility of the PV project is risky and relies either on expensive storage systems or severe curtailment of the generation of PV systems. This means that the PV system will have a higher effective cost of energy, and its installed panels will be effectively underutilized. At the same time, they are already limited in physical installation space, which makes this curtailment option even less favorable.

While some recommendations are offered based on the traffic conditions, Figure 5.10 exposed that variables other than the traffic affect the PV Utilization and warrant our attention. For this reason, more work is recommended on a more comprehensive list of Key Performance Indicators (KPIs) that could bring better insights into sizing and placement.
Furthermore, more research is needed into the integration of more loads into the trolleygrid (EV chargers, for example), to create a more constant base load for the PV system, both increasing its utilization by the same advantages of the aggregated scenario and sharing the cost of sustainable energy production among multiple stakeholders.

Finally, the scenarios of this chapter focused primarily on energy-neutral PV sizing per substation, and most of the sizing recommendations came tied with certain utilization values. However, these utilization values are not easily obtained without extensive grid and RES modeling, which is not readily available to most grid operators. Also, an inves-

tigation is still needed to look at different PV sizes and at combined substations in an effort to increase the techno-economic feasibility of the PV system.

To answer this, the following chapter proposes a simple estimation approach to the calculation of the utilization of a PV system of any size at any trolleygrid substation or combination of substations.

6

ESTIMATING THE PERFORMANCE OF PV SYSTEMS IN TROLLEYBUS GRIDS

"Voi che sapete
Che cosa è Amor,
Donne, vedete
S'io l'ho nel cor..?"

Voi Che Sapete - Act II, Le Nozze di Figaro (Mozart)

```
You who know
what love is,
Ladies, look and see
If I have it in my heart..?
```

This chapter is based on [79]: I. Diab, A. Saffirio, G. R. Chandra-Mouli, and P. Bauer, "A simple method for sizing and estimating the performance of PV systems in trolleybus grids," Journal of Cleaner Production, p. 135623, 2022.

As the previous chapter explained, no consensus exists yet on the placement or sizing of PV systems at the traction substations, and no method is available for easy estimation of the PV system utilization performance. The latter is crucial for understanding the need for storage, grid exchange, or even power curtailment, and has a direct impact on the technical and financial feasibility of the project.

The chapter begins with an explanation of PV integration in trolleybus grids in Section 6.1. Section 6.2 details the methodology used for the analysis in this chapter. Then, Section 6.3 presents the results of the 11 KPI studies made on the trolleygrids of Arnhem, The Netherlands, and Gdynia, Poland. From this analysis, Section 6.4 explains the formulated third-degree polynomial for the PV system performance estimation, which is expanded in Section 6.5 into an advised methodology for the sizing of these systems and their placement. Finally, Section 6.6 offers some conclusions and future work recommendations.

It is important to note at this stage that the contribution of this chapter is in exposing the existence of clear mathematical trends and plateaus that allow the estimation of the PV system performance in trolleygrids and offer sizing and combination insights. As of now, the derived trends in this chapter are purely empirical, and future works are encouraged to identify the underlying variables that describe these trends.

6

6.1. INTRODUCTION

While the electrification of urban transportation is already a mature and efficient method of sustainable urban transport [205], the solution is only meaningful if the supply power comes from sustainable sources. So far, the global transport sector still relies heavily on fossil fuels and accounts for about 24% of total GHG emissions [199], [206]. In Europe, this number stands at 40% [207].
PV systems are an attractive solution for the sustainable electrification of transport networks as they are DC systems like these networks, scalable, and easy to install in an urban environment. So far, PV systems are the most promising and also most implemented source for this type of application [11], [16], [22], [50], [80], [208]–[212]. However, there is still no consensus on methods of PV sizing or placement, and no readily accessible ways for grid operators to estimate the success and performance of these systems except by outsourcing detailed, complex, and costly modeling tools [11].

6.1.1. THE TROLLEYBUS GRID WITH PV IN LITERATURE

The sizing and placement of PV systems in trolleygrids and the degree of independence they can offer from the LVAC grid is an understudied field. This lack of research leaves trolley cities unable to estimate -or worse, unaware of- their PV potential. For example, as seen in the literature and in this chapter, the direct utilization of the generated PV system power by trolleybus(es) can vary significantly from substation to substation within the same city, from around 10% to 80% [11], [208], [209].
This creates the urgent need for an estimation method for the PV performance in trolleygrids, to avoid the installation of economically unfeasible PV systems at low-potential substations and/or at non-optimal system sizes. So far, the studies in the literature have

been mostly statistical, limited to one PV system size, and did not go in-depth into analyzing the causes of these differences, nor offer simple ways to predict the PV performance at different substations [50], [208]–[214]. This chapter presents a method for this purpose.

CHAPTER CONTRIBUTIONS

This chapter offers the following 4 contributions:

1. A thorough study and assessment framework for the PV system direct utilization and load coverage at a single trolleygrid substation as a function of a number of readily-available grid parameters to the transport grid stakeholders using detailed and validated bus, grid, and PV models and two trolleybus countries as case studies (The Netherlands and Poland)

2. A simple, empirically-identified, three-variable function that allows stakeholders to quickly estimate and assess the potential and performance of a PV system of any size connected to a single trolley substation, instead of requiring a complex grid, PV, and bus modeling

3. The identification of a saturation plateau in the PV system performance at a single substation that challenges what has been previously reported in the literature that larger substations would always report a better PV utilization

4. A proposed methodology for the sizing of a decentralized PV system shared by a group of neighboring substations for increasing the system performance, based on a simple, empirically-identified, three-variable function instead of the complex grid, PV, and bus modeling

6.2. CHAPTER METHODOLOGY

To study the mismatch between the trolleygrid load and the PV generation, the following three subsections present first the PV system placement, then the modeling methodology for the load (the individual buses and then the substations), and finally, the PV output power modeling. In subsection D, some performance indicators are defined to assess the utilization of the PV system. Subsection E introduces the two case study cities used in this chapter.

6.2.1. PV SYSTEM PLACEMENT

For this chapter, the PV and storage are installed on the AC side (Figure 5.5), which admittedly reduces the efficiency of the connection, since the generated solar energy has to be converted from DC to AC and then back to DC to supply the buses. However, while alternatively installing the PV on the DC side would reduce the system losses by using fewer power conversion steps, this configuration would not allow the PV to send its excess energy back to the main AC grid (substation diode rectifiers). Even if storage is installed, considerable curtailment of the PV power is expected, as the required seasonal storage would be unrealistically large[209], [214]. Moreover, placing the PV system on

Table 6.1: Comparison of the two case study grids of this chapter.

Parameter	Gdynia	Arnhem
Number of Bus Lines	12	6
Number of buses	84	42
Number of sections	30	43
Number of SS (Substations)	10	18
Section/Substation ratio	3	2.4
Bus/Substation ratio	8.4	2.3
Average bus traffic per substation	3.1	1.1
Yearly grid energy demand [Normalized]	1.00	0.747
Average yearly substation energy demand [Normalized]	0.10	0.041
Length of sections - average [km]	1.3	1.1
Average daily sunshine duration [h]	4.4	4.0
Average yearly irradiance [kWh/m^2]	225	190

the DC side could introduce strong voltage fluctuations on the section due to the intermittent PV power generation and the difficulty of gauging an output set-point. This is because the short-term variability of the PV output can present power fluctuations of 45-90% of the rated power of the system, and would indeed require more sophisticated converters for the trolleygrid stability [208], [215], [216].

Another solution is to replace the unidirectional substations with reversible or bidirectional substations equipped with inverters that allow exchange from the DC to the AC side [10], [38] from both the PV and the braking buses. However, this requires an overhaul of the trolleygrid infrastructure and is out of the scope of this chapter.

For these reasons, the PV system is placed in this chapter on the AC side for the PV integration in the trolleybus grid.

6.2.2. CASE STUDY DEFINITION

The trolleygrids of the cities of Arnhem, the Netherlands, and Gdynia, Poland, are taken as case studies for this research. The choice is made for these two cities as they have very different trolleygrid characteristics but a similar solar profile, allowing for a more generalizable study. It is an important validation that despite the stark differences between the trolley networks of Gdynia and Arnhem, the proposed methods in this chapter are still valid, as will be shown in the coming sections. Table 6.1 provides an overview of the key characteristics of the two grids.

Compared to the Arnhem grid, the Gdynia trolleygrid is characterized by double the number of bus lines and bus fleet size and a higher yearly load demand. Meanwhile, the Arnhem grid is fragmented into more sections and substations than the Gdynia grid. Namely, the Arnhem grid is characterized by 43 sections fed by 18 substations, while in Gdynia, 30 sections are fed by 10 substations. Finally, Gdynia substations see about 3 times the average traffic than those in Arnhem would see. These two cities offer thereby two very different trolleygrids infrastructures under a similar sun profile. All PV systems at the substations have been sized for ζ=1 (net energy neutral) unless otherwise stated.

6.3. FAMILIES OF VARIABLES THAT AFFECT THE PV UTILIZATION, U_{PV}

Any variable that influences or measures the direct PV utilization can be traced back to having an effect on, or a measure of any of these three levels/families:

- The **PV Output** (e.g., solar irradiance), and/or
- The **Load** (e.g., HVAC demand), and/or
- The **PV** $\cap$ **BUS**, which is the total time duration when there is simultaneously a bus demand (load) and a non-zero PV generation

For example, cloud coverage can affect the **PV Output** by reducing the irradiance, but can also affect the **PV**$\cap$**BUS** if the clouds block the sun generation completely. Recurring traffic lights can delay the presence of a bus on a section and cause more regenerative braking, both of which are phenomena that can alter the **Load** under a substation. If the regenerative braking is high enough, the braking bus can completely supply another bus on the section and effectively *mask* it from the PV, affecting the **PV**$\cap$**BUS**.
Using full-year bus, grid, and PV simulations for all substations in Arnhem and Gdynia, Table 6.2 summarizes the KPIs studied in this chapter, their effect on the three influence levels mentioned above, and their correlations to PV Utilization (curve fit and R-squared values [217]). Five of these KPIs are then explained in detail in the following sections.

Table 6.2: KPI correlation to the PV Utilization, U_{PV}, across the simulated traction substations of Arnhem and Gdynia (**H**: High, **L**: Low, **x**: none).

Substation KPI Parameter	Effect on/ Measure of PV	Load	PV∩BUS	Best fit [type, R^2]	Comments
Equivalent sun hours, ESH [h]	**H**	x	x	N/A	All substations in a city would have the same value for this KPI; **More details in Section 6.3.1**
After-sunset fraction of daily bus schedule[%]	**L**	x	**L**	Log, **0.08**	All substations have a value of 10-20% for this KPI; no correlation can be observed
Yearly average transmission losses [%]	x	**H**	x	Linear, **0.22**	While this KPI gives a clear indication of the bus traffic and load, it offers no insights on the other levels
Total supplied catenary distance, d_{ss} [m]	x	**L**	**L**	Log, **0.39**	Shortcoming: No indication of traffic; e.g: end-of-line sections can be long yet empty; **More details in Section 6.3.2**
Specific Traffic KPI $\overline{N_{bus}}/d_{ss}$ [bus/km]	x	**L**	**L**	Log, 0.51	Shortcoming: Same KPI value if 2bus/1km or 1bus/0.5km, overlooking their different braking energy recovery & PV∩BUS
Specific Energy KPI E_{ss}/d_{ss} [MWh/km]	x	**H**	**L**	Log, 0.63	Shortcoming: Despite high bus and traffic insight, not much indication into the section length and hence not into PV∩BUS
Yearly average bus traffic: $\overline{N_{bus}}$ [bus]	x	**H**	**L**	Log, 0.84	Shortcoming: Similar substation KPI value if 1 bus, or if 2 buses half the time and 0 otherwise; **More details in Section 6.3.4**
Distance energy KPI $E_{ss} \cdot d_{ss}$ [MWh.km]	x	**L**	**H**	Log, 0.86	Shortcoming: Similar KPI values for long sections with low energy demand and short sections with high demand
Traffic distance KPI $\overline{N_{bus}} \cdot d_{ss}$ [bus.km]	x	**L**	**H**	Log, 0.86	Shortcoming: Similar KPI values for long sections of low traffic and short sections of high traffic
Yearly energy demand: E_{ss} [MWh]	x	**H**	**H**	Log, **0.93**	**More details in Section 6.3.3**
Traffic energy KPI: $E_{ss} \cdot \overline{N_{bus}}$ [MWh.bus]	x	**H**	**H**	Log, **0.91**	**More details in Section 6.3.5**

Table 6.3: Change of the U_{PV} and Λ (in percentage points) for the same PV system (sized for Gdynia as a benchmark) when subjected to the yearly sun profiles of different cities.

Sun profile	Gdynia	Arnhem	Szeged	Athens
ESH [h]	4.4	4.0	5.5	7.6
Irradiance [W/m^2]	140	130	180	210
PV System Total Size (at all substations) [MWp]	6.57 (ζ=1)	Gdynia system	Gdynia system	Gdynia system
Change in Grid Median $U_{\mathbf{PV}}$ [percentage points]	benchmark	+1.4	-0.9	-1.3
Change in Grid Median Λ [percentage points]	benchmark	-0.5	+5.5	+10

6.3.1. KPI: YEARLY IRRADIANCE AND EQUIVALENT SUN HOURS

A sun hour is equivalent to 1000 W/m^2 collected in 1 hour of sunlight. Equivalent Sun Hours (ESH) is then not only influenced by the sunrise and sunset times, but also by the local cloudiness that can block out the sun [218]. This parameter has thereby an impact on the output of the PV installed capacity and on the time of the day during which the trolleybus is able to *see* and utilize this output, i.e., **PV∩BUS**.

In Table 6.3, the change in U_{PV} and Λ are shown as a function of these two parameters for a median of all studied Gdynia substations. For these simulations, the same PV systems at each substation of Gdynia were subjected to the same bus load demand, yet to different sunshine profile data (read: ESH) of Arnhem, Gdynia, Szeged (Hungary), and Athens (Greece) for one year of operation. The trolleygrid U_{PV} is not affected noticeably between the four cases. On the other hand, the Λ varies by more than 10 percentage points.

This can be better understood when deconstructing the PV Utilization as the result of two mismatches between the traction substation load demand and the PV generation: A temporal or horizontal mismatch (the moments where there is generation but no load, and vice versa), and a power or vertical mismatch (the moments when the generation and load are not equal, but still not zero).

The temporal mismatch (i.e., **PV∩BUS**) can be visualized by revisiting Figure 5.1(b), where the effect is clear on the low PV utilization as a consequence of the mismatch between the infrequent bus presence and the PV generation. This is an inherent behavior in any transportation network. Furthermore, there would be many bus operation hours after sunset (i.e., zero generation), which then adds to this effect.

Secondly, a sunnier city profile means both an increase in sun hours as well as peak irradiance. This means that the increase in ESH is also an increase in the magnitude and frequency of the PV power peaks and its mismatch with the trolleygrid demand, taking away from any obtained U_{PV} advantage from one city sun profile over the other. This means that while sunnier locations offer a better temporal/horizontal match between load and generation, they offset this benefit by a larger power/vertical mismatch, for the

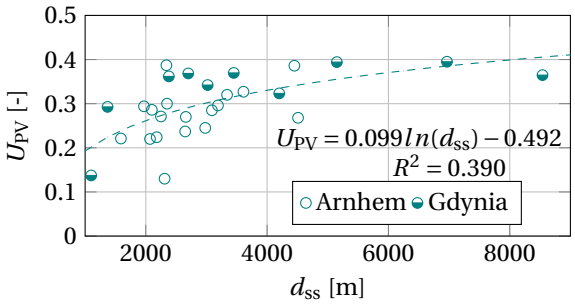

Figure 6.1: PV Utilization, U_{PV}, as a function of the distance covered by each substation, d_{ss}. No trend can be concluded for this KPI.

same PV system size.
Finally, it might sound counter-intuitive that the same PV system size would have the same utilization when subjected to the much sunnier profile of, for example, a city like Athens. It is good to recall then that the PV Utilization is a parameter that looks at the matching between load and generation, and is normalized to the PV generation (see Eq. 5.12). It is the load coverage of Eq.5.13 that offers insight into the amount of energy consumed. This justifies why, as seen in Table 6.3, there can be more load coverage (total generation) with a sunny profile while keeping a similar utilization (i.e.,*portion* of the power that is not in excess).
In summary, the study of these two sun parameter KPIs in detail justifies the low influence of **PV Output** in Table 6.2 and the high influence of **PV∩BUS**, on the other hand. This also validates the counter-intuitive phenomena in the later sections of this chapter of why both the Arnhem and Gdynia substations, despite their major grid architectural and operational differences, agree on the same KPI trend curves and exhibit a common PV system performance behavior.

6.3.2. KPI: SUBSTATION TOTAL SUPPLIED CATENARY DISTANCE: d_{ss}

The increase in the value of this KPI could be expected to reflect higher total demands and traffic under a substation. However, more buses would also mean higher chances of sharing the regenerative braking power, P_{net}, instead of the use of braking resistors, P_{BR}. This could bring down the demand on the substation, P_{load}, creating more excess generation than would have been expected. These opposing phenomena justify the lack of a trend between the U_{PV} and the d_{ss} in Figure 6.1. The total length of the supply zone of a substation does not offer a trend as it includes a number of contradicting variables (explained above) and does not offer enough information about the trolleygrid infrastructure and traffic. For example, Substation Q in Arnhem (previously seen in Figure 5.1) has a d_{ss} of 2.31 km and a low U_{PV} of 13% as it is covering the low-traffic end-of-line areas of a bus route. On the other hand, Substation D with a similar d_{ss} of 2.34 km and yet a U_{PV} of 38.6% is covering busy and central roads. In short, the d_{ss} parameter carries within it too many contradicting parameters to offer any usable trend for the estimation of PV performance in trolleygrids, and will not be considered any further.

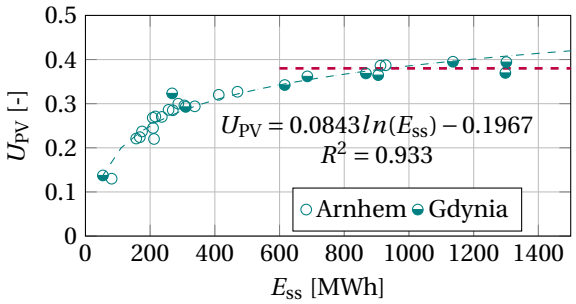

Figure 6.2: PV Utilization, U_{PV}, as a function of energy demand of each substation, E_{ss}. A plateau is observable starting 600 MWh.

6.3.3. KPI: SUBSTATION YEARLY ENERGY DEMAND: E_{SS}

The Substation Load Demand gives a direct indication of the bus power demand as well as the bus traffic and an indirect insight into the bus braking energy recovery. This indirect insight comes from the fact that high utilization of braking energy would already be reflected in a lower substation demand. These powerful insights can be contrasted with the d_{ss} KPI which would not offer information on the traffic and braking.

Figure 6.2 shows the correlation between the PV utilization and the substation energy demand in MWh. A strong logarithmic correlation exists with an R^2 value of over 0.93, indicating a good fit.

This fit seems to reach a plateau (the red dotted line) for values over 600 MWh. The substations of 686 and 1298 MWh report almost the same PV utilization at 36.18% and 36.97%, respectively. The 5 substations in between, a mix of Arnhem and Gdynia substations, hover around this same U_{PV} value.

This contradicts the previous proposition in the literature that a larger substation would always see a better PV utilization [11], [208], [209]. The main reason is that PV utilization is also subject to seasonal variations. The large PV systems would over-produce in the high-irradiance summer months when the buses typically run on less-frequent timetables and without the considerable HVAC heating demand. Large PV systems, therefore, would see a low utilization in the summer months, bringing down their average yearly U_{PV} value.

6.3.4. KPI: SUBSTATION YEARLY AVERAGE BUS TRAFFIC: $\overline{N_{BUS}}$

Another important, and yet readily available grid parameter is the average traffic under a substation, $\overline{N_{bus}}$, from bus schedules. A trend is also observable in Figure 6.3, although its R^2 value is only at 0.835, which is lower than the one found between U_{PV} and E_{ss}. However, the advantage of this KPI is that it visually disperses the substations on the trend curve more than the previous KPI. For example, the two Arnhem substations of around 900MWh are now considerably apart, at values of $\overline{N_{bus}}$ equal to 2.8 and 4.6. However, the two substations share the same U_{PV} (38.6% and 38.7%). This confirms the existence of a plateau in the PV Utilization and motivates the inclusion of $\overline{N_{bus}}$ in the performance estimation. The U_{PV} plateau can be observed in Figure 6.3 for values of

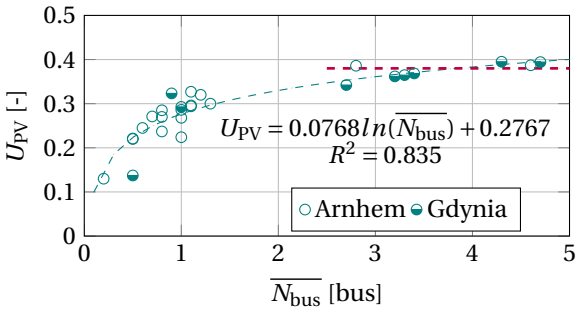

Figure 6.3: PV Utilization, U_{PV}, as a function of the substation average traffic, $\overline{N_{bus}}$. A plateau is observable starting 2.5bus.

$\overline{N_{bus}}$ above 2.5 bus (red dotted line).
These plateaus are an unavoidable consequence of both the daily mismatch between the intermittent bus scheduling and the PV generation (recall Figure 5.1), and the seasonal mismatch explained in the previous KPI subsection. This urges trolleygrid cities to integrate more smart grid components such as electric vehicle chargers or stationary storage systems into their infrastructure in the hope of increasing the substation U_{PV} values. These additional base loads can thereby help push this intrinsic saturation plateau to higher performance values by utilizing the PV generation when there is no (or little) bus demand, making the PV system more economically feasible and reducing the need for storage, exchange with the AC grid, or curtailment.

6.3.5. KPI: SUBSTATION TRAFFIC ENERGY: $E_{SS} \cdot \overline{N_{BUS}}$

To combine the trend of the energy substation demand KPI, E_{ss}, and the dispersing effect of the substation average bus traffic KPI, $\overline{N_{bus}}$, a new KPI is defined as the substation Traffic Energy: $E_{ss} \cdot \overline{N_{bus}}$.
Although this KPI does not have a physical interpretation, it mathematically combines two important trolleygrid substation parameters and offers insights into PV utilization and sizing. In Figure 6.4, the substations clearly communicate whether they are at the plateau of performance, or whether they are *behind the knee* of the performance curve. This offers a clear insight to trolleygrid operators on which PV systems need to be resized and/or combined with other systems. Section V addresses this latter topic in more detail.
Another advantage of this KPI over the E_{ss} KPI is that it better estimates the performance of a combined PV system (a PV system serving multiple substations). For example, a centralized PV system for the whole Arnhem grid has a U_{PV} of 42% from previous simulations in Chapter 5. The E_{ss} KPI curve would over-estimate this at 53%, while the Energy Traffic KPI curve places it at 41%. Section V addresses the topic of substation combination in more detail.

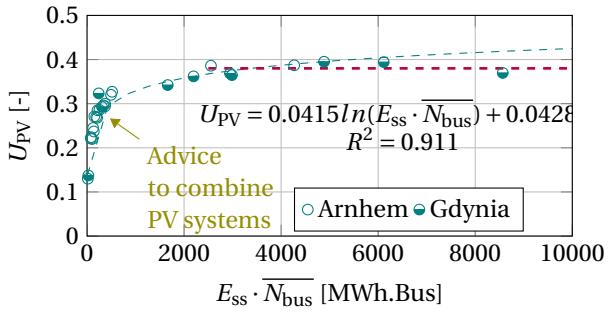

Figure 6.4: PV Utilization, U_{PV}, as a function of the substation traffic energy, $E_{ss} \cdot \overline{N_{bus}}$. A plateau is observable starting at 2200 MWh.Bus and underachieving substations (left-hand group) are exposed.

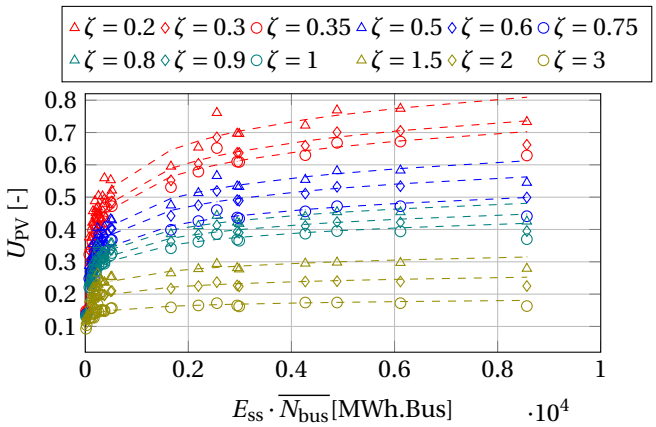

Figure 6.5: PV Utilization, U_{PV}, of Arnhem and Gdynia substations for different PV system sizes (as the energy-neutrality ratio ζ) against the defined Traffic Energy KPI $E_{ss} \cdot \overline{N_{bus}}$[MWh.Bus]. This is an extension of Figure 6.4 for any ζ between 0.2 and 3.

6.4. U_{PV} PERFORMANCE ESTIMATION

The strong trend between U_{PV} and $E_{ss} \cdot \overline{N_{bus}}$ observed in Figure 6.4 for energy-neutral PV system sizes (ζ=1) can also be observed for other system sizes, as reported in Figure 6.5. These trends at different system sizes observed are of the form $a \cdot ln(E_{ss} \cdot \overline{N_{bus}}) + b$. The a and b coefficients of the different curves are plotted in Figure 6.6 as a function of the normalized system size (ζ of Eq.5.15), and described analytically in Eq.6.1 and Eq.6.2. This method, summarized by the flowchart of Figure 6.7, offers then a quick and straightforward way for the U_{PV} estimation of any PV system at any substation without the need for complex grid and PV models.

$$a = 0.0215\zeta^3 - 0.1494\zeta^2 + 0.3369\zeta - 0.1680, \quad R^2 = 0.998 \tag{6.1}$$

$$b = -0.0082\zeta^3 + 0.0553\zeta^2 - 0.1305\zeta + 0.1244, R^2 = 1 \tag{6.2}$$

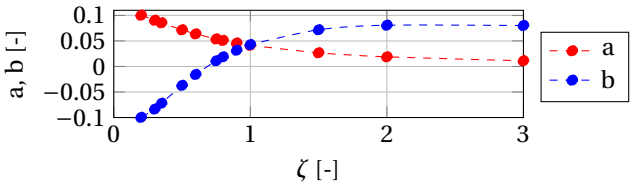

Figure 6.6: Coefficients a and b for the different ζ of Figure 6.5.

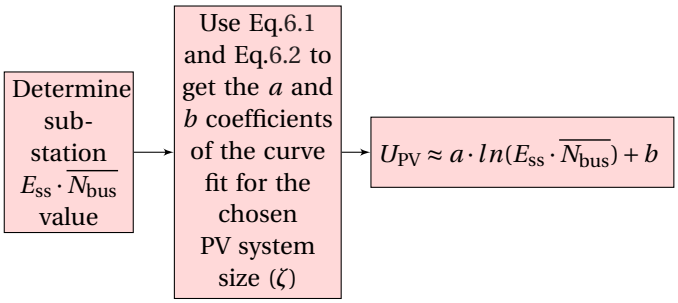

Figure 6.7: The proposed methodology in this chapter to approximate the PV utilization of a trolleybus substation using the suggested, empirically-derived third-degree polynomial and without the need for complex PV, bus, or grid modeling.

6.5. SUGGESTED SIZING APPROACH FOR SUBSTATION COMBINATION

The logarithmic trends described in this chapter showed a sharp rise in PV system performance, followed by a saturation plateau. Any substation sitting before the knee-point on the performance curve is then experiencing a lower U_{PV} than is achievable for other substations in their city with a higher Traffic Energy KPI.

This invites the installation of a semi-decentralized PV system combining service to neighboring substations in a way that moves their combined performance towards the knee and the plateau of the utilization curve. An example of these substations is highlighted in Figure 6.4 (golden arrow).

On the other hand, substations already on the plateau should not be destined for large PV system sizes as their utilization saturates rapidly. In fact, they should be sized at a value lower than energy-neutral sizes (i.e. ζ <1) as they can offer high U_{PV} values at these small system sizes (Figure 6.5), and bring thereby a better technical and economic feasibility. However, at those sizes, the load coverage will not be as high as can be predicted. This bespoke trade-off is left to the stakeholders.

Cities aiming to build new, sustainable trolleygrids should also be aware of the saturation points in the curve because larger, higher traffic substations would come with higher transmission losses, for the same fraction of U_{PV}, as the resulting large system size would probably need to be built at a distance from the substations, with additional transmission cables.

Figure 6.8 shows the example of combining two or three neighboring Arnhem substa-

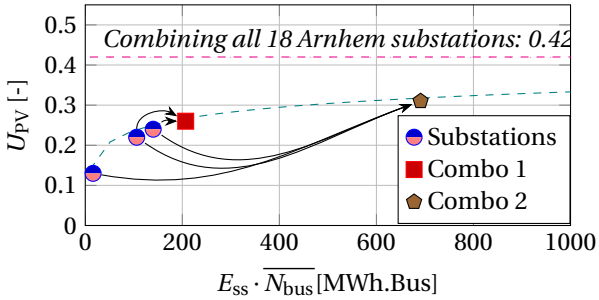

Figure 6.8: Example of the suggested sizing method: The U_{PV} of three neighboring Arnhem PV systems and of two of their combinations. As expected, the combinations outperform their individual constituents and their U_{PV} also sits on the same prediction trend curve derived in this chapter.

tions of low U_{PV}. Two important observations can be reported. Firstly, the combined PV system does indeed outperform any of its individual constituents, validating this encouraging message to trolleygrid cities to adopt this sizing method. This is a consequence of the higher traffic and continuous load that a combination of substations can offer, compared to a single substation. This brings about a better match between the PV generation and the substation load. Mathematically, this translated to a higher Traffic Energy KPI value. Secondly, a greatly beneficial result is that the performance of the combined PV systems can also be estimated using the previously reported trends, as these combos also sit on the trend curve. As explained in the previous section, this KPI curve can also be used up to the whole city grid (centralized PV system) as verified by comparing the results to those from the previous calculations in [11].

6.6. CONCLUSIONS

PV integration in urban transportation networks so far has neither a clear methodology nor consensus for the placement and sizing of PV systems, nor an available tool to estimate the performance of the PV systems easily. This chapter offered a simple approach for PV integration in trolleybus grids by examining two case study cities of very different characteristics of trolleygrid architecture, bus traffic, and substation power demands. However, common trends for both cities were still observed, which paved the way for a generalizable methodology.

A number of KPIs were studied, but a strong trend was reported between the PV direct utilization and the here-defined KPI of Substation Traffic Energy - a multiplication of the yearly energy demand of the substation and the average traffic it sees.
This empirically derived, logarithmic trend of the form $a \cdot ln(E_{ss} \cdot \overline{N_{bus}}) + b$ was also shown to be extendable to different PV system sizes. The a and b coefficients were analytically described using a simple third-degree polynomial for any normalized PV system size ζ. This allows trolleybus cities to quickly and efficiently estimate the performance of any PV system on any substation without the need for the grid, PV, and bus modeling.
Despite the fact that the first KPI (Yearly Irradiance and Sunshine Duration) showed a

weak trend between the PV input parameters and the PV utilization, future work is invited to include more cities of different sunshine profiles to confirm further that the offered polynomial fit is indeed suitable for the study of different trolleygrid cities.

Moreover, the trends observed offer strong insights and advice to these cities on possibilities for the placement and sizing of the PV systems and how to combine substations for increased benefit. This can be done using the same performance estimation trend proposed in this chapter. It is important to repeat again that the contribution of this chapter is in exposing the existence of clear mathematical trends and plateaus that allow the estimation of the PV system performance in trolleygrids and offer sizing and combination insights. As of now, the derived trends in this chapter are purely empirical, and future works are encouraged to identify the underlying variables that describe these trends.

The chapter also exposed performance saturation plateaus not previously reported in the literature, around 38% of direct utilization for an energy-neutral PV system. These plateaus are an uncompromising consequence of the mismatch between the intermittent bus scheduling and the PV generation that is to be expected in any trolley city.
This echoes again the crucial conclusion of the previous chapter that the integration of multiple loads, such as EV chargers, into trolleygrid infrastructures, is not only an opportunity but a necessity for the sustainability of these transport grids.

However, the analysis has so far focused only on AC-side storage that is connected to the PV system directly. This placement option does not offer the benefits of recuperating braking energy, reducing catenary voltage drops, and reducing line transmission losses. Such reductions in energy demand and performance enhancements could prove critical to the economic cost/benefit analysis of a PV system with connected storage.
Thus, one crucial investigation remains then on the performance of DC-side storage, whether on-board or off-board, before a decisive conclusion on the outlook of renewables integration in trolleygrids. This is the topic of the upcoming chapter.

7

COMPARISON OF ON-BOARD AND STATIONARY STORAGE SOLUTIONS FOR TROLLEYGRIDS WITH PV SYSTEMS

"Potria novel vigore
il pianto mio recarti..
ma .. ravvivar l'amore?
il pianto mio, ah no, non può.."

Ah, Non Credea Mirarti - Act II, La Sonnambula (Bellini)

Maybe a new life
my tears could replenish in you..
But .. to revive the love?
My tears, oh no, can never do .."

This chapter is based on Comparison of On-board and Stationary Storage Solutions for Trolleygrids with PV Systems. I Diab, K Giitsidis, GR Chandra-Mouli, P Bauer *(Submitted)*

A number of traction networks already use on-board and stationary storage systems to reduce the traction substation energy demand and reduce the line losses and voltage drops. However, their effect on the grid power profile is not yet studied at traction substations with PV systems, which already face severe power mismatches between the generation and load profiles.
This chapter investigated two common on-board energy storage system (OESS) technologies (LTO and supercapacitors) and two common stationary energy storage system (SESS) technologies (LTO and flywheels) under different substation and PV system sizes and profiles.
The chapter starts with a short introduction and motivation in Section 7.1. Section 7.2 looks into the modeling methodology for the on-board and stationary storage, and defines the suggested indicators and case studies for this chapter as well as the power management schemes. Then, Sections 7.3 and 7.4 present the case study results of the OESS and SESS analysis, respectively, which are then extended in Section 7.5 into generalized recommendations for sizing and placement in trolleygrids beyond the case studies. Finally, Section 7.6 concludes the chapter.

7.1. INTRODUCTION

Energy storage devices are traditionally implemented in transport grids to recuperate braking energy, reduce voltage drops, and reduce line transmission losses [6], [7], [21], [37], [80], [219]–[221]. Storage devices can be placed either on-board (on-board energy storage systems, OESS) or off-board at the traction grid section or substation level (stationary energy storage systems, SESS).
The advantages of the former are that the harvesting of braking energy is done on the vehicle, reducing transmission losses. This energy is then also used directly at the vehicle in moments of higher power demands. The power management is straightforward, and a battery size of the order of a few kWhs is sufficient for this purpose. Meanwhile, SESS is not placed on the vehicle and does not add to its traction demand. This absence of weight limitation also allows for larger SESS to be installed, which can help the substation in shaving power peaks, and its more sophisticated power management schemes and placement options along the grid can help control the line voltage and transmission losses to desired levels.
Many works are already rethinking transport networks such as trolley grids as multifunctional, active grids by integrating into them renewable energy sources (RES) like solar PV [11], [44]–[47], [73]–[76], [79], [82], EV chargers [16], [23], [67], [165], [222], and other smart grid loads and fleets [12], [15], [22], [36], [183].
However, the bus timetabling creates frequent moments of no-load for a PV system connected to a trolleygrid substation, as seen in the Figure **??** simulations of substation Q in the city of Arnhem, the Netherlands [11]. As illustrated in Figure 5.2, in the absence of storage systems, this requires curtailment of the excess energy and/or exchange with the AC grid (if the PV system has a path to the AC side such as in Figure 5.5). Both of these disadvantages the techno-economic feasibility of the PV project [80].

7.1.1. THE NEED FOR A STUDY ON STORAGE FOR TRACTION GRIDS WITH PV SYSTEMS

While PV and storage systems have been researched separately in traction grids, to the best knowledge of the authors, no work has investigated a comparison of storage solutions for a traction substation with a connected PV system.
This investigation is crucial to determine the net constructive or destructive effect of the on-board or stationary storage placement on the direct utilization of the generated PV power by the traction grid.
As can be seen in Table 7.1, there are multiple advantages and disadvantages to OESS and SESS solutions. For example, on-board storage is efficient in shaving the traction power peaks and thereby reducing under-generation mismatch between the PV and the substation demand. However, this can be disadvantageous in moments of high PV generation if it causes an over-generation mismatch by reducing the load demand. Meanwhile, stationary storage systems are beneficial as they supply the vehicles with stored PV power even after sunset or before sunrise, thereby reducing the substation demand throughout the day. However, their connection to the DC catenary means that they interfere with the loads and increase both the voltage drops and transmission losses.
Consequently, an intuitive conclusion cannot be straightforwardly obtained on the comparison of storage placement options. This chapter aims to bridge this knowledge gap.

7.1.2. TRACTION STORAGE TECHNOLOGIES IN THE LITERATURE

This chapter looks at three technologies interesting for the purpose of traction grids as per the available literature: Li-ion batteries, Supercapacitors, and flywheels.

Lithium-titanate-oxide (LTO) batteries are gaining attention in traction grids as they provide much higher charging and discharging currents compared to the other types of batteries, suitable for vehicle accelerations and braking [14], [95], [99], [153], [175], [219]. They are interesting as both on-board and stationary applications because of their comparatively high energy density, cycle life, and safety (for the former) and low self-discharge and high efficiency (for the latter).
Capacitors and *supercapacitors* (SC) are also used in transportation grids [6], [41], [150], [223], [224]. Their ability to provide and receive high currents in a very short time makes them suitable for uses with high electric power peaks, such as the abrupt acceleration of vehicles. Finally, flywheels are also commonly used in transport grids as their main advantage compared to other storage methods is their higher number of cycles. Especially as a stationary application, their relatively lower energy density does not constitute a problem [88], [89]. Their major disadvantages are their self-discharge and their response time when used in large-scale power applications, which can have an order of magnitude of some seconds rather than milliseconds compared to other energy storage systems [130]. For the examined application of this work, the flywheel system is in the order of 200kW, where the response time can be quicker than a second and is therefore not accounted for in the modeling [144], [225], [226].

Table 7.1: Comparison of the advantages and disadvantages of DC-side on-board and stationary storage solutions in traction substations with PV systems.

	On-board Storage (OESS)	Stationary Storage (SESS)
Advantages to the PV Direct Utilization	• Reduces the *masking** of loads from the PV by harvesting the braking energy • Reduces the under-generation power mismatch by shaving the traction peaks • Relatively small (sized for one vehicle) • Efficient braking energy recuperation and peak-shaving (present on the bus) • Resilient to self-discharge (acceleration demand comes soon after braking)	• Reduction of the *masking* of loads from the PV by harvesting the braking energy (subject to line voltage and battery SOC limitations) • Support during under-generation power mismatch • No effect on the vehicle weight and space constraints • Present on the section to harvest the PV energy in moments of zero-traction loads • Present on the section to deliver stored PV energy in moments of no PV generation (after sunset, for example) • Occupancy of space at the substation, not on the vehicle
Disadvantages to the PV direct Utilization	• Increases the over-generation mismatch by shaving the traction peaks • Leaves the section with the vehicle (does not help in the moments of zero loads) • Increases the weight and occupied space on a vehicle	• Relatively large (sized for the traffic of one substation) • Increases the line losses and voltage drops while charging the excess PV energy as it is connected to the DC catenary like the other loads • Susceptible to self-discharge as the energy can be retained for long periods (depending on the power management scheme and traffic conditions) • Efficiency of braking energy recuperation and peak shaving depends on placement location and line voltage (yet never as efficient as storage onboard the vehicle itself)

* Masking is when a braking vehicle fully supplies the power demand of another load, effectively masking it from the substation and PV

7.1.3. CHAPTER CONTRIBUTIONS

The chapter has the following contributions:

1. The detailed comparison of on-board and stationary storage solutions for traction substations with PV systems, under a full year of simulations using detailed and verified trolleybus, trolleygrid, storage, and PV models

2. The proposal of a PV-focused charging scheme for traction DC-side storage that reduces costs and complexity by not needing any dedicated grid and bus sensors or wireless communication between them

7.2. MODELING METHODOLOGY

7.2.1. MODELING OF OESS AND SESS

Table 7.2 summarizes the characteristics of the commercial storage solutions studied in this chapter as reported by their manufacturers [100], [136]–[138], [145].

These specifications allow for a detailed modeling of the storage systems that takes into account their charging and discharging efficiencies, self-discharge, and maximum power exchange. To create a suitable pack from these modules, multiple modules are connected in strings and in parallel.

Table 7.2: Module characteristics for the Supercapacitor [136]–[138], LTO battery [100], and Flywheel [145] used in this chapter (full details in the appendix).

	Storage Technology		
Variable	**SC**	**LTO**	**FW**
Capacity (Wh)	53	1500	32000
Module voltage (V_{DC})	48	24	550-750
Module resistance, charging (mΩ)	6	4.5	86% round-trip efficiency
Module resistance, discharging (mΩ)	6	4.3	
Self-discharge (% per day)	11.3	0.1	11.6
Maximum power exchange (kW)	3.4	12	8

These pack systems are designed then as follows:

Supercapacitors: Maxwell® Technologies BMOD0165 P048 C0B module. For the 1.5kWh configuration: 14x2 modules for 1.484kWh of capacity and 95.4kW of maximum power exchange [136]–[138].

LTO Batteries: Altair® Nanotechnologies 24V 70AH battery module. For the 1.5kWh configuration: 1 module for 1.50 kWh of capacity and 12kW of maximum power exchange [100].

Flywheels: Amber Kinetics M32 flywheel. For the 129kWh configuration: 1x4 modules of 128kWh capacity and 32kW of maximum power exchange [145].

7.2.2. INDICATORS FOR ASSESSING THE STORAGE SYSTEM PERFORMANCE

The assessment of the benefit that a PV-oriented storage system brings to the PV-augmented trolleygrid is on two levels: Energy and Voltage.

The energy benefit is in the relieving of the substation of some load coverage, recuperation of braking energy, and reduction of line losses.
This reduction in the energy demand (denominator of Eq.5.15) increases the here-defined **Gain in Effective System Size**, $\Delta\zeta$, for the same installed PV system, as described by:

$$\Delta\zeta \triangleq \zeta_{\text{with ESS}} - \zeta_{\text{without ESS}} \tag{7.1}$$

This factor is measured in percentage points [p.p.].
For example, an installed PV system, supposedly designed to cover half of the yearly load (i.e. $\zeta = 0.5$), is now combined with a storage system that successfully reduces the substation demand and renders the installed PV system effectively sized for 55% of the yearly load. This means a $\Delta\zeta$ of 5 p.p. according to Eq.7.1.
This is then not the relative 10% increase in the value of ζ from 50% to 55%. Opting for an absolute measure in percentage points allows a comparison of the absolute benefit added regardless of the PV system sizes studied in this chapter, by keeping the values normalized to the original substation load demand instead of to the PV system.

To judge the effect of the storage system on the voltage drops, the minimum voltage value per year and the average voltage values among the scenarios do not show enough nuances. This is because the storage would most frequently see the nominal substation voltage because of the absence of a traction load explained in Section 7.1.
For this, the yearly **Change in Cumulative Voltage Drops**, Δ_{VY}, is defined. This parameter presents the yearly relative reduction in the cumulative (integral) voltage drops on the section, calculated as:

$$\Delta_{VY} \triangleq \frac{\int_{\text{year}}(V_s - V_{\min}(t)\big|_B)\,dt - \int_{\text{year}}(V_s - V_{\min}(t)\big|_S)\,dt}{\int_{\text{year}}(V_s - V_{\min}(t)\big|_B)\,dt} \tag{7.2}$$

Where the B and S indices refer to the *Baseline* and *Studied Scenario*, respectively.

7.2.3. CASE STUDY DEFINITION: SUBSTATIONS

There is a difference in the performance of a PV system connected to a traction substation depending on the length of the catenary that it supplies and on the average traffic that it observes [11], [79].
For this purpose, this chapter needs to confirm the benefit of the PV system by looking at at least two traction substation types. The examined trolleygrid is that of the city of Arnhem, The Netherlands.
For this chapter, the choice is for:

- **Section 25 under Substation 9 (SS9)**: A relatively short (less than 1000m) catenary zone with up to 5 buses at a time in traffic density. A PV system of 129kW$_p$ can deliver the yearly energy demand of this section [11].
- **Section 23 under Substation 12 (SS12)**: A relatively long (more than 2000m) catenary zone at most 3 buses at a time in traffic density. A PV system of 195kW$_p$ can deliver the yearly energy demand of this section [11].

7.2.4. POWER MANAGEMENT SCHEMES FOR THE STORAGE SYSTEMS

POWER MANAGEMENT SCHEME FOR OESS

The power management scheme for on-board storage can be straightforward and rule-based as is typical in the literature [148], [227]–[231]. This is first because the placement of this storage on board the vehicle itself allows it to recuperate the braking energy in a more effective way compared to stationary storage, and that makes it a priority objective. Second, the relatively small size of typical on-board storage makes it impractical for them to focus on recuperating the PV excess generation as it would compete with the braking energy over the available battery capacity, which is not practical from an energy transmission efficiency point of view.
For this, the power management scheme of the on-board storage studied in this chapter is the typical scheme found commonly in the literature that recuperates the braking energy of the vehicles and delivers it in moments of high load. Here in this chapter, the storage delivers the power when the vehicle has a demand of over 100kW.

POWER MANAGEMENT SCHEME FOR SESS

For the Stationary storage system, as it is not tied to one vehicle, the power management scheme has to be more sophisticated.
The power generation of the PV system and the power demand of the substation can be measured and communicated (wirelessly) to the storage system. However, if such sensors and communication networks have not been set up for technical or economic reasons, the power management scheme based on the grid state estimator of Chapter 4 offers a fair estimate of the substation power demand.
Once the power excess or deficit is calculated by the difference between the estimated substation demand and the PV generation (measured or forecast), the storage system acts at this charge or discharge power set-point value as much as the upper and lower SOC and technology limitations allow it.

7.3. RESULTS: ON-BOARD ENERGY STORAGE SYSTEMS

Figure 7.1 shows the performance of the OESS in a one-year simulation of the Arnhem Grid sections 23 (Substation 12) and 25 (Substation 9). OESS systems typically have a few kWhs installed capacity, and hence this study looks at multiples of 1.5kWh (1.5, 3.0, and 4.5kWh) according to the commercially available technologies as detailed in the appendix.

The first observation is that supercapacitor systems consistently perform better than LTO systems. This is because the former has a higher power exchange capability that is not available to the LTO system. According to the technology limitations (see appendix), the largest LTO battery studied here, of 4.5kWh, can only exchange 36kW of power. This can leave most of the braking energy unharvested as it typically is at the order of 200kW. Moreover, the battery cannot supply more than 36kW to support the bus during acceleration peaks.
This last point also explains why supercapacitors of different sizes seem to behave almost identically, as their technical limitations are already at or above the order of magnitude that the grid operation requires. This means that a small supercapacitor already of-

fers interesting returns. Meanwhile, small LTO battery sizes do not have this advantage. This makes the supercapacitors economically attractive in two parts: First, the smaller sizes can already pick up near-maximum benefits, and second, the mass of smaller storage sizes would also translate to lower increases in traction power demands.

The second observation is that while the OESS can give a net benefit in reducing the demand for the traction substation, there is no directly observable benefit to the utilization of the PV system.
However, as the work in [11], [79] shows, the U_{PV} increases rapidly with the decrease of the PV system size in high-traffic sections. Consequently, there is a benefit to the PV utilization that can be obtained at high-traffic sections (like section 25) by allowing the installation of a smaller (thereby, better performing) PV system at this substation to meet its full energy demands.
Unfortunately, according to [11], [79], this benefit cannot be guaranteed at low-traffic substations as the mismatch problem is more in timetabling (absolute absence of loads) rather than a mismatch between generation and local demand. In such cases, an on-board storage device that leaves the section when a bus leaves would have no benefit on timetabling mismatch, which is the more pronounced problem at low-traffic substations.

7.4. RESULTS: STATIONARY ENERGY STORAGE SYSTEMS

Figure 7.2 shows the performance of the SESS in a one-year simulation of the Arnhem Grid sections 23 (Substation 12) and 25 (Substation 9).
For the energy-neutral size ($\zeta = 1$), the storage at each section is chosen to store one hour of peak PV generation (i.e., 195kWh at section 23 and 129kWh at section 25), as well as larger order of magnitudes of 500 and 1000 kWh. With the half-energy-neutral PV system ($\zeta = 0.5$), the studied storage sizes are half of those mentioned above.
An interesting contrast between the SESS and OESS cases is that the presence of larger stationary energy storage systems decreases the gain in system size, $\Delta\zeta$. This is a consequence of the DC-side placement of the storage that now acts as a load on the section as it charges the PV excess power. With other buses in traction mode on the line, this increases the voltage drops on the section and, consequently, the transmission losses. This also explains why the cases of smaller PV system sizes (i.e., generation peaks) have a better performance when coupled with storage like in Figures 7.2(d) and 7.2(b). This conclusion can be further validated by Figure 7.3 where it is clear that the presence of a DC-side SESS increases the voltage drops on a section in most cases, and more severely when coupled with larger PV systems (Figures 7.3(c) and 7.3(a)) versus smaller PV systems (Figures 7.3(d) and 7.3(b)).
Furthermore, this harvested PV energy cannot be stored seasonally as it is lost to self-discharge. This is especially true in the case of flywheels, where the relatively high self-discharge rate makes them consistently a less attractive solution than LTO batteries in terms of gain in system size and increase in PV utilization.
This can be proven by Figure 7.4 which shows the SOC of the 1000kWh LTO (upper left, blue) and Flywheel (upper right, red) during a year of operation under the same load of section 23. The SOC in the flywheel case is seen as subject to charging/discharging

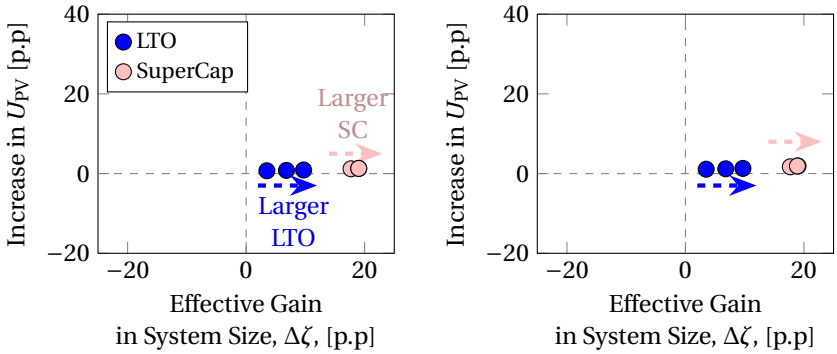

((a)) Section 25 in Arnhem, with $\zeta = 1$.

((b)) Section 25 in Arnhem, with $\zeta = 0.5$.

((c)) Section 23 in Arnhem, with $\zeta = 1$.

((d)) Section 23 in Arnhem, with $\zeta = 0.5$.

Figure 7.1: Simulation results of the yearly effective gain in the system size and in PV Utilization in percentage points (p.p) observed with supercapacitor and LTO on-board energy storage (OESS) of 1.5, 3.0, and 4.5kWh.

and self-discharge losses that reduce the amount of stored energy compared to the LTO under the same conditions. The lower plot of Figure 7.4 shows a one-week excerpt of a spring-time operation whereby the energy lost due to the difference in technologies is visible as the difference between the blue LTO and red flywheel curves.

However, an advantage of SESS over OESS is the increase in the PV system utilization in all the studied cases, including the high-losses flywheel scenarios. This is because the presence of a storage system when the buses are not present on the section is the key advantage of SESS over OESS. This allows the PV system to store its excess energy in moments of zero load. However, the benefit is still limited as the SOC of the stationary storage systems maxes out early in the year and no energy can be picked up in the summer when the mismatch is high. Furthermore, the fully charged storage system can no longer recuperate the braking energy of the buses on the sections. This is particularly important in the summer months in this case study since the summer schedule is less frequent than the winter one, and the buses are more likely to find themselves with excess braking energy since the HVAC demand is low and there are not many receiving buses on the section.
In conclusion, for stationary storage systems, it is better to use smaller LTO battery sizes along with the installation of smaller than energy-neutral PV system sizes.

7.5. ANALYSIS AND GENERALIZATION OF THE RESULTS

This chapter investigated on-board and stationary storage solutions for traction substations with PV systems with two case studies: A long, low-traffic substation and a short, high-traffic substation.

In terms of technologies, supercapacitors proved to be superior to LTO batteries in reducing the substation energy demand, and, thereby, the size of the PV system needed for the same emissions-reduction goal. This is because supercapacitors have a higher power exchange capability that efficiently harvests the braking energy dips and shaves the acceleration power peaks of the vehicles.
On the other hand, the reduced power peaks create larger mismatches between generation and load at peak PV hours. Furthermore, the on-board storage leaves the trolleygrid section with the vehicle and does not offer any harvesting sink for the excess PV power in the frequent moments of no traffic caused by timetabling. Therefore, the net effect is that both supercapacitors and LTO batteries are not helpful in increasing the utilization of the installed PV system (limited to 0.5-2% in this case study). The benefit can be obtained indirectly as smaller system sizes are needed now. But as pointed out in the literature [11], [79], this is only beneficial in high-traffic substations where the PV utilization increases rapidly with smaller system sizes.
Conclusively, at low-traffic substations, there is little utilization benefit in reducing the PV system size since the mismatch between generation and load is mostly temporal (horizontal offset) rather than in power (vertical offset).

For stationary storage, LTO batteries performed better than flywheels. This is because the latter have higher self-discharge rates that are damaging in such applications of long storage times. This is not the case with on-board storage and the high discharge rate of

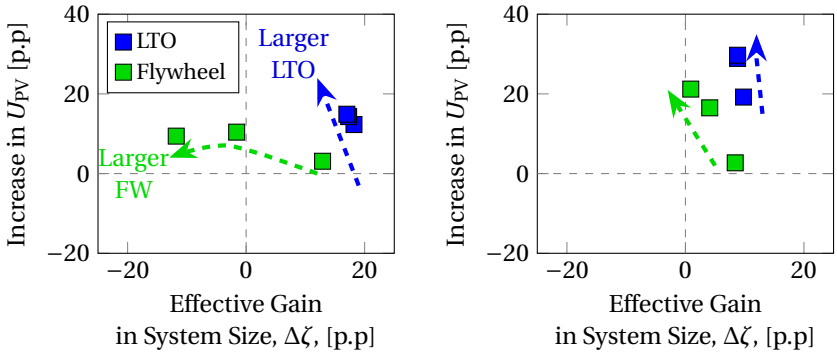

((a)) Section 25 in Arnhem, with $\zeta = 1$.

((b)) Section 25 in Arnhem, with $\zeta = 0.5$.

((c)) Section 23 in Arnhem, with $\zeta = 1$.

((d)) Section 23 in Arnhem, with $\zeta = 0.5$.

Figure 7.2: Simulation results of the yearly effective gain in the system size and in PV Utilization in percentage points (p.p) observed with flywheels and LTO stationary energy storage (SESS).

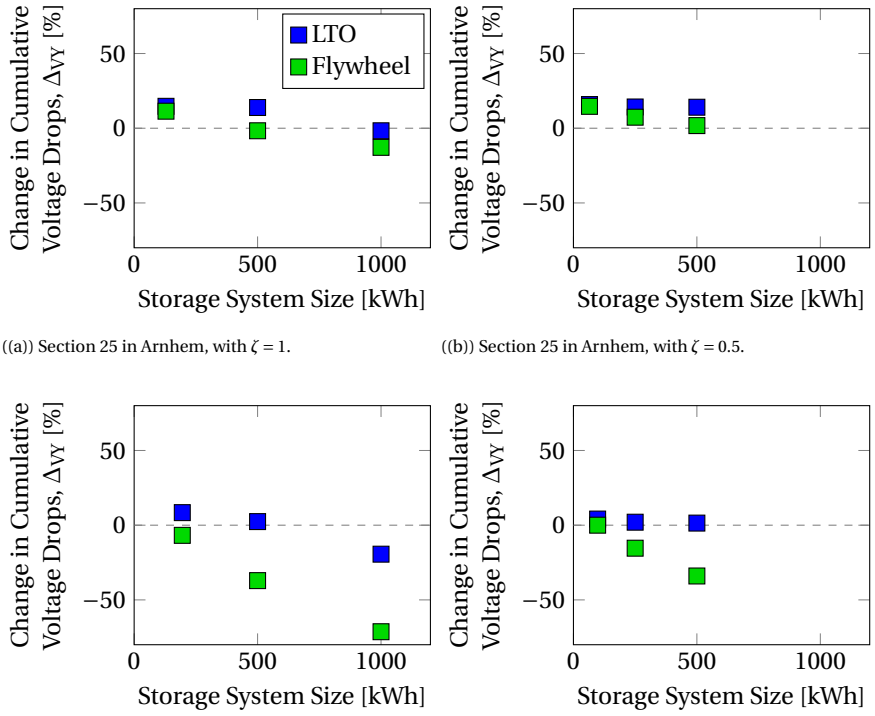

((a)) Section 25 in Arnhem, with $\zeta = 1$.

((b)) Section 25 in Arnhem, with $\zeta = 0.5$.

((c)) Section 23 in Arnhem, with $\zeta = 1$.

((d)) Section 23 in Arnhem, with $\zeta = 0.5$.

Figure 7.3: Simulation results of the yearly change in cumulative voltage drops, Δ_{VY}, of Eq. 7.2, for different flywheel and LTO battery sizes in Arnhem.

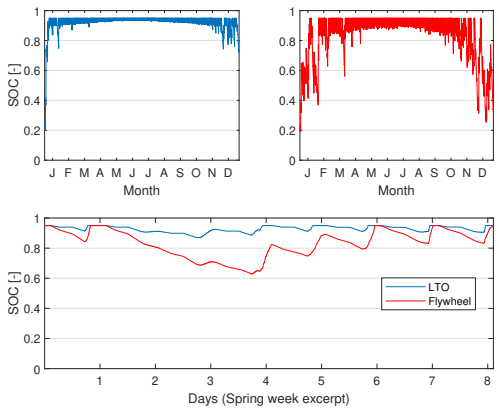

Figure 7.4: SOC comparison under the same operational conditions of LTO (blue) and Flywheel (red) technologies for a 1000 kWh installed capacity at section 23. The Flywheel has an inferior performance due to dis/charging efficiencies and self-discharge.

supercapacitors since the bus acceleration occurs after each deceleration, and the energy is not stored for long periods of time.
Since the stationary storage on the DC side now charges through the substation feeder cable like any other traction load, some technology and size scenarios increased the demand, and the voltage drops on the substation. This made it so that the higher the storage size, the higher the demand on the substation, and the voltage drops.
However, stationary storage played a direct role in increasing PV system utilization. This worked best with smaller PV system sizes, which is incidentally also the preferred scenario regarding line voltage drops.
However, such benefits for the utilization could also be obtained by placing the storage directly on the AC side with the PV system, which would also increase the transmission efficiency between the PV and the storage. This is motivated by the fact that the voltage drop reduction of the DC-side storage system does not seem to offer an attractive offset to the disadvantages.

In conclusion, on-board supercapacitors are the preferred method for reducing the required PV system size in case of economic and spatial installation limitations. However, no benefit is offered in terms of reducing the grid exchange and power curtailment, especially at low-traffic substations.
In terms of increasing the direct utilization of the PV system and minimizing the exchange with the grid, stationary LTO batteries are a favorable solution, but only to be coupled with relatively large PV systems at high-traffic substations, or with relatively small PV systems at low-traffic substations. However, the benefits do not seem to outweigh the convenience of placing the storage system on the AC side with the PV system.

7.6. CONCLUSIONS

This chapter compared on-board and stationary energy storage solutions for traction substations with PV systems.
On-board storage was found to be most beneficial in reducing the substation energy demand and, thereby, the required PV system size. Especially supercapacitors when compared to LTO batteries. However, it has little effect on the increase in direct PV utilization.
Meanwhile, stationary storage was found to be only effective in the case of small systems at low-traffic substations or with large PV systems at large substations. This is considering LTO battery storage as flywheels were not suited. Nonetheless, the effect of stationary storage systems on the line voltage did not outweigh their sophisticated power management schemes, and it is more advisable to place the stationary storage on the AC side with the PV system for PV-augmented trolleygrids.
In both cases, the increase in PV utilization is limited and subject to losses in transmission and storage self-discharge. A hybrid OESS-SESS solution and other power management schemes are still encouraged as a possible future work investigation.
However, the inherent limitations of trolleygrid timetabling and PV seasonal variations repeat the previous calls in Chapters 5 and 6 for a multi-functional transport grid with base loads, such as EV chargers, as the most suitable path toward the techno-economic feasibility of sustainable transport grids again.
For this, the coming part of the thesis looks at the multi-functional trolleygrid with dif-

ferent methods of base-load creation.

PART III

SMART NON-TRACTION LOADS AND COMPONENTS IN TROLLEYGRIDS

Part II arrived to the conclusion that the techno-economic feasibility of renewables in trolleygrids cannot be attained without the presence of a base load. This Part looks first at the feasibility and performance of three of these possibilities: Energy storage on the DC side whether on-board the vehicle, stationary, or a hybrid thereof (Chapter 8), EV chargers connected to the DC catenary (Chapter 9), and residential loads near the traction substations (Chapter 10).

In Chapter 8, it was clear that stationary storage is the best storage solution, especially when placed at the mid-of-line (halfway between the substation and the end-of-line). Fortunately, the half-and-half hybrid solution of onboard and stationary storage behaves closer to the favorable stationary storage case. This means that current sunk costs in onboard energy storage investments can be extended and not rendered redundant in the future when implementing stationary storage.

In Chapter 9, the potential of EV chargers is investigated to see what is the maximum amount of electric cars that could be charged from the DC catenary without breaking the traction grid's power, voltage, or current limitations. Surprisingly, over 200 EVs can be charged per day from a single trolley substation, highlighting again how traction grids are oversized and underutilized. EV chargers seem then like a promising solution to make the trolleygrid multi-functional and multi-stakeholder while providing crucial services for the energy transition in otherwise congested areas. Specific conclusions are drawn in this chapter on the sizing, placement, and intervention methods to increase this potential.

In that vein, Chapter 10 also looks at another way of making the trolleygrid multi-functional and multi-stakeholder while providing crucial services for the energy transition. The suggestion is to couple the trolleygrid to nearby residential loads via the Low Voltage AC grid. In this manner, the households can provide the desperately needed rooftop installation space and base loads to the traction network, which in return provides both the peak load and investment possibilities to enhance the techno-economic feasibility of renewables integration.

However, the concern is that the simultaneous integration of a few of these solutions can interfere with the performance of one another and possibly even restrict the available capacity for the integration of new, sophisticated bus fleets such as in-motion-charging trolleybus. This concern is the topic of Part IV later in this thesis.

8

Comparison of On-board, Stationary, and Hybrid Storage Solutions in Trolleygrids

"Largo al factotum della città! Largo!
[..]*Pronto a far tutto,*
la notte e il giorno
sempre d'intorno in giro sta!"

Largo al Factotum - Act I, Il Barbiere di Siviglia (Rossini)

Make way for the handyman of the city! Make way!
Ready to do anything,
night or day,
always around and going around!

This chapter is based on Comparison of On-board, Stationary, and Hybrid Storage Solutions in Trolleygrids. I Diab, GR Chandra-Mouli, P Bauer *(Submitted)*

Traction networks like trolleybuses implement storage solutions placed either on-board the vehicle or stationary (wayside), mainly for the recuperation of braking energy. Other benefits can be obtained in terms of reducing power losses, voltage drops, or increasing the substation spare capacity. However, there is no clear consensus yet on which placement option (or a hybrid combination of both) is the most beneficial, especially when looking ahead toward the multi-functional trolleygrids.
The chapter starts with a short introduction and motivation in Section 8.1. Section 8.2 looks into the modeling methodology for the on-board and stationary storage, and defines the suggested indicators and case studies for this chapter as well as the power management schemes. Then, Sections 8.3, 8.4, and 8.5 present the case study results of the Energy, Voltage, and Power analysis, respectively, which are then extended in Section 8.6 into generalized recommendations for sizing and placement in trolleygrids beyond the case studies. Finally, Section 8.7 concludes the chapter.

8.1. INTRODUCTION

Energy storage devices are traditionally implemented in transport grids to recuperate braking energy, reduce voltage drops, and reduce line transmission losses [6], [7], [21], [37], [80], [219]–[221]. Storage devices can be placed either on-board (on-board energy storage systems, OESS) or off-board at the traction grid section or substation level (stationary energy storage systems, SESS).
The advantages of the former are that the harvesting of braking energy is done on the vehicle, reducing transmission losses. This energy is then also used directly at the vehicle in moments of higher power demands. The power management is straightforward, and a battery size of the order of a few kWhs is sufficient for this purpose. Meanwhile, SESS is not placed on the vehicle and does not add to its traction demand. This absence of weight limitation also allows for larger SESS to be installed, which can help the substation in shaving power peaks, and its more sophisticated power management schemes and placement options along the grid can help control the line voltage and transmission losses to desired levels.
Storage solutions are crucial for the feasibility of future traction grids by reducing the energy consumption of the grids and creating more space for the integration of smart loads by creating more spare power capacity and keeping higher line voltages.

8.1.1. THE NEED FOR A STUDY ON STORAGE FOR TRACTION GRIDS

While storage systems have been researched separately in traction grids, to the best knowledge of the authors, no work has investigated a comparison of storage system placement between on-board, stationary, and a hybrid on-board and stationary system. This investigation is crucial to determine the preparedness of the future traction grids in terms of energy, power, and voltage as they move towards multi-functional grids.
There are multiple constructive and destructive advantages and disadvantages to OESS and SESS solutions (see Table 7.1 in Chapter 7). For example, on-board storage is efficient in shaving the traction power peaks and thereby creating more spare traction

substation capacity. However, they leave the grid section with the vehicle and thereby cannot help the smart loads of the multi-functional grid the way the stationary storage can. Moreover, they tend to be relatively small as they are carried by the vehicle, and can thereby not offer active voltage support. Meanwhile, the connection to the DC catenary of the SESS means that they interfere with the loads and increase both voltage drops and transmission losses while charging. Furthermore, as they are not on-board the vehicles, they are less efficient than the OESS in braking energy harvesting.
Consequently, an intuitive conclusion cannot be straightforwardly obtained on the comparison of storage placement options. This chapter aims to bridge this knowledge gap.

8.1.2. CHAPTER CONTRIBUTIONS

The chapter has the following contributions:

1. The detailed comparison of on-board and stationary storage solutions for traction substations with PV systems, under a full year of simulations using detailed and verified trolleybus, trolleygrid, storage, and PV models

2. The proposal of a PV-focused charging scheme for traction DC-side storage that reduces costs and complexity by not needing any dedicated grid and bus sensors or wireless communication between them

8.2. MODELING METHODOLOGY

8.2.1. MODELING OF OESS AND SESS

Lithium-titanate-oxide (LTO) batteries are gaining attention in traction grids as they provide much higher charging and discharging currents compared to the other types of batteries with excellent strain endurance, suitable for vehicle accelerations and braking [14], [95], [99], [153], [175], [219]. They are interesting as both on-board and stationary applications because of their comparatively high power density, cycle life, discharge at low temperature, and safety (for the former) and low self-discharge and high efficiency (for the latter).

The LTO Batteries used are Altair® Nanotechnologies 24V 70AH battery modules with up to 5C as a charge/discharge rate [100]. Table 12.1 summarizes the characteristics as reported by the manufacturer [100], [136]–[138], [145].
These specifications allow detailed modeling of the storage systems that take into account their charging and discharging efficiencies, self-discharge, and maximum power exchange. To create a suitable pack from these modules, multiple modules are connected in strings and in parallel.

8.2.2. INDICATORS FOR ASSESSING THE STORAGE SYSTEM PERFORMANCE

The assessment of the benefit that a storage system brings to a trolleygrid is on three levels: Energy, Power, and Voltage.
The energy benefit is straightforwardly obtained by looking at the reduction in the substation's yearly energy demand compared to the baseline (no storage).
The power performance is judged by the reduction in the maximum substation peaks in

Table 8.1: Module characteristics for the LTO battery [100] used in this chapter.

Variable	Value
Capacity (Wh)	1500
Module voltage (V_{DC})	24
Module resistance, charging (mΩ)	4.5
Module resistance, discharging (mΩ)	4.3
Self-discharge (% per day)	0.1

a year which affects the available spare capacity for the integration of more loads, such as EV chargers or more sophisticated fleets, such as IMC buses.
To judge the effect of the storage system, the yearly **Change in Cumulative Voltage Drops**, Δ_{VV}, defined in Eq.7.2 of Chapter 7, is a properly nuanced approach to the cumulative voltage drops. As a reminder, this parameter presents the yearly relative reduction in the cumulative (integral) voltage drops on the section.

8.2.3. CASE STUDY DEFINITION: SUBSTATIONS AND STORAGE TECHNOLOGY

For this chapter, the choice of case studies is the same as in defined in the case study of Chapter 7 in Section 7.2.3. Namely, that is the short, high-traffic Section 25 under Substation 9 (SS9) and the long, low-traffic Section 23 under Substation 12 (SS12).
Each LTO module is of 1.5kWh capacity, to see the effect of larger OESS systems, up to 3 modules are installed of 4.5kWh, which already are at the order of 500kg before accounting for power converters and other components (read: reducing passenger capacity by about 10-15 passengers). For a fair comparison, Arnhem has 39 buses at 18 substations, so for a fair comparison among the placement scenarios of the same total installed storage capacity in the grid, the SESS is sized at 9kWh per substation. For the hybrid scenario, the installed size is half of each of the OESS and SESS scenarios.

The placement scenarios are:

- **Baseline**: Baseline scenario with no storage
- **OESS**: OESS scenario
- **S-EOL**: SESS at the end-of-line (EOL) of the section
- **S-MOL**: SESS at the mid-of-line (MOL) of the section
- **H-EOL**: Hybrid system with the SESS at the end-of-line (EOL) of the section
- **H-MOL**: Hybrid system with the SESS at the mid-of-line (MOL) of the section

8.2.4. POWER MANAGEMENT SCHEMES FOR THE STORAGE SYSTEMS

POWER MANAGEMENT SCHEME FOR OESS

The power management scheme for on-board storage can be straightforward and rule-based, as is typical in the literature [148], [227]–[231]. This is first because the placement

of this storage on board the vehicle itself allows it to recuperate the braking energy in a more effective way compared to stationary storage, and that makes it a priority objective. Second, the relatively small size of typical on-board storage makes it impractical for them to focus on recuperating the PV excess generation as it would compete with the braking energy over the available battery capacity, which is not practical from an energy transmission efficiency point of view.
For this, the power management scheme of the on-board storage studied in this chapter is the typical scheme found commonly in the literature that recuperates the braking energy of the vehicles and delivers it in moments of high load. Here in this chapter, the storage delivers the power when the vehicle has a demand of over 100kW.

POWER MANAGEMENT SCHEME FOR SESS

The power management scheme of the SESS is based on the State Estimator of Chapter 4, which was developed previously into an SESS-specific charging scheme in Chapter 7. With the power on the section estimated, the charging/discharging of the battery should also ensure that it does not break the upper and lower voltage limitations of the grid.
With further mathematical manipulation of Eq.4.2, it can be proven that, from a measured voltage V_M in the presence of other loads on the section, a desired voltage V^* can be obtained by injecting/demanding a power P^* described as:

$$P^* = -\frac{(V^* - V_M)(V^* + V_M - V_s)}{R_\sigma} \tag{8.1}$$

This derivation allows the estimation of the power values to reach critical line voltage states. For example, the power to reach the upper cut-off voltage limit of the trolleygrid, V_{COH}, can be described by the P_{COH} term:

$$P_{COH} \triangleq -\frac{(V_{COH} - V_M)(V_{COH} + V_M - V_s)}{R_\sigma} \tag{8.2}$$

Similarly, maintaining a voltage threshold V_{TH} can be assured by the power value P_{TH}:

$$P_{TH} \triangleq -\frac{(V_{TH} - V_M)(V_{TH} + V_M - V_s)}{R_\sigma} \tag{8.3}$$

Finally, Eq.8.1 can be manipulated to find the power value, P_{ZP} that does not break the spare capacity and voltage limits by assuming in Eq.8.4 below that the estimated power is at the end of the line, at L m from the substation:

$$P_{ZP} \triangleq \frac{(V_s - V_{ZP} - \rho L\frac{P_{est}}{V_{ZP}})(V_{ZP} + \rho(L - X_\sigma)\frac{P_{est}}{V_{ZP}})}{R_\sigma} \tag{8.4}$$

Where ρ is the overhead line resistivity in Ω/m.
From this, the charging and discharging powers, P_{ch} and P_{dch}, can be set in a way that breaks neither the power, nor the voltage, nor the battery technology limitations:

$$\begin{cases} P_{ch} = -\min(P_{tech}, P_{TH}, P_{ZP}) & \text{, charging} \\ \\ P_{dch} = \min(P_{tech}, P_{TH}, P_{est}, P_{COH}) & \text{, discharging} \end{cases} \tag{8.5}$$

Where P_{tech} is the maximum power exchange allowed by the technology. These derivations form the basis of the charging scheme for the SESS and the SESS-component of the Hybrid placement solution as detailed in the flowchart of Figure 8.1.
In this chapter, the LTO battery is operated with a C-rate up to 5, where the efficiency becomes as low as 95%. Moreover, V_{TH} is taken as 600V and the V_{COH} is the 740V typical of a trolleygrid [3].
In the following section, the results of the analysis are presented.

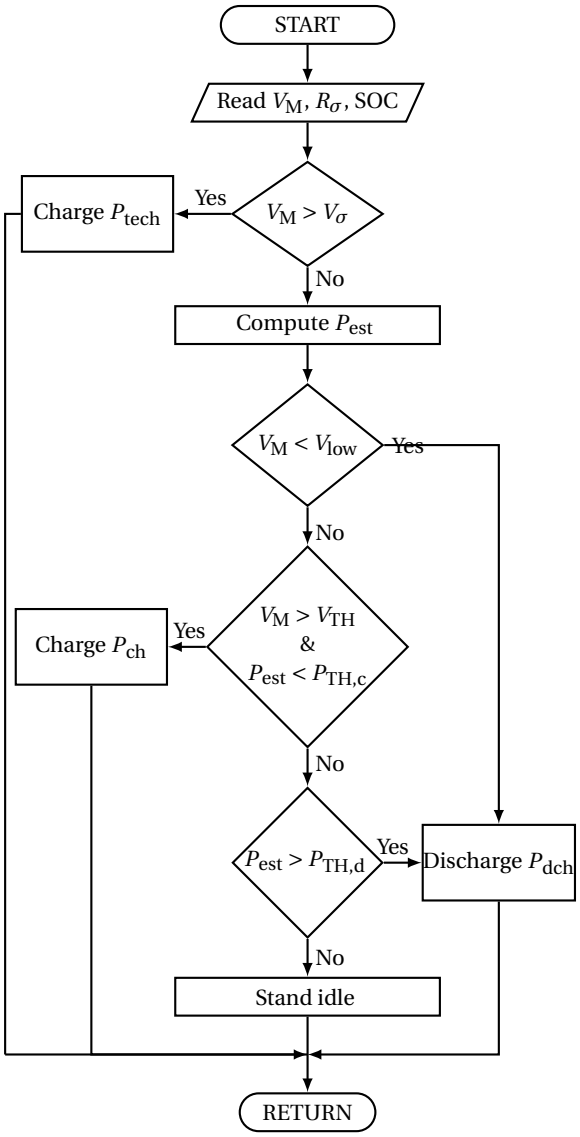

Figure 8.1: The proposed SESS power management flowchart.

8.3. RESULTS: YEARLY ENERGY DEMAND SAVINGS

Figure 8.2 shows the savings in the energy demand at each studied section.
The first observation is that the energy savings come primarily from the recuperation of otherwise-wasted braking energy, much more than from a reduction in transmission losses. This is to be expected, as the transmission losses are about 3-4% of the typical substation demand, while the available braking energy is about a third of the traction power demand [20], [40], [80], [183]. However, the observed energy savings are 10.3-19.0%, meaning that there is still a considerable theoretical amount of energy that can be saved. Yet this would need larger storage sizes, and given the battery costs, efficiency, transmission losses for charging and discharging on the section, technology power limitations, and self-discharge, it can be expected that the gains would diminish rapidly with increasing battery sizes.
The second observation is that OESS performs worse than all other placement options at both locations. This is expected as the relatively smaller size of the OESS limits the harvesting of the braking energy, and its efficient presence on board the vehicle next to the braking motor does not seem to offset this benefit, as observed in the figure. Furthermore, the OESS performs slightly poorer than the other methods when considering the savings in transmission losses alone at 0.5-0.6% versus 0.6-0.8%. This can be explained by how the SESS acts on the general line losses when it detects a voltage drop, while the OESS can *"waste"* its energy on an acceleration that occurs near the feed-in point, for example, where the vehicle could have been supplied efficiently anyhow. Additionally, the OESS recuperates some of the braking energy, but the C-rate limitation leaves some of it unharvested. This remaining lower braking energy can now find it more difficult to supply other buses because it cannot reach the required voltage level for successful braking energy sharing [16]. Consequently, the remaining braking energy is wasted in the braking resistors despite the presence of a load-demanding vehicle on the line. Contrarily, the SESS does not have this problem since the braking bus acts as a (high-power) source for both the SESS and any other vehicle on the line and finds it easier to reach higher voltages.
Thirdly, the hybrid solutions perform as a combination of the OESS and SESS, rather than achieving a synergetic outcome higher than both. However, this is still regarded as a positive outcome as it means that existing fleets with OESS should not worry about investment redundancy if they decide to install SESS systems for future needs such as solar PV energy harvesting or EV charger supply.
Moreover, there is not a significant difference between the EOL and MOL placement in either study.
Finally, it is interesting to note that the OESS is the only system that behaves better in a low-traffic substation than in a high-traffic substation, as expected from previous findings in the literature [156]. This can be explained by the fact that the work in [156] looked at stationary supercapacitors at the substation busbar, meaning that the braking energy was sent to the substation and the power shaving happened at the substation as well, rather than enhancing the braking energy recovery and line transmission losses. It can be said then that a stationary storage system at the substation housing behaves like an on-board storage and is less effective and more redundant with more vehicles on the line ready to accept the braking energy. However, stationary storage systems on the DC

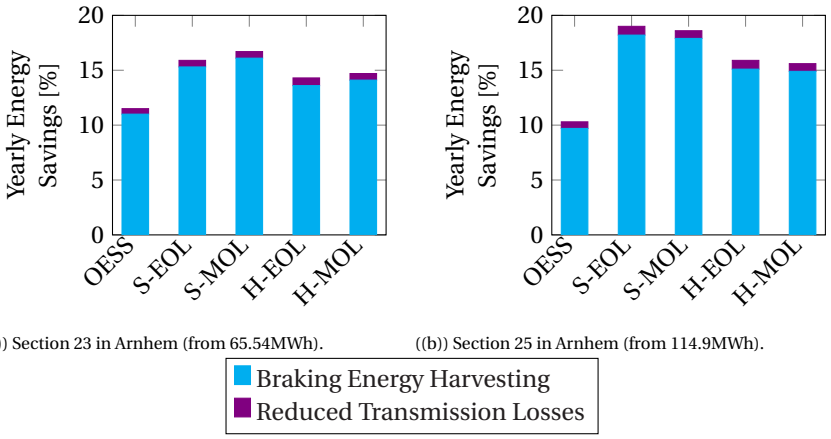

((a)) Section 23 in Arnhem (from 65.54MWh).

((b)) Section 25 in Arnhem (from 114.9MWh).

Figure 8.2: Simulation results of the yearly energy savings for each storage placement at each section.

side offer increasing benefits with higher traffic by enhancing the power flow among the vehicles and directly reducing transmission losses.

8.4. RESULTS: VOLTAGE DROPS REDUCTIONS

Figure 8.3 places the storage scenarios on a 2-D map of the lowest line voltage in a year and the change in cumulative voltage drops defined by Eq.7.2.

The first observation is that in both studies, the absolute minimum line voltage in a year brought by the implementation of storage systems is higher than the baseline and yet barely distinguishable among the individual solutions.

On the other hand, the cumulative voltage drops are more severe in the EOL placement options at the long, low-traffic section 23, even more than the baseline. This is because a storage device at the EOL has a contradicting purpose. First, it can act like a bilateral (dual substation) connection for the substation and effectively reduce voltage drops by tackling the voltage dips that are far from the substation. However, its periodic charging comes with higher voltage drops because of this longer distance. This can be observed in Figure 8.4 where the SESS at the end-of-line in charging-mode causes voltage dips worse than those seen in the baseline scenario. Overall, the numbers in Figure 8.3 show that while the minimum observed line voltage is enhanced in the EOL cases, the voltage sits lower overall compared to the other scenarios.

Moreover, in both studies, the OESS seems to offer the same voltage effect, albeit a bit lower, as expected, in the higher traffic study of section 25. This can be explained by the fact that the OESS *homogenizes* the bus demand by shaving the same peaks and dips in the profiles triggered at the same threshold values. On the contrary, the SESS gives the same response *regardless* of the bus positions and load profiles, which makes its performance more sensitive to the local traffic and load conditions.

Another observation is that the EOL options join the OESS in the high-traffic scenario at the shorter, high-traffic substations. This can be explained by the fact that the high traffic and, in consequence, the higher braking energy available allow the battery to charge

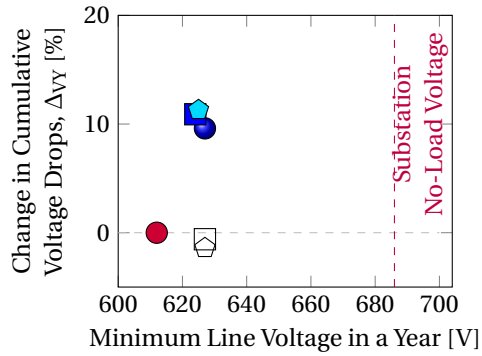

((a)) Section 23 in Arnhem.

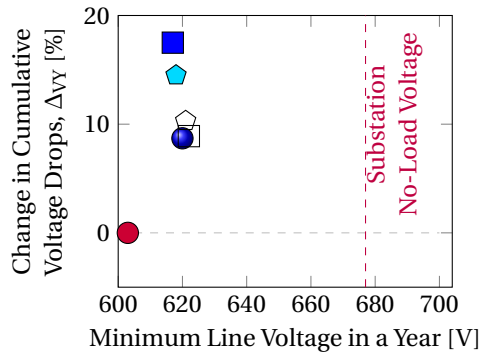

((b)) Section 25 in Arnhem.

Figure 8.3: Simulation results of the yearly minimum observed voltage and the change in cumulative voltage drops, Δ_{VY}, of Eq. 7.2, for different battery placement scenarios.

sufficiently and not rely on long-distance charging from the substation. In this case, the bilateral benefits of the EOL placement become apparent.
Finally, it can be seen that SESS MOL placement in both studies is superior or at least equal to the other scenarios, for the same reasons mentioned above. This, coupled with the energy performance, makes the SESS placement at the MOL the best option so far for a generalized storage recommendation.

8.5. RESULTS: SPARE SUBSTATION CAPACITY

Figure 8.5 shows the maximum recorded power peaks and the substation spare capacity that can be thereby afforded by the 800kW-rated substations in this study.
While the voltage and energy performances of the studied placement options were different, the power demand peaks that the substation sees with any storage device in place seem to be almost equal. In all cases, this is better than the baseline case. In the low-

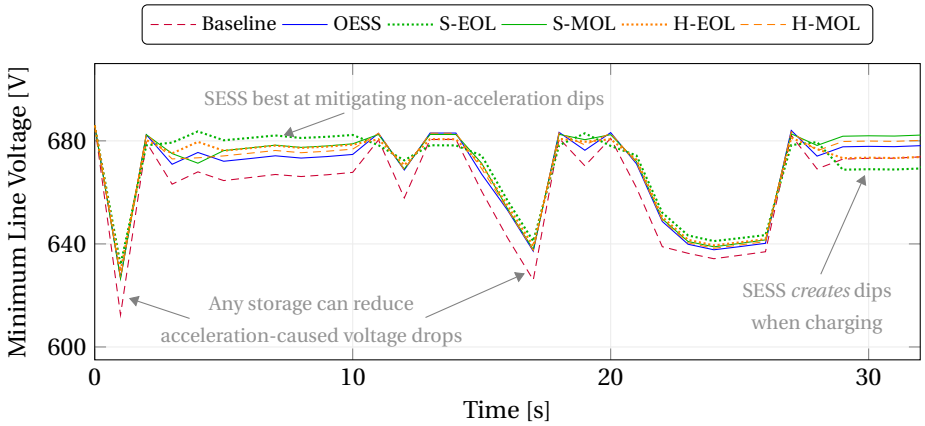

Figure 8.4: Minimum line voltage on section 23 (excerpt of a summer day with the lowest yearly dip).

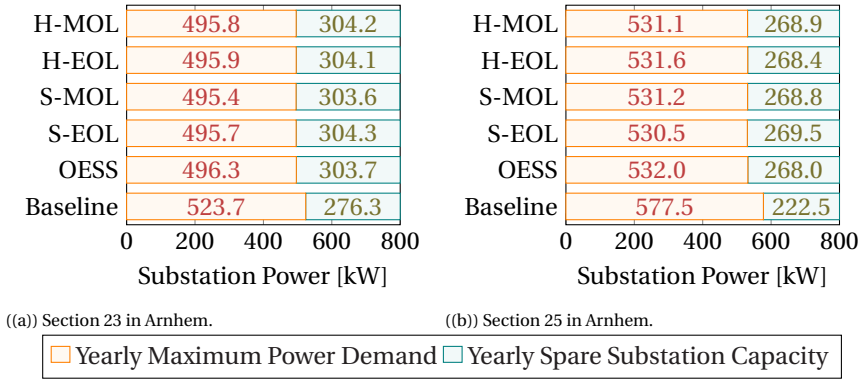

((a)) Section 23 in Arnhem.

((b)) Section 25 in Arnhem.

Figure 8.5: Simulation results of the yearly energy savings for each storage placement at each section.

traffic section 23, the power peaks were already low enough, and the storage systems added about 10% of extra spare capacity. This leaves more room for the addition of smart loads, such as EV chargers, to the trolleygrid.
Interestingly, the storage devices add over 20% of spare capacity to the high-traffic substation, bringing it to the baseline level of the low-traffic substation. This is a crucial benefit in load management since EV chargers, for example, might be demanded near the busier urban areas serviced by multiple lines, such as train stations or city centers.

8.6. Analysis and Generalization of the Results

8.6.1. On-board energy storage systems

OESS systems trailed behind the stationary and hybrid solutions in terms of overall performance. However, their performance seemed to be less sensitive than the other cases to a change of environment between a long, low-traffic scenario and a short, high-traffic

one. This is a crucial conclusion since OESS systems are placed on the vehicles themselves and therefore pass through a variety of substation profiles. It can be expected then that OESS systems will retain their performance throughout the vehicle trips through the transport network.
However, the added weight and volume constraints to the vehicle do not seem to offset their benefit in a full-OESS scenario, and it is more advisable to use smaller OESS devices in a hybrid scenario.

8.6.2. STATIONARY ENERGY STORAGE SYSTEMS

SESS systems performed the best among the three options, and better at the MOL than the EOL placement. More critically, SESS at the EOL should be avoided in long, low-traffic sections as they actually contribute to an overall lower voltage.
SESS systems also were found to be more efficient in high-traffic substations when placed on the DC side such as in this chapter, which is contrary to previous reports in the literature about diminishing benefits with higher traffic of SESS at the substation busbar.

8.6.3. HYBRID ENERGY STORAGE SYSTEMS

HESS consistently performed between the OESS and SESS values, with a slight tendency toward the SESS performance. This is a positive outcome as it means that already-made investments in OESS are not made redundant when augmented with (relatively small) SESS systems, creating a hybrid system. While this would not bring the benefit of a full SESS system implementation, it is still a positive step for traction networks with an already existing OESS fleet.

8.7. CONCLUSIONS

This chapter looked at a comparison of a fixed total storage capacity when implemented as on-board, stationary, or hybrid (on-board and stationary) battery storage solutions for trolleygrids.
The OESS performance was similar in both the low- and high-traffic environment when looking at the energy, voltage, and increase in spare power capacity. However, this performance was lower than that of the SESS and HESS solutions. This makes it a less attractive choice since the benefits brought by this on-board placement do not offset the weight and space disadvantages.
The SESS performance was superior or at least as good as the other options in every case, especially when considering the mid-of-line positioning. This performance was also against previous trends in the literature that warned that storage systems are less useful in higher-traffic environments.
Finally, the Hybrid systems proved to be a sound next-step investment for fleets that are already equipped with OESS. This is because the benefit increased when compared to the full-OESS case rather than creating a destructive effect of the two storage systems competing over the same available energy.
Future works are urged for more storage positions other than the MOL and EOL, and on different mixes than 50-50% for the hybrid storage.

9

ASSESSING AND INCREASING THE POTENTIAL OF EV CHARGERS INTEGRATION INTO TROLLEYGRIDS

"Du! Du! Du!
Du wirst sie zu befreien gehen
Du wirst der Tochter Retter sein..
Ja! Du wirst der Tochter Retter sein!"

O Zittre Nicht - Act I, Die Zauberflöte (Mozart)

```
You!  You!  You!
You will go to free her
You will be the savior of my daughter..
Yes!  You will be the savior of my daughter!
```

This chapter is based on "Methods for Increasing the Potential of Integration of EV Chargers into the DC Catenary of Electric Transport Grids: A Trolleygrid Case Study," K vd Horst, I Diab, GR Chandra-Mouli, P Bauer, in eTransportation, 2023, p.100271 **and** "Increasing the integration potential of EV chargers in DC trolleygrids: A bilateral substation-voltage tuning approach," I. Diab, G. R. C. Mouli, and P. Bauer, in 2022 International Symposium on Power Electronics, Electrical Drives, Automation and Motion (SPEEDAM), 2022, pp.264–269.

The traction substations of urban electric transport grids are oversized and underutilized in terms of their capacity. While their over-sizing is an unfortunate waste, their under-utilization creates the major hurdle for the integration of renewables into these grids due to the lack of a base load. Therefore, integrating smart grid loads such as EV chargers is not only an opportunity but a necessity for the sustainable transport grid of the future.
This chapter quantifies the potential for EV charger integration in trolleygrids and examines six methods for increasing this integration potential. These higher substation no-load voltage, a higher substation power capacity, a smart charging method, adding a third overheard parallel line, adding a bilateral connection, and installing a multi-port converter between two substations. From the case studies, the most promising and cost-effective method seems to be introducing a bilateral connection, bringing a charging capacity for up to 175 electric cars per day. Meanwhile, other costly and complex methods, such as fleet-aware smart charging with grid state sensors and communication, can offer charging room for over 200 electric cars per day.

Section 9.1 begins with an introduction to the integration of EVs in transport grids in general and trolleygrids in particular. Then, Section 9.2 proposes the six methods for increasing EV integration. Section 9.3 details the methodology for the EV demand modeling. The results are discussed in Section 9.4 and 9.5 for the designed theoretical case study and the Arnhem case studies, respectively. As the bilateral connection emerges as the best option for the integration of EV chargers, a substation-tuning method is suggested and investigated in Section 9.6 to motivate further research into the larger potential that can be harvested from the further tuning of the suggested methods in this chapter. Then, the analysis of the full results is generalized in Section 9.7 into more universal recommendations for the EV charger integration in trolleygrids beyond the investigated case studied. Finally, Section 9.8 concludes the chapter.

9.1. INTRODUCTION

Today, EV charging infrastructures are a critical bottleneck for the diffusion of electric vehicles (EVs). The barrier is the unavailability of spare charging capacity in the increasingly congested electricity grids that are not designed for more of such high, variable, and inconsistent power demands [157]–[160].
For this, urban electric public transport networks are being researched to host smart grid loads, like EV chargers, by integrating them into their infrastructures [3], [11], [15], [16], [67], [161], [232]. This is because, as explained in earlier chapters, these grids are historically sized for the worst-case scenarios of power demand, and can be better utilized by smart grid loads and appropriate power management.
There is also a benefit for the transport grids as this creates a base load on their substations in the moments of no vehicle traffic. This can reduce the need for expensive storage systems when, for example, a solar PV system is connected to the traction substation. This can be illustrated by the example of Figure 5.1(b) of the trolleybus grid of Arnhem, the Netherlands, where the lack of a base load jeopardized the techno-economic feasibility of the integration of renewables [11], [80].

Table 9.1: Overview of the projects with the integration of EV chargers into traction networks powering trolleybuses and trams.

Location	*Traction network*	*Description/objective*
Solingen, Germany [35], [36], [83], [162], [163]	Trolleybus	Investigating the potential of integrating decentralized renewable power generation (e.g., photovoltaics), charging stations for EVs, and stationary battery storage into the existing DC trolleybus infrastructure.
Gdynia, Poland [32]–[34], [164], [165]	Trolleybus	Analyzing the available capacity of the traction grid of Gdynia to charge electric cars. Furthermore, Smart Grid solutions for urban traction supply systems are introduced to improve the efficiency and stability of the traction network.
Edinburgh, Scotland [29], [30], [166]	Tram	Electrical capacity for EV charging systems based on four different charging control strategies are assessed and tested on the public tram system. The various connection topology, earthing methods, and stability criteria are considered.
Lisbon, Portugal [28]	Tram	Integration of bidirectional EV chargers into a DC catenary grid for trams. The authors looked into the concept V4G with an associated fuzzy control method. Furthermore, the benefits of an energy storage system in a catenary grid are demonstrated.
Sheffield, UK [26], [27]	Tram	Method to improve the energy efficiency of trams with the use of static energy storage systems and EV batteries in the public tram network. Current flow measurements and tram GPS data were used to simulate the energy flow in the catenary grid using a MATLAB/Simulink model.

9.1.1. INTEGRATION OF EV CHARGERS IN PUBLIC ELECTRIC TRANSPORTATION GRIDS

The integration of EV chargers directly into transport infrastructures is an emerging topic. While a number of studies exist on this theme, they mostly deal with simplified grid models and/or a lumped-energy methodology that does not consider the operational violations on the DC side of the transportation grid that an extra charging load could bring. Unfortunately, this is often overlooked in the literature, and while some works already tackle the integration of EV chargers in transport grids such as trams and trolleybuses (Table 9.1), they deal mostly with:

- Simplified grid models that do not calculate and/or consider the resulting grid power, voltage, and current violations, and/or
- An analysis of measurements that offer insight only into one case of a relatively small charger, and does not quantify the potential of the grid beyond it, and/or
- A focus on harvesting the baseline spare capacity of a specific EV charger case study, but without offering insights on how to increase this capacity and/or optimize the EV charger placement
- A focus on a local case study without an analysis that could serve the extrapolation of the results beyond the local studied grid

To start with the first point: As mentioned, transportation grids are oversized to account for rare occurrences of high power demands. These moments should still be considered

when integrating EV chargers so as not to violate the substation power rating. However, as with the maximum power limit, there are maximum line current and minimum line voltage limitations dictated by the overhead cable temperature limit and the vehicle current collector, respectively. Table 11.6 gives an example of the limitations of the trolleygrid of the city of Arnhem, the Netherlands, which is the case study city later in this chapter. It is then important for any transport grid study to consider all three violations simultaneously. Meanwhile, none of the studied cities reported in Table 9.1 account for this.

For example, the work in Gdynia [165] starts with historical measurements of the minimum line voltage and adds to them an estimated voltage drop based on the superposition principle. This approach has three limitations: First, the transport grid deals with (mechanical) power-source loads whose power flow cannot be accurately computed linearly by the superposition principle. Second, the superposition principle would ignore the combined voltage drop effect of all the load currents at the substation feeder cable (additional non-linearity in the solution). Third, the moments of maximum power, current, and voltage do not necessarily occur at the same moment; hence, a historical maximum/minimum of each parameter cannot be studied independently. For example, a high load near the substation would not necessarily create a large voltage drop. This is why *instantaneous* measurements or simulations of the current, voltage, and power must be *simultaneously* studied. Beyond this work, other studies either ignore studying the voltage drop, such as the works in Edinburgh [29] or Sheffield [26], or look only at averaged values of the voltage drops and not in absolute terms such as the work in Solingen [163], or overlook the reported line voltages as low as 350V such as the Lisbon study [28].

Regarding the second point, on the vehicle charger size, the study of Gdynia [165] and Lisbon [28] look at one fast charger up to 50kW, while the study in Solingen [163] goes up to 132kW in steps of 22kW. Meanwhile, the study in Sheffield [26] only mentions the advantages of EV charging, and the study in Edinburgh [29] finds an energy equivalent of the available EV charging power from the spare energy capacity afforded by historical substation measurements.

Regarding the third point, only the Edinburgh [29] study looks at the maximal achievable EV potential from the grid, while the other studies suffice themselves with one charger. Still, unlike the work proposed in our chapter here, none of the studies attempt to study methods to increase this EV potential beyond the instances of first violations of Power, Voltage, and/or Current.

Finally, all of the studies limit themselves to investigating their local case study, without any analysis that could serve as lessons-learned and extrapolation to other transport grids based on their local traffic intensity, section lengths, and desired EV charger location along the line.

9.1.2. CHAPTER CONTRIBUTIONS

This chapter offers the following contributions:

1. Three detailed case studies of EV charger integration in electrical public transport grids that use comprehensive and verified vehicle, grid, and *simultaneously* takes into account the effect on the grid power, voltage, and current violations, as op-

Table 9.2: Example of Trolleygrid Limitations: Arnhem, The Netherlands

Violation	Limitation	Allowable continuous duration
Maximum Substation Power*	$100\% < P_s \leq 120\%$	10 consecutive seconds
	$P_s > 120\%$	Never
Minimum Line Voltage	$400\text{V} < V_{min} < 500\text{V}$	120 seconds [233]
	$V_{min} \leq 400$ V	Never [234]
Maximum Current	$I_{max,1} < 880$ A	50 minutes [83], [165]
	$I_{max,2} < 1200$ A	30 minutes [59]

*Limit currently tolerated by the trolleygrid operator

posed to the less comprehensive studies in the literature that focus only on one or two of the three violations, while using simplified grid models

2. Detailed comparison of six methods for *increasing* the EV charger integration potential, namely a higher substation voltage, a higher substation power capacity, a smart charging method, adding a third overheard parallel line, adding a bilateral connection, and installing a multi-port converter, in terms of quantifying their additional EV charging potential at any location on a general trolleygrid section

3. An analysis and thereafter a general extrapolation of the three case study results into a set of generalizable suggestions on the sizing and placement of EV chargers in any section of a given trolleygrid depending on the traffic intensity, section length, and desired EV charger location along the line

9.1.3. CHAPTER STRUCTURE

The chapter starts with an introduction to EV chargers in public electric transport grid in section 1, and suggests six methods in section 2 for increasing this integration potential. Section 3 presents the modeling methodology for the various subsystems of the simulations used in the three case studies of this chapter: The theoretical case study of section 4, and the two case studies of Arnhem, The Netherlands, in section 5. Section 6 offers a summary of the recommendations of this work in terms of the sizing and placement of EV chargers in electric public transport networks. Finally, section 7 closes with recommendations and future works.

9.2. SIX METHODS FOR INCREASING THE EV INTEGRATION POTENTIAL

To increase the integration potential of EV chargers, while respecting the grid limitations, this section studies six methods designed to tackle the power, voltage, and current limitations. This diverse set of proposed methods is important so as to offer a customized solution that can cater to the common violations at each substation. For example, short sections (a few hundred meters) would not typically see serious voltage drops in their short overhead cables and therefore do not benefit from a solution that primarily tackles

the voltage drops. Table 9.3 summarizes the six methods and their intended mitigation use.

Table 9.3: Summary of the six methods addressed in this chapter and their positive (+), negative (-), or neutral (o) effects on reducing the grid violations in power, voltage, and current, as well as their effect on the transmission losses and the braking energy recuperation.

	Reduces violations of:			Effect on:	
	Power	Voltage	Current	RI^2 losses	BR* losses
Higher Substation Voltage	+	++	+	+	-
Higher Substation Power Limit	++	0	0	0	0
Third paralleled Line	+	++	++	++	+
Bilateral Connection**	++	++	++	++	+
Fleet-Aware Smart Charging	++	++	++	+	++
Multi-port Converter	-	-	-	+	+

*Breaking energy recuperation, **Unless both substations are heavily loaded

1. **Substation level**

   1.1 *Increasing the substation nominal voltage*
   This method increases the overall line voltage by increasing the substation no-load voltage setpoint via the traction transformer taps. This is not therefore a dynamic voltage-compensation method, but a one-time physical intervention. This method shifts the whole line voltage up, moving away from the critical voltage levels of 500V and 400V. Consequently, it also reduces the line current for the same power demand. A disadvantage is that the on-board braking resistor would be activated more frequently since the voltage is now closer to the upper limit of the grid. As a result, the total power consumption could be increased by this method, unless the reduction in transmission losses compensates for the loss in unharvested braking energy. This method invites the transport grid operators to rethink the substation no-load voltage set-points, not as a trade-off between braking energy harvesting and transmission losses, but also to take into account a desired minimum line voltage. In summary, as reported in Table 9.3, this method can directly reduce the voltage drops, and indirectly the power and current violations. This would reduce transmission losses, but has a negative effect on the braking energy recuperation (braking resistor activation).

   1.2 *Increasing the substation power limit*
   The substation power limit can be increased either by accepting a less conservative limit for the transformer overload or by an upgrade of the existing infrastructure to add capacity.
   As reported in Table 9.3, while this method directly addresses the power violations, it changes nothing in the grid operation and power flow, however, and has therefore no effect on any other grid states or operations.

2. **Grid infrastructure level**

   2.1 *Adding an extra overhead paralleled line*
   The impedance in the overhead wires is effectively reduced by adding an extra overhead cable in parallel to the existing cables (typically two existing cables, one for each side of the road). Since the power flow solution is non-linear (voltage source supply with power-source loads), this ratio in the reduction of the impedance would bring about an even more considerable reduction in the voltage drop than that ratio.
   As reported in Table 9.3 then, this has a direct positive impact on current and voltage violations. Additionally, this has an indirect positive impact on power losses, and a more effective braking energy sharing, both of which lead to a reduction of the substation power demand.

   2.2 *Introduction of a bilateral connection*
   The introduction of a bilateral connection splits the section load supply to two different substations. As summarized in Table 9.3, this consequently reduces the line current, the line voltage drops, and the resistive losses. Additionally, it increases the effectiveness of braking energy sharing by more frequently exposing the braking vehicle to power-accepting nodes. Consequently, the power demand on each substation is lowered. It is worth noting still that this recuperation of the braking energy is only a passive benefit and, thereby, not the most effective solution.
   On the other hand, due to the larger supply zone, faults in the system could occur more often per supply zone and influence a larger area, which is the main reason for the hesitation toward bilateral connections. Furthermore, it is worth noting that the power-sharing in a bilateral scenario is heavily influenced by the voltage of each substation [16].

3. **EV charging level**

   3.1 *Introduction of a smart charging with a fleet-aware power management scheme*
   Smart Charging controls the charging power continuously with respect to time [235]–[237]. With smart charging, the EV charging load could be reduced at moments when the loads are high, by measuring the instantaneous substation and fleet vehicles' powers and locations and wirelessly communicating them to the EV charger. With this, a power flow calculation (such as in [3], [19], [62]) can compute the voltage at every power node on the trolleygrid section, and the total power demand at the traction substation.
   Based on this information, the allowed EV charging power is chosen at each instant as the maximum desired power that would not violate the local grid power, voltage, and current limitations such as those in Table 11.6 for the Dutch grid of Arnhem. The power output of the EV charger is determined from this calculation. This is referred to in this chapter as Fleet-Aware Smart Charging and illustrated in Figure 9.1.
   In brief, an EV charger with a Fleet-Aware Smart Charging power management scheme receives the state (power, voltage, location, etc.) of each trol-

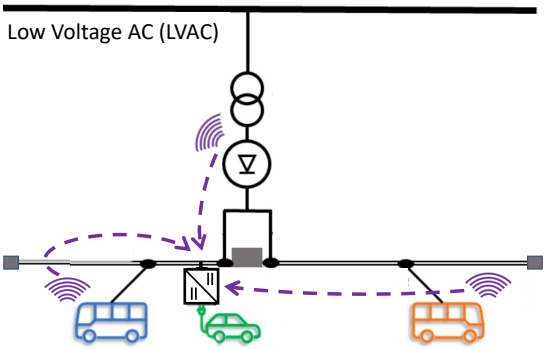

Figure 9.1: Illustration of Fleet-Aware Smart Charging: In this method, the substation and the vehicles on the section communicate their states to the EV charger (power, voltage, location) and the latter computes its allowable charging power that would not break any of the grid limitations at any node on the line (not just at the charger).

leybus and substation and load connected to a section. Then, implementing any readily available power flow calculation method from the literature calculates the maximum power it can draw at that instant that would not break any of the power, voltage, or current limitation of the local trolleygrid. This method is important because the small section lengths, moving loads, and severe voltage drops that can occur in transportation grids make the handling of EV chargers more complex than in regular distribution networks. An EV charger looking to maximize its power demand at a given instance needs to consider not only the available spare power capacity but also its effect on the line minimum voltage and maximum current for any vehicle on the section. For this, the EV charger's control algorithm should not only communicate with the supplying substation to compute the spare capacity (conventional smart charging). The controller needs to also communicate with all the moving vehicles of the fleet on the section to know their position and power demand, which is used to find the maximum allowable charging power that simultaneously respects the three grid limitations. The complexity of this method makes it hard to implement as it requires a lot of sensors, processors, and wireless communication between them. One alternative could be to use the available GPS bus data and the substation state (conventional smart charging) to estimate the state of each note on the grid, but that requires the development of a grid state estimator.

Another concern that can be raised is the Quality-of-Service (QoS) of EV charging. According to [238], the QoS can be examined on three levels: The energy delivered, the time of charging, and the variation of the charging power. However, the purpose of this method is to avoid the short moments of spare capacity dips that can occur on a trolley section, meaning that the charging is not significantly disturbed on a frequent basis. For example, a trolleybus

acceleration lasts less than 10 seconds from 0 to its 300kW peak [3], which means that the high power moments when the FASC method intervenes by curtailing the power is in the order of a few seconds. Furthermore, as seen in Figure 5.1(b), the timetabling creates long periods of absolute zero-load on the traction substations where the QoS is fully ensured. The QoS is then not a significant concern with this method, especially with the rise of incentives such as in [239] that suggest payable schemes for users who require a perfect QoS.

By virtue of its design, this method is beneficial in all aspects as reported in Table 9.3. The only possible drawback can be that it is not as intensive in the reduction of losses as, for example, the bilateral connection since its function is to maximize the power drawn, and not reduce the losses. This maximization of the harvesting of the available power justifies why it is reported as having such a considerable effect on the braking energy recuperation.

3.2 *Introduction of a multi-port converter*
A multi-port converter (two inputs, one output) can be used to charge an EV from two separate traction substations. This is done by connecting each of the two input ports to a section of each substation. It is suggested as an alternative to a bilateral connection if a charger is desired near the section separation (end-of-line). In this manner, each substation is loaded with only half of the power demand of the EV charger. This is different from the bilateral case because only the charger is simultaneously fed from the two separate substations in this configuration and not the trolleybuses. This offers the charger the benefits of a bilateral connection without the related concerns for faults. This solution is further detailed and explored in [67].
The downside of this solution is that it can add more voltage, current, and power violations as it adds a load to the end-of-line of two sections. However, this method reduces the losses in supplying the converter when no buses are on the section (as shown in [67],) and increases the braking energy recuperation by harvesting it from two trolleygrid sections. The reported results are in Table 9.3.

9.3. MODELING METHODOLOGY

9.3.1. DEFINITION OF THE THREE CASE STUDIES

This chapter presents three case studies for EV integration. By choosing different grid parameters (grid layout, traffic, etc.), the cases help quantify and thereafter extrapolate the EV potential to various locations.
The three cases are:

- Supply zone T: Theoretical case study, as typically performed in literature, using a trapezoidal velocity profile on two very long sections (over 1200m). The long section would mostly suffer from voltage problems
- Supply zone A: Case study from Arnhem with actual bus velocity and power data

Table 9.4: Grid parameters were used for the theoretical study [3], [11], [165].

Theoretical Grid Parameters	Value	Unit
Total track length	4569	[m]
Section lengths	[1500; 1500; 1569]	[m]
Overhead line resistivity	172	[mΩ/km]
Feed-in point location	[0; 3000; 3000]	[m]
Feed-in cable length	[100; 100; 100]	[m]
Feed-in cable resistivity	56.6	[mΩ/km]
Substation Rated Power	[800; 800]	[kW]

Table 9.5: The characteristics of the supply zones investigated in the case study.

Supply zone	Substation & powering section(s)	$V_{\text{nom,ss}}$	Bilateral between sections
T	SS_1 = 111 SS_2 = 112 & 113	SS_1 = 650 V SS_2 = 650 V	111 & 112
A	SS_{12} = 23 & 24 SS_{13} = 2 & 3	SS_{12} = 686 V SS_{13} = 698 V	23 & 2
B	SS_9 = 25 SS_{14} = 26 & 27 & 41	SS_9 = 677 V SS_{14} = 628 V	25 & 26

on two medium-to-long sections and with a low traffic

- Supply zone B: Case study from Arnhem with actual bus velocity and power data on two medium-to-short sections and with a high-traffic

The case studies are simulated for the worst-case scenario of high auxiliary demand (heating) and the highest traffic schedule (winter workday, day 268 in the year). The detailed information on all supply zones is in Tables 9.4, 9.5, and 9.6. From these, Table 9.7 alerts of the risks of violations at each supply zone as predicted by the key grid parameters [11].
In the theoretical study, Substation 1 is powering section 111, while Substation 2 is powering sections 112 and 113. The chosen parameters are based on typical trolleygrid parameters and summarized in Table 9.4. This section uses the same limitations and parameters previously described in tables 11.6, 9.5, and 9.6.

9.3.2. CREATING AND QUANTIFYING A REPRESENTATIVE CHARGING PROFILE

For a representative EV charging power demand, two charging profiles are derived from measurements of 10000 public charging transactions in The Netherlands in 2019 [240]. One charging profile is for the weekdays (7235 transactions), and the other is for the weekend days (2765 transactions). The charging profiles have a time step of 1 second.
Figure 9.2(a) provides an example of a few of the recorded 1000 transactions and Figure 9.2 shows the resulting power distribution profile from the 10000 transactions, normalized to a unity value. This unity demand is then multiplied by a constant factor to create

Table 9.6: The characteristics of the sections where the EV chargers are placed for the case study.

Supply zone	Section	Length [m]	Feed-in point location [m]	Feed-in cable length [m]
T	111	1500	0	100
	112	1500	1500	100
A	23	850	80	98
	2	1300	1210	300
B	25	860	100	180
	26	650	550	70

Table 9.7: Risk of violations at each supply zone from key grid parameters.

		Risk at Supply Zone		
	Effect on violations	T	A	B
Section Length	V, I	High	Medium	Low
SS Nominal Voltage	V, I	High	Low	Medium
Average Traffic	P, V, I	Medium	Medium	High
Peak Traffic	P, V, I	Low	Medium	High

the EV charging demand curve for the EV charger at any rated power in this study. As observed, the demand peak is around 9:00 during the weekdays and around 15:30 during the weekends.
From that, the number of EVs charged per day, referred to in this chapter as # of EVs/day, is calculated by:

$$\#\text{ of EVs/day} = \frac{\eta_{\text{con}} \cdot \eta_{\text{EV}}}{E_{\text{batt}}} \sum_{t=1}^{86400} P_{\text{EV}} \tag{9.1}$$

Where:
η_{con} is the DC/DC converter efficiency of the EV charger, assumed at 98%, η_{bat} is the battery charging efficiency, assumed constant at 95%, E_{batt} is the EV battery size of 60 kWh, and P_{EV} is the per-second charging power profile output of the studied scenario, summed over the 86400 seconds of the day.

9.4. RESULTS: THEORETICAL GRID CASE STUDY

The purpose of this section is to present the results of the case study of a theoretical grid, as is commonly approached in literature. This study will highlight the impact of the six methods on long sections of low substation voltage and low, yet constant traffic. Along with the case study of the Arnhem trolleygrid in the section, this offers generalized results by looking at different infrastructure topologies and bus traffic intensity.

9.4.1. A CLOSER LOOK AT SOME RESULTS: HIGHER SUBSTATION NOMINAL VOLTAGE

Substation voltages are typically designed as a trade-off between the minimum line voltage and the facilitation of regenerative braking energy sharing between far buses [11],

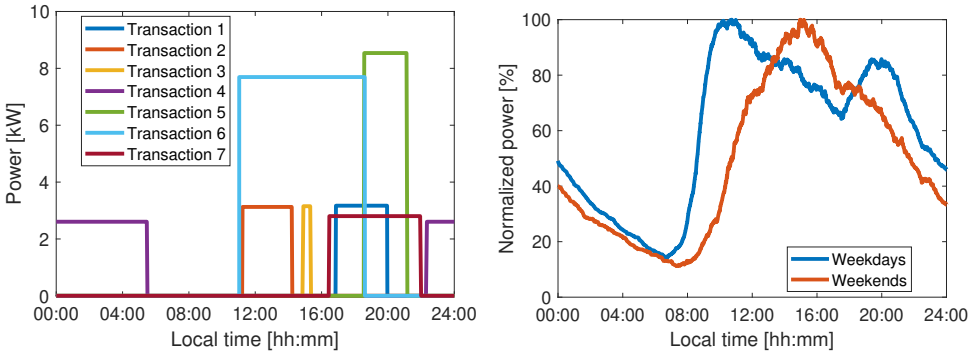

((a)) Various charging transactions.

((b)) EV power profile distribution over a day.

Figure 9.2: The EV charging demand used in this chapter from 1000 measured transactions in [240], (a) example of a few measured transactions, (b) summation curve of the 1000 transactions, normalized to a unity value.

[14], [16], [80]. A section with a low substation voltage can not allow EV charger integration as it would quickly experience voltage (and consequently power and current) violations. Such sections benefit from higher substation voltages and offer a smart base load that would still allow efficient harvesting of the regenerative braking energy.
The effects of this method are observable in Figure9.3, showing the minimum substation voltage required to allow the EV charger integration at any location on the section, and the grid violations that limit if the substation voltage is lower.
For example, In the case of a 200kW charger, an EV charger of this size can only be implemented at 1050m from the substation if the substation voltage is at least 670V. Otherwise, the simulations have shown that there would be voltage violations (blue dashed zone in the figure). Meanwhile, this charger at 300m from the substation could still be feasible with as low as 650V. On the other hand, a 350kW charger at 1050m from the substation cannot be guaranteed with a simple tuning of the substation voltage (the teal-blue curve is discontinued). As the Figure shows, this is because there is a power violation at this charger size (red dashed zone) that a mere voltage upgrade cannot solve.
The 100kW charger is feasible anywhere on the section. However, as these two long sections have a relatively low substation voltage, it is expected that the voltage is indeed the limiting factor for chargers up to 250kW far from the feed-in point. For 300kW and 350kW, power violations become the limiting factor, which is expected as these large values are almost half of the rated substation power of 800kW. Tuning the nominal voltage of a substation to a higher level is indeed an effective solution, especially at the end-of-line (EOL) of a long section of low, yet constant traffic.

9.4.2. A CLOSER LOOK AT SOME RESULTS: HIGHER SUBSTATION POWER LIMIT

The effects of this method are observable in Figure9.4, showing the effect of various maximum substation power tolerances on the EV charging potential for section 111 for different charger locations along the section. The simulated values are shown as [Multiple of substation rated power, continuous violation duration], for example, as [120%, 10s] to

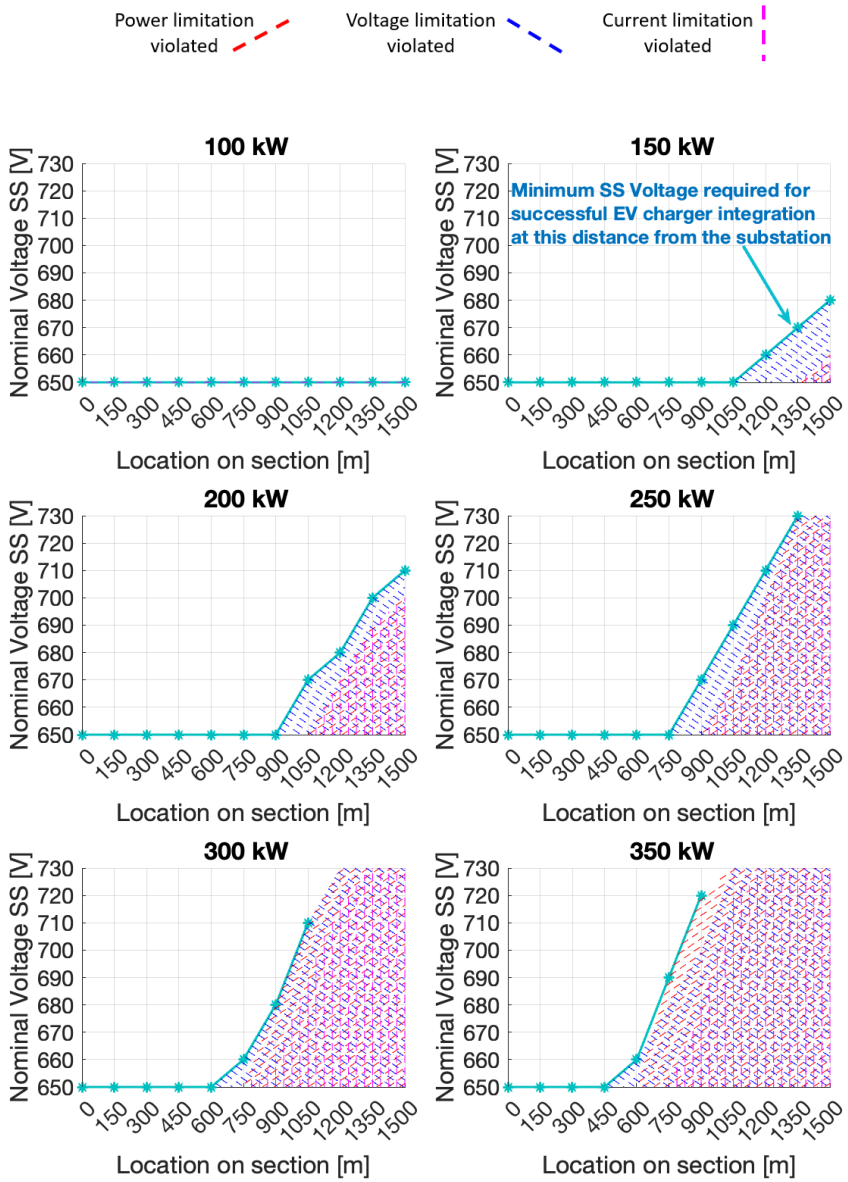

Figure 9.3: The minimum substation voltage required for the successful EV charger integration of a certain size at any location on the section. The zone and type of the limiting grid violations are shown with dashed lines.

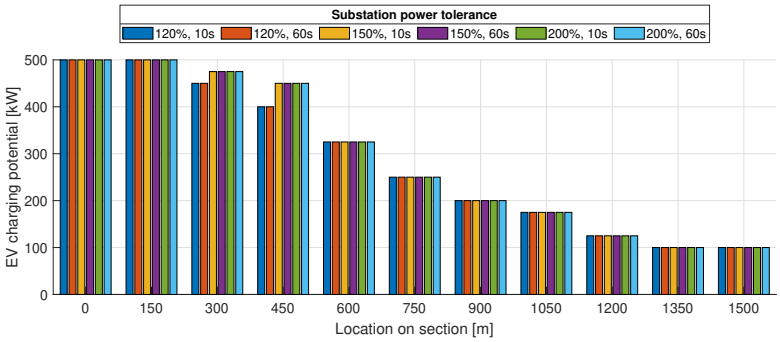

Figure 9.4: Effect of various maximum substation power tolerances on the EV charging potential for section 111 for different charger locations: [Multiple of substation rated power, continuous violation duration].

show that the power demand at the substation is tolerated to go as high as 120% of the rated power for 10 consecutive seconds. No considerable benefit, if any, is brought on by changing the substation power limit in this section. These results were expected as long sections of low, yet constant traffic do not have a more pronounced voltage problem than a power problem. Consequently, accepting a more lenient power peak tolerance would do little, if any, to increase the potential for EV integration.

9.4.3. A CLOSER LOOK AT SOME RESULTS: FLEET-AWARE SMART CHARGING

Figures 9.5(a) and 9.5(b) display the different loads on the section when a 500kW EV charger is placed at 400 meters from the feed-in point with a ramp-up/down speed of 3 kW/s and 9 kW/s, respectively.

The ramping up and down is activated when the EV charger detects a rise or drop, respectively, in the available spare capacity. The ramping is helpful from a stability perspective to avoid harsh fluctuations on the line from the chargers connecting/disconnecting in full. This allows the charger to follow the spare capacity trend in a smooth fashion and account for the delays in the telemetry and the processing time of the data used to compute the spare capacity.

As seen in the figures, the higher ramp-up/down converter can respond faster to various bus loads, with better peak shaving as a result. Such an example can be best offered at 9:05 when the violating power peak at 3kW/s is avoided at the 9kW/s scenario. Still, more examples can be observed in multiple power peaks, albeit non-violating, being shaved.

9.4.4. OVERVIEW OF THE SIX GRID METHODS - THEORETICAL STUDY

The previous subsections provided a closer look and a detailed analysis of three methods. The results of all six methods for the theoretical supply zone are summarized in Figure 9.6 and Table 9.8 summarizes the numerical results for all the grid methods. As expected, the long, low-traffic sections 111 and 112 are restrained by the voltage limitation when it comes to the integration of additional load.

Consequently, the voltage-oriented solutions of higher SS voltage, extra paralleled line

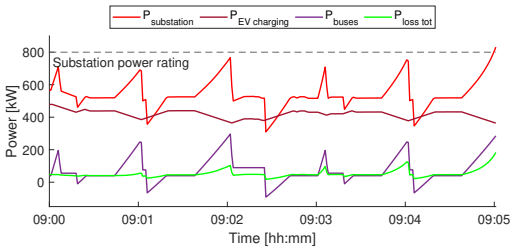

((a)) Loads on section 111 with a ramp-up/down speed of 3 kW/s.

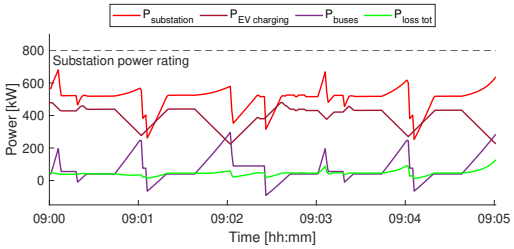

((b)) Loads on section 111 with a ramp-up/down speed of 9 kW/s.

Figure 9.5: The substation power (buses + EV + line losses) for an EV charger at 400m. It is noticeable at 9:05 that the faster response of the management system allows the grid to avoid a power violation that occurs with the slower response.

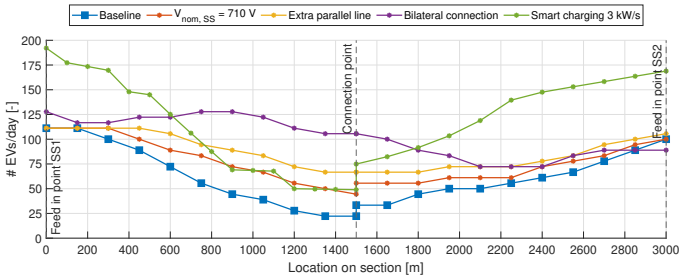

Figure 9.6: Summary of various grid methods on the maximum achievable EV charging potential on the theoretical sections 111 (left) and 112(right). Grid methods: increasing substation power and the multi-port converter are excluded from this graph as they showed no benefit.

Table 9.8: Supply zone T: effect of grid methods on the maximum achievable EV charging potential in the theoretical study (*Achievable with one charger **Achievable with one charger at the connection point).

Grid method	**Section 111** [# of EV/day]		**Section 112** [# of EV/day]		**Sec. 111+112** [# of EV/day]
	Max.	Mean.	Max.	Mean.	Max.
Baseline	111	63	100	60	211
Substation voltage	111	81	100	71	211
Substation power	111	65	111	74	222
Extra overhead line	111	93	106	80	217
Bilateral connection	128*	119*	106*	86*	128*
Fleet-aware smart charging	182	110	167	126	349
Multi-port converter	22	0	33	0	56**

seem more effective -especially at EOL (end of line)-, as well as the bilateral connection, which seems even more effective at MOL (mid of line) in addition to the EOL. Meanwhile, the power-oriented solution of increasing the substation limit has no noteworthy benefit. Furthermore, the multi-port converter (two inputs, one output) offers less potential for EV charging compared to the baseline. This is an inherent consequence of its end-of-line placement and of the voltage drops that it brings to both sections to which it is connected.

On the contrary, the smart charging method produces the highest benefit at the SOL (start of line) of both sections, while its benefit is less pronounced at MOL/EOL for section 111, and EOL of 112.
This can be explained by the fact that the fleet-aware smart charging only looks for harvesting the *attainable* charging power available, without increasing the spare capacity of the substations in any way. As both sections have very low traffic (read: power demand), there is a lot of spare capacity whenever smart power management is involved.
However, there is no active management solution that would help the limiting voltage drops at the EOL, and those need a passive solution that boosts the voltage altogether, such as substation voltage, paralleled lines, bilateral connections, or a combination of these.
The MOL advantage of 112 is that this section is powered along with another section (namely 113,) by one substation. This gives the advantage to the Smart Charging method as it has all the necessary information at the substation level, not only the section level. This information is hidden from the other, mostly-passive methods, that only have local, section-level information. This is why with section 111, powered alone by a substation, this all-knowing advantage of the Fleet-Aware smart charging method disappears at the MOL.

9.5. REULTS: ARNHEM GRID CASE STUDY

9.5.1. A CLOSER LOOK AT SOME RESULTS: PARALLELED LINES

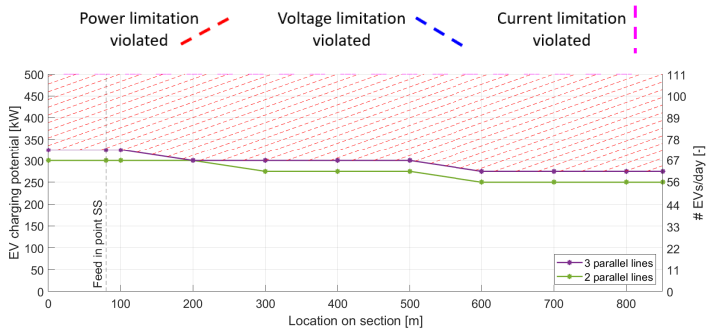

Figure 9.7: Effect of adding extra paralleled overhead wire on the maximum achievable EV charging potential on section 23, day 268. The colored area indicates the limiting factor in the three paralleled overhead wire scenario.

Table 9.9: Section 23: comparison of energy consumption substation and transmission losses with an extra paralleled line. The size of the EV charger is the maximum potential in that specific location for the two paralleled line case.

Location [m]	EV charger [kW]	E_{SS} [kWh/day]		$E_{loss,trans}$ [%]	
		2 lines	3 lines	2 lines	3 lines
0	300	4970	4959 (-0.22%)	0.89	0.68 (-23.6%)
200	300	4987	4970 (-0.34%)	1.24	0.90 (-27.4%)
400	275	4686	4649 (-0.79%)	2.53	1.75 (-30.8%)
600	250	4365	4313 (-1.19%)	3.57	2.41 (-32.5%)
800	250	4424	4350 (-1.67%)	4.85	3.23 (-33.4%)

SUPPLY ZONE A

Figure 9.7 shows the EV charging potential for two paralleled overhead lines (baseline scenario) and three paralleled overhead lines. The EV charging potential is 25 kW higher for most locations on section 23. With the introduction of an extra paralleled line, the power rating of the substation is still the limiting factor. In contrast to the results found in the sections of the theoretical study, the substation power tolerance is the limiting factor on this section and not the minimum line voltage. Therefore, the effect of this method is negligible. Adding an extra paralleled reduces the substation power slightly by reducing the transmission losses, and increases the EV charging potential. But the effect of the reduction on the voltage drop is more significant, as shown in the case study, and this method should be used in such environments. Table 9.9 summarizes the energy savings associated with introducing the additional paralleled overhead line. This method has the highest effect on the reduction of the energy consumption of the substation when placing the EV charger further away from the feed-in point (EOL). With a 250 kW EV charger, adding an extra paralleled line reduces the energy use by 74 kWh/day. This is -1.67% of the SS energy, but 33.4% of the transmission losses.

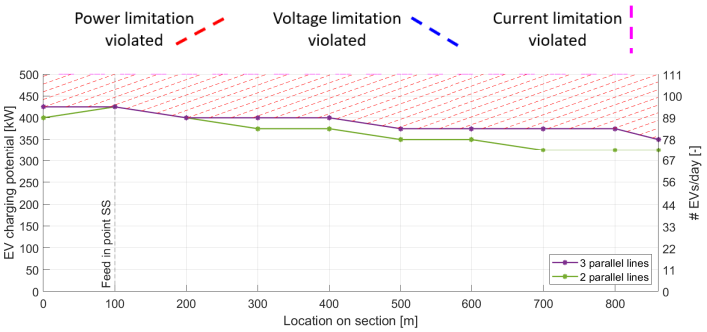

Figure 9.8: Effect of adding extra paralleled overhead wire on the maximum achievable EV charging potential on section 25, day 268. The colored area indicates the limiting factor in the three paralleled overhead wire scenarios.

SUPPLY ZONE B

Figure 9.8 shows the EV charging potential for two paralleled overhead lines (baseline scenario) and the three paralleled overhead lines scenario. Depending on the location of the EV charger, the potential increases between 25 and 50 kW. This is expectedly similar to the results of supply zone A because the substation power limitation is the limiting factor here as well.

9.5.2. A CLOSER LOOK AT SOME RESULTS: INTRODUCING A BILATERAL CONNECTION

SUPPLY ZONE A

In supply zone A, a bilateral connection between sections 23 and 2 is possible. Substation 12 is powering sections 23 and 24, whereas substation 1 is powering sections 2 and 3. The substation nominal voltages are 686 V and 698 V, respectively. The effect of this grid method is shown in Figure9.9. In the bilateral connected scenario, the maximum EV charging potential is between the connection point and substation 13. In this region, substation 13 supplies most of the power to the charger. The colored area indicates the limiting factor for the bilateral case.

SUPPLY ZONE B

Due to the relatively significant difference of $V_{\text{nom, SS}}$, 677 V vs. 628 V, the introduction of the bilateral changes the power source for the trolleybuses and EV chargers in supply zone B [16]. For the baseline simulation, the EV charging potential on section 26 is zero at every location, as seen in Figure 9.10. With the bilateral connection between sections 25 and 26, substation 9 can power section 26. Therefore, the loads on section 26 can be also served by substation 9, and more EV potential can be created.
However, the EV charging potential decreases at some point on section 25.

Figure 9.11 shows the energy shared between the two substations on supply zone B when an EV charger of 100 kW is integrated on the sections. Due to the higher nominal voltage of substation 9 compared to substation 14, most of the supplied power is supplied by substation 9 [16].

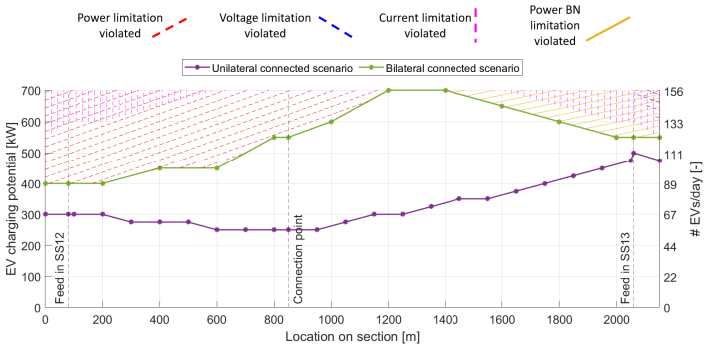

Figure 9.9: Effect of introducing bilateral connections between sections 23 (left, 0-850 m) and 2 (right, 850-2150 m) on the maximum achievable EV charging potential.

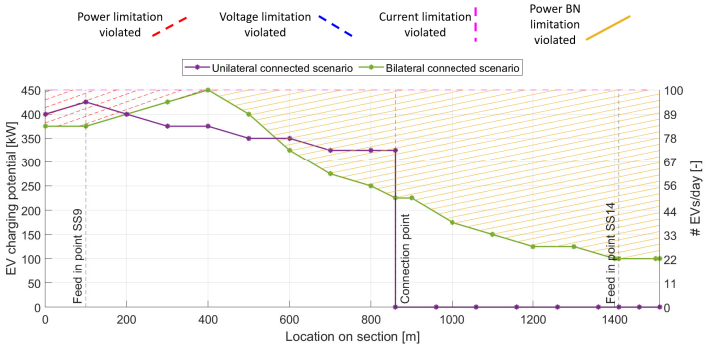

Figure 9.10: Effect of introducing bilateral connections between sections 25 (left, 0-860m) and 26 (right, 860-1510m). The power limitation at the bilaterally connected substation P_{BN} is also shown

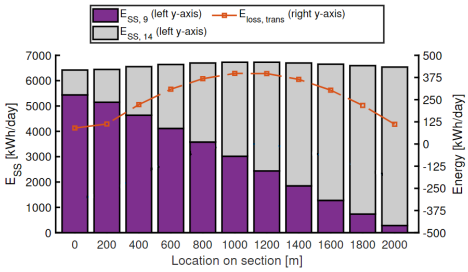

Figure 9.11: Energy share of the two substations in supply zone A (left axis). A 400 kW EV charger is placed at different locations on sections 23 and 2. The orange line (right axis) shows the cables' energy losses due to transmission losses

9.5.3. A CLOSER LOOK AT SOME RESULTS: MULTI-PORT CONVERTER

A Multi-port converter between 25 and 26 would not be feasible, as section 26 has no power capacity. The EV charging potential at the connection point of the sections is then 0kW. This highlights the key difference between a multi-port and a bilateral connection, in how the multi-port brings to the grid the disadvantages of the EOL placement (lower voltages and higher line currents), while bringing none of the benefits of the bilateral connection. Indeed, as is presented later, a bilateral connection does create an EV charging potential at section 26.

9.5.4. OVERVIEW OF THE SIX GRID METHODS - ARNHEM CASE STUDIES

The previous subsections provided a closer look and a detailed analysis of three methods. Figures 9.12 and 9.13 and tables 9.10 and 9.11 summarize the results of the six proposed methods as well as as a combination of the capacity-building increasing ones (case 1): $V_{\text{nom, SS}} = 710$ V, an extra paralleled overhead line, and a substation power rating of 1100 kW. The 1100 kW is 300kW more than the current limit of 800, and that is the power of one accelerating bus with the heating system on.
In supply zone A, section 23 is medium length with a medium-high substation voltage and thereby does not have a voltage or line current problem. It is expected then that the substation voltage and extra paralleled line methods do not contribute to any benefit, while the other power-centric methods did.
By contrast, section 24 is a long section supplied by a substation that feeds another long section. While the traffic is medium in average values and peak-values on the section, its connection to another long section of similar traffic means there are many instances of low spare grid capacity (as opposed to short sections that do not see bus traffic for long). This explains why the static power solutions of "Case 1" and "increasing the power limit" did not offer much additional potential to the section, as did the "load-shifting" methods of smart charging and bilateral connection. In short, this section had a lot of spare capacity once the load (especially the peaks) could be shifted or shared, rather than a fixed increase in power capacity. Interesting to note that as this section is long, the extra line had a clear positive impact at EOL.
Supply zone B clearly had a power problem, especially at section 26. It was expected that voltage and current methods do not produce tangible benefits.
Two interesting phenomena appear in these results. The first is that, unlike supply zone A, section 26 did not benefit from smart charging. This is explained by the fact that this overloaded section (high traffic, connected to a substation that feeds 3 sections) does need a fixed increase in capacity. Here, the bilateral method, increase of substation limit, and Case 1 create an EV charging potential that did not exist.
The other interesting phenomenon is that the introduction of a bilateral connection showed a decrease in the EV potential at some locations on 25. This is to be expected as the bilateral connection coupled to section 25 with section 26, which had no spare capacity and is of a much lower substation voltage. Therefore, section 25 had to supply many loads of substation 26.

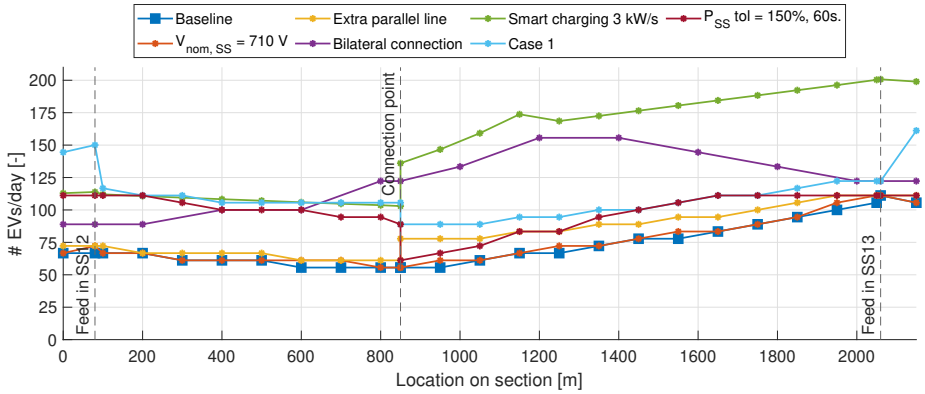

Figure 9.12: Summary of various methods on the maximum achievable EV charging potential in supply zone A sections 23 and 2 on day 268. Case 1: $V_{\text{nom, SS}} = 710$ V, an extra paralleled overhead line is added to the section, and the substation power rating is increased to 1100 kW.

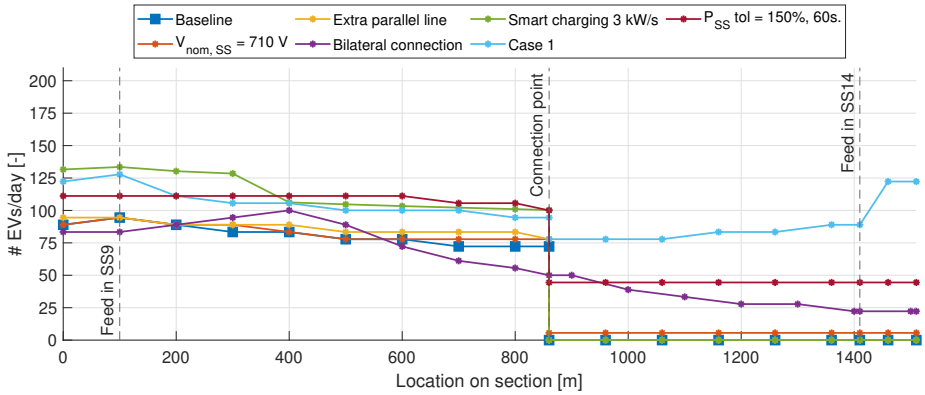

Figure 9.13: Summary of the effect of various methods on the EV charging potential in supply zone B sections 25 and 26. Case 1: $V_{\text{nom, SS}} = 710$ V, an extra paralleled overhead line is added to the section, and the substation power rating is increased to 1100 kW.

Table 9.10: Supply zone A: effect of grid methods on the EV charging potential for the case study on day 268 of the year. *Achievable with one charging facility. **Achievable with one charging facility at the connection point of the sections.

Grid method	**Section 23** [# of EV/day]		**Section 2** [# of EV/day]		**Section 23+2** [# of EV/day]
	Max	Mean	Max	Mean	Max
Baseline	67	61	111	82	178
Substation voltage	72	63	111	83	183
Substation power	111	103	111	96	222
Extra overhead line	72	66	111	94	183
Bilateral connection	122*	103*	156*	137*	156*
Fleet-aware smart charging	114	108	201	178	315
Multi-port converter	56	0	56	0	111**
Case 1	150	115	161	109	311

Table 9.11: Supply zone B: effect of grid methods on the EV charging potential for the case study. *Achievable with one charging facility. **Achievable with one charging facility at the connection point of the sections.

Grid method	**Section 25** [# of EV/day]		**Section 26** [# of EV/day]		**Section 25+26** [# of EV/day]
	Max	Mean	Max	Mean	Max
Baseline	94	81	0	0	94
Substation voltage	94	83	6	6	100
Substation power	111	109	44	44	156
Extra overhead line	94	87	0	0	94
Bilateral connection	100*	78*	50*	30*	100*
Fleet-aware smart charging	134	114	0	0	134
Multi-port converter	72	0	0	0	72**
Case 1	128	106	122	91	250

9.6. INCREASING FURTHER: CONTROLLING THE BILATERAL CONNECTION LOAD SHARE BALANCE BY SUBSTATION VOLTAGE TUNING

As it emerges from the analysis in this chapter, the bilateral connection is an excellent candidate for increasing the integration potential of EV chargers in trolleygrids. However, the load sharing between the two substations can be unbalanced such as in the case of supply zone B. Even more, the EV charger placement can be restricted to a specific location (a parking lot, for example), that is too far from the bilateral substation to receive its full benefit.

This section investigates a solution to further increase the potential for integration of EV chargers in the trolleygrid under bilateral connections, without additional infrastructure costs. This is done by simply tuning the nominal (no-load) voltages of bilaterally connected substations by changing the transformer tap position. It should be stressed

here that this is a mechanical, one-time design alteration and not a dynamic control of the tap positions on a continuous basis.

9.6.1. POWER FLOW IN TROLLEYGRIDS WITH BILATERALLY CONNECTED SUBSTATIONS

LOAD POWER-SHARE CALCULATIONS

Figure 9.14 shows a bus between two substations, drawing a power P_b. Its voltage is v_b and it draws a current i_b.

$$P_\mathrm{b} = v_\mathrm{b} \cdot i_\mathrm{b} \tag{9.2}$$

Defining the impedances as

$$R_i \triangleq R_{\mathrm{f},i} + R_{\mathrm{l},i} \quad i = 1,2 \tag{9.3}$$

And assuming that the two substations SS1 and SS2 are at a voltage differential ΔV_ss of

$$\Delta V_\mathrm{ss} \triangleq V_{\mathrm{s},1} - V_{\mathrm{s},2} \tag{9.4}$$

And defining the voltage drop ΔV as the voltage drop between the bus and the second substation, SS2:

$$\Delta V \triangleq V_{\mathrm{s},2} - V_\mathrm{b} \tag{9.5}$$

The power delivered by each substation can be written as:

$$P_1 = V_{\mathrm{s},1}\left(\frac{\Delta V + \Delta V_\mathrm{ss}}{R_1}\right) \tag{9.6}$$

$$P_2 = V_{\mathrm{s},2}\frac{\Delta V}{R_2} \tag{9.7}$$

Eq.9.2 can be rewritten as:

$$P_\mathrm{b} = (V_{\mathrm{s},2} - \Delta V)\cdot\left(\frac{\Delta V_\mathrm{ss} + \Delta V}{R_1} + \frac{\Delta V}{R_2}\right) \tag{9.8}$$

Giving:

$$R_\mathrm{b}\Delta V^2 + [R_2\Delta V_\mathrm{ss} - R_\mathrm{b}V_{\mathrm{s},2}]\Delta V + [R_1R_2P_\mathrm{b} - R_2V_{\mathrm{s},2}\Delta V_\mathrm{ss}] = 0 \tag{9.9}$$

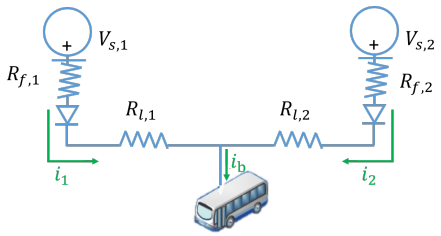

Figure 9.14: Nomenclature of the parameters used to study the case of one bus powered by two bilateral substations

where R_b is defined as the line impedance between the two substations

$$R_b \triangleq R_1 + R_2 \tag{9.10}$$

Solving the quadratic equation of Eq.9.9 gives:

$$\Delta V = \frac{R_b V_{s,2} - R_2 \Delta V_{ss}}{2R_b} - \frac{\sqrt{[R_b V_{s,2} - R_2 \Delta V_{ss}]^2 - 4R_b[R_1 R_2 P_b - R_2 V_{s,2} \Delta V_{ss}]}}{2R_b} \tag{9.11}$$

The power delivered by each substation can then be obtained by inserting Eq.9.11 into Eq.9.6 and Eq.9.7.

EFFECT OF BILATERAL PARAMETERS ON THE LOAD POWER-SHARE

Combining Eq.9.11 with Eq.9.6 and Eq.9.7 shows how for the same power demand and position of the load (i.e., line impedance), the share of each substation from the power delivered is a function of $V_{s,2}$ and ΔV_{ss}.

However, it can be mathematically shown, by computing the partial derivatives, that the two parameters do not have the same effect on the power-sharing when considering the typical order of magnitude of the parameters as seen in a trolleygrid.

Firstly, in terms of $V_{s,2}$:

$$\frac{\partial \Delta V}{\partial V_{s,2}} \approx \frac{1 - \dfrac{R_b V_{s,2}}{\sqrt{R_b^2 V_{s,2}^2 - 4P_b R_1 R_2 R_b}}}{2R_b} \tag{9.12}$$

For typical values of substation voltages at the order of 600-750V, i.e. $\mathcal{O}(V_{s,2}) = \mathcal{O}(10^2)$, and of line resistances at the order of 0.1Ω, i.e. $\mathcal{O}(R) = \mathcal{O}(10^{-1})$, and bus powers of $\mathcal{O}(P_b) = \mathcal{O}(10^5)$, it can be concluded that:

$$\frac{\partial \Delta V}{\partial V_{s,2}} \approx \frac{1 - \dfrac{\mathcal{O}(10^{-1})}{\sqrt{\mathcal{O}(10^{-2})}}}{2 \cdot \mathcal{O}(10^{-1})} \tag{9.13}$$

Leading to:

$$\frac{\partial \Delta V}{\partial V_{s,2}} \approx 0 \tag{9.14}$$

Which is confirmed in the next subsection.

Meanwhile, in terms of ΔV_{ss},

$$\frac{\partial \Delta V}{\partial \Delta V_{ss}} \approx \frac{-R_2 + 3\dfrac{R_b R_2 V_{s,2}}{\sqrt{R_2^2 V_{s,2}^2 - 4P_b R_1 R_2 R_b}}}{2R_b} \tag{9.15}$$

For typical values of difference in substations voltages of the order of tens of volts, i.e. $\mathcal{O}(\Delta V_{ss}) = \mathcal{O}(10^1)$, and the other parameters chosen above, it can be concluded that:

$$\frac{\partial \Delta V}{\partial \Delta V_{ss}} \neq 0 \tag{9.16}$$

Effectively meaning that tuning the absolute magnitude of the substation voltages would not have a significant effect on the load power share of each substation for any typical trolleygrid. Meanwhile, tuning the voltage difference between the two bilateral substations, ΔV_{ss}, would have a direct effect.
The above mathematical derivations are validated by the hypothetical case study in Figure 9.15 where it is observed that the load sharing fraction of SS1 is more affected by ΔV_{ss}, while the substation voltage is fixed (the differences within the sets of red and sets of blue lines) than by $V_{s,2}$ while the ΔV_{ss} is constant (the differences between the curve lines holding the same marker).
In the remaining part of this section, simulations of a trolleygrid substation with actual bus traffic will allow the validation of these results.

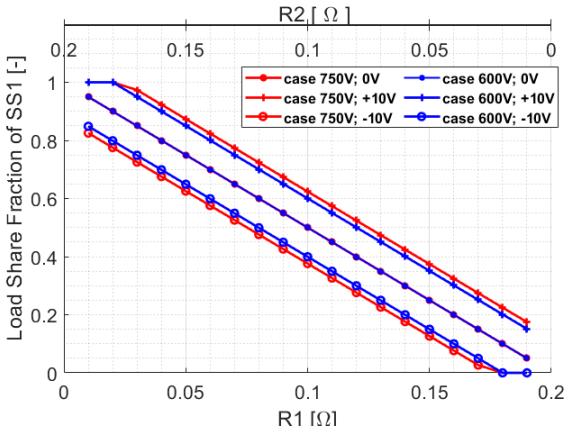

Figure 9.15: Load share fraction of SS1 for different cases of $[V_{s,2}, \Delta V_{ss}]$ for a situation such as Figure 9.14 with $R_b = 0.2\Omega$ and P_b=300kW. It is observed that changing $V_{s,2}$ (curves of the same marker) has a far lower effect on the fraction than ΔV_{ss} has (curves of the same color)

9.6.2. CASE STUDY EXAMPLE: ZONE A

The simulations are run for Zone A for a full day, for the worst-case scenario of a high-traffic schedule with a high HVAC demand. The day chosen is an October day, using a baseline of 690V as $V_{s,2}$. The results are tabulated in Table 9.12, where it can be seen that the power share of substation 1 can change by up to 7.5 percentage points by the tuning of the substation voltage difference. Additionally, the substation would see almost 90% of its day as a zero load period, available completely for EV charging.
A closer look at the results is presented in Figure 9.16 for the half-hour span between

Table 9.12: Summary of results of Load Share Fraction and Zero-load time for the SS1 in the case study of Figure 3.12 for different values of ΔV_{ss}

ΔV_{ss}	Average Load Share Fraction	Daily Zero-load time
+10V	45.9%	84.3%
+5V	48.0%	84.4%
0V	46.0%	87.3%
-5V	43.4%	88.9%
-10V	38.4%	89.2%

8.30 am and 9.00 am. The zero load instances can be observed. With ΔV_{ss} of 10V, for example, SS1 is engaged most of the time for more than 50% of the load, and during moments where it had not been previously engaged in supplying the load. It is especially interesting to note the peak demand moments before 9:00 am, where SS1 had no share of the power demand, leaving it completely to SS2, and then in the case of +10V, became engaged in more than half of the load. This, again, shows the benefit of this method.
It is worth noting, however, that this load shifting will also have an effect on the recuperation of braking energy and transmission losses. A more detailed study into the expected benefits or losses is urged, yet, as expected, this method already proves that more benefits can still be harvested by combinations and fine-tuning of the methods investigated in this chapter.

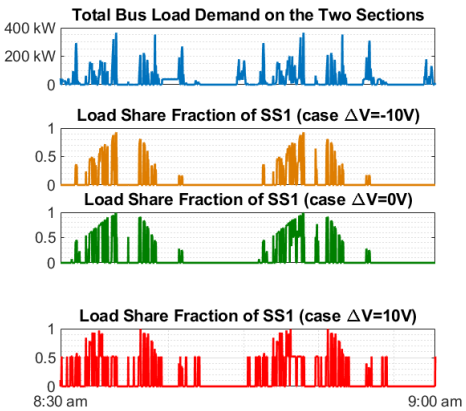

Figure 9.16: A closer look at the load share fractions between the two bilaterally connected substations based on different values ΔV_{ss} for 30 minutes during the day

9.7. RECOMMENDATIONS FOR INCREASING METHOD, PLACEMENT, AND SIZING OF EV CHARGERS IN PUBLIC TRANSPORT NETWORKS

The results of the previous sections offer insights into the best method to increase the EV chargers integration, placement, and sizing, for an array of different transport grid landscapes.

9.7.1. SUGGESTIONS FOR THE CHOICE OF THE POTENTIAL-INCREASING METHOD

- Increasing the substation voltage: This method is best suited for an EV charger placement at the EOL of long, low average traffic, low peak traffic sections. Otherwise, there is no mentionable benefit. This can be seen in detail in the results of Section 9.4.1.

- Introduction of an extra paralleled line: This method has the same suggestions as the above one. It is worth mentioning, however, that increasing the substation voltage is an effectively cost-less solution, and is therefore preferred over this method. This can be seen in detail in the results of Section 9.5.1.

- Increasing the substation power limit: This method is most effective for locations with medium to high average traffic densities. If the traffic congestion happens in peaks only, it is better to go for instantaneous relief solutions, such as Fleet-Aware Smart Charging, rather than increasing the substation capacity. This can be seen in detail in the results of Section 9.4.2.

- Fleet-Aware Smart Charging: This method is always a good solution to draw the available grid power for the EV chargers. Trivially, it is not beneficial in locations of high average and peak traffic intensities, as these locations have no spare capacity to be harvested. This method only harvests the attainable spare capacity but does not *create* any compared to the baseline, as is the case with a bilateral connection or the addition of a paralleled line, for example. The main advantage of this method shows up at sections that are supplied by a substation that feeds multiple sections, as this method, by its sensors and communication, can actively avoid violating the grid limits. However, this method is expensive (sensors) and requires reliable wireless communication. This can be seen in detail in the results of Section 9.4.3.

- Introduction of a bilateral connection: This method is best suited at the MOL and EOL of long sections, but has an overall visible benefit at almost any location. The only exception is when placing an EV charger on a section that is then bilaterally connected to a section with no spare capacity, as this would cause a reduction of the local spare capacity since a part of it goes to its neighboring section (case study of supply zone B). This can be seen in detail in the results of Section 9.5.2. However, as Section 9.6 shows, a fine-tuning of the substation voltages can overcome this hurdle.

- Use of a multi-port converter: Unfortunately, this method is not recommended as it always produced results lower than the baseline. The reason the MPC has a poor performance is that it presents to the grid all the disadvantages of a load at the EOL (more severe voltage drops and higher currents and losses), without any of the benefits of a bilateral connection since the vehicle loads on the two sections are still galvanically isolated. This can be seen in detail in the results of Section 9.5.3.

9.7.2. SUGGESTIONS FOR THE SIZING OF EV CHARGERS

There is a charging potential for 150-200 EVs per day anywhere along long sections of medium-to-low traffic that are fed alone or with one other section from their substation, as long as it is with the fleet-aware smart charging method. It is also possible at MOL and EOL of long, medium-to-low traffic sections that are bilaterally connected to another mid-to-low traffic section. Care should be considered at the SOL of very long sections that are supplied by a substation that feeds multiple sections, as only the smart charging method could prove beneficial, for a low EV charging potential of about 75 EVs per day. Care is also advised at MOL of high average and peak traffic densities that are supplied by a substation that feeds multiple sections, as the EV charging potential is also limited. This is because the MOL sees a lot of violations as it has neither the benefit of being close to the feed-in point nor that of being close to the EOL and the bilateral connection.

9.7.3. SUGGESTIONS FOR THE PLACEMENT OF EV CHARGERS

EV chargers are placed where there is a parking availability and a need for a charger. However, when the placement offers some flexibility, the following recommendations are presented:

- Place the EV charger at SOL when implementing Fleet-Aware Smart Charging, except at sections with high average and peak traffic densities that are supplied by a substation that feeds multiple sections. In that case, SOL is advised with a bilateral connection or increasing the substation power capacity.
- Place the EV charger at MOL when implementing fleet-aware smart charging or a bilateral connection at long, medium average, and peak traffic sections. Avoid the MOL placement at sections with high average and peak traffic densities that are supplied by a substation that feeds multiple sections, for the reasons previously explained.
- Place the EV charger at EOL for long, medium-to-low average, and peak traffic sections that are supplied by a substation that feeds multiple sections when adding a bilateral connection. These sections have voltage and power violations, and benefit the most from a bilateral connection

9.8. CONCLUSIONS

This chapter presented six methods for increasing the integration potential of EV chargers in electric public transport grids, assessed their benefit, and offered recommendations on the placement and sizing.

In conclusion, there is no single solution that fits all types of sections and their parameters (length, average traffic, peak traffic, etc.). For this purpose, Section 9.7 offers a detailed, tailored suggestion for each method, sizing, and placement option.

However, some general conclusions can still be made regardless of the specific grid layout or size and location of the EV charger. For example, the multi-port converter (two inputs, one output) was found to be worse than the baseline, regardless of the case study, as it presented to the grid all the disadvantages of a load at the end-of-line of two sections (more severe voltage drops and higher currents and losses), without any of the benefits of a bilateral connection.
The bilateral connections are the most beneficial and cost-efficient solution in all cases except for a section coupled with an already congested section. This is because no spare capacity could be provided in that case. On the contrary, in the case study of supply zone B, the combined spare capacity dropped compared to the baseline since the congested section was exploiting the spare capacity of the uncongested section. However, proper fine-tuning of the substation voltage can overcome this problem, as derived and validated in this chapter.
Fleet-Aware Smart Charging with sensors and wireless communication can increase the potential significantly by continuously sensing and analyzing the grid states to avoid grid violations. It is a costly and complex solution. This is because it requires sensors at each trolleybus, substation, and power load, as well as wireless communication between them and the EV charger that processes the data and finds the allowed instantaneous charging power that would not violate the grid power, voltage, or current limits neither at the EV charger nor any other node on the section. Furthermore, this method is only suitable for sections with a spare capacity since Fleet-Aware Smart Charging only harvests the available capacity but does not create any.

Future work is needed in testing more combinations of grid methods and quantifying their effects. More urgently, a cheaper yet reliable method of estimating the grid states, such as the one developed in Chapter 4, is crucial to harvest the outstanding benefits of Fleet-Aware Smart Charging with sensors, but without the costs and complexity of such an added infrastructure.
This chapter has proven that EV chargers can be integrated into trolleygrids, both allowing for more chargers integration in the city without additional capacity building and offering the base load needed for the integration of renewables at traction substations. However, with the increased demand for EV chargers comes an increased need for more PV panels and installation space. The coming chapter looks at another possibility for providing a base load to traction grids while simultaneously offering them the needed PV installation space: A shared solar system between traction substations and nearby residential loads.

10

A Multi-Stakeholder PV System Shared by Transportation and Residential Loads

"Měsíčku na nebi hlubokém,
světlo tvé daleko vidí,
po světě bloudíš širokém,
díváš se v příbytky lidí."

Song to the Moon - Act I, Rusalka (Dvořák)

Moon high and deep in the sky
Your light travels far,
You travel around the wide world,
and see into people's homes.

This chapter is based on: A Shared PV System for Transportation and Residential Loads to Reduce Storage and Curtailment: Two Trolleygrid Case Studies. I Diab, N Damianakis, GR Chandra-Mouli, P Bauer *(Submitted)*

The challenges and opportunities of PV integration in either transport or residential networks are complementary to each other. The residential stakeholders offer both the base electrical load and the physical installation space needed by the traction stakeholder, who brings the peak load and investments to the former. In that aim, this chapter proposes and investigates a multi-stakeholder PV system that can be shared by transport and nearby residential loads.

Section 10.1 starts with a short introduction to the challenges for PV integration in transport and residential networks, and motivates the suggestion of a shared PV system.
Section 10.2 then details the modeling methodology for the residential loads, while that of the trolleygrid and PV have been previously detailed in Chapters 3 and 5, respectively. Then, Section 10.3 offers the results of the benefits to the direct PV Utilization (PV and Load matching) of the combined system. To prove the benefit of the shared system is not a mere consequence of an effective under-sizing of the solar PV system, Section 10.4 looks at the benefits to the load coverage of the combined system according to the share of each stakeholder. Finally, section 10.5 closes with conclusions and recommendations.

10.1. INTRODUCTION

Renewable energy systems like solar photovoltaic (PV) offer scalable, decentralized, and sustainable power supply at increasingly competitive costs [241]. However, their intermittent generation profile creates a major hurdle for their techno-economic feasibility. This is because the power mismatch between this generation and the connected load requires storage systems and/or exchange with the main city grid (when allowed). In more practical choices, the most economical option is to curtail the excess power. These options are illustrated in Figure 5.2.
The first solution of using storage systems is high in both losses (transmission, self-discharge, battery efficiency, etc.) and system costs. Meanwhile, for the second solution of using the local, the grid requirements impose strict export limitations on the power sent to the AC grid -if allowed at all -to maintain the stability and controllability of the grid. Finally, curtailment directly influences the effective energy cost of the PV system and, in environments where the available space for PV implementation is already limited, can jeopardize the techno-economic feasibility of the project or its implemented scale.
Consequently, it is in the techno-economic interest of the PV system stakeholders to increase the direct utilization of their PV system output by the load. However, matching demand and generation is a different challenge depending on the type of load profile. Below are two examples of such profiles: Urban traction loads and residential dwellings loads.

10.1.1. CHALLENGES FOR PV SYSTEM INTEGRATION IN URBAN TRACTION GRIDS

Catenary traction grids like trams or trolleybus are segmented into substations that consist of a step-down transformer and a rectifier that turns the Low Voltage AC to a Low

Voltage DC at about 650-750V, depending on the traction substation and the trolley city. The load profile of such traction networks is particular in two aspects. First, the load is stochastic and unpredictable both in time and location since the vehicles are moving with the city traffic [22], [183]. Second, when the vehicle exits the supply zone of one substation and enters another, the load suddenly disappears from the first substation. In that sense, traction grids are particular grids with no base loads and with high, unpredictable power peaks caused by vehicle acceleration (about five times that of cruising traction [3], [14], [20]).
Previous works in the literature [11], [79], [80] have proven that the direct utilization of an energy-neutral sized, traction-substation-connected PV system (Figure 5.5) can be as low as 13% in low-traffic substations, and quickly reaches a plateau of about 38% with busier substations. This means that if the excess generation is curtailed, less than 40% of the PV energy is used from a system that was sized to feed 100% of the load. The effective energy cost is thereby more than 2.5 times higher than that of the installed capacity. If the system is undersized to reduce the absolute amount of energy wasted, less of the traction load is covered. Other works have also shown the sizing limitation of a traction-grid-connected PV system because of the load and generation mismatch [81].
This has motivated calls in the literature for the integration of more base loads into traction networks [16], [79], [80], [165].

10.1.2. CHALLENGES FOR PV SYSTEM INTEGRATION FOR URBAN ELECTRIFIED HOUSEHOLD DEMANDS

The residential sector is one of the most significant users of energy, accounting for about a quarter of total global energy use [242].
In an effort to decarbonize this load sector, its heating and transportation demands are increasingly electrified in the form of Heat Pumps (HPs) and private Electric Vehicles (EVs) [243].
However, a challenge with coupling PVs and HPs is that the higher periods of PV generation occur when the buildings are not occupied, and the HPs are not in their periods of higher demand. Therefore, energy storage and demand response are necessary for PV rooftops with minimum grid power exchange [244], [245].
However, the simultaneous installation of energy storage, heat pumps, and PV panels can be costly for a household and demotivate projects of demand electrification.

10.1.3. ADVANTAGES OF A SHARED PV INFRASTRUCTURE FOR TRANSPORT AND RESIDENTIAL LOADS (THIS CHAPTER)

The challenges and opportunities of PV integration in either transport or residential networks are complementary to each other. In the case of the former, there is an absence of a base load during the day, yet power peaks occur frequently and during daylight hours. In the latter's case, a base load is present, yet not enough load peaks occur during the higher generation periods.
In that regard, there is an expected synergy in coupling traction substations and nearby residential loads in increasing the overall matching between load and generation. Furthermore, rooftop PV systems can offer physical installation space which is otherwise scarcely available in urban environments for the transport grids.

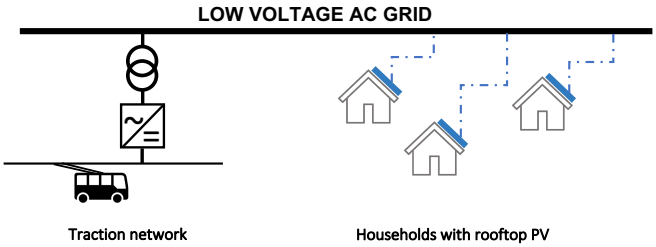

Figure 10.1: The suggested multistakeholder in this chapter: Traction substations like trolleybuses and nearby households can form one load entity via the Low Voltage AC grid to reduce the need for energy storage.

This suggestion is illustrated in Figure 10.1, where traction grids such as trolleybus grids that are fed from the LVAC network can aggregate their load demand with that of nearby residential homes. This aggregated load can be served by rooftop PV systems. It is important to point out that there is no active load control in this method, but rather a bundling of stakeholders for a scenario somewhat equivalent to an on-site Power Purchase Agreement with solar assets (see [72] for the example of Dutch railways and wind power).

10.1.4. CHAPTER CONTRIBUTIONS

This chapter offers the following contributions:

1. The proposition of a shared PV system for combining the (base) load of residential networks with the (peak) load of transport grids to create a multi-stakeholder renewable energy generation and transport system

2. A detailed study of the decrease in the need for storage, MVAC grid exchange, and/or curtailment for the proposed multi-stakeholder PV system using comprehensive and verified trolleybus, trolleygrid, heat pump, and PV models for one year with a per-second resolution

3. A detailed study of the increase in the direct load coverage out of an effective PV system size in the proposed multi-stakeholder PV system case using comprehensive and verified trolleybus, trolleygrid, heat pump, and PV models for one year with a per-second resolution

10.2. MODELING METHODOLOGY

10.2.1. CASE STUDY DEFINITION

There is a difference in the performance of a PV system connected to a traction substation depending on the length of the catenary that it supplies and on the average traffic that it observes [11], [79]. For this purpose, this chapter needs to confirm the benefit of the shared PV system by looking at at least two traction substation types. The examined trolleygrid is that of the city of Arnhem, The Netherlands.
For this chapter, the choice is for:

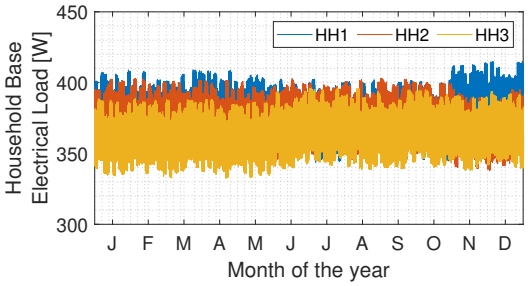

Figure 10.2: The three household load profiles used in this study based on publicly available data on the electricity demand of Dutch private dwellings [246].

- Substation 9 (SS9): A relatively short (less than 1000m) catenary zone with up to 5 buses at a time in traffic density
- Substation 12 (SS12): A relatively long (more than 2000m) catenary zone at most 3 buses at a time in traffic density

To study these grids, the simulations are run per second for a full year of operation. The PV systems, expected to primarily be rooftop systems, first supply the residential loads (closest) and then send the remaining energy through the LVAC connection to the nearby traction loads. The total losses are around 4.5% as derived in Chapter **??**.

10.2.2. HOUSEHOLD DEMAND MODELING: ELECTRIC LOADS AND HEATING

ELECTRIC LOADS

The electric loads of the households have been modeled with the use of Probability Distribution Function (PDF) electricity profiles for the Netherlands of 2021. These profiles are downloaded from the NEDU open database [247], and they are categorized into E1A and E1B for the residential sector. The E1A profiles are generated with the use of only the day-meter, whereas also a night meter is used for the generation of the E1B.
Three final consumption profiles of a household are calculated by scaling its estimated yearly consumption PDF, as depicted in Figure 10.2.

HEATING DEMAND MODEL

The heating model includes mainly the Building, space & domestic hot water (DHW), insulation, and power consumption models, which will be briefly explained as follows. Regarding the building model, the typical Dutch terraced building type has been selected since it represents more than 50% of Dutch households. The buildings' specifications (dimensions, materials, and conductivity values) are summarized in Table 10.1.

$$T_{\mathrm{bw}}(t+\Delta t) = \frac{\dot{Q}_{\mathrm{gain}}(t) - \dot{Q}_{\mathrm{los}}(t)}{C_{\mathrm{tot}}} \Delta t + T_{\mathrm{b}}(t) \tag{10.1}$$

where:

$$C_{\mathrm{tot,b}} = C_{\mathrm{b}} + V_{\mathrm{b}} C_{\mathrm{air}} \rho_{\mathrm{air}} \;\&\; C_{\mathrm{tot,w}} = V_{\mathrm{tank}}\, C_{\mathrm{wat}}\, \rho_{\mathrm{wat}} \tag{10.2}$$

Table 10.1: Building parameters used in this chapter.

Surface (surf)	**Material**	**Area A (m^2)**	**Thickness d (m)**	**Conductivity U (W/mK)**
Floor (fl)	Wood	90	0.03	0.18
Front/Back Walls (fw/bw)	Brick	15x5	0.23	1
Side Walls (sw)	Brick	6x8	0.23	1
Roof (rf)	Clay	15x4.25	0.015	0.72

$$\dot{Q}_{\text{gain,b}}(t) = \dot{Q}_{\text{hp}}(t) + \dot{Q}_{\text{ir}}(t) \;\&\; \dot{Q}_{\text{gain,w}}(t) = \dot{Q}_{\text{hp}}(t) \tag{10.3}$$

$$\dot{Q}_{\text{ir}}(t) = G_{\text{inc}}(t)\ w_{\text{b}}\ s_{\text{b}} \tag{10.4}$$

$$\dot{Q}_{\text{los}}(t) = \dot{Q}_{\text{cond}}(t) + \dot{Q}_{\text{vent}}(t) \tag{10.5}$$

$$\dot{Q}_{\text{cond,b}}(t) = \sum_{\text{surf}}^{\text{surfaces}} (d_{\text{surf}} U_{\text{surf}} A_{\text{surf}})(T_{\text{b}}(t) - T_{\text{a}}(t)) \tag{10.6}$$

$$\dot{Q}_{\text{cond,w}}(t) = U_{\text{tank}} A_{\text{tank}}(T_{\text{tank}}(t) - T_{\text{a}}(t)) \tag{10.7}$$

$$\dot{Q}_{\text{vent}}(t) = C_{\text{air}}\ \rho_{\text{air}}\ r_{\text{b}}(T_{\text{b}}(t) - T_{\text{a}}(t)) \tag{10.8}$$

Regarding the space & DHW heating/cooling model, equation (10.1) dictates that the temperature of the next timestep for both the building and the DHW tank depends on the total heat gains $\dot{Q}_{\text{gain}}$ & losses $\dot{Q}_{\text{los}}$ as well as the total heating capacity C_{tot}. According to (10.2), the total building capacity $C_{tot_{\text{b}}}$ is the sum of the building heating capacity itself C_b and the capacity of the air inside, while the total DHW tank capacity is the capacity of the total water stored $C_{tot_{\text{w}}}$. The heating gains of the DHW tank $\dot{Q}_{\text{gain,w}}$ is the HP output $\dot{Q}_{\text{hp}}$, while for the building, the gained heat by irradiation is also included $\dot{Q}_{\text{ir}}$, as dictated by (10.3). According to (10.4), $\dot{Q}_{\text{ir}}$ depends on the total incident building irradiation G_{inc}, the building window-to-wall ratio w_b & the solar heat gain coefficient s_b. Equation (10.5) shows that the total heating losses $\dot{Q}_{\text{los}}$ are the sum of the conduction losses $\dot{Q}_{\text{cond}}$ and the ventilation losses $\dot{Q}_{\text{vent}}$, which for the building are modeled in (10.6) & (10.8), respectively. The DHW tank losses $\dot{Q}_{\text{cond,w}}$ are only conductive and are modeled in 10.7).

$$U_{des} = \frac{1}{\dfrac{d_{\text{surf}}}{U'_{\text{surf}}} + \dfrac{d_{\text{ins}}}{U'_{\text{ins}}}} \tag{10.9}$$

Regarding the insulation model, the walls and roof of the buildings are insulated according to (10.9). With use of 80mm Expanded Polystyrene (EPS) of U = 0.024W/mK & 110mm PIR Board (Celotex) of U = 0.019W/mK, the walls and roof conductivities U'_{walls} & U'_{roof} have been decreased to comply with the new regulations ($0.28 W/m^2K$ & $0.17 W/m^2K$,

respectively). It is then assumed here that the buildings in the future are well insulated, and floor heating using a heat pump would be sufficient.

$$P_{\text{hp}}(t) = \frac{\dot{Q}_{\text{hp}}(t)}{\text{COP}(t)} \tag{10.10}$$

$$\text{COP}(t) = 7.90471 e^{-0.024(T_{\text{ret}}(t) - T_{\text{a}}(t))} \tag{10.11}$$

$$\begin{aligned} \dot{Q}_{\text{hp}}(t) &= \dot{m}_{\text{wat}} C_{\text{wat}} (T_{\text{sup}} - T_{\text{ret}}(t)) \\ \leftrightarrow T_{\text{ret}}(t) &= T_{\text{sup}} - \frac{\dot{Q}_{\text{hp}}(t)}{\dot{m}_{\text{wat}} C_{\text{wat}}} \end{aligned} \tag{10.12}$$

Finally, the power consumption model is modeled in (10.10) - (10.12). The HP power consumption P_{hp} depends on the HP heating output $\dot{Q}_{hp}$ and the Coefficient of Performance (COP). The latter is estimated by regression from 10 different HP models in [248] and is dictated by (10.11). Finally, (10.12) models the HP output, which depends on the water flow rate $\dot{m}_{\text{wat}}$, the water-specific heating capacity C_{wat} and the difference of the supply and return water temperature, T_{sup} & T_{ret}, respectively.
The considered HP in this work is an ON-OFF reversible Air-Sourced Heat Pump (ASHP), which uses floor heating for space heating. The specifications, such as the HP heating output, have been acquired by the Dimplex LIK 8MER module [249], which has a rated flow water rate $\dot{m}_{\text{wat}} = 0.8 m^3/h$ and uses supply temperatures T_{sup} of 35°C, 50°C & 18°C for floor-heating, DHW & floor-cooling, respectively. The heating model represents a temperature controller, which keeps the building temperature within the desired interval [21°, 23°] as long as the building is occupied. In this regard, the buildings have been considered to be empty during 8:00 - 14:00 on weekdays. Moreover, the use of DHW has been considered once per day, every day at 6:00, which then is always prioritized against space heating.

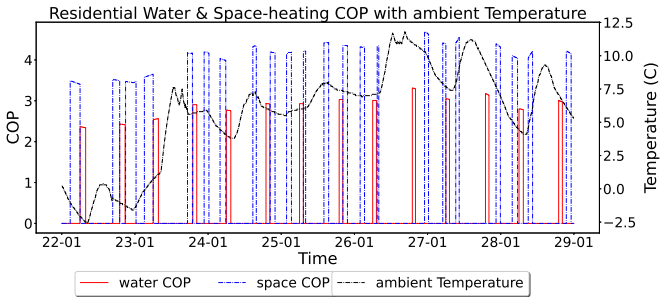

Figure 10.3: Simulation example of a week of residential Space-Heating and DHW COPs and ambient Temperature during Winter.

In Figures 10.3 and 10.4, key results of the heating model for a Winter week are summarized. As it can be observed in Figure 10.3, the space-heating COPs are always higher than the DHW COPs, reaching up to the value of 4.2. This is due to the lower heating temperature, that is used for the floor heating, because the COP always depends on the

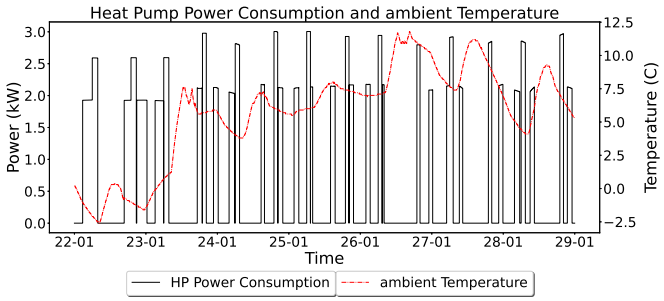

Figure 10.4: Simulation example of a week of residential HP power consumption and ambient temperature during winter.

difference of the source and sink temperatures. This also can be seen, by observing the trend of both COPs during ambient temperature increases. Finally, Figure 10.4 depicts the HP power consumption versus the ambient Temperature during the same week. Due to the different COPs, the low consumption pulses are related to the space-heating, while the high pulses belong to the DHW. The average consumption for space-heating fluctuates around 2kW, while it can reach approximately up to 3kW for DHW use.

10.3. RESULTS: BENEFITS IN DIRECT PV UTILIZATION

As mentioned earlier, households can reduce the PV curtailment by providing the load demand in the frequent moments of zero or low load demands at traction substations. This can be illustrated in the one-hour extract of the PV system performance at SS12 in Figure 10.5. The figure compares two systems of the same size: A single traction stakeholder and a shared stakeholder system between the traction substation and 15 households.
The PV generation is almost fully utilized (100% U_{PV}) at numerous instances in the combined system. Meanwhile, utilization of up to 80% is ensured when the single stakeholder system is in full-curtailment mode (no bus demand).
These results are further discussed in this section.

10.3.1. CASE OF A LONG, LOW TRAFFIC SUBSTATION

Figure 10.6(a) shows the PV system utilization, U_{PV}, at a long yet low traffic traction substation. With increasing PV system sizes, U_{PV} is lower as the mismatch between the generation and load is higher. The knee of the curve can be seen at about 40kW, which is the value of the bus auxiliaries and, therefore, constitutes a sort of "base load" for the traction substation power demand when and if a bus is present on the section. For systems lower than this knee value, U_{PV} rapidly increases as such small PV systems generate powers that are consumed almost in full when and if a bus is present on the section. This "when and if" condition dictated by the timetabling is the reason the U_{PV} does not reach 100%. However, smaller system sizes are not particularly attractive as they do not cover a large part of the traction load.

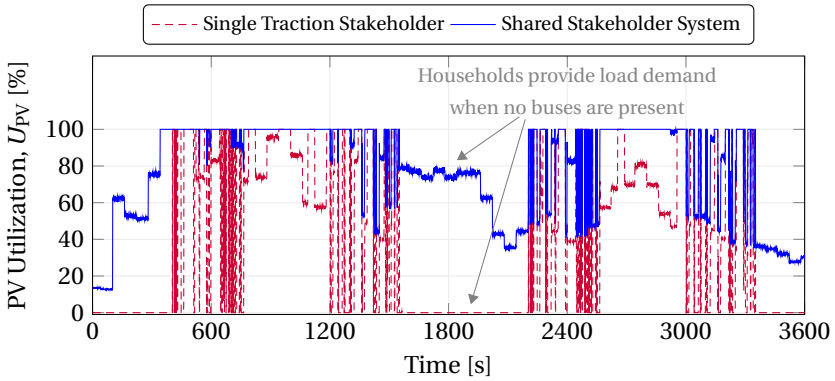

Figure 10.5: Comparison of the PV Utilization between the single and combined stakeholder systems (one-hour excerpt of a July day at Substation 12 without or with 15 households).

For substation 12, the net energy-neutral PV system size ($\zeta = 1$) is 195kW and of a U_{PV} of 25.6%. Consequently, 74.4% of the PV generation needs to be stored, exchanged with the AC grid, and/or curtailed.
Figure 10.7(b) shows the U_{PV} for different numbers of connected households, N_h . The curves go from 3 to 60 houses, in steps of 3, to represent each of the 3 available household profiles of Figure 10.2.
Figure 10.6(c) shows the increase in the U_{PV} when the PV system serves a combined traction-residential load. In this case, the energy-neutral PV system of 195kW is at about 29% in U_{PV}, creating a net reduction in generation mismatch of absolute 3.4 percentage points. Obviously, this PV system is now covering more loads, and therefore, this system size is no longer considered "energy neutral" for the combined load. The effect on the load coverage is discussed in the following section of this chapter. However, the key takeaway from the U_{PV} analysis is the observable net jump in the utilization curves when comparing Figures 10.6(a) and 10.7(b) to Figure 10.6. The values in the latter figure reach, in many cases, up to 100% utilization, which argues that the benefits of this shared system are not otherwise reachable by a simple under-sizing of the PV system in the single-stakeholder cases.

10.3.2. CASE OF A SHORT, HIGH TRAFFIC SUBSTATION

The results of Substation 9, in Figure 10.7, validate the previous results and conclusions of Substation 12.
For this substation, despite the high traffic that the substation experiences, a consequence of its short supply zone length is that it does not have many bus and traffic-light stops. Furthermore, the buses could enter and exit the section without activated auxiliaries (mainly heating/cooling). This leaves the U_{PV} with a similar knee around 40kW, yet smaller system sizes do not bring the accelerated increase observed in long-supply-zones substations as seen in Figure 10.7(a).
However, Figure 10.7(c) shows the same positive jump in the U_{PV} curves as seen in the case of long, low-traffic substations with values above the curves of both Figures 10.7(a)

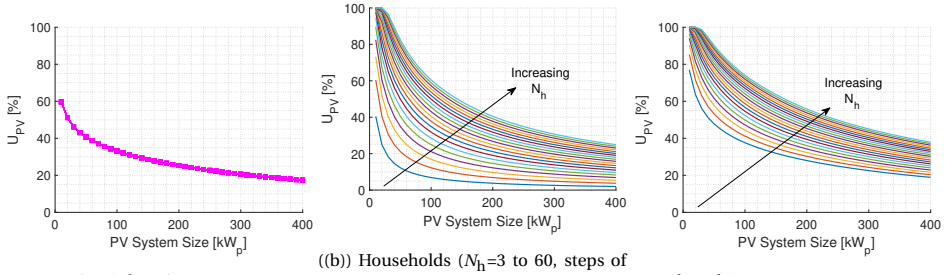

((a)) Traction Substation 12.

((b)) Households (N_h=3 to 60, steps of 3).

((c)) Shared System.

Figure 10.6: Benefit in direct PV utilization, U_{PV}, for the individual stakeholders and the shared system for a Long, Low Traffic substation in a one-year simulation.

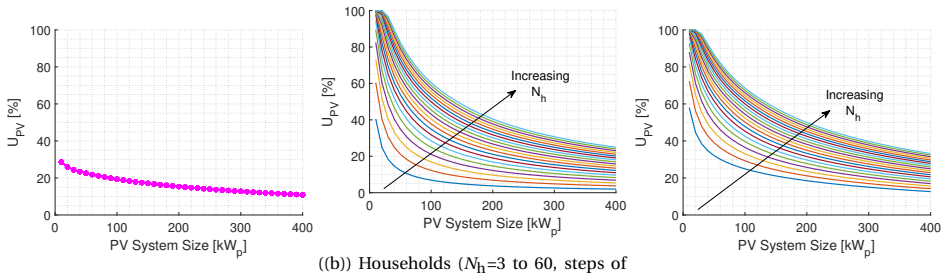

((a)) Traction Substation 9.

((b)) Households (N_h=3 to 60, steps of 3).

((c)) Shared System.

Figure 10.7: Benefit in direct PV utilization, U_{PV}, for the individual stakeholders and the shared system for a Short, High Traffic substation in a one-year simulation.

and 10.6(b).

10.4. RESULTS: BENEFITS IN LOAD COVERAGE

The PV system utilization was shown to have a positive effect at both low and high-traffic substations when sharing their PV system with any number of households. However, it is still important to study the individual traction load coverage of these shared PV systems to ensure that this benefit does not effectively come from an implicit under-sizing approach since the PV system now serves two load types.

Figure 10.8 shows the load coverage of the individual traction and residential systems. From an energy perspective, the share of each stakeholder in the PV system can be established from the energy it utilized over a year. This can be used to define an *effective* PV system size for each stakeholder to help quantify the benefit of the shared system.

For example, it is deduced from the simulations that a 200kWp (kW peak) PV system connected to SS 12 and 3 households delivers directly 80% of its power to the traction substation over the year and 20% to the households. This *effectively* means that the energy that the traction substation receives is *equivalent* to having installed an 80kWp system. However, the simulations show that an 80kWp system would give SS12 about 1% less direct load coverage than an 80% share of a 100kWp multi-stakeholder system. This validates

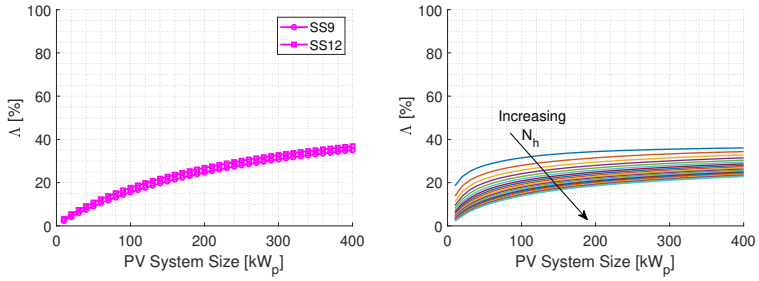

((a)) Traction Substations.

((b)) Households.

Figure 10.8: Direct Load Coverage by a PV system connecting only to a traction substation or to households.

first the claim that the benefit in utilization is not the consequence of an implicit undersizing, and second that the combined system offers better coverage per kWp installed than a single-stakeholder system. These results for all PV system sizes and household numbers are presented in Figure 10.9(a) and Figure 10.9(b), respectively. Since none of the curves in these figures cross below the zero value, it can be concluded that there is always a net benefit on the load coverage from a combined system that goes hand in hand with a net benefit in direct utilization. The energy-neutral system of 198kW for this substation ($\zeta = 1$) can be traced in Figure 10.9(b) to an increase of about 5 percentage points.
This means that a shared, multi-stakeholder system offers both less of a need for storage, curtailment, and grid exchange, as well as a net benefit in the direct load coverage (kWh delivered) per installed capacity (kWp installed).
These results are also valid for the short, high-traffic substation SS9, as can be seen in Figure 10.10. The energy-neutral system of 129kW for this substation ($\zeta = 1$) can be traced in Figure 10.10(b) to an increase of about 6-7 percentage points. While the net percentage point benefit there is seen above 10% for large system sizes, it is important to keep in mind that this substation has an energy-neutral system size of 129kW rather than the 198kW of SS12. In that regard, a 400kWp system is relatively much larger for this substation than it is for the other substation, and would directly cover significantly more of the load yet at the expense of a lower PV utilization.

10.5. CONCLUSIONS AND RECOMMENDATIONS

This chapter looked at a multi-stakeholder PV system shared between traction substations and nearby residential dwellings. In the shared system, the residential demand is expected to provide a base load to the PV system, while the traction demand provides peak demand periods. Together, this would offer a better matching of generation and load and make the system more techno-economically feasible by reducing the need for storage, AC grid exchange, and curtailment. Moreover, rooftop PV systems would offer the traction substations the otherwise-scarce urban space to install the PV panels.
In terms of the direct PV utilization, U_{PV}, there was a positive benefit in combining any traction substation with any number of households.

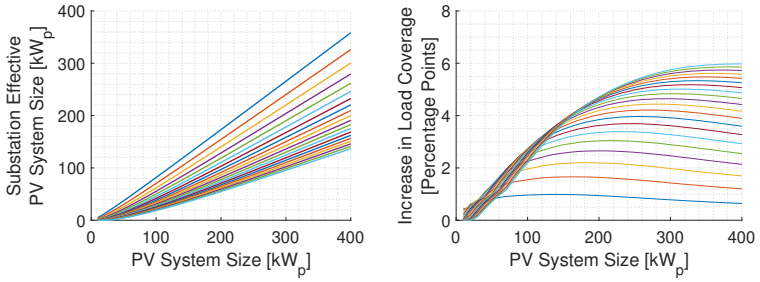

((a)) Effective PV System size. ((b)) Load Coverage Comparison.

Figure 10.9: Effective PV System size based on the share of output consumed from the installed PV system (left) and the increase in load coverage compared to a single-stakeholder system of that effective size (right) for Substation 12.

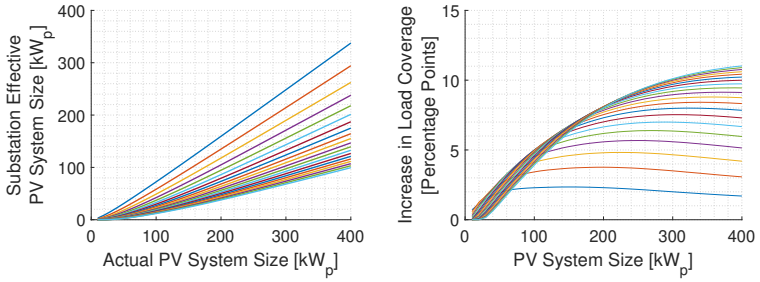

((a)) Effective PV System size. ((b)) Load Coverage Comparison.

Figure 10.10: Effective PV System size based on the share of output consumed from the installed PV system (left) and the increase in load coverage compared to a single-stakeholder system of that effective size (right) for Substation 9.

This benefit is shown to be an intrinsic benefit of the shared system and not an implicit consequence of the effective undersizing of the PV system, as it now delivers two load demands.
Furthermore, the shared PV system is shown to deliver more direct energy to the loads per effective kWp installed. Here, there was also a positive benefit for any combination of traction substations and households. This meant that the return on the investment in a share of a combined system brings more load coverage than having installed a dedicated PV system to one stakeholder of the size of that share.
Future works are urged to look at an optimal sizing approach to the number of connected households and PV system size at a traction substation with respect to costs, physical space available, and the use of storage.

PART IV

POWER MANAGEMENT SCHEMES AND SYNERGETIC DESIGN SCHEMES

Part III looked at different base loads that could transform transport networks into multi-functional and multi-stakeholder infrastructures while aiding the techno-economic feasibility of its renewables projects.

However, the concern was the possibility that simultaneously implementing these solutions could lead to them cannibalizing each other's benefits and leaving no spare capacity for the implementation of new and sophisticated trolleybus fleets such as In-Motion-Charging (IMC) buses - a hybrid between battery buses and trolleybuses.

To start with the latter, Chapter 11 looks at two more sophisticated methods to allow IMC buses to charge from an increasingly congested grid. The first method is the Adaptive Charging method which adapts the bus charging power according to its location on the grid. This proved to be sufficient to electrify some diesel bus lines fully or reduce their terminal charging time by as much as 64% while operating the existing trolleybus fleets and without the need for grid extensions.
One particular route of interest is bus line 352: an intercity bus route from Arnhem to Wageningen that is being designed as an IMC route. Given the large battery size needed and the relatively short catenary charging time, the Valley-Charging method is developed to allow for the successful implementation of this project in parallel with existing trolley fleets. The Valley-Charging method is an instantaneous measure-estimate-charge scheme based primarily on the trolleygrid state estimator developed in Chapter 4. This method with the estimator proved successful, and even almost equal to the case of all-knowing and wirelessly communicating sensors, but without the need for such expensive and cumbersome elements and communication.

Finally, Chapter 12 looks at different possibilities of combining trolleybus fleets and multi-functional components together. EV chargers were found to be the most beneficial in terms of controllable and useful base load and creating a multi-functional transport grid. However, the presence of an EV base load renders residential loads redundant from a base load perspective. Residential loads should still be considered as they allow for the rooftop installation space, and surely when integrating IMC buses without EV chargers. EV chargers, being able to recuperate braking energy, also render storage (both onboard and stationary) redundant. Energy storage is still useful in its stationary form when IMC buses are implemented but again becomes redundant in an IMC+EV+Storage scenario.
In any case, transport infrastructure like those of the trolleygrid can and should be sustainable, multi-functional, and multi-stakeholder backbones to congested city grids.

11

ENABLING THE FLEETS OF THE FUTURE: BATTERY CHARGING SCHEMES FOR IN-MOTION-CHARGING TROLLEYBUSES

"Deh! Non volerli vittime
Del mio fatale errore!
Deh! Non troncar sul fiore
Quell'innocente età!"

Deh! Non Volerli Vittime - Act II, Norma (Bellini)

Ah! Do not let them be victims
Of my fatal mistake!
Ah! Do not cut down, still in their blossoming,
those still at that innocent age!

This chapter is based on: "An Adaptive Battery Charging Method for the Electrification of Diesel or CNG Buses as In-Motion-Charging Trolleybuses," I Diab, R Eggermont, GR Chandra Mouli and P Bauer, in IEEE Transactions on Transportation Electrification **and** A Valley-Charging Method for the Electrification of Buses as IMC Trolleybuses in Congested Grid Areas. M Bistřický, I Diab, GR Chandra-Mouli, P Bauer *(Submitted)* **and** "Toward a better estimation of the charging corridor length of in-motion-charging trolleybuses," I. Diab, G. R. Chandra Mouli, and P. Bauer, in 2022 IEEE Transportation Electrification Conference Expo (ITEC), 2022, pp.557–562

In-Motion-Charging (IMC) buses are becoming a key player in sustainable urban transport as they combine the advantages of both trolleybuses (overhead supply mode) and e-buses (on-board battery mode): Reduced battery sizes, shorter charging times, and increased route flexibility.
The IMC bus, as explained in Section 11.1, runs as a trolleybus while also charging an on-board battery from the overhead lines. This battery energy is then used to power the IMC bus when the bus rides independently of the overhead cables.
The contributions of this chapter start by Section 11.2 offering a correction to the battery energy-pick calculation commonly found in literature, by including the effects of both the stopping and moving times of a typical IMC bus.
This accuracy in modeling the bus power demand is important as IMC buses already form a challenge for power-congested trolleygrid areas, and this is, in fact, the biggest bottleneck for their implementation. In that aim, this chapter first offers an Adaptive charging approach for the IMC battery in Section 11.3. This method is less conservative than the present (Regular) IMC charging scheme and takes into account the local historical congestion level of the substation that the IMC bus is under. The Adaptive Charging is tested both in a theoretical study and in Section 11.4 in a case study of four bus lines in Arnhem. The results are contrasted to the conventional IMC charging scheme in Section 11.5, which then paves the way for a fine-tuning of the Adaptive method for the case study substation in Section 11.6.
An even less conservative approach is the Valley-Charging scheme presented in Section 11.7. This method uses already-existing bus measurements to estimate the available charging power for the IMC buses at every instant and can thereby electrify bus fleets without infrastructure upgrades or wirelessly communicating grid state sensors. This method is successfully validated in a case study on Bus Line 352 of the city of Arnhem in Section 11.8 and 11.9 and is found, in the comparison in Section 11.10, to have picked up almost the entirety of the available spare capacity while retaining all of the economic, range extension, and technical benefits.
Section 11.11 then offers conclusions and recommendations for future works.

11.1. INTRODUCTION

11.1.1. IMC BUSES AS THE NEXT GENERATION OF ELECTRIC BUSES

Trolleybuses are making a comeback into the urban transport landscape as a replacement for diesel buses, pushed by recent advancements in battery technologies and electric mobility [3], [250]–[254] as well as the drive for sustainable electric transportation [11], [255]–[257]. In particular, In-Motion-Charging (IMC) buses are destined to become a key urban transportation player. These buses are a hybrid between trolleybuses and e-buses, where the vehicle runs as a trolleybus while also charging an on-board battery from the overhead lines (Figure 11.1). This battery energy is then used to power the IMC bus when the bus rides independently of the overhead cables.
The benefit is that IMC buses can use the existing trolleygrid infrastructure where their route overlaps with it to charge the battery, and operate in battery-mode outside of it. This increases the utilization of the trolley infrastructure and reduces the battery size

Table 11.1: Comparison of different IMC and non-IMC bus charging schemes[14], [22], [69], [80], [258], [259].

	Opportunity Charging Battery Bus	**Trolleybus (no storage)**	**IMC - Regular Charging (Conventional)**	**IMC - Adaptive Charging (This Chapter)**	**IMC - Valley Charging (This Chapter)**
Source for bus power	On-board battery	From the catenary, while in-motion	From the catenary, while in-motion, and from the battery when outside the catenary	From the catenary, while in-motion, and from the battery when outside the catenary	From the catenary, while in-motion, and from the battery when outside the catenary
Source for battery power	Overnight and Stationary Chargers	From the catenary, while in-motion	From the catenary, while in-motion	From the catenary, while in-motion	From the catenary, while in-motion
Harvesting of braking energy	Yes	Only for auxiliaries	Auxiliaries and battery	Auxiliaries and battery	Auxiliaries and battery
Battery charging power from catenary	No	No	Fixed charging value for Ψ and Π *for the whole trolleygrid*	Fixed charging value for Ψ and Π *under each substation*	Estimates and charges the available spare capacity for Ψ and Π *at every instant*

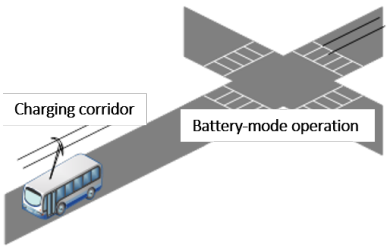

Figure 11.1: The IMC bus can operate as a trolleybus (charging corridor) or an e-bus (battery mode).

needed for the bus route [14].
Presently, the IMC battery charging power is set conservatively to the minimum of all the spare capacities of the traction substations found along the bus route. This can render most electrification projects techno/economically infeasible as not enough energy is picked up for the battery-mode operation, and long charging times at bus terminals are required.
This chapter proposes then two more liberal charging schemes: Adaptive Charging and Valley Charging as explained in Table 11.1.
However, before delving into the more sophisticated IMC charging schemes, Section 11.2 addresses one of the key gaps in the analysis of the IMC buses in the literature, which is neglecting the difference between the IMC bus moving and standing powers.

11.1.2. CHAPTER CONTRIBUTIONS

This chapter offers the following contributions:

1. The detailed derivation of the actual energy picked-up by an IMC battery during a realistic drive cycle and the quantification of the error produced when adopting instead the existing calculation methods in the literature

2. The proposition of a new charging method for IMC trolleybus batteries, namely the Adaptive Charging method that can offer more room for the integration of IMC buses and reduction of infrastructure size and costs and of bus battery charging times

3. A theoretical proof of concept, analytical quantification, and detailed technical feasibility case study of a new charging method (Adaptive Charging) for the electrification of diesel/CNG bus lines as IMC buses using the existing infrastructure

4. Analysis of maximum substation powers and minimum line voltages using comprehensive and verified bus traction and auxiliaries load models and trolleygrid models, as well as accounting for both the standing and moving charging powers of IMC buses, for the study of the impact of bus electrification on the existing infrastructure, unlike the insufficient and yet typical energy and power analyses found in literature when studying transport grids

5. The proposition, derivation, and detailed explanation of a new battery charging scheme, namely Valley-Charging, for the successful electrification of buses as In-Motion-Charging trolleybuses even in congested grid areas, and without the need for additional and/or communicating real-time grid sensors

6. A detailed case study that implements and investigates an example of the electrification of a CNG bus line as a proof of concept and as a suggestion of design choices for the Valley-Charging parameters

7. A comparison of the proposed Valley-Charging scheme to both the most sophisticated IMC scheme in literature (namely, Adaptive Charging) and to the all-knowing "Best Case" scenario of communicating real-time sensors at every power node and every substation on the grid

11.2. ACCURATE CALCULATION OF THE PICKED-UP IMC BATTERY ENERGY: CHARGING CORRIDOR LENGTH EXAMPLE

IMC buses run under the catenary as a trolleybus but are also equipped with an onboard battery. This battery is charged while the bus is in motion under the route segment with overhead wires (the charging corridor). This gives the IMC bus both the route and range flexibility of a BEB, but with a smaller battery size which is needed only to cover the catenary-less part of the bus route (the battery-mode operation). The IMC battery charging power is different per trolleybus city and is limited by factors such as the IMC battery capacity and technology, the available grid capacity, and the ratio of the battery-mode route length to that of the charging corridor.

Important to note that the IMC bus draws a lower battery charging power when standing

(referred to as Π in this chapter) than the power it draws when moving (here, Ψ). This is not to overheat and damage the point of connection of the bus to the catenary when standing still.
The picked-up battery energy by the IMC bus under the charging corridor, E_{up}, can be written as:

$$E_{\text{up}} = \eta_{\text{ch}} \cdot P_{\text{batt}} \cdot \frac{l_{\text{c}}}{\overline{v}} \tag{11.1}$$

Where η_{ch} is the battery charging efficiency, P_{batt} is the battery charging power, l_{c} is the length of the charging corridor, and $\overline{v}$ is the average bus speed under the charging corridor. This equation is then used to estimate the necessary length of the charging corridor for completing a trip of a certain distance on battery-mode.
However, in practice, the charging power of an IMC bus that is standing still (referred to in this chapter as Π) is much lower than the charging power it can consume while moving (referred to in this chapter as Ψ). This is a consequence of the current limitation of the overhead cable, which can reduce the standing battery charging power to as much as a third of the moving charging power, so as not to overheat the connection point from the current collector to the overhead cables [250]. Unfortunately, this difference in charging powers, and therefore the energy picked up by the battery, is not typically considered when estimating the length of charging corridors [250].
Figure 11.2 shows the error in the E_{up} calculation between different velocity profiles according to the percentage of moving time during the trip. The charging duplet (Ψ; Π) is taken as (150kW; 50kW). The figure exposes the error in neglecting the stopping time of the vehicle, with errors as high as -33% for a charging corridor of 2km (8kWh from an assumed 12kWh). The error comes from the fact that an average velocity of 24km/hr at 100% moving (charging 150kW) is different than the scenario with an average velocity of 24 km/hr at 50% moving, as that means the vehicle was stopped half of the time (limited to 50kW charging) and then did not spend a lot of time charging at 150kW, as it sped through the charging corridor at 48km/hr. Both these scenarios, however, have an average velocity of 24km/hr and are not discriminated by equation 11.1.
To show the impact of considering both the moving and standing charging powers, this section looks into the effect of neglecting the standing power on a key IMC network design feature: The charging corridor length.

11.2.1. ANALYTICAL ESTIMATION OF THE CHARGING CORRIDOR LENGTH

Consider a charging corridor of length l_{c} (km) for an IMC bus that needs to cover a total route length of l_{tot} (km). The IMC bus can charge Π (kW) for the time t_{s} (h) that it is standing still, and Ψ (kW) for the time t_{m} (h) that it is in motion. The round-trip efficiency of battery charging is η, and the bus consumes a specific energy of e in kWh/km. The total trip time, Δt (h), is defined as:

$$\Delta t \triangleq t_{\text{s}} + t_{\text{m}} \tag{11.2}$$

In terms of the total average velocity under the charging corridor, $\overline{v}$, the charging corridor length can be expressed as:

$$l_{\text{c}} = \overline{v} \cdot \Delta t \tag{11.3}$$

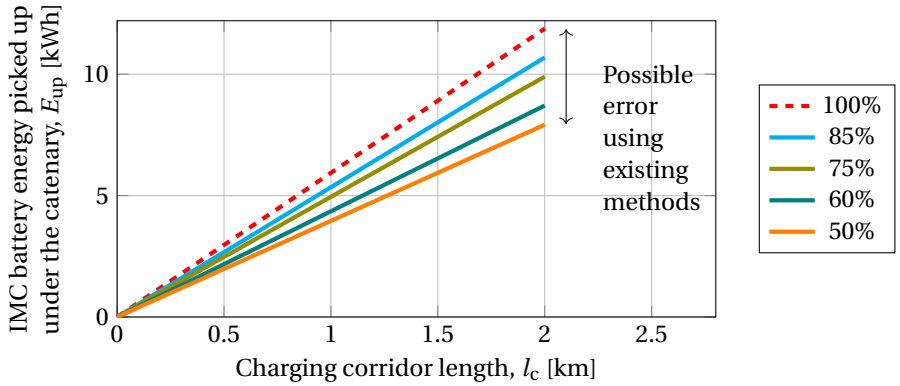

Figure 11.2: IMC battery energy picked up as a function of the traveled distance (150kW moving/50kW standing) for an average bus velocity of 24km/hr. The different lines show the fraction of the moving time of the bus during the trip; e.g., at 50%, the bus moved at 48km/hr for half the time and was stopped for the other half (average velocity of 24km/hr).

While in terms of the average *moving* velocity, $\overline{v}_m$, that excludes the zero values of the stopping time, the charging corridor length can be expressed as:

$$l_c = \overline{v}_m \cdot t_m \tag{11.4}$$

Combining Eq.11.2 and Eq.11.4:

$$t_s = \Delta t - \frac{l_c}{\overline{v}_m} \tag{11.5}$$

The battery energy balance between the total charged energy (left-hand side) and the total discharged energy (right-hand side) is then:

Energy picked up under l_c = Energy discharged during the remaining part of the trip (that is $l_{tot} - l_c$) (11.6)

or in terms of the variables previously defined:

$$\Pi \cdot t_s + \Psi \cdot t_m = (l_{tot} - l_c)\frac{e}{\eta} \tag{11.7}$$

Finally, combining Eq.11.5 and Eq.11.7:

$$\frac{l_c}{l_{tot}} = \frac{e}{e + \eta[\Psi \cdot \frac{1}{\overline{v}_m} + \Pi(\frac{1}{\overline{v}} - \frac{1}{\overline{v}_m})]} \tag{11.8}$$

This offers the ratio of the charging corridor length to the total route length. For comparison, following the common trend in literature to ignore the difference in the allowed charging powers between moving and standstill periods [250], the ratio would only take

Table 11.2: Characteristics of the measurements of 7 exemplary trolleybus trips in Arnhem.

Trip	Length	Duration	$t_s/\Delta t$	$\overline{v}$	$\overline{v}_m$
Oosterbeek to Velp, trip 1	11.7 km	44 min	43.3%	15.8 km/hr	21.6km/hr
Oosterbeek to Velp, trip 2	11.9 km	41 min	36.7%	17.4 km/hr	25.5km/hr
Burgers Zoo to Het Duifje, trip 1	10.5 km	39 min	37.7%	16.2 km/hr	24.9km/hr
Burgers Zoo to Het Duifje, trip 2	10.4 km	39 min	29.4%	16.0 km/hr	24.6km/hr
Het Duifje to Burgers Zoo	9.90 km	40 min	29.4%	14.9 km/hr	22.3km/hr
Presikhaaf to Schuytgraaf	15.1 km	47 min	31.8%	19.3 km/hr	24.6km/hr
Rijkerswoerd to Geitenkamp	12.7 km	46 min	35.6%	16.6 km/hr	21.6km/hr
Average	**11.7 km**	**42.3 min**	**34.8%**	**16.6 km/hr**	**23.6km/hr**

Table 11.3: The moving (Ψ) and standing (Π) battery charging power for IMC buses in different cities **IMC_Esslingen**, **IMC_Solingen**, **IMC_UITP**, [81], [250].

Charging Power	Gdynia	Esslingen	Gdynia II (Study)	Solingen	Prague	Szeged	Eberswalde
Ψ [kW]	120	150	250	240	120	130	240
Π [kW]	90	50	80	200	50	81	90

Ψ into account and would be expressed as:

$$\frac{l_c}{l_{tot}} = \frac{e}{e+\eta\cdot\frac{\Psi}{\overline{\overline{v}}}} \qquad \text{(As found in literature)} \tag{11.9}$$

11.2.2. CASE STUDY: QUANTIFYING THE ERROR IN THE ESTIMATION OF THE CHARGING CORRIDOR LENGTH

The following case study investigates the error in the charging corridor estimation between the literature method (Eq. 11.9) and the method proposed in this chapter (Eq. 11.8) by using measured data from the Dutch trolleygrid city of Arnhem. The error is defined as:

$$\text{Error} = \frac{\text{Result of Eq. 11.8} - \text{Result of Eq. 11.9}}{\text{Result of Eq. 11.8}} \tag{11.10}$$

The case study city is Arnhem (the Netherlands), which is a trolleybus city with 6 lines (12 routes both ways). Table 11.2 shows the analyzed characteristics of the measurements done on 7 trips on some of these routes, courtesy of the HAN University of Applied Sciences. It is observed that the bus stopping time can account for as much as 34.8% of the whole trip time, on average. This average stopping time as well as the average velocities reported in the table are taken as the values for the case study. Additionally, in this chapter, e is taken as 3 kWh/km [3], [4] and η is 0.9.

THE CASE OF IMC REGULAR CHARGING

Figure 11.3 shows the percentage error (Eq. 11.10) between the method commonly found in literature and the more accurate method presented in this chapter for multiple charging values of several trolley cities. The charging power duplets ($\Psi;\Pi$) of these cities are

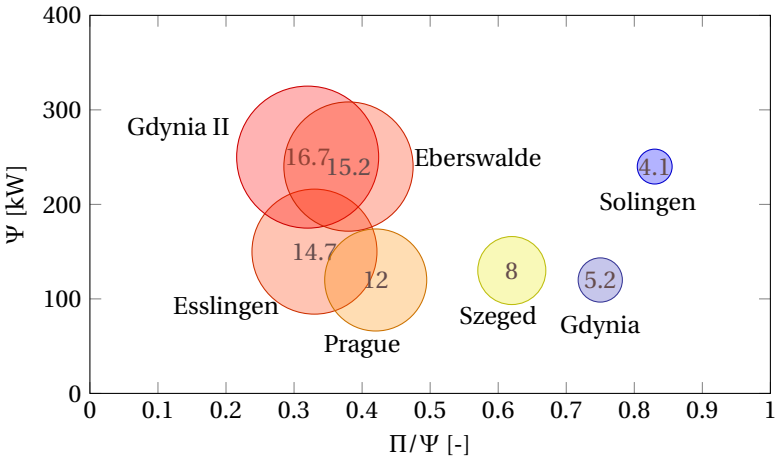

Figure 11.3: Percentage Error (Eq. 11.10) between the method commonly found in literature and the more accurate method presented in this chapter for multiple charging values of several trolleycities. The bubble size reflects the error value, in percentage.

presented in Table 11.3. The x-axis shows the ratio of the standing to moving charging powers (Π/Ψ) and the y-axis shows the absolute value of the moving charging power, Ψ, in kW.
The results quantify two intuitive insights. First, the error is drastically lower when the ratio between the standing and the moving charging powers is higher, as in the Solingen or Gdynia case. However, as can be seen in the figure, scenarios of such high Π to Ψ ratios are not typically the case for IMC systems. Second, the error is lower when the moving charging power is lower. Interestingly though, this effect is not as drastic as that of the ratio of the two charging powers. For example, the Prague and Gdynia cases move from 12% to 5.2% error by going from a ratio of 0.42 to 0.75 at the same moving charging power, Ψ, of 120 kW. This urges especially the cities of low Π/Ψ ratio to be more critical with their charging corridor length calculations.

EXTENSION TO THE CASE OF IMC ADAPTIVE CHARGING

Adaptive charging can also be route-dependent. For example, while going downhill, an IMC bus is allowed to collect more battery energy because its traction power demand is negligible. However, when going uphill on the same road, the bus should collect less energy from its battery, as the bus traction demand is already significant.
In the Adaptive charging scenario, accounting for two different charging power duplets (namely 1 and 2) under the same charging corridor and route, the energy balance of Eq.11.7 can be rewritten as:

$$(\Pi_1 \cdot t_{s,1} + \Pi_2 \cdot t_{s,2}) + (\Psi_1 \cdot t_{m,1} + \Psi_2 \cdot t_{m,2}) = (l_{tot} - l_c)\frac{e}{\eta} \tag{11.11}$$

Moreover, the result of Eq.11.8 can be extended to N different sections with their charging duplets as:

$$\frac{\Sigma_{i=1}^{N} l_{\mathrm{c},i}}{\Sigma_{i=1}^{N} l_{\mathrm{tot},i}} = \frac{e}{e+\eta\cdot[\Sigma_{i=1}^{N}\Psi_i\cdot\frac{1}{\overline{v}_{\mathrm{m},i}}+\Sigma_{i=1}^{N}\Pi_i(\frac{1}{\overline{v}_i}-\frac{1}{\overline{v}_{\mathrm{m},i}})]} \tag{11.12}$$

11.3. THE ADVANTAGES OF ADAPTIVE CHARGING: THEORETICAL PROOF OF CONCEPT

Electrification of urban public transport is gaining momentum, pushed by ambitious zero-emission policies. For example, almost half of the EU member states have set a 75% target for zero-emission bus sales by 2030 [260], [261]. This steep increase poses a challenge for electric transport infrastructures looking to electrify their diesel or CNG fleets. On the other hand, the existing urban transport networks, such as trams or trolleybus grids, tend to be both oversized and underutilized in terms of their power capacity [3], [12], [14], [79], [80]. This invites investigations into using this spare capacity for the sustainable electrification and charging of electric vehicle fleets without the need for major urban grid infrastructure updates and investment costs [11], [16], [262]–[264]. Presently, an IMC bus has a fixed charging power duplet throughout its operation (Ψ while moving, and Π while standing still, as explained earlier). This charging power is chosen and fixed in a very conservative way according to the expected spare capacity of the *most congested* substation on the IMC bus route. This leaves the other, less-congested zones with underutilized spare capacity that could have allowed an extension of the battery-mode operation and/or reduced the required charging corridor length. This is referred to in this chapter as *Regular Charging*.

This chapter suggests an *Adaptive Charging* approach that changes the battery charging power duplet (Ψ, Π) depending on the spare capacity of the trolleygrid substation it is currently under (Figure 11.4). This spatial condition can be easily implemented by making use of the existing GPS signal found on most buses or of an integral of the bus velocity to estimate its position on the route.

11.3.1. QUANTIFICATION OF THE BENEFIT OF ADAPTIVE CHARGING WITH THE CASE OF ONE CONGESTED AND ONE UNCONGESTED ZONE

In a regular IMC charging situation, combining Eq.11.5 and Eq.11.7 yields the length of the batter-mode route feasible with the picked up energy under the catenary, L_{BM}:

$$L_{\mathrm{BM}} = \frac{\eta\cdot L_{\mathrm{ch}}}{e\cdot\overline{v}_{\mathrm{m}}}\left[\Psi+\Pi(\frac{\overline{v}_{\mathrm{m}}}{\overline{v}}-1)\right] \tag{11.13}$$

In an Adaptive Charging scenario, considering a charging corridor that consists of a congested substation zone and an uncongested zone, the energy balance of Eq.11.7 can be re-written as:

$$(\Pi_{\mathrm{c}}\cdot t_{\mathrm{s,c}}+\Pi_{\mathrm{u}}\cdot t_{\mathrm{s,u}})+(\Psi_{\mathrm{c}}\cdot t_{\mathrm{m,c}}+\Psi_{\mathrm{u}}\cdot t_{\mathrm{m,u}}) = L_{\mathrm{BM,A}}\cdot\frac{e}{\eta} \tag{11.14}$$

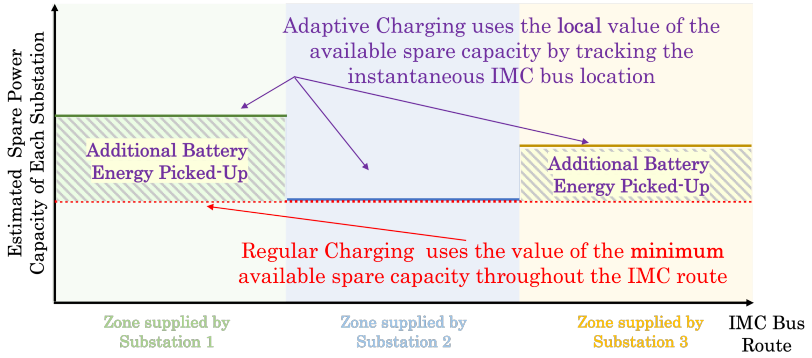

Figure 11.4: Illustrative example of the different IMC battery charging methods presented in section 11.3.

Accounting thereby for two different charging power duplets (Ψ, Π), where the c and u subscripts refer to the congested and uncongested zones, respectively, and $L_{\mathrm{BM,A}}$ is the battery-mode route length obtained by Adaptive Charging. The net additional benefit in the achievable battery-mode distance obtained from Adaptive Charging over Regular Charging, ΔL_{BM}, is in the difference between Eq. 11.13 and Eq. 11.14.
Indeed, by defining the ratio of the congested to uncongested velocities as ϕ, the ΔL_{BM} can be expressed as:

$$\frac{\Delta L_{\mathrm{BM}}}{L_{\mathrm{u}}} = \frac{\eta}{e \cdot \overline{v}_{\mathrm{m,c}}} \left[(\phi \Psi_{\mathrm{u}} - \Psi_{\mathrm{c}}) + (\frac{\overline{v}_{\mathrm{m,c}}}{\overline{v}_{\mathrm{c}}} - 1)(\phi \Pi_{\mathrm{u}} - \Pi_{\mathrm{c}}) \right] \tag{11.15}$$

This value is always larger than zero since, by definition, $\phi \in]0,1]$ and thereby $\phi \Psi_{\mathrm{u}} \in]\Psi_{\mathrm{c}}, \Psi_{\mathrm{u}}]$. Moreover, $\overline{v}_{\mathrm{m}} \geq \overline{v}$, also by definition. Consequently, the benefit ΔL_{BM} is a sum of strictly positive terms and is thereby always strictly positive, and Adaptive Charging will always lead to an increase in the potential for picked-up energy by the battery.
Looking at values of the typical order of magnitude for a trolleybus (see: the case study later), it can be shown that the length of the added battery-mode can be at the order of a few L_{u}, i.e., in the range of kilometers. This can have significant implications on reducing the length of the charging corridors or increasing the length of the battery-mode sections, as well as on the economical and technical feasibility of the bus electrification projects.

11.3.2. GENERALIZATION OF THE RESULTS FOR N SECTIONS

When multiple sections are involved, such as in Figure 11.4, the net increase in the feasible battery-mode operation distance, $\Delta L_{\mathrm{BM,N}}$ can be obtained by an extension of Eq.11.15 to N substations as:

$$\Delta L_{\mathrm{BM,N}} = \frac{\eta}{e} \sum_{i=1}^{N} \frac{L_i}{\overline{v}_{\mathrm{m,c}}} \left[(\phi \Psi_i - \Psi_{\mathrm{c}}) + (\frac{\overline{v}_{\mathrm{m,c}}}{\overline{v}_{\mathrm{c}}} - 1)(\phi \Pi_i - \Pi_{\mathrm{c}}) \right] \tag{11.16}$$

Where the subscript "c" is reserved for the most congested substation among the N substations, i.e., the one with the least spare capacity. The same analysis as the one that

Table 11.4: Illustrative comparison of the Adaptive (this chapter) and Regular IMC charging methods.

		IMC Charging Power
Adaptive Charging	**SS1**	Ψ_1
	SS2	Ψ_2
	SS3	Ψ_3
Regular Charging	**For all three SS**	$\min(\Psi_1, \Psi_2, \Psi_3) = \Psi_2$

followed Eq.11.15 can show here as well how the benefit described by Eq.11.16 is also always strictly positive.
To revisit Figure 11.4 as a way of an example, the 3 substations shown have 3 spare capacities for charging: Ψ_1 for SS1 (relatively high), Ψ_2 for SS2 (relatively low), and Ψ_3 for SS3 (relatively medium). For simplicity, the standing charging powers (for example, Π_1), are not mentioned here but their design choice follows this same process.
Table 11.4 shows this charging powers decision process. The Adaptive Charging method uses the locally available spare power capacity, which increases the amount of picked-up energy relative to the Regular Charging method. The latter is more conservative and is the method currently used in all IMC applications. The Regular Charging method uses the minimum of the spare capacities throughout the network, which leaves out a lot of unharvested spare capacity. Fleets using Regular Charging can be upgraded to Adaptive Charging by tracking the bus position by methods such as GPS tracking, a velocity-measurement integral with a look-up table, or others.

11.4. THE ADVANTAGES OF ADAPTIVE CHARGING FOR A FULL BUS LINE: THE ARNHEM CASE STUDY

To quantify the total benefit of Adaptive Charging for a fleet of operating buses, the following sections present the results of a case study of the electrification of 4 bus lines in the Dutch city of Arnhem. The substations have a rated power limit of 800 kW, except for the Arnhem Central Station (Arnhem CS, substation 4), which was being increased to a capacity of 1800 kW by the time of this research.
Four diesel bus lines in Arnhem, namely lines 4, 13, 29, and 352, are suggested as candidates in this chapter for electrification by IMC Adaptive Charging. As summarized in Table 11.5, these lines have routes that are independent of each other, other than the unavoidable exception of the Arnhem Central Station.
As mentioned earlier, the two obstacles to the integration of IMC buses are the substa-

Table 11.5: The four studied diesel bus lines in Arnhem, with the trolleygrid substations (SS) and sections (SCT) that they cross marked with a checkmark. All bus lines pass through SCT 5 of SS 4 which is the Arnhem Central Station (ACS).

Bus	**Route under**	L_{BM}	**SS**	**1**		**2**			**3**		**4**			**5**			**9**	**10**	**12**	
Line	**the catenary**	**(one-way)**	**SCT**	**2**	**3**	**14**	**15**	**16**	**12**	**36**	**5**	**6**	**8**	**17**	**18**	**35**	**25**	**22**	**23**	**24**
4	ACS-De Praets	5.6 km									✓						✓			
13	ACS-Graaf Ottoplein	1.4 km				✓					✓	✓	✓							
29	ACS-Velp	25.2 km						✓	✓		✓	✓		✓	✓			✓		
352	ACS-Oosterbeek	12.1 km		✓	✓						✓								✓	✓

Table 11.6: Example of Trolleygrid Limitations: Arnhem, The Netherlands (*Busines-as-usual: Limit currently tolerated by the trolleygrid operator).

Violation	Limitation	Allowable continuous duration
Maximum Substation Power*	$100\% < P_s \leq 150\%$	10 seconds
	$P_s > 150\%$	Never (Undesired)
	$P_s > 200\%$	Never (Severe)
Minimum Line Voltage	$V_{min} \leq 490V$	Never; 500V is typically tolerated [233], [234]
Maximum Line Current	$I_{max,1} > 880$ A	3000 seconds [83], [165]
	$I_{max,2} > 1200$ A	1800 seconds [59]

tion power and line voltage limitations. Small power peaks are commonly withstood by transformers, and for this study, a limit of 1 hour per year (3600s) of operation up to 150% of the rated substation power is deemed acceptable. This number is close to a daily 10 seconds of such an operation that is currently reported in measurements on the Arnhem grid. No value above this is accepted. On the other hand, a minimum line voltage between 450V and 500V is not welcomed since it means curtailment of the bus power, yet still is acceptable if the voltage is not lower than that. This means that no voltage under 450V would be accepted because the grid's lower operational limit is 400V as mentioned in the introduction.
These limits of the substation power demand, P_{ss}, as a function of its rated power and of the minimum line voltage, V_{min}, are summarized in Eq.11.17 and Table 11.6:

$$P_{ss} \begin{cases} \leq 100\% \text{ rated} & \text{, Acceptable} \\ > 100\% \& \leq 150\% \text{ rated} & \text{, Acceptable up to 3600s per year} \\ > 150\% \text{ rated} & \text{, Not Acceptable} \end{cases} \tag{11.17}$$

$$V_{min} \begin{cases} \geq 500V & \text{, Acceptable} \\ < 500V \& > 450V & \text{, Acceptable, although undesired} \\ \leq 450V & \text{, Not Acceptable} \end{cases} \tag{11.18}$$

11.4.1. SUGGESTED ADAPTIVE CHARGING POWER LEVELS

The different IMC charging powers levels are:

- **No IMC:** Keep the studied buses as diesel buses
- **IMC - no charging:** Transform the diesel buses into IMC buses, but do not charge the battery under *this* specific section. This means that the bus only consumes traction and auxiliaries power from the catenary and Π =0kW and Ψ=0kW.
- Π **kW;**Ψ **kW:** All the 4 studied bus lines electrified, and charging the battery at Π kW while stopped and Ψ kW while moving. The different duplets are studied in this chapter, according to existing and future IMC charging powers from European cities [14], [22]

The ***IMC - no charging*** suggestion is a key feature of the Adaptive Charging method where the IMC bus completely refrains from charging under a congested section of the

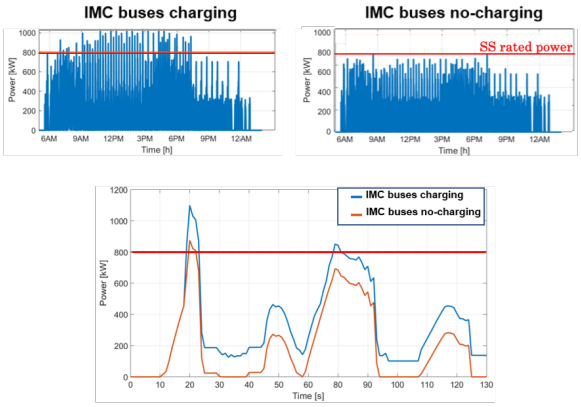

Figure 11.5: One-day simulation of the SS1 power demand including IMC bus line 352 both when the IMC buses are charging at 150kW (top left) or in No-charging mode (top right). A zoom-in on two minutes of operation (bottom) shows how the No-charging mode of Adaptive Charging can reduce both the severity and the number of power breaches.

trolleygrid but still runs as a trolleybus rather than in battery-mode. To highlight an example, Figure 11.5 shows one day of operation of SS 1 with the significant reduction of almost all power violations by switching to no-charging mode, yet still operating as a normal trolleybus and not depleting the battery.

11.4.2. AN EXTENSION OF THE TROLLEYBUS MODELLING INTO AN IMC TROLLEYBUS

The trolleybus model from Chapter 3 is now extended and the IMC bus powers are given by Eq.11.19.
While in traction mode, the bus power, P_{bus}, is the traction power and battery powers, P_{tr} and P_{batt}, and the auxiliaries demand of the HVAC load (Heating, Ventilation, and Air Conditioning), P_{HVAC}, and other base loads, P_{base}, such as the bus lighting, information screens, door opening, and closing motors, the control systems, etc.
The power is capped at 500kW, which is the maximum commercially available power for an IMC bus currently: The IMC500 by Kiepe Electric.
During braking, the bus power is the auxiliaries power, P_{HVAC}, plus the battery power P_{batt}, and the excess energy, P_{BR}, that is wasted in the on-board braking resistors.

$$P_{\text{bus}} = \begin{cases} P_{\text{tr}} + P_{\text{HVAC}} + P_{\text{base}} + P_{\text{batt}} & \text{, traction \& } < 500\text{kW} \\ 500\text{kW} & \text{, traction \& } \geq 500\text{kW} \\ P_{\text{BR}} + P_{\text{HVAC}} + P_{\text{base}} + P_{\text{batt}} & \text{, braking} \end{cases} \tag{11.19}$$

$$P_{\text{batt}} = \begin{cases} \Psi \quad [\text{kW}] & \text{, when moving} \\ \Pi \quad [\text{kW}] & \text{, when standing, e.g. at a traffic light} \end{cases} \tag{11.20}$$

Table 11.7: The yearly number of power demand breaches on each substation of the case study simulations (with IMC buses charging at $[\Pi;\Psi] = [100\text{kW};150\text{kW}]$). The unacceptable breaches, according to Eq.11.17, are marked in bold.

		Substation							
		1	2	3	4	5	9	10	12
Total yearly number of	>100% but ≤ 150%	**91708**	3093	**24031**	0	190	0	11	**3806**
Rated Power Breaches [s]	>150%	**14**	0	**1974**	0	0	0	0	0
Acceptable Breaches as per Eq.11.17?		**No**	Yes	**No**	Yes	Yes	Yes	Yes	**No**
Next Study Suggestion*		Try IMC-no charging	Higher Power	Try IMC-no charging	Higher Power	Higher Power	Higher Power	Higher Power	Try IMC-no charging

*see example results in Figure 11.8

11.5. ADAPTIVE COMPARISON: FULL YEAR WITH IMC REGULAR CHARGING AT $[\Pi;\Psi] = [100\text{kW};150\text{kW}]$

11.5.1. YEARLY POWER DEMAND ANALYSIS UNDER IMC REGULAR CHARGING

Table 11.7 shows the simulated yearly power demand on the Arnhem substations with the electrified IMC buses charging at $[\Pi;\Psi] = [100\text{kW};150\text{kW}]$. To simulate the most demanding conditions for the substation power and line voltage, regenerative power sharing between buses will be excluded as well as bilateral connections.

Substations 1, 3, and 12 are already ruled out on the basis of their excessive power breaches as set by Eq.11.17. These substations can probably still benefit from the electrification as IMC buses with no-charging mode. This means that an IMC bus running under these substations would pick up less energy and would need to compensate for it elsewhere. However, this is still a major advantage over Regular Charging as the latter would have deemed the whole electrification project unfeasible when faced with this information. Further investigations of these lines are then conducted in the next section of this chapter.

On the other hand, substations 2, 4, 5, 9, and 10 are capable of integrating these electrified bus fleets, and at these battery-charging powers, as no unacceptable breach levels were flagged. In the next section of this chapter, these substations will be investigated to see if they can handle an even higher IMC charging power.

First, however, a voltage study is conducted to look at possible violations of the minimum line voltage limits.

11.5.2. YEARLY MINIMUM VOLTAGE ANALYSIS YEARLY POWER DEMAND ANALYSIS UNDER IMC REGULAR CHARGING

If a trolleybus sees the low voltage of 500V the on-board power control will intervene [265] and curtail its demand. This results, for example, in the bus HVAC system shutting off and the bus not being able to accelerate. At 400V, the power to the bus is completely shut off.

For this analysis, any occurrence of the minimum line voltage below 500V is undesired, and the limit of 400V is a serious violation. Comparing this to a situation with IMC buses (see figures 11.6 and 11.7) it can be noticed that sections 2 and 22 of substations 1 and 10 now also have voltage drops below 500 V. While this is undesired, it is still feasible

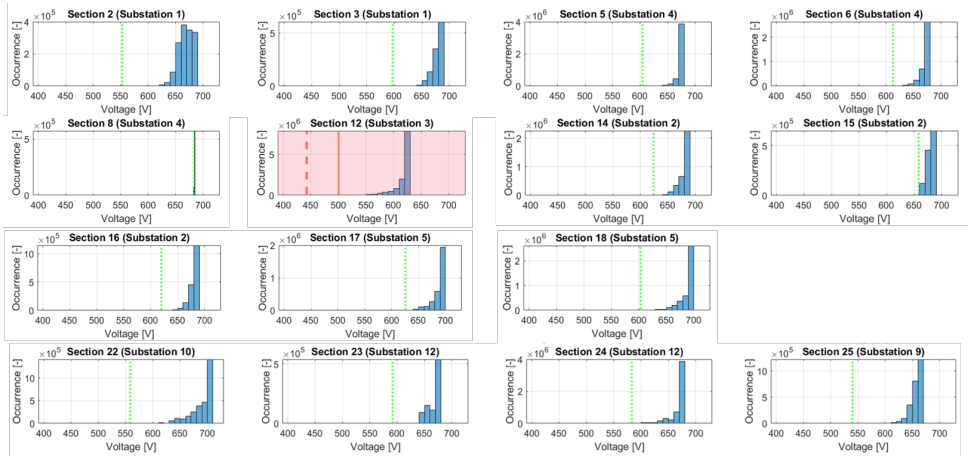

Figure 11.6: Histogram of the yearly minimum line voltage on each section in this study for the present trolley-grid (Without IMC buses). The lowest recorded voltage is indicated by a green dotted line if the limit of 500V of Eq.11.18 is not exceeded, and a red dotted line otherwise. Also per Eq.11.18, orange-colored plots flag an unwelcome yet tolerated operation, while red-colored plots flag an unacceptable operation (IMC charging not feasible).

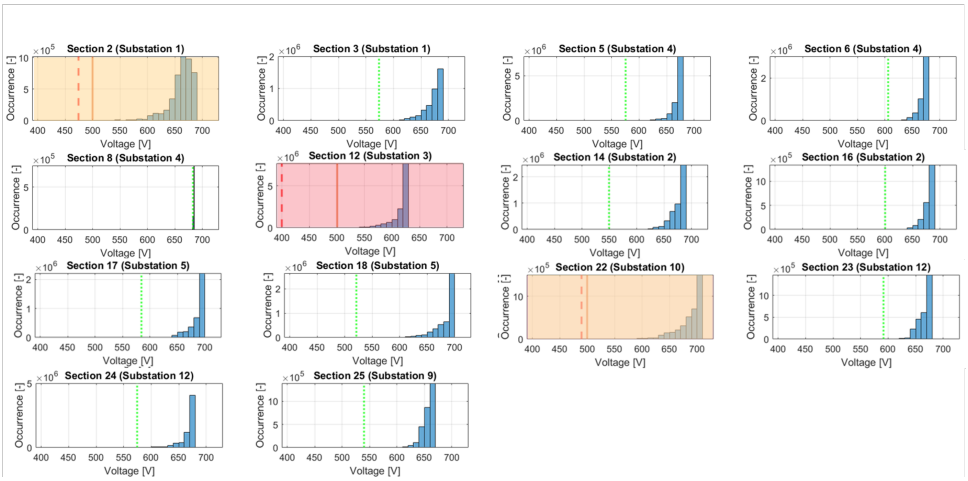

Figure 11.7: Histogram of the yearly minimum line voltage on each section in this study for the present trolley-grid (Without IMC buses). The lowest recorded voltage is indicated by a green dotted line if the limit of 500V of Eq.11.18 is not exceeded, and a red dotted line otherwise. Also per Eq.11.18, orange-colored plots flag an unwelcome yet tolerated operation, while red-colored plots flag an unacceptable operation (IMC charging not feasible).

Table 11.8: Comparison of the Adaptive (this chapter) and Regular IMC charging methods for the studied bus lines in Arnhem and the maximum power that can be drawn [Π standing; Ψ moving] from the substations that supply them. As explained in section 11.3, the Regular Charging method uses the most conservative charging power throughout the whole bus route.

		Line 4	Line 13	Line 29	Line 352
Adaptive Charging ([Π standing; Ψ moving])	**SS1**				No Charging
	SS2		[200;300kW]	[200;300kW]	
	SS3			No Charging	
	SS4	[100;150kW]	[100;150kW]	[100;150kW]	[100;150kW]
	SS5			[100;150kW]	
	SS9	[200;500kW]			
	SS10			[200;300kW]	
	SS12				No Charging
Regular Charging ([Π standing; Ψ moving])	**For any SS on the route**	[100;150kW]	[100;150kW]	No Charging	No Charging

according to Eq.11.18.
The minimum voltage of section 12 of substation 3 drops even further to the minimum of 400 V. Substation 3, therefore, does not seem to allow the electrification of bus line 29. This is already an expected result as this congested substation caters to all 6 conventional trolleybus lines in Arnhem.
No other substations are then excluded by the 150kW charging scheme and the chosen substations can be studied for higher charging powers. If a higher charging power is chosen in the end for a substation, it is worth keeping in mind that a possible voltage under 500V would then first momentarily curtail the battery charging power, and not the bus traction power, and is thereby acceptable although undesired outcome as it affects seconds of battery charging rather than a shutting-down of the bus. This justifies why the voltage analysis is not repeated in the upcoming section.

11.6. ELECTRIFICATION OF BUS LINES WITH ADAPTIVE CHARGING: SUBSTATION ANALYSIS

11.6.1. ANALYSIS OF DIFFERENT IMC CHARGING POWERS

The results of other IMC charging powers are presented in Figure 11.8. Power demand throughout the day is shown in blue while the substation limit (i.e. 800 kW for all substations except substation 4 which is built for 1800 kW) is indicated with a red dashed line. Across the board, an increase in power demand can be observed when looking from left to right. For substations 2, 9, and 10 this power demand increase is relatively small. On the other hand, substations 1 and 4 show drastic increases in power demand.
Battery charging of IMC buses waiting for their next trip at Arnhem CS even causes the power demand for substation 4 to constantly be above zero from early in the morning to at least 7 PM. Substations 3, 5, and 12 show power demands that do increase quite a lot but this mostly shows up as short peaks instead of a constant increase.
This indicates that substations 2, 9, and 10 could supply the buses with a higher charging power to compensate for a decrease in charging power on other sections.

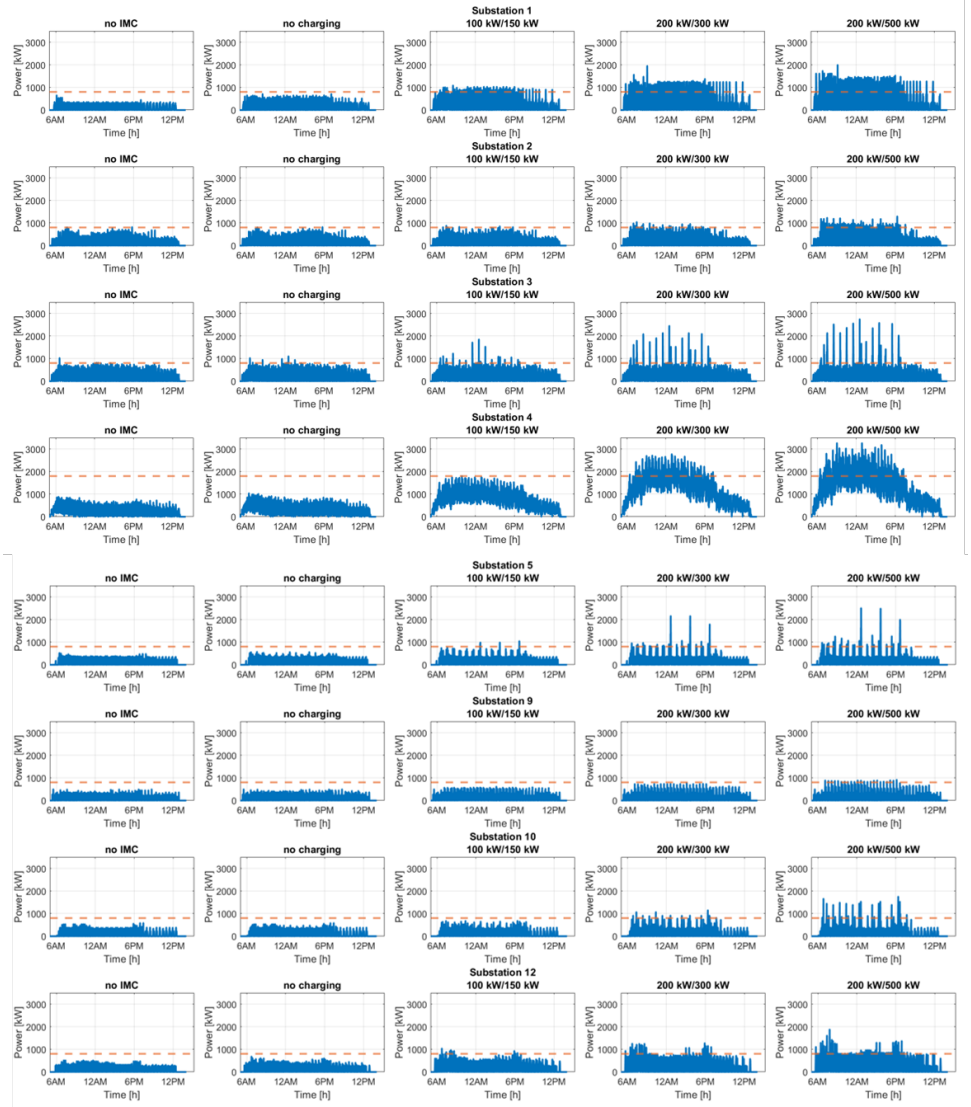

Figure 11.8: Closer look at the substation power demand on a Regular Weekday schedule for five IMC battery charging schemes.

Table 11.9: Comparison of the energy picked up by the IMC battery, route feasibility, and extra charging time needed for Adaptive Charging (this chapter) or the conventional Regular Charging methods, with e=3kWh/km [14].

		Feasible energy pick-up (Integral of the battery charging power curve with the values in Table 11.8)		**Additional time needed at an opportunity charger (Eq. 11.21 with P_{op}=100kW, η_{op}=0.94)**		
Bus Line	**Energy needed for a battery-mode round trip (=2*$L_{BM} \cdot e$)**	**Regular Charging**	**Adaptive Charging**	**Regular charging**	**Adaptive Charging**	**Time saved**
4	33.8 kWh	9.6 kWh	25 kWh	15.4 min	5.6 min	64%
13	8.3 kWh	16.2 kWh	26.2 kWh	0 min	0 min	N/A
29	151.3 kWh	0 kWh	59.5 kWh	96.6 min	58.6 min	39%
352	72.6 kWh	0 kWh	2 kWh	46.3 min	45.1 min	3%

The suggested Adaptive Charging approach is summarized in Table 11.8, by adopting the highest possible charging power at each substation according to the power and voltage limitations described earlier. Regular Charging is the most conservative, as previously explained, and adopts the most conservative charging power of any substation on the bus route throughout the whole route. The first IMC bus line considered is bus line 4, which passes under substations 4 and 9. It can be seen that substation 9 can take charging powers up to 500 kW without exceeding the power demand limit too often. However, these charging powers are so far unachievable with the available bus technology. For substation 4, the limit is [100kW;150kW]. If needed, bus line 4 can shift thereby the battery charging from under substation 4 to under substation 9.
Bus line 352 passes under substations 1, 4, and 12. As substations 1 and 12 show power limit breaches even at low charging powers, the charging power should be shifted to another section. However, substation 4 cannot compensate for more than 150kW of charging. For this IMC bus line, no solution can be found without an increase in the substation capacity or the installation of small stationary storage that can momentarily relieve the substation by assisting in load coverage.
As can be seen from the first four columns of Table 11.9, the picked-up energy, while increased with Adaptive Charging, is not sufficient for the full catenary-electrification of lines 4, 29, and 352.
In case the electrification of the diesel lines is not feasible using only the charging corridor, an additional opportunity charger at the end-of-line can be used to help charge the battery from its current state, E_b, to its needed energy level for the trip, E_{trip}. For this, Adaptive Charging has also the advantage of reducing the charging time.

11.6.2. ADAPTIVE CHARGING AS A WAY TO REDUCE CHARGING TIMES

To increase the total battery energy, E_b, to its needed energy level for the trip, E_{trip}, the additional charging time needed at an opportunity charger, t_{op}, for a charging session at a power, P_{op}, and total converter+battery efficiency of η_{op} is:

$$t_{op} = \begin{cases} \dfrac{E_{trip} - E_b}{\eta_{op} \cdot P_{op}} & \text{, if } E_{trip} \geq E_b \\ 0 & \text{, otherwise} \end{cases} \tag{11.21}$$

When a charger of 100kW is installed, the suggested Adaptive Charging scheme presented in Table 11.8 leads to the results in Table 11.9. It is seen that the method proposed in this chapter can reduce the charging times needed at the terminals by up to 64%, or almost 40 minutes.
The electrification of diesel line 13 is feasible with both Regular and IMC charging and is highly urged to be implemented to offset the carbon emissions of the present diesel buses. Bus line 4 can require as little as 5.6 minutes of opportunity charging when using the here-suggested Adaptive Charging method. This time window can be easily worked into the bus timetables and delays, as opposed to the 15.4 minutes needed with Regular Charging. Bus lines 29 and 352 are not as promising, unfortunately, as significant opportunity charging time is still needed even with Adaptive Charging. However, it is important to note that bus 29 would pick up no energy under the Regular Charging method, needing thereby to be electrified as a full BEB if an electrification project is underway. With Adaptive Charging, more than a third of its energy demand can be picked up from under the existing catenary, translating into a reduction by up to a third of the needed battery capacity. This brings benefits in costs, space, and traction energy from the reduced battery mass. Line 352 on the other hand is limited by its congested substations, and a new, more sophisticated and instantaneous charging scheme is urged for a future investigation.

11.7. BEYOND ADAPTIVE: A VALLEY-CHARGING METHOD WITHOUT ADDITIONAL SENSORS

Despite having an underutilized spare energy capacity, traction grids can frequently have short periods of power congestion problems. These moments should be considered when integrating smart loads such as IMC buses or EV chargers so as not to violate the traction substation power rating, maximum line current, or minimum line voltage limitations. For example, the trolleybuses in Arnhem curtail their power when they measure a voltage under 500V and completely shut off at 400V [3].
Consequently, tapping into the unused capacity of these grids requires intelligent power management schemes and ample information on the traction grid state. What renders these systems even more complex is that their power demand constantly varies in time and location. Therefore, gathering the necessary grid state information requires a large array of sensors wirelessly communicating between themselves, the traction substation, and a local data processor for each grid supply zone. This increases the cost and complexity of the system [266].
Conveniently, some information is already available at each power node (bus, EV chargers, etc.) because of the smart protection systems (e.g., measurements of overhead connection point voltage, current, and node power) and of vehicle live position sensing (GPS tracking for user apps, for example).
This chapter aims to use only the already-available local data at a node to estimate the state of the traction substation and the number of non-zero power nodes on the same grid section. This state estimation can be then used to better manage and integrate IMC fleets, smart loads, and renewables into traction networks and render them more sustainable, better utilized, and multi-functional.

Table 11.10: Summary of the Boolean variables used in the Valley-Charging Method and their logic.

Boolean Variable	Action	Purpose	Value	
			1	0
B_{TRF}	Flag if the vehicle is present on a high traffic section (from pre-defined GPS look-up table)	Reduce Charging	High Traffic	Low Traffic
B_{SOC}	Flag if the battery SOC exiting the charging corridor would not be sufficient (from a charging estimate over the remaining charging corridor length)	Ensure minimum SOC is attained	Not Enough	Enough
B_{EOL}	Flag if the vehicle is close to exiting the section (from GPS position and section length data)	Not to carry a section's estimations into the next	Yes	No
B_{D}	Flag if the vehicle is in the direction exiting the charging corridor (from GPS position)	Prioritize charging for vehicles on the way out of the corridor	Exiting	Not Exiting
B_{σ}	Flag if there are multiple vehicles on the section (From the V-sigma condition)	Ensure sharing of the estimated local spare capacity	Multiple Vehicles	Possibly Alone

The flowchart of the Valley-Charging method is presented in Figure 11.9, and a summary of the Boolean "B" variables is offered in Table 11.10.
The first computational step of the valley charging method is to estimate P_{av}, the available spare power for IMC charging on a section (Section 11.7.1). Obviously, this available power cannot always be demanded in full by the IMC vehicle for fear that it could cause a grid voltage violation if, for example, the IMC vehicle is too far from the substation feed-in point.
For this, there is an upper cap setting depending on the vehicle's position and if the IMC vehicle is believed to be alone (single: $P_{\text{cap, s}}$) or not (multiple: $P_{\text{cap, m}}$) on the section. This cap is explained in Section 11.7.2 and flagged by the Boolean B_{σ} (Section III-F).
Additionally, enforcing some charging limitations and vehicle prioritization is necessary. For example, sections labeled as high-traffic should be treated as no-charging zones (B_{TRF}, section III-D) unless the battery SOC forecast is flagged as insufficient by the time the vehicle is expected to leave the charging corridor (B_{SOC}, section III-E). The IMC vehicle moves to a designed safe charging level in the latter case. Also, to ensure reliable operation, charging priority is given to vehicles in the direction out of the charging corridor over the vehicles just entering the charging zone (B_{D}, section III-G).
Finally, IMC vehicles near the End-Of-Line of a section flag the B_{EOL} Boolean and switch to charging at the safe-charging level. This is to make sure that an IMC vehicle does not enter a new section while demanding a high charging power that it was allowed by the section it was previously under (section III-C). The variable L_{sct} in this chapter refers to the section length and is used to flag this boolean.

11.7.1. AVAILABLE SPARE CHARGING POWER: P_{AV}

When a node is alone on a section, its measured node voltage, V_{M}, can be used to estimate the substation spare capacity, P_{spare}, as derived in Chapter 4.

11.7.2. CAPPED CHARGING POWER: $P_{\text{CAP,S}}$ & $P_{\text{CAP,M}}$

Unfortunately, the IMC bus cannot always demand the violations-free available charging power as it might thereby cause a grid violation. For example, if an IMC bus is near the end of a section with another bus, despite having a certain available power, drawing it might be acceptable from a power point of view but could cause a voltage violation.
For this, there should be a cap on the maximum allowable charging power that a vehicle

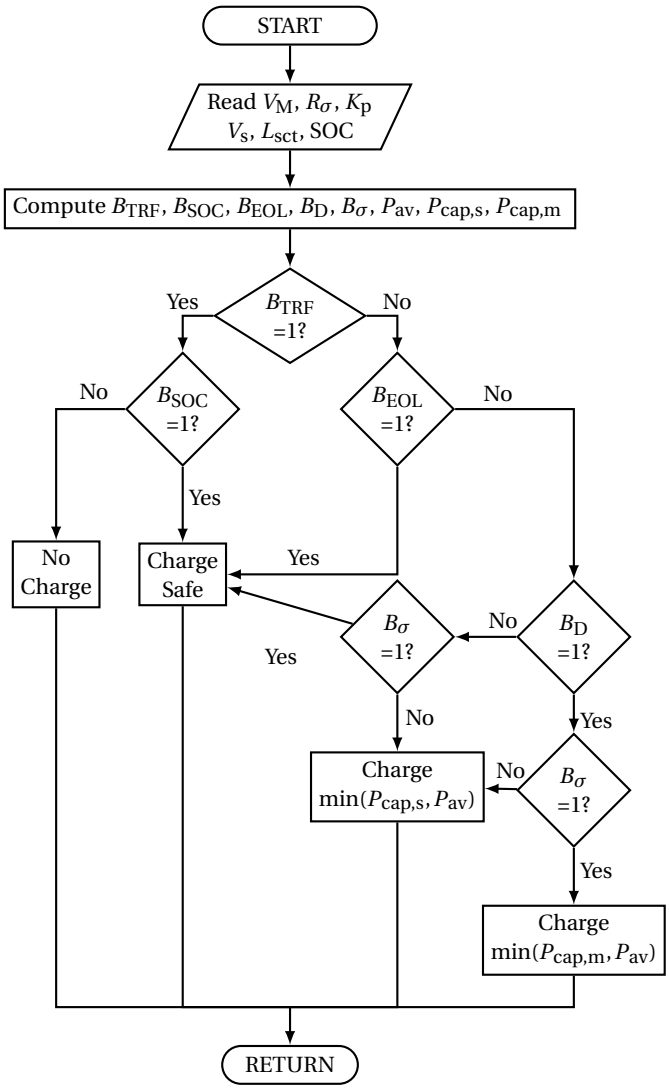

Figure 11.9: The Valley-Charging method flowchart developed in this thesis.

can draw whether it is alone ($P_{\text{cap,s}}$) or not ($P_{\text{cap,m}}$) on a section.
The value of $P_{\text{cap,s}}$ can be easily obtained from Kirchhoff's laws by studying the minimum IMC bus power value that would violate any of the three grid limitations of current, voltage, and power. Such calculation methods are readily available in the literature on traction grid modeling [3], [62].
In a similar fashion, the value of $P_{\text{cap,m}}$ can be obtained by a design choice for the specific IMC project based on the number of expected vehicles on the line. For example, for a low-traffic zone, the procedure of $P_{\text{cap,s}}$ can be repeated with one extra bus at the end of the line drawing a certain amount of power. In short, this value is left to be computed as conservatively as the IMC bus operator decides.

11.7.3. REDUCED CHARGING AT SECTION END-OF-LINE: B_{EOL}

Another concern to be addressed is that the IMC bus can enter a congested grid section with the generous charging set-point from a previous section, depending on the charging power setpoint update time. To avoid this, the IMC bus charging power should be reduced at a designed safe distance from any section's end-of-line. In this chapter, this is controlled by the Boolean B_{EOL}.

11.7.4. REDUCED CHARGING AT HIGH-TRAFFIC AREAS: B_{TRF}

High-Traffic areas that face power congestion problems are expected to have low and capped spare capacity. This is why it is advisable to overrule the Valley-charging setpoint at such sections. The IMC bus can easily flag its presence in a historically congested area by comparing its location (GPS) to a pre-defined look-up table. In this chapter, this is controlled by the Boolean B_{TRF}.

11.7.5. CONCERN ABOUT THE EXPECTED BATTERY SOC GAIN: B_{SOC}

The valley-charging method has a number of conflicting constraints, and its output is dictated by the instantaneous grid state. Therefore, the battery SOC gain under the charging corridor might not be sufficient to complete the battery-mode route on certain trips. The IMC bus should then override the estimator and switch to a low, safe charging value once such a status is predicted (from a product of the expected time left under the corridor and the expected average charging power). In this chapter, this is flagged by the Boolean B_{SOC}.

11.7.6. THE V-SIGMA CONDITION: B_{σ}

When a power node (such as the IMC bus) is alone on a grid section, its voltage, V_{σ}, can be written analytically as derived in Chapter 4 in Eq. 4.2. As a reminder, a key grid state can be derived from the calculation of V_{σ}. Per definition, The V-sigma voltage is the voltage expected when a node is *alone* on a section. It follows logically, then, that if a measured nodal voltage, V_{M}, were to be outside of this range, the studied node is not alone on the section, and there exists *at least* one other node. In this chapter, this is flagged by the Boolean B_{σ}.
However, because of the welcomed sharing of braking energy between nodes, it is advised to avoid assuming that a measured nodal voltage V_{M} equal to V_{σ} implies that the node is alone on the section. This mathematical coincidence can arise from the fact that

Table 11.11: Technical specifications of Line 352 (*-Planned Expansion at Arnhem Centraal).

Substation Number Label	Supplied Line352 Sections	SS nominal voltage [V]	SS rated power [kW]
SS 21	37 & 38	685	2600*
SS 12	23 & 24	686	800
SS 1	2 & 3	698	800

Figure 11.10: Illustration of the catenary grid layout for the charging corridor of Bus Line 352.

some nodes are supplying regenerative power, thereby masking some of the expected voltage drop effects of other nodes. Also, a vehicle/node could be momentarily not drawing power or close enough to the section feed-in point that it is not causing an observable voltage drop. This is again a motivation not to interpret $V_{\mathrm{M}} \approx V_{\sigma}$ as a sign that a node is alone on the section -that is to say:

$$\begin{cases} B_{\sigma} = 0 & \text{(Single node)} \quad , \text{if } V_{\mathrm{M}} \approx V_{\sigma} \\ B_{\sigma} = 1 & \text{(No information)} \quad , \text{if otherwise} \end{cases} \tag{11.22}$$

11.7.7. IMC BUS CHARGING PRIORITY: B_{D}

When multiple vehicles are detected on the line, it is useful to prioritize the vehicles that are on their way out of the charging corridor and heading toward battery-mode operation. The IMC bus GPS location can define this. This chapter labels this direction-priority by the Boolean B_{D}.

11.8. VALLEY-CHARGING CASE STUDY: REVISITING THE ARNHEM-WAGENINGEN LINE 352

As a reminder, Line 352 in Arnhem runs from the Arnhem Central Station (Arnhem Centraal) to the city of Wageningen. At the time of this research, the bus is powered by CNG. The bus route overlaps for over 4 kilometers with the existing trolleygrid from Arnhem Centraal to the bus stop at Oosterbeek and then continues for another 12.1 km to Wageningen. Under the catenary, a bus on route 352 crosses the supply zones of substations 1, 12, and 21, and their sections as summarized in Table 11.11 and illustrated in Figure 11.10. These sections are shared with the conventional trolleybus line 1 (not IMC).
This case study aims to electrify bus line 352 as a Valley-Charging IMC bus, using the Arnhem Centraal-Oosterbeek catenary as a charging corridor for the Oosterbeek-Wageningen battery mode. The major bottleneck for this project is that this bus route overlaps with trolley line 1, sometimes leaving little-to-no spare capacity on the grid, as seen with the

Adaptive Charging case.

11.8.1. VALLEY-CHARGING METHOD DESIGN FOR LINE 352

Section 11.7 of this chapter introduced the Valley Charging logic and its parameters. A number of these parameters were left as a design choice based on the IMC project. Here, the design choices for line 352 are presented.
First, the estimator is updated every 3 seconds. This is a choice to ensure the estimator does not update too fast (grid stability and battery health issues) or too slow (missing out on dynamic changes like an 8-10 seconds acceleration). For this, and considering the average trolleybus speed of 16m/s [22], a rounded-up value of 50m from the EOL is chosen for B_{EOL}. Third, the Boolean B_{TRF} is flagged as high traffic (value 1) only under Substation 21, which serves Arnhem Centraal. The safe charging power is set as 50kW - a value as low as the bus's heating/ventilation system demand. For the $P_{\text{cap,m}}$ calculations, it is assumed that there are two buses at the EOL: One trolleybus drawing the average power of 70kW [3], and one IMC drawing the average power of 70kW and the EOL-safe-charging value of 50kW - netting a total of 190kW demand at the EOL.

11.8.2. CASE STUDY PERFORMANCE CRITERIA

The study follows the battery SOC of the 9 buses dedicated to Line 352, namely vehicles number 40 to 48 of the Arnhem fleet. It is worth noting that buses 44, 45, and 47 only operate in the morning and evening, while the other buses go back and forth between Arnhem and Wageningen. The batteries are LTOs of 130kWh capacity and are cycled between 20% and 90%.
The operation is subject to three limitations in power, voltage, and current as summarized in Table 11.6

11.9. RESULTS OF IMC BUS ELECTRIFICATION WITH VALLEY-CHARGING OF LINE 352

11.9.1. VALLEY-CHARGING VERSUS ADAPTIVE CHARGING

Earlier in this chapter, the Adaptive Charging method was proposed for Line 352 but was insufficient in terms of picking up the needed energy for the battery-mode operation.
Indeed, Figure 11.11 shows a comparison of the IMC electrification project of Line 352 under the Valley Charging method proposed in this chapter (Figure 11.11(a)) and the Adaptive charging method deemed more sophisticated than the conventional charging approach (Figure 11.11(b)).
The Adaptive charging method is not sufficient for the IMC bus to pick enough energy for its trip in any of the studied cases. Meanwhile, the Valley-Charging approach is capable of securing the successful operation of all 9 buses of the newly electrified fleet even without breaching the SOC limits.

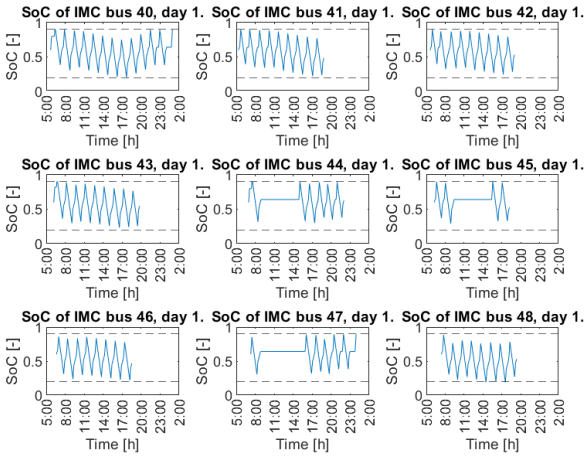

((a)) Valley-Charging.

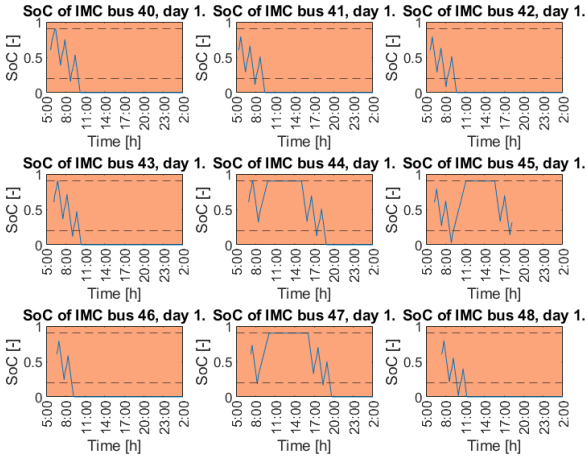

((b)) Adaptive Charging.

Figure 11.11: Comparison of SOC of IMC trolleybuses on Day 1 with the Valley-Charging and Adaptive Charging approaches. Buses 44, 45, and 47 only operate in the morning and evening.

Table 11.12: Power, voltage, and current violations per each of the six representative days of this case study.

Parameter	Day 1	Day 117	Day 197	Day 200	Day 268	Day 305
Power	460	443	370	367	386	454
Voltage	0	3	4	0	0	0
Current	1060	448	471	501	732	927

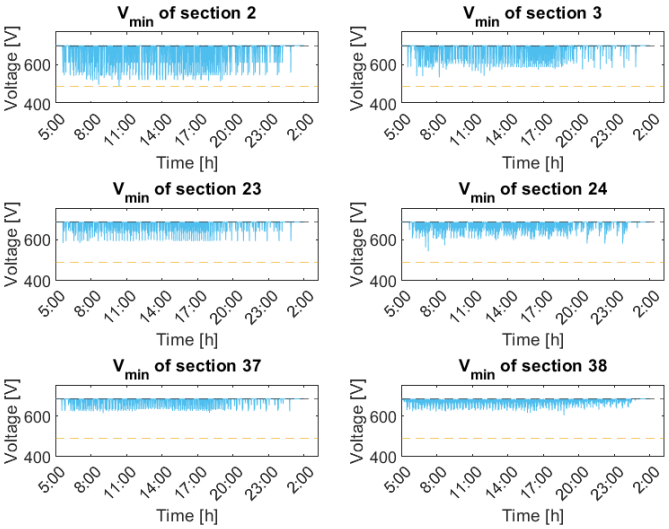

Figure 11.12: Minimum line voltage for each section of Line 352 on Day 1. Horizontal dashed black lines represent the nominal voltage of each substation. Yellow, horizontal dashed lines represent the voltage threshold limit.

11.9.2. ASSESSING THE GRID VIOLATIONS WITH VALLEY-CHARGING

The grid impact of the IMC bus is assessed in terms of the previously defined voltage, current, and power violations. The violations for the six studied representative days are presented in Table 11.12, and the results for Day 1 are explored in more detail below as an example. First, the minimum line voltage at each second, V_{min}, is visualized in Figure 11.12. The figure shows of the six sections of the IMC bus 352 route for one of the six representative days, namely Day 1. For all sections except section 2, the minimum line voltage sits comfortably above the violation threshold.

Unfortunately, while section 2 does not reach the threshold on this day, it does so on a few occasions on other days, as reported in Table 11.12. The reason is that section 2 is a long section, halfway on the Arnhem-Oosterbeek charging corridor, and can see many vehicles in both traffic directions. This can cause an unexpected voltage drop that even the estimator cannot predict with its multiple-vehicle power cap. This justification will be revisited and validated in Section 11.10 of this chapter, with possible solutions.

Figure 11.13 shows the maximum line current on each of the six sections for Day 1. In this case, even a visual estimate from the figure shows how the average value sits com-

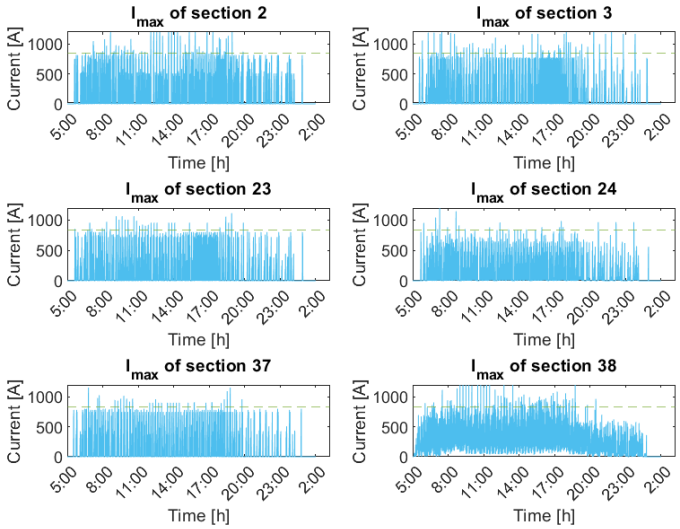

Figure 11.13: Maximum line current for each section of Line 352 on Day 1. Green, horizontal dashed lines represent the current threshold limit.

fortably below the threshold. While individual peaks occur above the limit, they do not last long enough to be considered a violation.

Finally, the power violations at the three substations can be seen in Figure 11.14 for Day 1. The power demand breaches the rated substation power at 460 instances. However, only one is over 150% of the substation's rated capacity (violation), and two are of a duration of 10 seconds (borderline). This means that the operation of the IMC buses in Valley-Charging mode can be deemed acceptable for two reasons. First, it is worth mentioning again that the grid simulation used in this chapter looks at the worst-case scenario by not curtailing the trolleybus traction/HVAC power. In reality, then, some of these breaches would be avoided by the buses themselves. Second, one expected violation per day of operation is still tolerated compared to the techno-economic consequences of upgrading the substation capacity, especially since this limitation is a business-as-usual operation for the current trolleygrid.

11.10. COMPARISON OF VALLEY-CHARGING AND THE "BEST-CASE SCENARIO" OF USING COMMUNICATING SENSORS

The Valley-Charging method has proven to be superior to the other IMC battery charging methods in performance and in the feasibility of the electrification project. This section compares the Valley-Charging method to the so-called Best-Case scenario for a performance evaluation in more absolute terms. In the Best-Case scenario, each IMC bus has full information on all the grid states of power, voltage, current, and position of all vehicles and whether they are IMC buses or regular trolleybuses. In such a scenario,

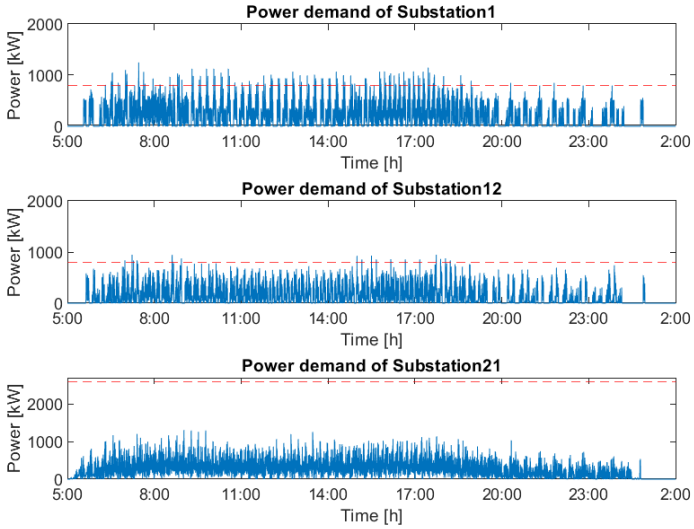

Figure 11.14: Maximum substation power demand for each substation of Line 352 on Day 1. Red, horizontal dashed lines represent the current threshold limit.

each IMC bus knows perfectly the battery-charging power it can demand so as not to violate any grid limit. Obviously, the inconvenience of this latter method is the need for a large array of sensors communicating wirelessly and computing and coordinating, in real-time, their power demands.

First, Table 11.13 summarizes the violations on the grid for each of the six representative days when the IMC buses are operating in the Best-Case scenario charging. While the violations are reduced significantly, a small number of them still occur. This is a consequence of the fact that the electrification of Line 352 alone, without battery-charging, causes violations on the line due to the increased traction demand (the Valley-Charging only controls the battery demand, not the traction and auxiliary). In that regard, Table 11.12 can be revisited, keeping in mind that these few violations are not the fault of the Valley-Charging estimator.

This is also an opportunity to revisit the claim made in Section 11.9 that the voltage violations on the trolleygrid section 2 are caused by the high traffic on section 2 and are indeed avoided by the all-knowing charger. One work-around for this value could be to stop the charging when the IMC vehicle voltage dips below a certain threshold. However, the voltage drops from such a scenario are too few to risk a change in operation. It is worth mentioning again that the grid simulation used in this chapter looks at the worst-case scenario by not curtailing the trolleybus traction/HVAC power. In reality, then, some of these breaches will be avoided.

In terms of the picked-up energy, a fortunate conclusion can be derived from Figure 11.15. This figure shows the energy collected by the IMC buses on each of the six representative days, both in Valley-Charging and Best-Case modes. The dashed, stacked

Table 11.13: Number of power, voltage and current limits violations per representative day. Best Case Scenario.

Parameter	Day 1	Day 117	Day 197	Day 200	Day 268	Day 305
Power	20	14	3	1	15	7
Voltage	0	0	0	0	0	0
Current	152	62	51	75	99	131

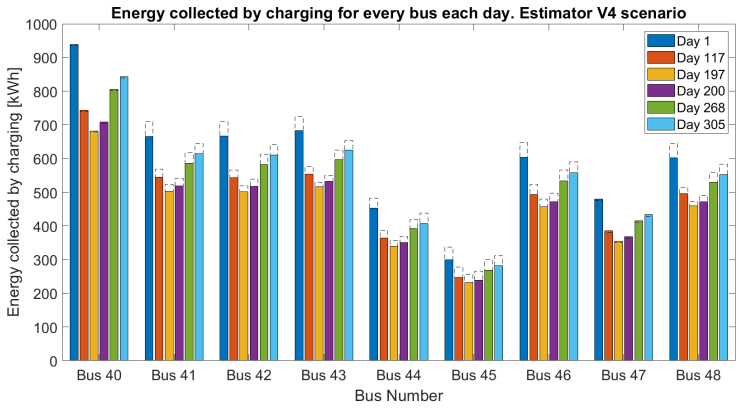

Figure 11.15: Energy collected by each bus of the Line 352 fleet on each representative day of the year using the estimator-based Valley-Charging of this chapter. Dashed transparent bars represent the full potential energy to be collected using communicating sensors rather than the here-proposed state estimator.

histogram portions represent the Best-Case mode.
Two important insights can be derived from this comparison. First, the Valley-Charging method performs almost identically to the Best-Case method yet without any of the costs, controls, or wireless communication required by the latter method. This validates the techno-economic superiority of the Valley-Charging method. Second, the additional picked-up energy is minimal enough (or even non-existent for buses 40 and 47. Therefore, no economically interesting reduction of the IMC battery size can be argued by more sophisticated charging schemes with real-time communicating sensors by claiming to pick-up more energy per charging cycle.

11.11. CONCLUSIONS

This chapter offered a method that improved the accuracy of the estimation of the charging corridor length of IMC buses from what was previously suggested in the literature. Errors as high as 16.7% were reported when compared to the more extensive calculation offered in this chapter. This could have drastic consequences on the reliable operation of the transportation grid, as the buses pick up a considerably lower energy amount than what is required for their battery-mode trips.
Additionally, an Adaptive Charging method for the IMC battery was also introduced that can better utilize the spare trolleygrid capacity and test with the case study of the electrification of four lines in Arnhem. One of the four lines was achievable without any need for additional grid extensions. For the other three lines, an opportunity charging point

was needed, and the Adaptive Charging method proved indeed to be superior to Regular Charging, with terminal-charging times reduced by up to 64%, or up to 40 minutes.
One of the four studied lines (bus line 352) was completely unachievable with Regular Charging, and unfortunately, the Adaptive Charging method was not enough either and could only pick up 3% of the required energy for the battery-mode trip. This is because the route of this bus had mostly congested substations that did not allow any IMC battery charging but did allow for the electrification of the buses in any case. Still, the IMC No-charging electrification can mean that the bus can be decarbonized and with a reduced battery size since it runs as a trolleybus under the charging corridor and not in battery-mode.
Line 352 was then revisited with the suggestion of another original battery-charging method: The Valley-Charging method. The method used available bus measurements and a developed grid state estimator to predict the available charging power for the IMC bus at every instant that would not break the power, voltage, or current limitations of the trolleygrid. Consequently, this allows the electrification of bus lines whose routes overlap with sections of a trolleygrid infrastructure, even in historically congested trolleygrid areas.
The method successfully harvested the full required trip energy from under the catenary on all six representative bus schedule days studied.
When compared to the all-knowing, Best-Case scenario (communicating sensors), the Valley-Charging method was shown to have almost achieved a similar energy harvesting potential. However, the Valley-Charging method obviously comes at a much lower cost as it does not require additional sensors and communication between them.
Overall, the Adaptive and Valley charging methods offered significant reductions in battery mass, cost, and volume when compared to a project of electrification by full Battery Electric Buses.
Future works are urged to verify the Valley-Charging method in other electrification projects. Additionally, since some power peak violations came from the addition of the bus fleet without even charging, it would be interesting to expand the Valley-Charging method with an even more conservative action than "No Charge" by switching to battery-mode operation for the traction/auxiliaries. This way, the IMC bus relieves the grid of all its power demand in moments of extreme congestion.
Finally, in terms of the vision of the sustainable, multi-functional trolleygrid of the future, it is important to study IMC buses in conjunction with renewable systems and smart loads (such as EV chargers) to understand the constructive and destructive effects they could have on the operation of the trolleygrid.

12

SYNERGY AND DYSERGY IN THE SUSTAINABLE, MULTI-FUNCTIONAL, AND MULTI-STAKEHOLDER TROLLEYGRIDS OF THE FUTURE

"Tutto questo avverrà,
te lo prometto!
Tienti la tua paura..
io, con sicura fede, l'aspetto!"

Un Bel Dì Vedremo - Act II, Madama Butterfly (Puccini)

All this will happen,
I promise you!
Hold back your fears..
I, with sure faith, await him!

This chapter is based on: Designing and Assessing the Sustainable, Multi-Functional, and Multi-Stakeholder Trolleygrids of the Future. I Diab, GR Chandra-Mouli, P Bauer *(Submitted)*

This chapter re-examines the oversized and underutilized high-power infrastructures of transport grids as a support to the increasingly congested urban grids. This is done by the integration of renewables, EV chargers, and storage systems in tandem with new, high-power fleets such as the In-Motion-Charging (IMC) trolleybuses.
In simulations of one year of operation, EV chargers are the best trolleygrid addition in terms of losses, voltage performance, and PV system performance. Also, their recuperation of over 30% of the available braking energy saves on expensive storage systems. Indeed, the conclusive advice is to install storage systems only to reduce the substation transformer overloading (by up to 34%, seemingly). The integration of IMC buses is still feasible even with EV chargers, and this combination provides enough of a base and peak load profile for better PV system performance. Otherwise, the base load can be provided by a multi-stakeholder solar system shared with neighboring households. Additionally, this shared rooftop solar provides transport grids with the otherwise-scarce physical installation space in urban environments.
The chapter starts with a short introduction and motivation in Section 12.1. Section 12.2 looks into the modeling methodology and defines the suggested indicators and case studies for this chapter and storage power management schemes. Then, Sections 12.3, 12.4, 12.5, 12.6, and 12.7 present the results of the yearly substation energy demand and losses, line voltage drops, transformer power overloading, PV utilization, and investment gains from the multi-shareholder system, respectively.
These results are then extended in Section 12.8 into generalized recommendations for trolleygrids. Finally, Section 12.9 concludes the chapter.

12.1. INTRODUCTION

Transport grids are oversized and underutilized high-power infrastructures which makes them ideal for the integration of renewables, EV chargers, and storage systems to support the increasingly congested urban grids. However, this must not interfere with the introduction of new, high-power fleets such as the In-Motion-Charging (IMC) trolleybuses. The trolleybus is a type of electric traction network where the bus is supplied by overhead lines (catenary), similar to the way a tram operates.

12.1.1. THE TROLLEYGRIDS OF THE FUTURE

Many works are already rethinking transport networks such as trolley grids as multi-functional, active grids by integrating into them renewable energy sources (RES) like solar PV [11], [44]–[47], [73]–[76], [79], [82], EV chargers [16], [23], [67], [165], [222], and other smart grid loads and fleets [12], [15], [22], [36], [183].
However, no comprehensive work exists yet that looks at the destructive and constructive effects of integrating many of these systems simultaneously. For example, EV chargers can pick up the available braking energy, rendering an installed storage system partially redundant. On the other hand, in the presence of IMC buses, the large on-board battery is already recuperating all of the braking energy.
Another example is that a shared PV system between residential and traction load cre-

ates a better matching load profile to the PV generation as it combines the base load of the former with the peak loads of the latter. However, a valid concern is that the integration of EV chargers in the trolleygrid can offset the benefit of the residential base load by offering an EV-charging base load.
For this, a detailed study is needed to quantify the effects of the simultaneous integration of EV chargers, storage, new fleets, and residential loads into the PV-augmented trolleygrid.

12.1.2. CHAPTER CONTRIBUTIONS

The chapter has the following contributions:

1. The quantification of the constructive and destructive effects of the different design options of the sustainable and multi-functional trolleygrid, under a full year of simulations, using detailed and verified trolleybus, trolleygrid, storage, and PV models

2. The quantification of the techno-economic performance of a multi-stakeholder PV system between the residential loads and the different design options of the sustainable and multi-functional trolleygrid, under a full year of simulations, using detailed and verified trolleybus, trolleygrid, storage, and PV models

12.2. MODELING METHODOLOGY

12.2.1. MODELING OF OESS AND SESS

Lithium-titanate-oxide (LTO) batteries are gaining attention in traction grids as they provide much higher charging and discharging currents compared to the other types of batteries with excellent strain endurance, suitable for vehicle accelerations and braking [14], [95], [99], [153], [175], [219]. They are interesting as both on-board and stationary applications because of their comparatively high power density, cycle life, discharge at low temperature, and safety (for the former) and low self-discharge and high efficiency (for the latter).

For this chapter, the choice is LTO Batteries. A commercially available example is Altair® Nanotechnologies 24V 70AH battery modules with up to 5C as a charge/discharge rate [100]. Table 12.1 summarizes the characteristics as reported by the manufacturer [100], [136]–[138], [145].
These specifications allow detailed modeling of the storage systems that take into account their charging and discharging efficiencies, self-discharge, and maximum power exchange. To create a suitable pack from these modules, multiple modules are connected in strings and in parallel.

12.2.2. INDICATORS FOR ASSESSING THE SYSTEM PERFORMANCE

PV INDICATORS

To quantify the percentage of solar power that is directly used by the loads on a trolleygrid, the **Direct PV Utilization** factor is used as defined in Eq.5.12 of Chapter 5.
Similarly, the **Direct Load Coverage**, Λ, is used as defined in Eq.5.13 of Chapter 5, as the

Table 12.1: Module characteristics for the LTO battery [100] used in this chapter.

Variable	Value
Capacity (Wh)	1500
Module voltage (V_{DC})	24
Module resistance, charging (mΩ)	4.5
Module resistance, discharging (mΩ)	4.3
Self-discharge (% per day)	0.1

fraction of the load that the output of the PV system can directly supply.
A valid concern in the multi-shareholder system is the question of whether the benefit obtained in the reduction of excess generation is not simply the result of the effective smaller share size of the traction network of this installed PV system.
In other terms, the question is:

If the traction network has a share X of a PV system of size ζ, would it not be better off installing a smaller, private system of size $\zeta_{private}$ equal to $X \cdot \zeta$?

Therefore, to quantify the net **Gain in Return on Energetic Investment**, the parameter Δ_{ROEI} is defined as the comparison between the traction load coverage offered by the shared PV system compared to that which would be offered by a smaller PV system of a size equal to the share of the traction substation from the shared system.
This can be mathematically described as:

$$\Delta_{ROEI} \triangleq \frac{\Lambda\Big|_{\zeta} - \Lambda\Big|_{\zeta_{private}}}{\Lambda\Big|_{\zeta_{private}}} \tag{12.1}$$

VOLTAGE INDICATOR
To judge the effect of the multi-functional system on the voltage drops, the minimum voltage value per year and the average voltage values among the scenarios do not show enough nuances. This is because the catenary line would most frequently see the nominal substation voltage because of the absence of a traction load explained in Section 12.1.
For this, the yearly **Change in Cumulative Voltage Drops**, Δ_{VY}, is used, as defined in Eq.7.2 of Chapter 7. This parameter presents the yearly relative reduction in the cumulative (integral) voltage drops on the section.

12.2.3. CASE STUDY DEFINITION: SUBSTATIONS AND SCENARIO SIZING

There is a difference in the power and voltage profiles of the traction substation depending on the length of the catenary that it supplies and on the average traffic that it observes [11], [79].
For this purpose, this chapter needs to examine at least two traction substation types, which is done by choosing the trolleygrid of Arnhem, The Netherlands, as a case study
For this chapter, the choice is for:

- **Section 25 under Substation 9 (SS9)**: A relatively short (less than 1000m) catenary zone with up to 5 buses at a time in traffic density.
- **Section 23 under Substation 12 (SS12)**: A relatively long (more than 2000m) catenary zone at most 3 buses at a time in traffic density.

The chosen battery size is 6 of the LTO modules described for a total of 9kWh. The battery system is placed halfway through each section.
Also halfway through the section is the EV charger, which has a randomized profile based on publicly available measured EV transactions offered by Elaad NL [240]. The charger has 4 modules of 30kW, as is commercially available for an EV charger connected to a trolleygrid [267]. This means that the EV charging profile varies from 0 to 120kW in steps of 30kW.
Furthermore, the IMC buses charge their battery by 150kW while moving and 50kW while standing, which is an already researched suggestion for the Arnhem grid [22], [183].
Finally, 12 households have been chosen as private stakeholders for the shared PV system. The electric loads of these households have been modeled as explained in Chapter 10.

12.2.4. POWER MANAGEMENT SCHEMES FOR THE STORAGE SYSTEMS

POWER MANAGEMENT SCHEME FOR OESS

The power management scheme for on-board storage can be straightforward and rule-based as is typical in the literature [148], [227]–[231]. This is first because the placement of this storage on board the vehicle itself allows it to recuperate the braking energy in a more effective way compared to stationary storage, and that makes it a priority objective. Second, the relatively small size of typical on-board storage makes it impractical for them to focus on recuperating the PV excess generation as it would compete with the braking energy over the available battery capacity, which is not practical from an energy transmission efficiency point of view.
For this, the power management scheme of the on-board storage studied in this chapter is the typical scheme found commonly in the literature that recuperates the braking energy of the vehicles and delivers it in moments of high load. Here in this chapter, the storage delivers the power when the vehicle has a demand of over 100kW.

POWER MANAGEMENT SCHEME FOR SESS

The power management scheme of the SESS is based on the State Estimator of Chapter 4, which was developed previously into an SESS-specific charging scheme in Chapter 7 and detailed further in Chapter 8.

12.3. RESULTS: YEARLY SUBSTATION ENERGY DEMAND AND LOSSES

Figure 12.1 shows the yearly substation energy demand and losses for the two studied substations in Arnhem. Four main observations can be reported.

First, the percentage of power losses when an EV charger is connected on the section is lower than the baseline in both high-traffic and low-traffic scenarios. On the one hand, this is a consequence of the more efficient braking energy harvesting caused by the presence of a power-demanding load on the section. On the other hand, as power losses increase exponentially with higher loads [3], the presence of a relatively low EV demand as the only load in the frequent cases of zero traffic causes the overall average to be lower than that of the baseline.
The second observation validates the theory mentioned above on the non-linearity of power losses at higher loads. In the low-traffic substation of Figure 12.1(a), the percentage of power losses in the EV+IMC+S case is similar to the baseline. Meanwhile, in the high-traffic case of Figure 12.1(b), the IMC and EV+IMC+S see loss percentages almost double those of the baseline. This shows that the shorter catenary length of the higher-traffic section is not sufficient as a measure for the efficient supply of the multi-functional trolleygrids, and more active approaches, such as substation no-load voltage tuning, should be investigated.
The third observation is how the storage scenarios sit vertically below their non-storage counterparts. This means that while the transmission losses in absolute terms are lower when storage is implemented, the substation energy demand remains virtually the same. This is a consequence of the charging/discharging losses of the storage system and the self-discharge, although the latter is only at 0.1% daily for the studied LTO technology. This is a crucial finding that warns of the uselessness of an (expensive) storage system in the multi-functional trolleygrid, as the braking energy is predominately picked-up by the IMC bus and/or the EV charger. Future investigations should then look at the role of larger storage devices and at the placement of storage devices for power peak-shaving at the substation DC-busbar, minimizing losses while charging the battery compared to the DC scenario.
Finally, it is clear from the scale of the total energy demand that the multi-functional trolleygrid has the capability of supplying many times the present-day loads that it caters to. This reserved and unused capacity must be explored for achieving the sustainable goals of electric transport, whether in enabling EV chargers or bus electrification as IMC buses.

12.4. RESULTS: YEARLY LINE VOLTAGE DROPS

Figure 12.2 shows the yearly minimum line voltage and the change in cumulative voltage drops for the two studied substations.
The first observation is that the line voltage sits considerably lower in the multi-functional grid, as is shown by the increase of up to 600% in the cumulative voltage drops (y-axis). This has two consequences. The first of which is that the transmission losses would be higher, but that has already been addressed in the previous section. The second concern is that the line voltage would typically be seen further from the nominal voltage and less robust in the face of traffic delays that threaten to aggravate the voltage drops. However, both the IMC buses with their battery and the EV chargers are capable of momentarily curtailing their loads and ensuring acceptable operation.
The previous justification is also validated by the yearly absolute minimum line voltage

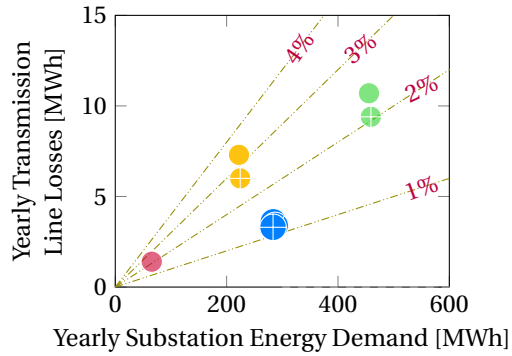

((a)) Section 23 in Arnhem.

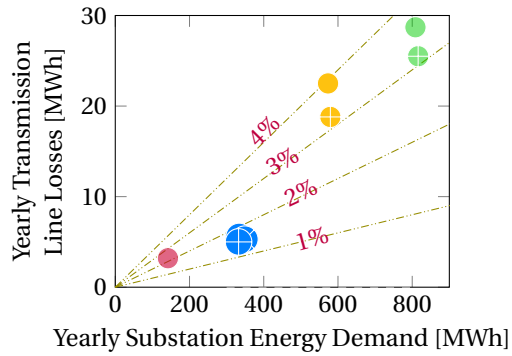

((b)) Section 25 in Arnhem.

Figure 12.1: Simulation results of the yearly substation energy demand and line transmission losses for all the studied scenarios.

that remains well above the cut-off voltage in all scenarios at both the high and low-traffic substations. In the high-traffic case of Figure 12.2(b), all IMC scenarios dip below the power curtailment line. However, the storage scenarios perform better in bringing the minimum voltage to regular operation levels. Consequently, larger storage systems could be investigated at high-traffic substations implementing IMC buses for the sake of maintaining an acceptable line voltage. Furthermore, more sophisticated IMC technologies are being researched [183] that can momentarily adjust the battery power in congested instances and compensate with momentary higher charging powers in other instances. Nonetheless, a more straightforward solution can be the investigation of a new, higher set-point for the substation no-load voltage that can better maintain a higher line voltage performance.

Furthermore, it is interesting to note that the cumulative voltage drops in the EV case

Table 12.2: Traction Substation Power Overloading from a rated 800kW for the studied scenarios at section 23.

Scenario	Yearly Peak Power [kW]	Peak Power Overload [%]	Yearly Total Overload Time [s]	Average Overload Session Time [s]	Average Overload Session Power [kW]	Average Overload Session Time Daily [s/day]
Baseline	623.7	0%	0	0.0	0.0	0.0
EV	674.7	0%	0	0.0	0.0	0.0
EV+S	674.7	0%	0	0.0	0.0	0.0
EV+O	628.3	0%	0	0.0	0.0	0.0
IMC	867.2	8%	3824	3.0	849.3	10.5
IMC+S	818.3	2%	3824	2.0	812.0	10.5
EV+IMC	1008.7	26%	3990	3.1	871.1	10.9
EV+IMC+S	1008.7	26%	3857	2.5	831.7	10.6

at the low-traffic substation are more severe than in the IMC scenario and much higher than the baseline, while the contrary is observed in the high-traffic scenario. This serves as an indicator that the presence of an EV charger is indeed less-intrusive than the existing traffic in high-traffic zones and does not pose a threat to the trolleygrid operation. In fact, the presence of storage in the EV case helps in keeping the cumulative voltage drops lower, albeit causing a lower absolute voltage as a possible consequence of the battery charging at an inopportune moment.
Finally, the IMC+EV scenario records lower cumulative voltage drops than the IMC and the EV scenarios put together. This signals again that the trolleygrid is underutilized, as otherwise, the IMC buses and EV chargers would have continuously overlapped and caused the expected non-linear, exponential increase in the voltage drops. This, again, is an example of the synergy that can be obtained in the multi-functional trolleygrid of the future.

12.5. RESULTS: YEARLY SUBSTATION POWER OVERLOADING

Tables 12.2 and 12.3 summarize the results of the substation overloading simulations for all the scenarios at sections 23 and 25, respectively.
At both locations, the EV placement does not cause any overloading on the substation throughout the year. Additionally, both locations also see a reduction in the average overloading session duration and magnitude when storage is applied, although the reduction is more pronounced at low-traffic substations. Furthermore, the cumulative yearly overload time is less an 70 minutes in all cases per year, signaling that overloading is indeed not a problem. This can be in part attributed to the short length of the sections that have already been designed to avoid power overloads and serves, in fact, as another promising suggestion for the design of the trolleygrid of the future.
Finally, it is interesting to note that storage in high-traffic scenarios can reduce the yearly overload time by as far as 34%. This supports the suggestion made earlier that storage systems should be investigated as voltage and capacity support for the traction substations in the multi-functional trolleygrid rather than the conventional focus on braking energy harvesting and reduction of transmission losses.

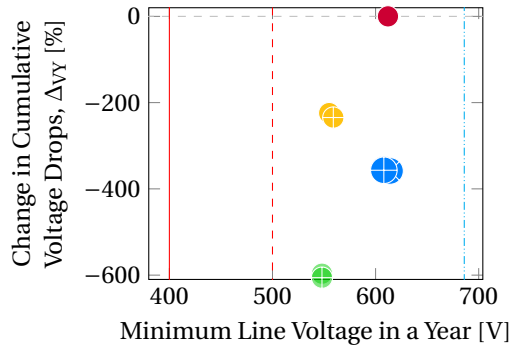

((a)) Section 23 in Arnhem.

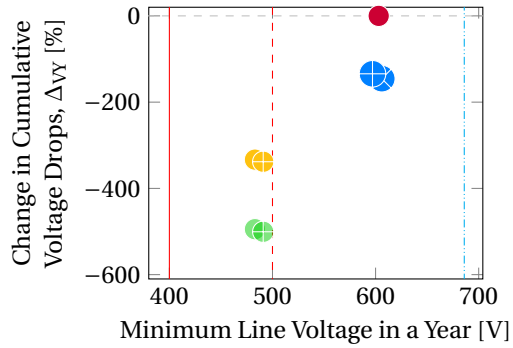

((b)) Section 25 in Arnhem.

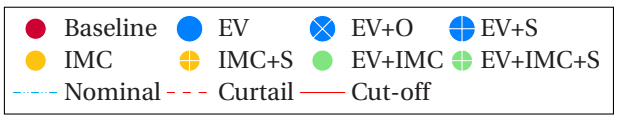

Figure 12.2: Simulation results of the yearly minimum line voltage and of the change in cumulative voltage drops as defined by Eq.7.2 for all the studied scenarios.

12.6. RESULTS: INCREASE IN THE PV UTILIZATION OF A MULTI-STAKEHOLDER PV SYSTEM

An increase in direct PV Utilization can be expected when the scenarios studied in this chapter are coupled with the neighboring households that can provide a base load for the PV operation. These results are presented in Figure 12.3 for sections 23 and 25 for the traction substation.

The PV Utilization in the multi-stakeholder case is divided into two components: The utilization obtained from the effective reduction in the PV system share dedicated to the traction network (blue), and an additional component resulting from the synergy in coupling traction and residential loads (orange).

Table 12.3: Traction Substation Power Overloading from a rated 800kW for the studied scenarios at section 25.

Scenario	Yearly Peak Power [kW]	Peak Power Overload [%]	Yearly Total Overload Time [s]	Average Overload Session Time [s]	Average Overload Session Power [kW]	Average Overload Session Time Daily [s/day]
Baseline	577.5	0%	0	0.0	0.0	0.0
EV	710.9	0%	0	0.0	0.0	0.0
EV+S	710.9	0%	0	0.0	0.0	0.0
EV+O	664.4	0%	0	0.0	0.0	0.0
IMC	959.0	20%	1682	2.7	847.9	4.6
IMC+S	904.9	13%	1171	2.3	840.0	3.2
EV+IMC	1045.7	31%	2290	2.7	850.5	6.3
EV+IMC+S	1045.7	31%	1522	2.4	848.2	4.2

The first observation is that the synergetic gain is the highest at each of the two locations in the baseline scenario. This is an expected outcome since the benefit of the multi-stakeholder system is that the households can provide the base load that is missing from traction networks. When the low or high-traffic substations are coupled with EV chargers, the need for a base load is met, and no sizeable benefit can be obtained from the coupling with residential loads.
However, in the low-traffic substation, a large synergetic benefit can still be obtained when IMC buses are implemented, as this is similar to the baseline where the traffic is sparse. Meanwhile, a negligible benefit is obtained in the IMC case at the high-traffic substation as the persistent traffic creates a sort of a base load similar to what residential loads would offer.
Two more observations can be attributed to the base load effect. The first of these is that the scenarios with stationary storage consistently outperform their storage-less counterparts in terms of PV Utilization, which is an expected outcome as the storage can save the excess PV energy actively, or passively while replenishing its SOC. The second of these observations is that the EV scenarios outperform other scenarios in terms of PV Utilization, given how they provide a relatively high and consistent base load.
Finally, in some cases at the high-traffic substation, the PV Utilization is reduced in the multi-stakeholder system. However, the reduction is negligible and stands at 0.55% in the worst case, which does not offset the major benefit of shared PV panel installation space offered by the multi-stakeholder system.

12.7. RESULTS: INVESTMENT GAINS IN A MULTI-STAKEHOLDER PV SYSTEM

Figure 12.4 shows the Load Coverage and the Gain in Return on Energetic Investment as defined by Eq.12.1 for all the scenarios when coupled with the residential loads.
The results here echo those of the PV Utilization. First, the baseline scenarios at both locations perform better in terms of the synergetic gain, as reflected in Δ_{ROEI} as high as 30.6%. This, as well as the null or slightly negative benefits of most scenarios except IMC in low-traffic substations, is a consequence of the same base load analysis explained in the previous section of this chapter.
Nonetheless, it is worth noting that the analysis here is limited to a fixed number of 12 dwellings, and hence further research is encouraged before a conclusive opinion can be made on the multi-stakeholder PV system in multi-functional trolleygrids. Furthermore,

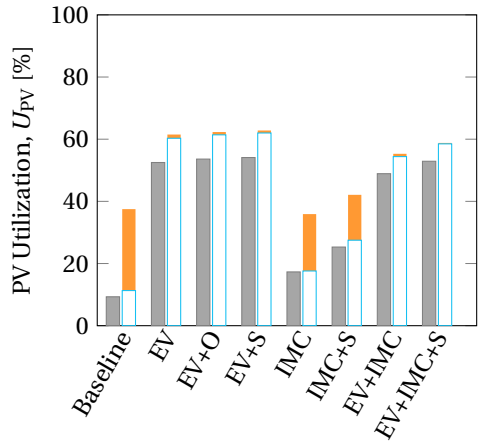

((a)) Section 23 in Arnhem.

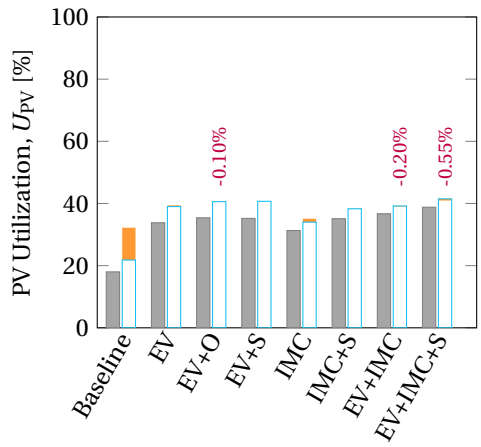

((b)) Section 25 in Arnhem.

Figure 12.3: Gain in the PV system utilization in the different multi-functional scenarios, without (gray) or with (colored stacked bars) a connection to the residential load of 12 dwellings.

a benefit similar to that observed with the baseline could possibly be harvested from a combination of neighboring substations that do not all have an EV charger, as suggested in previous works [79].

12.8. ANALYSIS AND GENERALIZATION OF THE RESULTS

Based on the results presented in this chapter, the present-dat trolleygrid is indeed confirmed as having the feasible capacity for becoming a sustainable, multi-functional, and multi-stakeholder grid.

Most certainly, the integration of EV chargers in transport grids is not only an opportunity but a necessity for the sustainability of transport grids and the feasibility of EV charging in congested urban environments. The synergy in the implementation is observed both in low and high-traffic zones, although more pronounced in the former. EV chargers are more efficient than storage devices in harvesting the braking energy of vehicles, as they directly serve it to an end-user rather than undergoing losses in reaching the battery, charging, storing, discharging, and reaching the load. Furthermore, they offer the critically required base load for the successful techno-economic feasibility of a PV system connection to the trolleygrid. Even in the absence of available braking energy, as in the case of IMC buses that harvest their own energy, EV chargers still show a synergetic performance with the trolleygrid, especially in the presence of a PV system.

Storage systems, whether on-board or stationary, have not shown a promising benefit that offsets their cost and size disadvantages. They become especially redundant in the presence of an EV charger as they begin to compete over the available braking energy. The one noticeable advantage of stationary storage is with the presence of IMC buses and PV systems at low-traffic substations, where the storage can assist in harvesting the excess PV energy.

Overall, storage systems have not proven to be particularly beneficial in the multi-functional grid in terms of voltage or transmission losses, which are catenary-side interventions. However, they have managed to reduce the duration and severity of the substation power overloading by up to 34%, which is a substation-side intervention. This motivates the recommendation to consider a substation-busbar placement of storage devices in the multi-functional grid as an effective capacity increase of the substation capacity.

In terms of PV integration, there is a clear net benefit in a multi-stakeholder system at low-traffic substations, especially when no base load is present, such as an EV charger. High-traffic substations, on the other hand, are less notable in their benefit. However, it is these substations that have a larger energy demand and, thereby, a higher need for PV panel installation space. This motivates the multi-stakeholder approach for its physical space benefit, even if it comes without the tempting additional economic benefit seen at low-traffic substations.

12.9. CONCLUSIONS

Transport grids such as the trolleygrid are oversized and underutilized, motivating research into integrating renewables, EV chargers, storage, and newer, more sophisticated

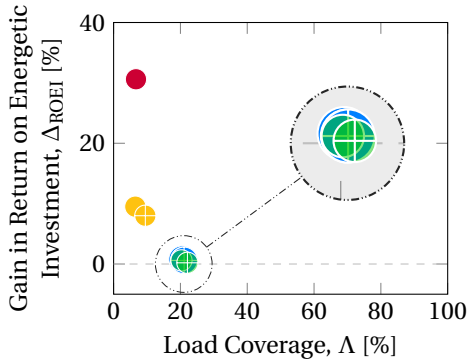

((a)) Section 23 in Arnhem.

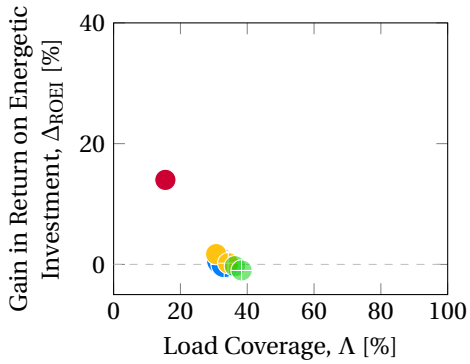

((b)) Section 25 in Arnhem.

Figure 12.4: Simulation results of the gain in the Return on Energetic Investment as defined by Eq.12.1 versus the yearly load coverage by the PV system, Λ, for each of the multi-functional grid scenarios connected to residential loads.

fleets into their infrastructures.

This chapter looked at the constructive and destructive effects of combining one or more of these possibilities into low and high-traffic trolleygrid sections.

while the power surges and voltage drops became more severe in the multi-functional trolleygrid, the breaches were not severe enough to disrupt the bus operation or render a scenario unfeasible.

EV chargers proved to be the most beneficial upgrade to current infrastructures. While simultaneously relieving the main AC grid of the charger load by tapping into the reserved capacity for the traction network, the EV charger showed synergy in the harvesting of braking energy and providing the critically needed base load for the successful techno-economic feasibility of the PV system. EV chargers can therefore replace storage systems on the catenary side of the trolleygrid while providing beneficial functionalities rather than a passive storage function.

Storage systems have indeed proven redundant in the presence of an EV charge. However, they still offered promising benefits in terms of reduction of the duration and severity of power overloading at the substation transformers, by up to 34%.

The multi-stakeholder PV system is most effective in low-traffic substations as it provides the necessary base load to reduce the need for storage, curtailment, and exchange with the AC grid. Nonetheless, this benefit is overshadowed by the presence of an EV charger. Still, there is a considerable benefit in the multi-stakeholder system in providing the needed physical installation space.

In conclusion, existing transport grid networks such as trolleygrid have the techno-economically feasible potential for the integration of more functionalities into their infrastructures, acting thereby as sustainable, multi-functional, and multi-stakeholder backbones to the congested urban electricity grids.

13

CONCLUSIONS AND FUTURE WORKS RECOMMENDATIONS

"L'avenir aura-t-il les charmes
De ces beaux jours déjà passés?
Adieu, notre petite table,
qui nous réunit si souvent.."

Adieu, Notre Petite Table- Act II, Manon (Massenet)

```
                    Will the future have the charm
Of these beautiful days that have already passed?
                         Farewell, our little table
                          that united us so often..
```

13.1. CONCLUSIONS

The goal of this thesis was to investigate how the existing trolleybus grid infrastructures could be re-designed as sustainable and multi-functional smart DC grids. This investigation was carried out in four parts, each addressing one of the four research gaps introduced as four research questions in Chapter 1.
This chapter gives the main conclusions for each research question and recommendations for future research.

What are the opportunities, challenges, and tools needed for designing and assessing the transformation of present-day trolleygrid infrastructures into sustainable, multi-functional grids?

Chapter 2 offered an extensive review of the changes happening in trolleygrids with the integration of renewables, smart grid loads, EV chargers, and new, sophisticated bus fleets with the capabilities of operating independently of the catenary. These complex multi-functional trolleygrids of the future face first the technical limitations of their own oversized and underutilized infrastructures, regularly shifting between instances of zero load (no bus) and high load demands and voltage dips (high traffic). The former creates the major techno-economic hurdle for renewables integration in these grids. Meanwhile, the latter discourages the integration of more electric loads into these grids or, at the very least, exposes the unreadiness of the present power management schemes to deal with the particularities of these sectionized, unidirectional grids and the spatial and temporal stochasticity of their loads.
Furthermore, some policy and economic hurdles prove to be problematic. First, contractual obligations do not allow traction grid operators to sell energy to third-party users. This legally constraints the integration, for example, of EV chargers in catenary grids. Second, the different decision-makers and investors in transport grids have different timelines, and that constrains both investment and tendering operations. Lastly, the lack of knowledge in storage system performance, particularly in degradation, and the infeasibility of grid-scale pilot projects deters investment possibilities. This should primarily be tackled by in-depth scientific research initiatives. The operation of multi-functional catenary grids should involve an array of partners from key operational stakeholders to the DSO/TSO and research/academic institutions to share both the operational expertise as well as the financial costs while being guided and connected via a coordinating body.
These complex future grids bring along new modeling requirements. The lump-sum approach, typical of heavy rail networks and concerned mainly with energy calculations, does not fit the study of trolleygrids when expected to house power electronic converters, smart loads, and renewable energy sources. More sophisticated models are needed to compute the line voltage and currents to conduct more sophisticated power management schemes and maintain minimum grid state requirements so as not to force the curtailment of traction loads. Such a model was presented in **Chapter 3**, and two of its main lessons are the importance of including the auxiliaries demand (mainly heating/cooling) in the grid modeling and the invalidity of modeling the bilateral substations as two unilateral substations.

This modeling methodology of Chapter 3 paved the way for a more global, mathematical approach to modeling transport grids. The model validates the common assumption of modeling catenary lines as purely resistive lines and requires the exact modeling of the substation voltage and bilateral status, the parallel lines, and the bus auxiliaries and braking energy. The assumption of ignoring the feeder cables is shown to be valid only for sections of relatively short cables and relatively low powers defined as per the acceptable error level of the modeler. Through a deeper understanding of the analytical rather than the numerical modeling of catenary networks, vital lessons and patterns were drawn that led to the Trolleygrid State Estimator. This estimator of **Chapter 4** compares the already-available measurements at a power node against a number of here-defined indicators and trends to help estimate, among others, the spare traction substation capacity available locally. This estimator is the basis of the successful power management schemes for the storage and IMC buses in this thesis, without the need for additional sensors across the trolleygrid and trolleybuses and/or wireless communication.

What is the outlook for renewables integration in present-day urban trolleygrids?

Chapter 5 started with the approach of powering the trolleygrid traction substations through decentralized PV systems at every substation, without storage, but the results were not satisfactory. In the case study of the Arnhem substations, the direct PV utilization was between 13-39% depending on the substation, with a weighted average of 31% for the whole city grid when considering energy-neutral PV system sizes at each location. Several different approaches attempted to find a more favorable sizing methodology for a better PV system performance, but the most promising solution seemed to be a hybrid PV-Wind system at the MVAC grid rather than the decentralized approach. It was interesting to note that some of the proposed methodologies, like the Marginal Utilization Approach, completely advised against PV system installations at certain traction substations. When further investigation, this advice seemed to be strongly coupled with the average traffic during sunlight hours under the substation, or the here-defined Traffic View Factor.
It is important, therefore, to find a simple and effective method for trolleygrid operators to estimate the performance of a PV system of any size connected to a certain traction substation. Such a method was offered in **Chapter 6** where a number of accessible Key Performance Indicators (KPI) were tested against the array of results for the two drastically different trolleygrids of Arnhem (NL) and Gdynia (PL). One KPI in particular, the here-defined Traffic Energy KPI, was the most promising. This KPI is a simple product of the yearly energy demand under a substation and its average traffic count and predicts, through a simple logarithmic curve, the performance of a PV system of any size at any traction substation. This KPI was also useful in calculating the performance of a combined PV system for neighboring substations. Interestingly, this study exposed the presence of a performance saturation plateau for every PV system at any substation. This is an inherent shortcoming of coupling the specific load traction profiles of transport grids with PV systems - a result of the vital absence of a base load.
This result carried into **Chapter 7** where comparing DC-side storage solutions for in-

creasing the PV system performance showed some interesting outcomes in terms of energy savings of over 20%. However, the study did not solve the problem of the absence of a base load since on-board storage systems vanished with the buses, and stationary storage systems were primarily in charging mode in low-traffic substations. This latter process is less efficient than simply placing the storage on the AC side with the PV system. Part II ends, therefore, with the conclusion that the multi-functional and multi-stakeholder approach to traction grids is not only an opportunity but a necessity in providing the critical base loads for the successful techno-economic feasibility of PV system integration into these grids.

How can the integration of smart non-traction loads and grid components be maximized to improve the techno-economic feasibility of the future sustainable, multi-functional trolleygrid?

From the possibilities of functionalities and components that can be added to the grid, this thesis looked at three: The storage solutions that are already present in many traction grids, the EV chargers that are currently being discussed and rolled out into traction networks, and the connection to residential loads that is an original suggestion of this thesis.
While storage is already implemented in traction grids in general, and trolleygrids in particular, no consensus exists yet on whether to implement on-board (OESS) or stationary (SESS) energy storage systems -or even a hybrid combination.
For that aim, **Chapter 8** presented this comparison. On-board storage is criticized for the disadvantage of leaving the section with the bus that holds it as well as adding to the traction demand of the bus by its presence onboard. This disadvantage is exacerbated by the performance in terms of the recuperation of braking energy, reduction of transmission losses, and voltage drops. Meanwhile, the benefits of stationary storage are heavily dependent on its placement location and power management scheme, yet a mid-line performance proved satisfactory. Furthermore, in the absence of components such as PV systems or EV chargers to "leave behind" when the on-board storage exits the section with the bus, there are no grid operation benefits to be gained from the presence of a stationary storage system on a section. Finally, the benefits of a hybrid system seemed to be mostly brought in by the SESS and therefore do not justify the extra costs of the SESS system in a hybrid storage situation. However, this is welcomed news as it means that a future investment decision in stationary storage would not render present investments in on-board storage redundant.
Chapter 9 investigated EV charger integration directly to the catenary of DC trolleygrids by examining multiple active and passive grid methods to increase the number of EVs charged in a day. These were: Increasing the substation voltage, adding a third parallel overhead cable, introducing a bilateral connection, introducing Smart Charging, increasing the substation power rating, and installing a multi-port converter. It was found that no single solution fits all types of sections and their parameters (length, average traffic, peak traffic, etc.). However, bilateral connections seem to be the most beneficial and cost-efficient solution in most cases, except for a section that is coupled with an already congested section. Smart charging with sensors and wireless communication can in-

crease the potential significantly by dynamically veering away from grid violations, but it is a costly and complex solution. This was one of the main motivations behind developing the estimator of Chapter 4. Overall, there was immense potential for up to 220 EVs to be charged from a single trolleygrid section. EV chargers are already a mature technology of smart grid loads, and their integration was expected indeed to be technically feasible in catenary grids.
EV chargers have also been shown to have a significant positive impact on the feasibility of RES integration into electric public transport grids, by providing a base load for the RES and avoiding costly solutions such as storage or exchange with the AC grid or curtailment. The benefit increases with bigger EV chargers, hence the importance of the methods explained in this chapter.
In the third study of possible future trolleygrid architectures, **Chapter 10** introduced a shared, multi-stakeholder PV system for traction substations and their nearby residential dwellings. The advantage of this method was to again investigate base load possibilities for the PV system performance, while also offering the crucially needed physical space for the implementation of the PV system. The shared system proved to be perfectly synergetic, offering better load coverage and less need for storage/curtailment at any combination of PV system and number of households.
In conclusion, of Part III, the multi-functional trolleygrid is shown to be feasible and energy efficient, offering more of the benefits of conventional storage systems while serving additional loads and functionalities. This motivates their study again as a base load for the sustainable trolleygrids.

What are suitable power management and design schemes for the trolleybuses and the trolleygrids of the future?

Part IV looked at the future of both trolleybuses and trolleygrids.
First, **Chapter 11** looked at the increasingly popular new generation of trolleybus fleets: The In-Motion-Charging trolleybus. This bus is a hybrid between trolleybuses and battery buses, offering range extensions compared to trolleys and with a more convenient charging on-the-go than the overnight charging common for battery buses. However, the IMC bus comes with an increased power demand from the available catenary. These power demand peaks and voltage drops threaten to hinder the integration of more smart loads in the future trolleygrids at the expense of newer bus fleets. Chapter 11 proposed two dynamic charging schemes for the IMC bus battery that satisfied both the IMC bus energy pick-up requirements as well as the power and voltage violations of the trolleygrid. The first method, the Adaptive Charging method, used the historically known spare substation capacities to change the battery charging setpoint per the locally available power. This worked best for short routes and managed to reduce any additional charging times by up to 64%. The second method, the Valley Charging method, made use of the trolleygrid state estimator of Chapter 4 to design a power management scheme that allowed the IMC bus to estimate and draw the available instantaneous spare substation energy while respecting both the voltage and current limitations. This method was successful in electrifying an intercity operation from Wagening to Arnhem, becoming the longest known battery-mode route of an IMC bus, and still only using the available cate-

nary and not disturbing the operation of other conventional trolleybuses. This method can then work efficiently with other loads integrated into the section.
Finally, **Chapter 12** looked at the combinations of the above fleets and components into trolleygrid sections. while the power surges and voltage drops became more severe in the multi-functional trolleygrid, the breaches were not severe enough to disrupt the bus operation or render a scenario unfeasible.
EV chargers proved to be the most beneficial upgrade to current infrastructures. While simultaneously relieving the main AC grid of the charger load by tapping into the reserved capacity for the traction network, the EV charger showed synergy in the harvesting of braking energy and providing the critically needed base load for the successful techno-economic feasibility of the PV system. EV chargers can therefore replace storage systems on the catenary side of the trolleygrid while providing beneficial functionalities rather than a passive storage function.
Storage systems have indeed proven redundant in the presence of an EV charge. However, they still offered promising benefits in terms of reduction of the duration and severity of power overloading at the substation transformers, by up to 34%.
The multi-stakeholder PV system is most effective in low-traffic substations as it provides the necessary base load to reduce the need for storage, curtailment, and exchange with the AC grid. Nonetheless, this benefit is overshadowed by the presence of an EV charger. Still, there is a considerable benefit in the multi-stakeholder system in providing the needed physical installation space.
Part IV ends, therefore, by painting the final picture of the trolleygrid of the future as a sustainable, multi-functional, multi-stakeholder grid with IMC buses, DC-side EV chargers, and shared PV infrastructure with nearby residential loads.

13.2. FUTURE WORKS

This thesis offered various tools, methods, and techno-economic lessons for designing and managing future trolleybus fleets and grids. This is the first step in the study of these multi-functional infrastructures, and some future works are necessary to form an even more complete picture.

THEORETICAL MODELS AND POWER MANAGEMENT SCHEMES

First, some aspects of the modeling still need further investigation. Primarily, while the calculation of the available braking power is a straightforward electro-mechanical task, the engagement of braking resistors is not very well understood and often simplified by a voltage droop control. This has direct consequences on the power flow in the catenary and rail networks.
Furthermore, unilateral and unidirectional substations are more studied than bilateral or trilateral and bidirectional substations. With the advancements in power electronics and protection devices, the latter group could become an increasingly important player in the trolleygrids of the future and this invites a strong research momentum into creating comprehensive grids models for their operation.
Finally, experimental verification of power management schemes such as the trolleygrid estimator is needed, especially in the dynamic-transients environments brought by the

integration of new bus fleets and smart grid loads. This is a tedious effort that demands cooperation between trolleybus, trolleygrid, and distribution service operators as well as research institutes. These legal and cooperative bottlenecks will, unfortunately, hinder many of the future solutions and validation efforts in transport networks and need to be addressed by policy and decision-makers.

PV SYSTEM ANALYSES

Second, while this thesis has offered an extensive study of PV systems in trolleygrids, key aspects are still important to investigate. The most trivial of these aspects is a DC-side connection of the PV system and a thorough study of its power, voltage, and line current benefits. Furthermore, for both these DC studies and the AC studies offered in this thesis, a detailed economic analysis is pivotal for decision-makers. This is especially crucial for the multi-stakeholder scenarios to better inform the design decisions and total cost of ownership for each stakeholder. Lastly, this thesis confined itself to the northern hemisphere, harsh winter trolleygrids. It is still important to see how the utilization plateaus and trends look like for harsh summer environments like the trolleygrid of Athens or of Marrakesh.

ADDRESSING IMPLEMENTATION HURDLES

Third, a stability analysis is another piece of the future trolleygrid puzzle that is an important next step. The integration of smart grid loads and their power electronics and aggressive power management schemes needs to be re-iterated based on their effect on the stability of the DC catenary networks. Another implementation hurdle is the physical space available for the installation of PV systems. A detailed case study is invited for the case of the multi-stakeholder PV system that takes into account the available space and the economic costs of such systems as well as their effect on the Low Voltage AC grid.

MORE UNIVERSAL IMC BATTERY CHARGING SCHEMES

Fourth, the available IMC charging schemes need to be translated into workable battery management systems in cooperation with trolleybus manufacturers. These charging schemes should also be extended to cover non-conventional trolleygrid architectures (forks, bilateral, trilateral, etc.) and bidirectional substations.

BIBLIOGRAPHY

[1] L. Brunton, "The trolleybus story", *IEEE Review*, vol. 38, no. 2, pp. 57–61, 1992.

[2] M. Wołek, M. Wolański, M. Bartłomiejczyk, O. Wyszomirski, K. Grzelec, and K. Hebel, "Ensuring sustainable development of urban public transport: A case study of the trolleybus system in gdynia and sopot (poland)", *Journal of Cleaner Production*, vol. 279, p. 123 807, 2021.

[3] I. Diab, A. Saffirio, G. R. Chandra Mouli, A. S. Tomar, and P. Bauer, "A Complete DC Trolleybus Grid Model With Bilateral Connections, Feeder Cables, and Bus Auxiliaries", *IEEE Transactions on Intelligent Transportation Systems*, vol. 23, no. 10, pp. 19 030–19 041, 2022.

[4] A. S. Tomar, B. Veenhuizen, L. Buning, and B. Pyman, "Estimation of the size of the battery for hybrid electric trolley busses using backward quasi-static modelling", in *Multidisciplinary Digital Publishing Institute Proceedings*, vol. 2, 2018, p. 1499.

[5] E. Sindi, M. Polis, G. Yin, L. Ding, *et al.*, "Distributed optimal power and voltage management in dc microgrids: Applications to dual-source trolleybus systems", *IEEE transactions on transportation electrification*, vol. 4, no. 3, pp. 778–788, 2018.

[6] D. Zhang, J. Jiang, W. Zhang, *et al.*, "Robust and scalable management of power networks in dual-source trolleybus systems: A consensus control framework", *IEEE transactions on intelligent transportation systems*, vol. 17, no. 4, pp. 1029–1038, 2015.

[7] D. Zhang, J. Jiang, W. Zhang, *et al.*, "Optimal power management in dc microgrids with applications to dual-source trolleybus systems", *IEEE Transactions on Intelligent Transportation Systems*, vol. 19, no. 4, pp. 1188–1197, 2017.

[8] D. Zhang, J. Jiang, W. Zhang, *et al.*, "Load prediction and distributed optimal control of on-board battery systems for dual-source trolleybuses", *IEEE Transactions on Transportation Electrification*, vol. 3, no. 1, pp. 284–296, 2016.

[9] D. Cornic, "Efficient recovery of braking energy through a reversible dc substation", in *Electrical systems for aircraft, railway and ship propulsion*, IEEE, 2010, pp. 1–9.

[10] Y. Warin, R. Lanselle, and M. Thiounn, "Active substation", in *World Congress on Railway Research*, Lille, 2011, pp. 22–26.

[11] I. Diab, B. Scheurwater, A. Saffirio, G. R. Chandra-Mouli, and P. Bauer, "Placement and sizing of solar PV and Wind systems in trolleybus grids", *Journal of Cleaner Production*, p. 131 533, 2022.

[12] R. F. Paternost, R. Mandrioli, R. Barbone, V. Cirimele, J. Loncarski, and M. Ricco, "Impact of a stationary energy storage system in a dc trolleybus network", in *2022 IEEE Transportation Electrification Conference & Expo (ITEC)*, IEEE, 2022, pp. 1211–1216.

[13] J. J. Mwambeleko, T. Kulworawanichpong, and K. A. Greyson, "Tram and trolleybus net traction energy consumption comparison", in *2015 18th International Conference on Electrical Machines and Systems (ICEMS)*, 2015, pp. 2164–2169. DOI: 10.1109/ICEMS.2015.7385399.

[14] M. Bartłomiejczyk, *Dynamic Charging of Electric Buses*. Gdańsk University of Technoligy, Faculty of Electrical and Control Engineering, 2018, ISBN: 9783110645071. [Online]. Available: https://books.google.cz/books?id=ziX%5C_vQEACAAJ.

[15] trolley:motion, *trolley:motion*, 2020. [Online]. Available: https://www.trolleymotion.eu/.

[16] I. Diab, G. R. C. Mouli, and P. Bauer, "Increasing the integration potential of ev chargers in dc trolleygrids: A bilateral substation-voltage tuning approach", in *2022 International Symposium on Power Electronics, Electrical Drives, Automation and Motion (SPEEDAM)*, 2022, pp. 264–269. DOI: 10.1109/SPEEDAM53979.2022.9841989.

[17] Š. Hamacek, M. Bartłomiejczyk, R. Hrbáč, S. Mišák, and V. Stỳskala, "Energy recovery effectiveness in trolleybus transport", *Electric Power Systems Research*, vol. 112, pp. 1–11, 2014.

[18] D. He, Y. Yang, Y. Chen, *et al.*, "An integrated optimization model of metro energy consumption based on regenerative energy and passenger transfer", *Applied Energy*, vol. 264, p. 114 770, 2020.

[19] R. Barbone, R. Mandrioli, M. Ricco, R. F. Paternost, V. Cirimele, and G. Grandi, "Novel Multi-Vehicle Motion-Based Model of Trolleybus Grids towards Smarter Urban Mobility", *Electronics*, vol. 11, no. 6, p. 915, Mar. 2022, ISSN: 2079-9292. DOI: 10.3390/electronics11060915.

[20] Vanhool, *A bus for the future, Leipzig, October, 2012*, www.trolley-project.eu, [Online; accessed 23-Feb-2020], 2012.

[21] D. Iannuzzi, D. Lauria, and P. Tricoli, "Optimal design of stationary supercapacitors storage devices for light electrical transportation systems", *Optimization and Engineering*, vol. 13, no. 4, pp. 689–704, 2012.

[22] I. Diab, G. R. Chandra Mouli, and P. Bauer, "Toward a better estimation of the charging corridor length of in-motion-charging trolleybuses", in *2022 IEEE Transportation Electrification Conference & Expo (ITEC)*, 2022, pp. 557–562. DOI: 10.1109/ITEC53557.2022.9814021.

[23] A. Fernández-Rodrıguez, A. Fernández-Cardador, A. P. Cucala, and M. C. Falvo, "Energy efficiency and integration of urban electrical transport systems: Evs and metro-trains of two real european lines", *Energies*, vol. 12, no. 3, p. 366, 2019.

[24] S. Rastegarzadeh, M. Mahzoon, and H. Mohammadi, "A novel modular designing for multi-ring flywheel rotor to optimize energy consumption in light metro trains", *Energy*, vol. 206, p. 118 092, 2020.

[25] R. Teymourfar, B. Asaei, H. Iman-Eini, *et al.*, "Stationary super-capacitor energy storage system to save regenerative braking energy in a metro line", *Energy Conversion and Management*, vol. 56, pp. 206–214, 2012.

[26] T. Zhang, R. Zhao, E. E. Ballantyne, and D. Stone, "Increasing urban tram system efficiency, with battery storage and electric vehicle charging", *Transportation Research Part D: Transport and Environment*, vol. 80, p. 102 254, Mar. 2020, ISSN: 13619209. DOI: 10.1016/j.trd.2020.102254.

[27] T. Zhang, E. E. Ballantyne, R. Zhao, and D. A. Stone, "Technical and economic feasibility of increasing tram system efficiency with EV batteries", *Transportation Research Part D: Transport and Environment*, vol. 91, p. 102 681, Feb. 2021, ISSN: 13619209. DOI: 10.1016/j.trd.2020.102681.

[28] P. Santos, P. Fonte, and R. Luis, "Improvement of DC Microgrid Voltage Regulation Based on Bidirectional Intelligent Charging Systems", in *2018 15th International Conference on the European Energy Market (EEM)*, Lodz: IEEE, Jun. 2018, pp. 1–6, ISBN: 978-1-5386-1488-4. DOI: 10.1109/EEM.2018.8469991.

[29] K. Smith, L. Hunter, S. Galloway, C. Booth, C. Kerr, and M. Kellett, "Integrated Charging of EVs Using Existing LVDC Light Rail Infrastructure: A Case Study", in *2019 IEEE Third International Conference on DC Microgrids (ICDCM)*, Matsue, Japan: IEEE, May 2019, pp. 1–7, ISBN: 978-1-72813-491-8. DOI: 10.1109/ICDCM45535.2019.9232726.

[30] T. Dragicevic, J. M. Guerrero, and J. C. Vasquez, "A Distributed Control Strategy for Coordination of an Autonomous LVDC Microgrid Based on Power-Line Signaling", *IEEE Transactions on Industrial Electronics*, vol. 61, no. 7, pp. 3313–3326, Jul. 2014, ISSN: 0278-0046, 1557-9948. DOI: 10.1109/TIE.2013.2282597.

[31] M. Bartłomiejczyk, L. Jarzebowicz, and R. Hrbáč, "Application of Traction Supply System for Charging Electric Cars", *Energies*, vol. 15, no. 4, p. 1448, Feb. 2022, ISSN: 1996-1073. DOI: 10.3390/en15041448.

[32] M. Bartłomiejczyk and M. Połom, "Multiaspect measurement analysis of breaking energy recovery", *Energy Conversion and Management*, vol. 127, pp. 35–42, Nov. 2016, ISSN: 01968904. DOI: 10.1016/j.enconman.2016.08.089.

[33] M. Bartłomiejczyk, "Smart Grid Technologies in Electric Power Supply Systems of Public Transport", *Transport*, vol. 33, no. 5, pp. 1144–1154, Dec. 2018, ISSN: 1648-4142, 1648-3480. DOI: 10.3846/transport.2018.6433.

[34] M. Bartłomiejczyk, "Bilateral power supply of the traction network as a first stage of Smart Grid technology implementation in electric traction", *MATEC Web of Conferences*, vol. 180, A. Szeląg, K. Karwowski, H. Gold, and A. Żurkowski, Eds., p. 02 003, 2018, ISSN: 2261-236X. DOI: 10.1051/matecconf/201818002003.

[35] M. Salih, M. Koch, D. Baumeister, M. Wazifehdust, P. Steinbusch, and M. Zdrallek, "Adapted Newton-Raphson Power Flow Method for a DC Traction Network including Non-receptive Power Sources and Photovoltaic Systems", in *2019 IEEE PES Innovative Smart Grid Technologies Europe (ISGT-Europe)*, Bucharest, Romania: IEEE, Sep. 2019, pp. 1–5, ISBN: 978-1-5386-8218-0. DOI: 10.1109/ISGTEurope.2019.8905722.

[36] M. Salih, D. Baumeister, M. Wazifehdust, *et al.*, "Impact assessment of integrating novel battery-trolleybuses, pv units and ev charging stations in a dc trolleybus network", in *2nd E-Mobility Power System Integration Symposium*, MOSI Symposium, 2018, pp. 1–6.

[37] A. Rufer, D. Hotellier, and P. Barrade, "A supercapacitor-based energy storage substation for voltage compensation in weak transportation networks", *IEEE Transactions on power delivery*, vol. 19, no. 2, pp. 629–636, 2004.

[38] M. Bartłomiejczyk and M. Połom, "Spatial aspects of tram and trolleybus supply system", in *8th International Scientific Symposium on Electrical Power Engineering (ELEKTROENERGETIKA)*, 2015, pp. 223–227.

[39] P. M. Santos, J. P. Trovao, and P. G. Pereirinha, "Sustainable trolleybus system: Rectifier substation technology improvement for energy efficiency and operational cost reduction", in *2014 IEEE Vehicle Power and Propulsion Conference (VPPC)*, IEEE, 2014, pp. 1–6.

[40] A. S. Tomar, B. Veenhuizen, L. Buning, and B. Pyman, "Estimation of the size of the battery for hybrid electric trolley busses using backward quasi-static modelling", *Proceedings*, vol. 2, no. 23, 2018, ISSN: 2504-3900. DOI: 10.3390/proceedings223149

[41] B. Destraz, P. Barrade, A. Rufer, and M. Klohr, "Study and simulation of the energy balance of an urban transportation network", in *2007 European conference on power electronics and applications*, IEEE, 2007, pp. 1–10.

[42] M. Bartłomiejczyk and M. Połom, "Multi-aspect measurement analysis of breaking energy recovery", *Energy conversion and management*, vol. 127, no. 1, pp. 35–42, 2016.

[43] C. Wu, B. Xu, S. Lu, F. Xue, L. Jiang, and M. Chen, "Adaptive eco-driving strategy and feasibility analysis for electric trains with onboard energy storage devices", *IEEE Transactions on Transportation Electrification*, vol. 7, no. 3, pp. 1834–1848, 2021.

[44] A. Capasso, R. Lamedica, L. Podestà, *et al.*, "A measurement campaign in a metro trains deposit/maintenance and repair site for PV production optimal sizing", in *2015 IEEE 15th International Conference on Environment and Electrical Engineering (EEEIC)*, IEEE, 2015, pp. 956–961.

[45] W. Weiying, W. Mingliang, L. Qi, and C. Weirong, "Method for improving power quality of metro traction power supply system with PV integration", in *2017 Chinese Automation Congress (CAC)*, IEEE, 2017, pp. 1682–1685.

[46] P. Arévalo, A. Cano, J. Benavides, and F. Jurado, "Feasibility study of a renewable system (PV/HKT/GB) for hybrid tramway based on fuel cell and super capacitor", *IET Renewable Power Generation*, vol. 15, no. 3, pp. 491–503, 2021.

[47] İ. Şengör, H. C. Kılıçkıran, H. Akdemir, B. Kekezoğlu, O. Erdinc, and J. P. Catalao, "Energy management of a smart railway station considering regenerative braking and stochastic behaviour of ESS and PV generation", *IEEE Transactions on Sustainable Energy*, vol. 9, no. 3, pp. 1041–1050, 2017.

[48] G. Stana and V. Brazis, "Trolleybus motion simulation by dealing with overhead dc network energy transmission losses", in *2017 18th International Scientific Conference on Electric Power Engineering (EPE)*, IEEE, 2017, pp. 1–6.

[49] J. J. Mwambeleko, T. Kulworawanichpong, and K. A. Greyson, "Tram and trolleybus net traction energy consumption comparison", in *2015 18th International Conference on Electrical Machines and Systems (ICEMS)*, IEEE, 2015, pp. 2164–2169.

[50] M. Salih, D. Baumeister, M. Wazifehdust, *et al.*, *Optimized positioning for storage systems in an lvdc traction grid with non-receptive power sources and photovoltaic systems*, Proceedings of the 9th Solar & Storage Integration Workshop, Dublin, 2019.

[51] D. Baumeister, M. Salih, M. Wazifehdust, *et al.*, "Modelling and simulation of a public transport system with battery-trolleybuses for an efficient e-mobility integration", in *1st E-Mobility Power System Integration Symposium*, 2017.

[52] P. Arboleya, B. Mohamed, and I. El-Sayed, "Dc railway simulation including controllable power electronic and energy storage devices", *IEEE Transactions on Power Systems*, vol. 33, no. 5, pp. 5319–5329, 2018.

[53] M. Wazifehdust, D. Baumeister, M. Salih, *et al.*, "Potential analysis for the integration of renewables and ev charging stations within a novel lvdc smart-trolleybus grid", 2019.

[54] G. Stana and V. Brazis, "Mathematical calculation of power transmission related parameters in simulations of overhead grid-connected electric public transport motion", in *2020 IEEE 61th International Scientific Conference on Power and Electrical Engineering of Riga Technical University (RTUCON)*, IEEE, 2020, pp. 1–6.

[55] G. Stana and V. Brāzis, "Trolleybus with ess motion simulation considering common mass increase and transmission losses", in *2017 IEEE 58th International Scientific Conference on Power and Electrical Engineering of Riga Technical University (RTUCON)*, IEEE, 2017, pp. 1–6.

[56] M. Bartłomiejczyk, "Modern technologies in energy demand reducing of public transport—practical applications", in *2017 Zooming Innovation in Consumer Electronics International Conference (ZINC)*, IEEE, 2017, pp. 64–69.

[57] B.-Y. Ku and J.-S. Liu, "Solution of dc power flow for nongrounded traction systems using chain-rule reduction of ladder circuit jacobian matrices", in *ASME/IEEE Joint Railroad Conference*, IEEE, 2002, pp. 123–130.

[58] KRUCH, *KRUCH Railway Innovations GmbH & Co. KG*, urlhttp://kruch.com/, [Online; accessed 16-6-2021], 2021.

[59] R. Barbone, R. Mandrioli, M. Ricco, R. F. Paternost, V. Cirimele, and G. Grandi, "Novel multi-vehicle motion-based model of trolleybus grids towards smarter urban mobility", *Electronics*, vol. 11, no. 6, p. 915, 2022.

[60] D. Iannuzzi, F. Ciccarelli, and D. Lauria, "Stationary ultracapacitors storage device for improving energy saving and voltage profile of light transportation networks", *Transportation Research Part C: Emerging Technologies*, vol. 21, no. 1, pp. 321–337, 2012.

[61] R. F. P. Paternost, R. Mandrioli, M. Ricco, *et al.*, "Energy storage management in support of trolleybus traction power systems", in *2022 International Symposium on Power Electronics, Electrical Drives, Automation and Motion (SPEEDAM)*, 2022, pp. 252–257. DOI: 10.1109/SPEEDAM53979.2022.9842162.

[62] M. Z. Chymera, A. C. Renfrew, M. Barnes, and J. Holden, "Modeling electrified transit systems", *IEEE Transactions on Vehicular Technology*, vol. 59, no. 6, pp. 2748–2756, 2010.

[63] A. Finlayson, C. Goodman, and R. White, "Investigation into the computational techniques of power system modeling for a dc railway", 2006.

[64] D. Iannuzzi and P. Tricoli, "Speed-based state-of-charge tracking control for metro trains with onboard supercapacitors", *IEEE Transactions on Power Electronics*, vol. 27, no. 4, pp. 2129–2140, 2011.

[65] J. Macedo and R. J. Rossetti, "Rush hour traffic conditions impact in electric bus performance: A case study in porto", *DSIE'17*, p. 65, 2017.

[66] D. Perrotta, B. Ribeiro, R. J. Rossetti, and J. L. Afonso, "On the potential of regenerative braking of electric buses as a function of their itinerary", *Procedia-Social and Behavioral Sciences*, vol. 54, pp. 1156–1167, 2012.

[67] A. Shekhar, G. C. R. Mouli, S. Bandyopadhyay, and P. Bauer, "Electric vehicle charging with multi-port converter based integration in dc trolley-bus network", in *2021 IEEE 19th International Power Electronics and Motion Control Conference (PEMC)*, IEEE, 2021, pp. 250–255.

[68] W. Wu, Y. Lin, R. Liu, Y. Li, Y. Zhang, and C. Ma, "Online ev charge scheduling based on time-of-use pricing and peak load minimization: Properties and efficient algorithms", *IEEE Transactions on Intelligent Transportation Systems*, 2020.

[69] M. Bartłomiejczyk, "Practical application of in motion charging: Trolleybuses service on bus lines", in *2017 18th International Scientific Conference on Electric Power Engineering (EPE)*, IEEE, 2017, pp. 1–6.

[70] M. Bartłomiejczyk, "Bilateral power supply of the traction network as a first stage of smart grid technology implementation in electric traction", in *MATEC Web of Conferences. Vol. 180*, EDP Sciences, 2018, pp. 1–6.

[71] M. Bartlomiejczyk, "Use of numerical methods in the analysis of traction energy systems—an overview of the practical examples", in *Proceedings of the First International Scientific Conference "Intelligent Information Technologies for Industry"(IITI'16)*, Springer, 2016, pp. 407–418.

[72] UITP, *The road to sustainability: Transition to renewable energy in public transport*, uitp.org.

[73] S. A. Al-Janahi, O. Ellabban, and S. G. Al-Ghamdi, "Technoeconomic feasibility study of grid-connected building-integrated photovoltaics system for clean electrification: A case study of Doha metro", *Energy Reports*, vol. 6, pp. 407–414, 2020.

[74] P. Arévalo, A. Cano, and F. Jurado, "Comparative study of two new energy control systems based on PEMFC for a hybrid tramway in Ecuador", *International Journal of Hydrogen Energy*, vol. 45, no. 46, pp. 25 357–25 377, 2020.

[75] L. P. Di Noia and R. Rizzo, "Analysis of integration of pv power plant in railway power systems", in *2019 8th International Conference on Modern Power Systems (MPS)*, IEEE, 2019, pp. 1–5.

[76] A. Cano, P. Arévalo, D. Benavides, and F. Jurado, "Sustainable tramway, techno-economic analysis and environmental effects in an urban public transport. a comparative study", *Sustainable Energy, Grids and Networks*, vol. 26, p. 100 462, 2021.

[77] M. Bartłomiejczyk, "Potential application of solar energy systems for electrified urban transportation systems", *Energies*, vol. 11, no. 4, p. 954, 2018.

[78] M. Wazifehdust, D. Baumeister, M. Salih, *et al.*, "Potential analysis for the integration of renewables and EV charging stations within a novel LVDC smart-trolleybus grid", 2019.

[79] I. Diab, A. Saffirio, G. R. Chandra-Mouli, and P. Bauer, "A simple method for sizing and estimating the performance of PV systems in trolleybus grids", *Journal of Cleaner Production*, p. 135 623, 2022.

[80] I. Diab, G. R. C. Mouli, and P. Bauer, "A review of the key technical and non-technical challenges for sustainable transportation electrification: A case for urban catenary buses", in *2022 IEEE 20th International Power Electronics and Motion Control Conference (PEMC)*, IEEE, 2022, pp. 439–448.

[81] M. Wołek, M. Wolański, M. Bartłomiejczyk, O. Wyszomirski, K. Grzelec, and K. Hebel, "Ensuring sustainable development of urban public transport: A case study of the trolleybus system in Gdynia and Sopot (Poland)", *Journal of Cleaner Production*, vol. 279, p. 123 807, 2021.

[82] M. Salih, D. Baumeister, M. Wazifehdust, *et al.*, "Impact Assessment of Integrating Novel Battery-Trolleybuses, PV Units and EV Charging Stations in a DC Trolleybus Network", 2018, p. 6.

[83] M. Wazifehdust, D. Baumeister, M. Salih, *et al.*, "Potential Analysis for the Integration of Renewables and EV Charging Stations Within a Novel LVDC Smart-Trolleybus Grid", in *International Conference on Electricitiy Distribution*, 2019, p. 5.

[84] S. Kratz, A. Schmidt, B. Krueger, R. Wegener, and S. Soter, "Power supply of a short-range public transportation system based on photovoltaics-potential analysis and implementation", in *2019 IEEE 46th Photovoltaic Specialists Conference (PVSC)*, IEEE, 2019, pp. 3077–3081.

[85] S. Kratz, B. Krueger, R. Wegener, and S. Soter, "Integration of photovoltaics into a smart trolley system based on SiC-Technology", in *2018 IEEE 7th International Conference on Power and Energy (PECon)*, IEEE, 2018, pp. 168–173.

[86] A. T. De Almeida, C. Inverno, J. L. de Almeida, J. A. S. Marques, and B. Santos, "Small-hydropower integration in a multi-purpose dam-bridge for sustainable urban mobility", *Renewable and Sustainable Energy Reviews*, vol. 15, no. 9, pp. 5092–5103, 2011.

[87] A. E. Díez and M. Restrepo, "A planning method for partially grid-connected bus rapid transit systems operating with in-motion charging batteries", *Energies*, vol. 14, no. 9, 2021, ISSN: 1996-1073. DOI: 10.3390/en14092550. [Online]. Available: https://www.mdpi.com/1996-1073/14/9/2550.

[88] H. Chen, T. N. Cong, W. Yang, C. Tan, Y. Li, and Y. Ding, "Progress in electrical energy storage system: A critical review", *Progress in natural science*, vol. 19, no. 3, pp. 291–312, 2009.

[89] I. E. Commission, *Electrical energy storage*, 2011.

[90] A. Du Pasquier, I. Plitz, S. Menocal, and G. Amatucci, "A comparative study of li-ion battery, supercapacitor and nonaqueous asymmetric hybrid devices for automotive applications", *Journal of power sources*, vol. 115, no. 1, pp. 171–178, 2003.

[91] M. Beaudin, H. Zareipour, A. Schellenberglabe, and W. Rosehart, "Energy storage for mitigating the variability of renewable electricity sources: An updated review", *Energy for sustainable development*, vol. 14, no. 4, pp. 302–314, 2010.

[92] Advanced Cell Engineering, *Advanced lfp cell technology with 200 wh/kg energy density*, www.advancedcellengineering.com, 2022.

[93] D. Rastler, "A white paper primer on applications costs and benefits", *Electric Power Research Institute, Tech. Rep.*, 2010.

[94] P. Nikolaidis and A. Poullikkas, "Cost metrics of electrical energy storage technologies in potential power system operations", *Sustainable Energy Technologies and Assessments*, vol. 25, pp. 43–59, 2018.

[95] T. Nemeth, P. J. Kollmeyer, A. Emadi, and D. U. Sauer, "Optimized operation of a hybrid energy storage system with lto batteries for high power electrified vehicles", in *2019 IEEE Transportation Electrification Conference and Expo (ITEC)*, IEEE, 2019, pp. 1–6.

[96] A. Burke and M. Miller, "Life cycle testing of lithium batteries for fast charging and second-use applications", in *2013 World Electric Vehicle Symposium and Exhibition (EVS27)*, IEEE, 2013, pp. 1–10.

[97] A. Harris, D. Soban, B. M. Smyth, and R. Best, "Assessing life cycle impacts and the risk and uncertainty of alternative bus technologies", *Renewable and Sustainable Energy Reviews*, vol. 97, pp. 569–579, 2018.

[98] X. Liu, K. Li, and X. Li, "The electrochemical performance and applications of several popular lithium-ion batteries for electric vehicles-a review", *Advances in Green Energy Systems and Smart Grid*, pp. 201–213, 2018.

[99] X. Hu, C. Zou, C. Zhang, and Y. Li, "Technological developments in batteries: A survey of principal roles, types, and management needs", *IEEE Power and Energy Magazine*, vol. 15, no. 5, pp. 20–31, 2017.

[100] Altair Nanotechnologies, *Altair Nanotechnologies: 24V 70Ah Battery Module*, `https://altairnano.com/products/battery-module/`.

[101] M. Baumann, J. Peters, M. Weil, and A. Grunwald, "Co2 footprint and life-cycle costs of electrochemical energy storage for stationary grid applications", *Energy Technology*, vol. 5, no. 7, pp. 1071–1083, 2017.

[102] L. Wang, Z. Wang, Q. Ju, W. Wang, and Z. Wang, "Characteristic analysis of lithium titanate battery", *Energy Procedia*, vol. 105, pp. 4444–4449, 2017.

[103] D. I. Stroe, A.-I. Stan, R. Teodorescu, D. Sauer, *et al.*, "Selection and performance-degradation modeling of limo 2/li 4 ti 5 o 12 and lifepo 4/c battery cells as suitable energy storage systems for grid integration with wind power plants: An example for the primary frequency regulation service", *IEEE Transactions on Sustainable Energy*, vol. 5, no. 1, pp. 90–101, 2014.

[104] A. Chatzivasileiadi, E. Ampatzi, and I. Knight, "Characteristics of electrical energy storage technologies and their applications in buildings", *Renewable and Sustainable Energy Reviews*, vol. 25, pp. 814–830, 2013.

[105] F. A. Farret and M. G. Simoes, *Integration of alternative sources of energy*. John Wiley & Sons, 2006.

[106] T. Yamamura, X. Wu, S. Ohta, *et al.*, "Vanadium solid-salt battery: Solid state with two redox couples", *Journal of Power Sources*, vol. 196, no. 8, pp. 4003–4011, 2011.

[107] A. Taniguchi, N. Fujioka, M. Ikoma, and A. Ohta, "Development of nickel/metal-hydride batteries for evs and hevs", *Journal of power sources*, vol. 100, no. 1-2, pp. 117–124, 2001.

[108] G. Pistoia, *Electric and hybrid vehicles: Power sources, models, sustainability, infrastructure and the market*. Elsevier, 2010.

[109] P. Li, "Energy storage is the core of renewable technologies", *IEEE Nanotechnology Magazine*, vol. 2, no. 4, pp. 13–18, 2008.

[110] C. J. Rydh and B. A. Sandén, "Energy analysis of batteries in photovoltaic systems. part i: Performance and energy requirements", *Energy conversion and management*, vol. 46, no. 11-12, pp. 1957–1979, 2005.

[111] J. Baker, "New technology and possible advances in energy storage", *Energy Policy*, vol. 36, no. 12, pp. 4368–4373, 2008.

[112] F. Dıaz-González, A. Sumper, O. Gomis-Bellmunt, and R. Villafáfila-Robles, "A review of energy storage technologies for wind power applications", *Renewable and sustainable energy reviews*, vol. 16, no. 4, pp. 2154–2171, 2012.

[113] I. Hadjipaschalis, A. Poullikkas, and V. Efthimiou, "Overview of current and future energy storage technologies for electric power applications", *Renewable and sustainable energy reviews*, vol. 13, no. 6-7, pp. 1513–1522, 2009.

[114] J. San Martın, I. Zamora, J. San Martın, V. Aperribay, and P. Eguia, "Energy storage technologies for electric applications", in *International Conference on Renewable Energies and Power Quality*, 2011.

[115] J. Kaldellis and D. Zafirakis, "Optimum energy storage techniques for the improvement of renewable energy sources-based electricity generation economic efficiency", *Energy*, vol. 32, no. 12, pp. 2295–2305, 2007.

[116] J. Kondoh, I. Ishii, H. Yamaguchi, *et al.*, "Electrical energy storage systems for energy networks", *Energy conversion and management*, vol. 41, no. 17, pp. 1863–1874, 2000.

[117] S. M. Schoenung, "Characteristics and technologies for long-vs. short-term energy storage", *United States Department of Energy*, 2001.

[118] R. Newnham, "Advantages and disadvantages of valve-regulated, lead/acid batteries", *Journal of power sources*, vol. 1, no. 52, pp. 149–153, 1994.

[119] N. Author, "Review of electrical energy storage technologies and systems and of their potential for the uk", *EA Technology*, vol. 1, p. 34, 2004.

[120] S. Schoenung, "Energy storage systems cost update a study for the doe energy storage systems program (report sand2011-2730)", *New Mexico and California, Sandia National Laboratories*, 2011.

[121] Z. Wen, J. Cao, Z. Gu, X. Xu, F. Zhang, and Z. Lin, "Research on sodium sulfur battery for energy storage", *Solid State Ionics*, vol. 179, no. 27-32, pp. 1697–1701, 2008.

[122] S. J. Kazempour, M. P. Moghaddam, M. Haghifam, and G. Yousefi, "Electric energy storage systems in a market-based economy: Comparison of emerging and traditional technologies", *Renewable energy*, vol. 34, no. 12, pp. 2630–2639, 2009.

[123] A. Bito, "Overview of the sodium-sulfur battery for the ieee stationary battery committee", in *IEEE Power Engineering Society General Meeting, 2005*, IEEE, 2005, pp. 1232–1235.

[124] A. Z. Weber, M. M. Mench, J. P. Meyers, P. N. Ross, J. T. Gostick, and Q. Liu, "Redox flow batteries: A review", *Journal of applied electrochemistry*, vol. 41, no. 10, pp. 1137–1164, 2011.

[125] L. Barote, R. Weissbach, R. Teodorescu, C. Marinescu, and M. Cirstea, "Stand-alone wind system with vanadium redox battery energy storage", in *2008 11th International Conference on Optimization of Electrical and Electronic Equipment*, IEEE, 2008, pp. 407–412.

[126] C. P. De Leon, A. Frıas-Ferrer, J. González-Garcıa, D. Szánto, and F. C. Walsh, "Redox flow cells for energy conversion", *Journal of power sources*, vol. 160, no. 1, pp. 716–732, 2006.

[127] Z. Yang, J. Zhang, M. C. Kintner-Meyer, *et al.*, "Electrochemical energy storage for green grid", *Chemical reviews*, vol. 111, no. 5, pp. 3577–3613, 2011.

[128] C. J. Rydh and B. A. Sandén, "Energy analysis of batteries in photovoltaic systems. part ii: Energy return factors and overall battery efficiencies", *Energy conversion and management*, vol. 46, no. 11-12, pp. 1980–2000, 2005.

[129] S. T. Revankar, "Chemical energy storage", in *Storage and Hybridization of Nuclear Energy*, Elsevier, 2019, pp. 177–227.

[130] X. Luo, J. Wang, M. Dooner, and J. Clarke, "Overview of current development in electrical energy storage technologies and the application potential in power system operation", *Applied energy*, vol. 137, pp. 511–536, 2015.

[131] P. Boer and J. Raadschelders, "Briefing paper: Flow batteries", *KEMA, Netherlands. Retrieved on*, vol. 18, 2013.

[132] W. Tong, *Wind power generation and wind turbine design*. WIT press, 2010.

[133] M. Winter and R. J. Brodd, "What are batteries, fuel cells, and supercapacitors?", *Chemical reviews*, vol. 104, no. 10, pp. 4245–4270, 2004.

[134] E. N. Power, "Capacitors age and capacitors have an end of life", *White paper*, 2008.

[135] S. C. Smith, P. Sen, and B. Kroposki, "Advancement of energy storage devices and applications in electrical power system", in *2008 IEEE Power and Energy Society General Meeting-Conversion and Delivery of Electrical Energy in the 21st Century*, IEEE, 2008, pp. 1–8.

[136] Maxwell Technologies, *Maxwell Technologies: New 48V Module (C0B)*, `https://maxwell.com/wp-content/uploads/2022/02/3001491-EN.7_48V-165F-C0B-Datasheet_20220216.pdf`.

[137] Maxwell Technologies, *Maxwell Technologies: Ultracapacitors Bus Application Brief*, `https://maxwell.com/wp-content/uploads/2021/08/Bus_Application_3000620_EN_1.pdf`.

[138] Maxwell Technologies, *Maxwell Technologies: Ultracapacitors Energy Storage Application Brief*, `https://maxwell.com/wp-content/uploads/2021/08/Energy_Storage_Application_Brief_3001003-EN_1.pdf`.

[139] L. Wagner, "Overview of energy storage technologies", in *Future Energy*, Elsevier, 2014, pp. 613–631.

[140] A. Vecchi, Y. liang Li, Y. Ding, P. Mancarella, and A. Sciacovelli, "Liquid air energy storage (laes): A review on technology state-of-the-art, integration pathways and future perspectives", *Advances in Applied Energy*, p. 100 047, 2021.

[141] H. Power, *Highview power storage, secure, clean power.*

[142] EASE European Association for Storage of Energy, *Energy storage technology descriptions - liquid air energy storage.*

[143] M. Akhurst, I. Arbon, M. Ayres, *et al.*, "Liquid air in the energy and transport systems: Opportunities for industry and innovation in the uk", 2013.

[144] G. Ries and H.-W. Neumueller, "Comparison of energy storage in flywheels and smes", *Physica C: Superconductivity*, vol. 357, pp. 1306–1310, 2001.

[145] Amber Kinetics, *Amber kinetics: M32 flywheel*, https://amberkinetics.com/wp-content/uploads/2020/05/Amber-Kinetics-DataSheet.pdf.

[146] H. L. Ferreira, R. Garde, G. Fulli, W. Kling, and J. P. Lopes, "Characterisation of electrical energy storage technologies", *Energy*, vol. 53, pp. 288–298, 2013.

[147] M. Falvo, R. Lamedica, and A. Ruvio, "Energy storage application in trolley-buses lines for a sustainable urban mobility", in *2012 Electrical Systems for Aircraft, Railway and Ship Propulsion*, IEEE, 2012, pp. 1–6.

[148] A. E. Dıez and M. Restrepo, "A planning method for partially grid-connected bus rapid transit systems operating with in-motion charging batteries", *Energies*, vol. 14, no. 9, p. 2550, 2021.

[149] A. Rufer, "Energy storage for railway systems, energy recovery and vehicle autonomy in europe", in *The 2010 International Power Electronics Conference-ECCE ASIA-*, IEEE, 2010, pp. 3124–3127.

[150] V. Brazis, L. Latkovskis, and L. Grigans, "Simulation of trolleybus traction induction drive with supercapacitor energy storage system", *Latvian Journal of Physics and Technical Sciences*, vol. 47, no. 5, p. 33, 2010.

[151] F.-c. Sun, B. Liu, and Z.-p. Wang, "Analysis of energy consumption characteristics of dual-source trolleybus", pp. 1–5, 2014. DOI: 10.1109/ITEC-AP.2014.6940838.

[152] S. Xie, M. H. Nazari, G. Yin, W. Chen, *et al.*, "Impact of stochastic generation/load variations on distributed optimal energy management in dc microgrids for transportation electrification", *IEEE Transactions on Intelligent Transportation Systems*, vol. 23, no. 7, pp. 7196–7205, 2021.

[153] L. Alfieri, A. Bracale, P. Caramia, D. Iannuzzi, and M. Pagano, "Optimal battery sizing procedure for hybrid trolley-bus: A real case study", *Electric Power Systems Research*, vol. 175, p. 105 930, 2019.

[154] Y. Liu, M. Chen, S. Lu, Y. Chen, and Q. Li, "Optimized sizing and scheduling of hybrid energy storage systems for high-speed railway traction substations", *Energies*, vol. 11, no. 9, p. 2199, 2018.

[155] H. Hayashiya, H. Itagaki, Y. Morita, *et al.*, "Potentials, peculiarities and prospects of solar power generation on the railway premises", in *2012 International Conference on Renewable Energy Research and Applications (ICRERA)*, IEEE, 2012, pp. 1–6.

[156] M. Bartłomiejczyk and S. Mirchevski, "Reducing of energy consumption in public transport—results of experimental exploitation of super capacitor energy bank in gdynia trolleybus system", in *2014 16th International Power Electronics and Motion Control Conference and Exposition*, IEEE, 2014, pp. 94–101.

[157] T. Unterluggauer, J. Rich, P. B. Andersen, and S. Hashemi, "Electric vehicle charging infrastructure planning for integrated transportation and power distribution networks: A review", *ETransportation*, p. 100 163, 2022.

[158] S. Rahman and G. Shrestha, "An investigation into the impact of electric vehicle load on the electric utility distribution system", *IEEE Transactions on Power Delivery*, vol. 8, no. 2, pp. 591–597, 1993.

[159] M. R. Khalid, M. S. Alam, A. Sarwar, and M. J. Asghar, "A comprehensive review on electric vehicles charging infrastructures and their impacts on power-quality of the utility grid", *ETransportation*, vol. 1, p. 100 006, 2019.

[160] G. Gruosso, A. Mion, and G. S. Gajani, "Forecasting of electrical vehicle impact on infrastructure: Markov chains model of charging stations occupation", *ETransportation*, vol. 6, p. 100 083, 2020.

[161] M. Bartłomiejczyk, "Practical application of in motion charging: Trolleybuses service on bus lines", in *2017 18th International Scientific Conference on Electric Power Engineering (EPE)*, May 2017, pp. 1–6. DOI: 10.1109/EPE.2017.7967239.

[162] M. Wazifehdust, D. Baumeister, M. Salih, *et al.*, "Predictive flexibility calculation for battery-trolleybuses", in *ETG-Kongress 2021 - Von Komponenten Bis Zum Gesamtsystem Fur Die Energiewende*, vol. 9, 2021, pp. 191–196, ISBN: 9783800755493.

[163] M. Weisbach, U. Spaeth, B. Schmuelling, and C. Troullier, "Flexible EV Charging Strategy for a DC Catenary Grid", in *2020 Fifteenth International Conference on Ecological Vehicles and Renewable Energies (EVER)*, Monte-Carlo, Monaco: IEEE, Sep. 2020, pp. 1–6, ISBN: 978-1-72815-641-5. DOI: 10.1109/EVER48776.2020.9243038.

[164] M. Bartłomiejczyk and M. Połom, "The impact of the overhead line's powersupply system spatial differentiation on the energy consumption of trolleybustransport: Planning and economic aspects", *Transport*, vol. 32, no. 1, pp. 1–12, Oct. 2015, ISSN: 1648-4142, 1648-3480. DOI: 10.3846/16484142.2015.1101611.

[165] M. Bartłomiejczyk, L. Jarzebowicz, and R. Hrbáč, "Application of traction supply system for charging electric cars", *Energies*, vol. 15, no. 4, p. 1448, 2022.

[166] K. Smith, S. Galloway, and G. Burt, "A review of design criteria for low voltage DC distribution stability", in *2016 51st International Universities Power Engineering Conference (UPEC)*, Coimbra: IEEE, Sep. 2016, pp. 1–6, ISBN: 978-1-5090-4650-8. DOI: 10.1109/UPEC.2016.8114089.

[167] M. Bartłomiejczyk, "Smart grid technologies in electric traction: Mini inverter station", in *2017 Zooming Innovation in Consumer Electronics International Conference (ZINC)*, IEEE, 2017, pp. 60–63.

[168] S. Nasr, M. Iordache, and M. Petit, "Smart micro-grid integration in DC railway systems", in *IEEE PES Innovative Smart Grid Technologies, Europe*, Istanbul, Turkey: IEEE, Oct. 2014, pp. 1–6, ISBN: 978-1-4799-7720-8. DOI: 10.1109/ISGTEurope.2014.7028913.

[169] M. Bartłomiejczyk and M. Połom, "Possibilities for developing electromobility by using autonomously powered trolleybuses based on the example of gdynia", *Energies*, vol. 14, no. 10, 2021, ISSN: 1996-1073. DOI: 10.3390/en14102971. [Online]. Available: https://www.mdpi.com/1996-1073/14/10/2971.

[170] M. Bartłomiejczyk and M. Połom, "Sustainable use of the catenary by trolleybuses with auxiliary power sources on the example of gdynia", *Infrastructures*, vol. 6, no. 4, 2021, ISSN: 2412-3811. DOI: 10.3390/infrastructures6040061. [Online]. Available: https://www.mdpi.com/2412-3811/6/4/61.

[171] F. Bergk, K. Biemann, U. Lambrecht, R. Pütz, and H. Landinger, "Potential of inmotion charging buses for the electrification of urban bus lines", *Journal of Earth Sciences and Geotechnical Engineering*, vol. 6, pp. 347–362, 2016.

[172] R. Beekman and R. Van Den Hoed, "Operational demands as determining factor for electric bus charging infrastructure", pp. 1–6, 2016.

[173] O. Vilppo and J. Markkula, "Feasibility of electric buses in public transport", *World Electric Vehicle Journal*, vol. 7, no. 3, pp. 357–365, 2015, ISSN: 2032-6653. DOI: 10.3390/wevj7030357. [Online]. Available: https://www.mdpi.com/2032-6653/7/3/357.

[174] A. Randhahn and T. Knote, "Deployment of charging infrastructure for battery electric buses", pp. 169–183, 2020.

[175] UITP, "In motion charging: Innovative trolleybus", May 2019. [Online]. Available: https://cms.uitp.org/wp/wp-content/uploads/2021/01/Knowledge-Brief-Infrastructure-May-2019-FINAL.pdf.

[176] K. Electric, "Articulated battery bus with imc500", kiepe.knorr-bremse.com/media/prospekte

[177] M. Bartłomiejczyk, "Practical application of in motion charging: Trolleybuses service on bus lines", May 2017. DOI: 10.1109/EPE.2017.7967239.

[178] D. Baumeister, M. Salih, M. Wazifehdust, *et al.*, "Modelling and simulation of a public transport system with battery-trolleybuses for an efficient e-mobility integration", 2017, 1st E-Mobility Power System Integration Symposium.

[179] V. Kiepe, "Articulated electric bus with in motion charging (imc)",

[180] London Reconnections, *New interurban long range trolleybus line for arnhem: Details*, https://www.londonreconnections.com/.

[181] M. Wołek, M. Wolański, M. Bartłomiejczyk, O. Wyszomirski, K. Grzelec, and K. Hebel, "Ensuring sustainable development of urban public transport: A case study of the trolleybus system in gdynia and sopot (poland)", *Journal of Cleaner Production*, vol. 279, p. 123 807, 2021, ISSN: 0959-6526. DOI: https://doi.org/10.1016/j.jclepro.2020.123807. [Online]. Available: https://www.sciencedirect.com/science/article/pii/S095965262033852X.

[182] M. Bartłomiejczyk and M. Połom, "The impact of the overhead line's power supply system spatial differentiation on the energy consumption of trolleybus transport: Planning and economic aspects", *Transport*, vol. 32, no. 1, pp. 1–12, 2017.

[183] I. Diab, R. Eggermont, G. R. C. Mouli, and P. Bauer, "An Adaptive Battery Charging Method for the Electrification of Diesel or CNG Buses as In-Motion-Charging Trolleybuses", *IEEE Transactions on Transportation Electrification*, pp. 1–1, 2023, doi10.1109/TTE.2023.3243022. DOI: 10.1109/TTE.2023.3243022.

[184] M. Pagliaro and F. Meneguzzo, "Electric bus: A critical overview on the dawn of its widespread uptake", *Advanced Sustainable Systems*, vol. 3, no. 6, p. 1 800 151, 2019.

[185] Green Zones EU, *E-buses fail in the cold – green-zones.eu*, urlhttps://www.green-zones.eu/en/blog-news/e-buses-fail-in-the-cold, (Accessed on 06/02/2022), Feb. 2021.

[186] B. Freudenberg and T. Knote, "Eberswalde final use case report", May 2015, Eliptic Project.

[187] M. Bartlomiejczyk, A. Jagiello, M. Wolek, M. Woronowicz, and O. Wyszomirski, "Gdynia final use case report", Jun. 2018, Eliptic Project.

[188] A. Náday, I. Tibor Tóth, Z. Á. Németh, and N. Újhelyi, "Szeged final use case report", Jun. 2018, Eliptic Project.

[189] A. Náday, I. T. Tóth, D. Z. Á. Németh, and N. Újhelyi, "Szeged final use case report", Eliptic Project, Tech. Rep., Jun. 2018. [Online]. Available: `http://www.eliptic-project.eu/sites/default/files/ELIPTIC%5C%20D2.20%5C%20Szeged%5C%20Final%5C%20Use%5C%20Case%5C%20Report.pdf`.

[190] UITP, *Large Scale Bus Electrification: The Impact on Business Models*, cms.uitp.org/wp/wp-content/uploads/2021/07, (Accessed on 06/02/2022), Jul. 2021.

[191] A. L. Rodrigues and S. R. Seixas, "Battery electric buses and their implementation barriers: Analysis and prospects for sustainability", *Sustainable Energy Technologies and Assessments*, vol. 51, p. 101 896, 2022.

[192] M. Bartłomiejczyk and R. Kołacz, "The reduction of auxiliaries power demand: The challenge for electromobility in public transportation", *Journal of Cleaner Production*, vol. 252, p. 119 776, 2020.

[193] Z. Ma, J. Xing, M. Mesbah, and L. Ferreira, "Predicting short-term bus passenger demand using a pattern hybrid approach", *Transportation Research Part C: Emerging Technologies*, vol. 39, pp. 148–163, 2014.

[194] R. Liu and S. Sinha, "Modelling urban bus service and passenger reliability.", 2007.

[195] Z. Wang, F. Chen, and J. Li, "Implementing transformer nodal admittance matrices into backward/forward sweep-based power flow analysis for unbalanced radial distribution systems", *IEEE Transactions on Power Systems*, vol. 19, no. 4, pp. 1831–1836, 2004.

[196] P. C. Sen, *Principles of electric machines and power electronics*. John Wiley & Sons, 2007.

[197] R. T. Birge, "The propagation of errors", *American Journal of Physics*, vol. 7, no. 6, pp. 351–357, 1939.

[198] C. Europea, *Together towards competitive and resource-efficient urban mobility*, 2013.

[199] C. Wang, W. Cai, X. Lu, and J. Chen, "CO2 mitigation scenarios in China's road transport sector", *Energy Conversion and Management*, vol. 48, no. 7, pp. 2110–2118, 2007, ISSN: 0196-8904.

[200] G. B. Alliance, "A vision for a sustainable battery value chain in 2030: Unlocking the full potential to power sustainable development and climate change mitigation", in *Geneva, Switzerland: World Economic Forum*, 2019.

[201] Koninklijk Nederlands Meteorologisch Instituut (KNMI), *Meteonorm world solar irradiance data*, 2019. [Online]. Available: `https://meteonorm.com`.

[202] A. H. Smets, K. Jäger, O. Isabella, R. van Swaaij, and M. Zeman, *Solar Energy: The physics and engineering of photovoltaic conversion technologies and systems*. UIT, 2016.

[203] J. Jonkman, S. Butterfield, W. Musial, and G. Scott, "Definition of a 5-mw reference wind turbine for offshore system development", National Renewable Energy Lab.(NREL), Golden, CO (United States), Tech. Rep., 2009.

[204] T. R. Oke, *Boundary layer climates*. Routledge, 2002.

[205] M. Bartłomiejczyk and M. Połom, "The impact of the overhead line's power supply system spatial differentiation on the energy consumption of trolleybus transport: Planning and economic aspects", *Transport*, vol. 32, no. 1, pp. 1–12, 2017, ISSN: 1648-4142.

[206] IEA, *Data overview, electricity statistics*, Web Page, 2020. [Online]. Available: `https://www.iea.org/subscribe-to-data-services/electricity-statistics`.

[207] M. Bartłomiejczyk and R. Kołacz, "The reduction of auxiliaries power demand: The challenge for electromobility in public transportation", *Journal of Cleaner Production*, vol. 252, p. 119 776, 2020, ISSN: 0959-6526.

[208] M. Bartłomiejczyk, "Potential application of solar energy systems for electrified urban transportation systems", *Energies*, vol. 11, no. 4, p. 954, 2018.

[209] M. Wazifehdust, D. Baumeister, M. Salih, *et al.*, "Potential analysis for the integration of renewables and ev charging stations within a novel lvdc smart-trolleybus grid", 2019, ISSN: 2960241509.

[210] Y. Liu, M. Chen, Z. Cheng, Y. Chen, and Q. Li, "Robust energy management of high-speed railway co-phase traction substation with uncertain pv generation and traction load", *IEEE Transactions on Intelligent Transportation Systems*, 2021.

[211] X. Zhu, H. Hu, H. Tao, and Z. He, "Stability analysis of pv plant-tied mvdc railway electrification system", *IEEE Transactions on Transportation Electrification*, vol. 5, no. 1, pp. 311–323, 2019.

[212] A. Zahedmanesh, K. M. Muttaqi, and D. Sutanto, "A cooperative energy management in a virtual energy hub of an electric transportation system powered by pv generation and energy storage", *IEEE Transactions on Transportation Electrification*, 2021.

[213] S. Kratz, A. Schmidt, B. Krueger, R. Wegener, and S. Soter, "Power supply of a short-range public transportation system based on photovoltaics-potential analysis and implementation", in *2019 IEEE 46th Photovoltaic Specialists Conference (PVSC)*, IEEE, 2019, pp. 3077–3081.

[214] M. Salih, M. Koch, D. Baumeister, M. Wazifehdust, P. Steinbusch, and M. Zdrallek, "Adapted newton-raphson power flow method for a dc traction network including non-receptive power sources and photovoltaic systems", in *2019 IEEE PES Innovative Smart Grid Technologies Europe (ISGT-Europe)*, IEEE, 2019, pp. 1–5.

[215] N. Brinkel, M. Gerritsma, T. AlSkaif, *et al.*, "Impact of rapid pv fluctuations on power quality in the low-voltage grid and mitigation strategies using electric vehicles", *International Journal of Electrical Power and Systems, Energy*, vol. 118, p. 105 741, 2020, ISSN: 0142-0615.

[216] S. Kratz, B. Krueger, R. Wegener, and S. Soter, "Integration of photovoltaics into a smart trolley system based on sic-technology", in *2018 IEEE 7th International Conference on Power and Energy (PECon)*, IEEE, 2018, pp. 168–173.

[217] S. Wright, "Correlation and causation", 1921.

[218] B. Wu, S. Liu, W. Zhu, M. Yu, N. Yan, and Q. Xing, "A method to estimate sunshine duration using cloud classification data from a geostationary meteorological satellite (fy-2d) over the heihe river basin", *Sensors*, vol. 16, no. 11, p. 1859, 2016.

[219] M. Bartłmiejczyk and L. Jarzebowicz, "Utility analysis and rating of energy storages in trolleybus power supply system", in *2020 Zooming Innovation in Consumer Technologies Conference (ZINC)*, IEEE, 2020, pp. 237–241.

[220] M. Ogasa, "Application of energy storage technologies for electric railway vehicles—examples with hybrid electric railway vehicles", *IEEJ Transactions on Electrical and Electronic Engineering*, vol. 5, no. 3, pp. 304–311, 2010.

[221] G. Krajačić, N. Duić, Z. Zmijarević, B. V. Mathiesen, A. A. Vučinić, and M. da Graça Carvalho, "Planning for a 100% independent energy system based on smart energy storage for integration of renewables and co2 emissions reduction", *Applied thermal engineering*, vol. 31, no. 13, pp. 2073–2083, 2011.

[222] I. Diab, G. R. C. Mouli, and P. Bauer, "Opportunity Charging of Electric Buses Directly from a DC Metro Catenary and Without Storage", in *2023 IEEE International Conference on Electrical Systems for Aircraft, Railway, Ship Propulsion and Road Vehicles International Transportation Electrification Conference (ESARS-ITEC)*, 2023, pp. 1–6. DOI: 10.1109/ESARS-ITEC57127.2023.10114818.

[223] M. Bartłomiejczyk and S. Mirchevski, "Reducing of energy consumption in public transport—results of experimental exploitation of super capacitor energy bank in gdynia trolleybus system", in *2014 16th International Power Electronics and Motion Control Conference and Exposition*, IEEE, 2014, pp. 94–101.

[224] V. Brazis, L. Latkovskis, and L. Grigans, "Simulation of trolleybus traction induction drive with supercapacitor energy storage system", *Latvian Journal of Physics and Technical Sciences*, vol. 47, no. 5, pp. 33–47, 2010.

[225] X. Qu, L. Tian, J. Li, C. Lou, and T. Jiang, "Research on charging and discharging strategies of regenerative braking energy recovery system for metro flywheel", in *2021 3rd Asia Energy and Electrical Engineering Symposium (AEEES)*, IEEE, 2021, pp. 1087–1095.

[226] P. Jandura, A. Richter, and Ž. Ferková, "Flywheel energy storage system for city railway", in *2016 International Symposium on Power Electronics, Electrical Drives, Automation and Motion (SPEEDAM)*, IEEE, 2016, pp. 1155–1159.

[227] M. Bartłomiejczyk and S. Mirchevski, "Reducing of energy consumption in public transport—results of experimental exploitation of super capacitor energy bank in gdynia trolleybus system", in *2014 16th International Power Electronics and Motion Control Conference and Exposition*, IEEE, 2014, pp. 94–101.

[228] M. Wołek, M. Wolański, M. Bartłomiejczyk, O. Wyszomirski, K. Grzelec, and K. Hebel, "Ensuring sustainable development of urban public transport: A case study of the trolleybus system in gdynia and sopot (poland)", *Journal of Cleaner Production*, vol. 279, p. 123 807, 2021.

[229] M. Yan, M. Li, H. He, J. Peng, and C. Sun, "Rule-based energy management for dual-source electric buses extracted by wavelet transform", *Journal of Cleaner Production*, vol. 189, pp. 116–127, 2018.

[230] Y. Han, Q. Li, T. Wang, W. Chen, and L. Ma, "Multisource coordination energy management strategy based on soc consensus for a pemfc–battery–supercapacitor hybrid tramway", *IEEE Transactions on Vehicular Technology*, vol. 67, no. 1, pp. 296–305, 2017.

[231] F. Ciccarelli, D. Iannuzzi, K. Kondo, and L. Fratelli, "Line-voltage control based on wayside energy storage systems for tramway networks", *IEEE Transactions on power electronics*, vol. 31, no. 1, pp. 884–899, 2015.

[232] K. van der Horst, I. Diab, G. R. C. Mouli, and P. Bauer, "Methods for increasing the potential of integration of ev chargers into the dc catenary of electric transport grids: A trolleygrid case study", *eTransportation*, p. 100 271, 2023.

[233] T. Brand, *Arnhems Trolleybusnet Onderzoek Bovenleidingnet*, Oct. 2012.

[234] CENELEC, *EN 50163 - Railway applications - Supply voltages of traction systems*, Nov. 2004.

[235] W. Vermeer, G. R. Chandra Mouli, and P. Bauer, "A multi-objective design approach for pv-battery assisted fast charging stations based on real data", in *2022 IEEE Transportation Electrification Conference Expo (ITEC)*, 2022, pp. 114–118. DOI: 10.1109/ITEC53557.2022.9814016.

[236] G. R. Chandra Mouli, J. Schijffelen, M. van den Heuvel, M. Kardolus, and P. Bauer, "A 10 kw solar-powered bidirectional ev charger compatible with chademo and combo", *IEEE Transactions on Power Electronics*, vol. 34, no. 2, pp. 1082–1098, 2019. DOI: 10.1109/TPEL.2018.2829211.

[237] O. Sadeghian, A. Oshnoei, B. Mohammadi-Ivatloo, V. Vahidinasab, and A. Anvari-Moghaddam, "A comprehensive review on electric vehicles smart charging: Solutions, strategies, technologies, and challenges", *Journal of Energy Storage*, vol. 54, p. 105 241, 2022.

[238] D. Danner and H. de Meer, "Quality of service and fairness for electric vehicle charging as a service", *Energy Informatics*, vol. 4, pp. 1–20, 2021.

[239] M. Erol-Kantarci, J. H. Sarker, and H. T. Mouftah, "Quality of service in plug-in electric vehicle charging infrastructure", in *2012 IEEE International Electric Vehicle Conference*, IEEE, 2012, pp. 1–5.

[240] ELAAD, *ElaadNL Open Datasets for Electric Mobility Research*, platform.elaad.io/analyses.

[241] IEA, *Approximately 100 million households rely on rooftop solar PV by 2030 – Analysis*, urlhttps://www.iea.org/reports/approximately-100-million-households, (Accessed on 03/22/2023), Sep. 2022.

[242] B. Asare-Bediako, W. Kling, and P. Ribeiro, "Future residential load profiles: Scenario-based analysis of high penetration of heavy loads and distributed generation", *Energy and Buildings*, vol. 75, pp. 228–238, 2014, ISSN: 0378-7788. DOI: https://doi.org/10.1016/j.enbuild.2014.02.025. [Online]. Available: https://www.sciencedirect.com/science/article/pii/S037877881400139X.

[243] R. Gupta, A. Pena-Bello, K. N. Streicher, *et al.*, "Spatial analysis of distribution grid capacity and costs to enable massive deployment of pv, electric mobility and electric heating", *Applied Energy*, vol. 287, p. 116 504, 2021, ISSN: 0306-2619. DOI: https://doi.org/10.1016/j.apenergy.2021.116504. [Online]. Available: https://www.sciencedirect.com/science/article/pii/S0306261921000623.

[244] L. Langer and T. Volling, "An optimal home energy management system for modulating heat pumps and photovoltaic systems", *Applied Energy*, vol. 278, p. 115 661, 2020, ISSN: 0306-2619. DOI: https://doi.org/10.1016/j.apenergy.2020.115661. [Online]. Available: https://www.sciencedirect.com/science/article/pii/S0306261920311570.

[245] W. Wei, C. Gu, D. Huo, S. Le Blond, and X. Yan, "Optimal borehole energy storage charging strategy in a low carbon space heat system", *IEEE Access*, vol. 6, pp. 76 176–76 186, 2018. DOI: 10.1109/ACCESS.2018.2883798.

[246] Centraal Bureau voor de Statistiek, *Energy consumption private dwellings by type of dwelling and regions, 2016*. [Online]. Available: http://statline.%20cbs.%20nl/StatWeb/publication.

[247] Vereniging Nederlandse Energie- Data Uitwisseling (NEDU), urlhttp://nedu.nl.

[248] R. O. Oliyide and L. M. Cipcigan, "The impacts of electric vehicles and heat pumps load profiles on low voltage distribution networks in great britain by 2050", in *International Multidisciplinary Research Journal*, vol. 11, 2021, pp. 30–45. DOI: 10.25081/imrj.2021.v11.7308.

[249] Dimplex. “Project planning manual heating and cooling with heat pumps”, Dimplex. (Feb. 11, 2008), [Online]. Available: https://www.dimplex-partner.de/fileadmin/dimplex/downloads/planungshandbuecher/en.

[250] M. Bartłomiejczyk, “Practical application of in motion charging: Trolleybuses service on bus lines”, in *2017 18th International Scientific Conference on Electric Power Engineering (EPE)*, IEEE, 2017, pp. 1–6.

[251] H. Fitzová and M. Matulová, “Comparison of urban public transport systems in the Czech Republic and Slovakia: Factors underpinning efficiency”, *Research in Transportation Economics*, vol. 81, p. 100 824, 2020.

[252] A. Kołoś and J. Taczanowski, “The feasibility of introducing light rail systems in medium-sized towns in Central Europe”, *Journal of Transport Geography*, vol. 54, pp. 400–413, 2016.

[253] L. Borowik and A. Cywiński, “Modernization of a trolleybus line system in Tychy as an example of eco-efficient initiative towards a sustainable transport system”, *Journal of Cleaner Production*, vol. 117, pp. 188–198, 2016.

[254] M. Bartłomiejczyk and M. Połom, “Spatial aspects of tram and trolleybus supply system”, *Proceedings of the 8th International Scientific Symposium on Electrical Power Engineering, ELEKTROENERGETIKA 2015*, pp. 211–215, 2015.

[255] Electric Mobility Europe, *Trolley:2.0 leaflet: New developments of modern trolleybus systems for smart cities*, 2018. [Online]. Available: https://www.trolleymotion.eu/trolley2-0/.

[256] M. Salin, D. Baumeister, M. Wazifehdust, *et al.*, “Impact assessment of integrating novel battery-trolleybuses, pv units and ev charging stations in a dc trolleybus network”, in *2nd E-Mobility Power System Integration Symposium | Stockholm, Sweden | 15 October 2018*, Oct. 2018.

[257] KiepeElectric, *DOUBLE-ARTICULATED ELECTRIC BUS WITH IN MOTION CHARGING LINZ, AUSTRIA*.

[258] P. Jandura, J. Kubín, and L. Hubka, “Electric energy monitoring for applying an energy storage systems in trolleybus dc traction”, in *2017 IEEE International Workshop of Electronics, Control, Measurement, Signals and their Application to Mechatronics (ECMSM)*, May 2017, pp. 1–6. DOI: 10.1109/ECMSM.2017.7945904.

[259] D. Turner and F. De Guzman, “San francisco muni trolleybus propulsion tests: The results”, *IEEE Transactions on Vehicular Technology*, vol. 35, no. 3, pp. 118–131, 1986. DOI: 10.1109/T-VT.1986.24080.

[260] European Commission, “Proposal for A Directive of the European Parliament and of the Council amending Directive 2009/33/EC on the promotion of clean and energy-efficient road transport vehicles”, pp. 1–76, 2017. [Online]. Available: https://eur-lex.europa.eu/legal-content/EN/TXT/?uri=CELEX%3A52017PC0653.

[261] B. Heid, M. Kässer, T. Müller, and S. Pautmeier, *The urban electric bus market | McKinsey*, 2020. [Online]. Available: https://www.mckinsey.com/industries/automotive-and-assembly/our-insights/fast-transit-why-urban-e-buses-lead-electric-vehicle-growth.

[262] M. Bartłomiejczyk, "Modern technologies in energy demand reducing of public transport — practical applications", in *2017 Zooming Innovation in Consumer Electronics International Conference (ZINC)*, May 2017, pp. 64–69. DOI: 10.1109/ZINC.2017.7968665.

[263] D. Patil, M. K. Mcdonough, J. M. Miller, B. Fahimi, and P. T. Balsara, "Wireless power transfer for vehicular applications: Overview and challenges", *IEEE Transactions on Transportation Electrification*, vol. 4, no. 1, pp. 3–37, 2017.

[264] B. J. Limb, Z. D. Asher, T. H. Bradley, *et al.*, "Economic viability and environmental impact of in-motion wireless power transfer", *IEEE Transactions on Transportation Electrification*, vol. 5, no. 1, pp. 135–146, 2018.

[265] Liandon, "Connexxion - Arnhems trolleybusnet Onderzoek bovenleidingnet", Tech. Rep., 2012.

[266] S. Xie, X. Hu, Z. Xin, and L. Li, "Time-efficient stochastic model predictive energy management for a plug-in hybrid electric bus with an adaptive reference state-of-charge advisory", *IEEE Transactions on Vehicular Technology*, vol. 67, no. 7, pp. 5671–5682, 2018. DOI: 10.1109/TVT.2018.2798662.

[267] Power Research Electronics B.V., *25kW Charger Datasheet*, http://www.pr-electronics.nl/media/documenten/25kW_Charger_datasheet_V13.180417.194545.pdf, (Accessed on 05/29/2023).

LIST OF PUBLICATIONS

JOURNAL PAPERS

1. "A Complete DC Trolleybus Grid Model With Bilateral Connections, Feeder Cables, and Bus Auxiliaries," I Diab, A Saffirio, GR Chandra Mouli, AS Tomar and P Bauer, in **IEEE Transactions on Intelligent Transportation Systems**, vol. 23, no. 10, pp. 19030-19041, Oct. 2022

2. "Placement and Sizing of Solar PV and Wind Systems in Trolleybus Grids", I Diab, B Scheurwater, A Saffirio, GR Chandra-Mouli, P Bauer **Journal of Cleaner Production** 352, 131533

3. "A Simple Method for Sizing and Estimating the Performance of PV Systems in Trolleybus Grids", I Diab, A Saffirio, GR Chandra-Mouli, P Bauer, **Journal of Cleaner Production** 384, 135623

4. "An Adaptive Battery Charging Method for the Electrification of Diesel or CNG Buses as In-Motion-Charging Trolleybuses," I Diab, R Eggermont, GR Chandra Mouli and P Bauer, in **IEEE Transactions on Transportation Electrification**

5. "Methods for Increasing the Potential of Integration of EV Chargers into the DC Catenary of Electric Transport Grids: A Trolleygrid Case Study," K vd Horst, I Diab, GR Chandra-Mouli, P Bauer, in **eTransportation**, 2023, p.100271

6. "A Traction Substation State Estimator for Integrating Smart Loads in Transport Grids Without Additional Sensors: Theory and Case Studies," I Diab, GR Chandra-Mouli, P Bauer, in **IEEE Transactions on Intelligent Transportation Systems**

7. A Shared PV System for Transportation and Residential Loads to Reduce Storage and Curtailment: Two Trolleygrid Case Studies. I Diab, N Damianakis, GR Chandra-Mouli, P Bauer, *Submitted*

8. Comparison of On-board and Stationary Storage Solutions for Trolleygrids with PV Systems. I Diab, K Giitsidis, GR Chandra-Mouli, P Bauer, *Submitted*

9. Comparison of On-board, Stationary, and Hybrid Storage Solutions in Trolleygrids. I Diab, GR Chandra-Mouli, P Bauer, *Submitted*

10. A Valley-Charging Method for the Electrification of Buses as IMC Trolleybuses in Congested Grid Areas. M Bistřický, I Diab, GR Chandra-Mouli, P Bauer, *Submitted*

11. Designing and Assessing the Sustainable, Multi-Functional, and Multi-Stakeholder Trolleygrids of the Future. I Diab, GR Chandra-Mouli, P Bauer, *Submitted*

12. The Next Generation of Sustainable, Multi-functional Trolleybus Grids: A Review of Trends, Research, and Challenges. I Diab, K Giitsidis, M Bistřický, K vd Horst, GR Chandra-Mouli, P Bauer, *Submitted*

CONFERENCE PAPERS

THIS THESIS

1. "Toward a better estimation of the charging corridor length of in-motion-charging trolleybuses," I. Diab, G. R. Chandra Mouli, and P. Bauer, in 2022 IEEE Transportation Electrification Conference & Expo (ITEC), 2022, pp.557–562

2. "Increasing the integration potential of EV chargers in DC trolleygrids: A bilateral substation-voltage tuning approach," I. Diab, G. R. C. Mouli, and P. Bauer, in 2022 International Symposium on Power Electronics, Electrical Drives, Automation and Motion (SPEEDAM), 2022, pp.264–269.

3. "A Review of the Key Technical and Non-Technical Challenges for Sustainable Transportation Electrification: A Case for Urban Catenary Buses," I. Diab, G. R. Chandra Mouli, and P. Bauer, in Proceedings of the 20th IEEE International Power Electronics and Motion Control Conference (IEEE-PEMC 2022), September 2022

OUTSIDE THIS THESIS

1. "Opportunity Charging of Electric Buses Directly from a DC Metro Catenary and Without Storage," I Diab, GR Chandra Mouli and P Bauer, in 2023 IEEE International Conference on Electrical Systems for Aircraft, Railway, Ship Propulsion and Road Vehicles & International Transportation Electrification Conference (ESARS-ITEC), Venice, Italy, 2023, pp. 1-6

2. "Increasing the Braking Energy Recuperation in Electric Transportation Grids Without Storage," I Diab, GR Chandra Mouli and P Bauer, in 2023 IEEE Transportation Electrification Conference & Expo (ITEC), Detroit, MI, USA, 2023, pp. 1-5

PRESENTATIONS AND OUTREACH

1. Invited to design and teach a one-week course on Trolleygrids of the Future (*Business NOT as usual*) to a group of 20 European students in the spring 2022 edition of the Board of European Students of Technology (BEST) course in Delft.

2. Invited to submit and present a paper on the Technical and Non-Technical Challenges for Sustainable Transportation Electrification during one of the plenary sessions of the 20th IEEE International Power Electronics and Motion Control Conference (IEEE-PEMC 2022) in Brasov, Romania.

3. Invited to be an external panel speaker on Challenges for Sustainable Transportation Electrification at the e-SMART final event within the Next Generation Mobility in May 2022 in Turin, Italy.

4. Invited to present on the Challenges for Sustainable Transportation Electrification to sustainability and/or innovation member(s) of Ricerca sul Sistema Energetico (RSE, Milan, Italy), Heineken (Amsterdam, The Netherlands), HTM Personenvervoer (The Hague public transport company, The Hague, The Netherlands), and coachbuilder and manufacturer of buses Van Hool (Online).

5. Invited to present on the Possibilities for Sustainable Electrification in Trolleygrids at the e-Webinar "Multipurpose Usage of Public Transport Infrastructure" of the EfficienCE project (Online, December 2021).

6. Invited to present on the Technical and Non-Technical Challenges for Sustainable Transportation Electrification at the AMS Institute Conference in February 2022.

7. Invited to present on the Transportation Grids of the Future at the Pro-Rail offices (Amersfoort, February 2022).

8. Invited to submit a magazine article on the trolleygrids of the future to the MAXWELL magazine of the electrical engineering faculty at TU Delft.

ACKNOWLEDGEMENTS

It takes a village to raise a child, but it surely takes a small town to support one through a PhD. I would like to express my gratitude to everyone who has been part of this journey.

First, the supervisory team. I would like to sincerely thank my promotor, Prof. Pavol Bauer. Thank you first of all for taking a chance on that kid who came with his mechanical and energy background and insisted on a PhD in Electrical Engineering. I hope I've made you proud in the end. Thank you as well for your valuable guidance, and for pushing me and my work on many occasions onto the national and international podiums.
Dear Gautham, I will be forever humbled by your patience and understanding, and your genuine appreciation of those around you. I am amazed by how you always had an open door and ear (despite your incredibly busy schedule) and treated everyone who came to you with interest, patience, and respect. You always show us that we all have something worthy of your time and learning, and it's beautiful what that does to one's confidence. From you, I have learned some of my most valuable lessons in separating Science from Engineering (finally!), time management, and teamwork.
I would also like to express my gratitude to all the members of my defense committee who have given me their valuable feedback (to the typos level, sometimes!) and agreed to be part of my journey.
A very grateful thank-you goes to Martijn Wackers for his help and feedback during -and long after- the course on writing a dissertation. Martijn, you are a lesson in generosity.

An immigrant's life is sadly never linear, and to be here I also needed to jump through some bureaucratic loops. I can't describe my gratitude to Prof Bauer, Prof Peter Palensky, and Dr René van der Swaaij for offering me the opportunity to stay in the country 2018 and work at the TU Delft. I will forever be angry at how effortlessly this whole life could have passed me by, and the unfairness of this border-frenzied world.
For that, I would also like to thank Dr. David Vermaas for trying so hard to carve me a place in this world; from being his TA when I needed work, to him trying the impossible to get me a PhD with him or with colleagues, and then even trying to find me a spot at his start-up. David, your kindness was never forgotten.
René, I am so grateful that my time in Delft in your SET program and your Online Courses guidance has come to a full-circle to see you on my committee on my Ph.D. defense day.

Working on the Online Courses was the final technical stretch I needed to complete my on-the-job bridging program (or apprentice) in Electrical Engineering. For that, I also owe an immense debt of gratitude to the late Prof Braham (Bram) Ferreira. Thank you for your patience, your radiating enthusiasm, and the engineering books and private lessons you have given me. You always joked that we had the same name, and I wish I'd one day bring it to a fraction of what you've paved ahead.

Thank you, Prof Thiago Batista Soeiro for your teaching as well, and for valuing my work and giving me confidence. Not once did I feel incompetent or that I lacked knowledge around you, but rather that I was inviting a friendly technical conversation from you. That is the true natural gift of teaching.
Finally, while this incredible group of people pushed me through the last stages of my Electrical Engineering transformation, I owe all of the motivation to go through it to Dr Jelena Popović, who was the first and only one to never doubt my cross-disciplinary jump or its motivation and offered so much of her time to have me finally pass the Electric Power Conversion course. Jelena, you are the role model in patience and generosity that I hope to bring into my teaching. I never forgot this.

In teaching, I have had the immense pleasure of working with such a vibrant and enthusiastic group of master students. I will always cherish Stella's enthusiasm and motivation that push you to offer more, Erné's persistent and unbending arguments that push you to communicate better, Habib's curiosity that pushes you to teach better, and Khalid's independence that pushes you to calibrate your management better.
To another group of students, I owe literal pages of this book as their incredible work became the basis of many journals and chapters.
Thank you, Bram Scheurwater, for your patience in being the first student when I barely understood the topic myself. Our work together challenged our whole vision of the project and diverted the research plan of my Ph.D on many occasions. Thank you for both that amazing work and for the flexibility in rethinking your thesis topic.
Thank you, Rik Eggermont, for setting up the basics of the IMC work. You have taken the project way beyond what we had originally planned and took so many overwhelming initiatives along the way that always left me in shock at the workload you took on. The world of IMC owes you a load of gratitude.
Thank you, Alice Saffirio, for so much more than I could count. I can clearly see the clear-cut division in my work before and after your thesis. You tied so many knots from previous work, offered so much during your thesis, and left so much to the future students to build on. You were so independent but also so involved and communicative that you always felt much more like a colleague than a student. Thank you a thousand times.
Then came the amazing trio: Kostas, Marek, and Koen. You three were definitely an example of the synergy that a solid research team can have!
Konstantinos Giitsidis, to say I was challenged by you would be an understatement! Thank you for always keeping me in check with your questions and digging up parts of my old research to make me prove it again to you. You brought back the motivation and the internal fire of the early research days that I had not had in years. I wish all PhDs an ego-cracking student like you in their third year! Thank you also for the immeasurable work on on-board storage and the comparison of storage technologies, and thank you for still staying in touch and randomly showing up at the office with Greek sweets.
Thank you, Marek Bistřický, for all you've done for the other half of the IMC chapter. The topic is lucky to have had two brilliant students like you and Rik. Thank you for your patience and your flexibility in doing your work as you waited for me to develop the grid estimator in parallel and figure it out on-the-go. I hope you would go back one day and

do that PhD on IMC trolleybuses.
And finally, thank you Koen van der Horst, for so much. You refused to be handed over blocks of codes to run and spent days understanding it line by line and pointing out improvement points. Your work topic was particularly turbulent as we kept receiving new information and needed to re- and re- and re-adjust our simulations. Your forward thinking and modularity in designing your code and output saved the day. Our work on EV is one of the key take-away of this thesis and the underlying thought of my postdoc research. I hope we soon get to see EV chargers in all transport grids.

All this work could obviously not have been done without the data and support of Abhishek Singh Tomar (HAN University of Applied Sciences), and Hans Aldenkamp and Niek Limburg from the trolley operator of Arnhem, Connexxion. I hope we continue to collaborate on many projects.

A very special thanks goes to Dr. Mikołaj Bartłomiejczyk. When I first joined the trolley project, a year into its launch, Mikołaj's work on trolleybuses gave me a solid foundation to catch up with years of trolleygrid and IMC knowledge. Mikołaj, you are an open and generous book, and I am immensely honored to have you on my committee and to have you go through my chapters and give them the technical scrutiny they need. I never would have thought that my work could reach a point of collaboration, and I can't wait for our future IMC publications.

I also would like to thank Rudolf Paternost for our ongoing collaboration. Although we started too late for our work to be included in this book, you have given me the motivation to write it better since I saw with you that my journey with trolleybuses is not over yet. I look forward to all of our future collaborations.

With the years working at the department and then the PhD, I have seen more than my share of PhD colleagues and staff.
To go back in time, Thank you, Nishant, for your (dearly missed) sustainability ethics, and for the countless hours of playing darts in your office to let the steam out. Wazzaaabi, your presence is missed daily -especially since your poster is hanging in my office.
Thank you, Victor, first of all for giving me my favorite defense committee story that I repeat three times a day, but surely as well for your (equally dearly missed) warmth and friendship at the office.
To counter that warmth and happiness, let's mention the original Mean Girls crew of Soumya, Nils, Udai, and Pavel! I enjoyed so much how tight-knit the group was back then, and all the dinners and parties and events we went to. Thank you for setting the bar so high for all of us (except you in MSc supervision, Soumya), and for the thousand and one jokes on SET and me not having a PhD. Wow.. joke is over now, I guess?
Mladen and Laurens you were both part of the old crew but also still around. Mladen, promise me you will never choose a career in politics -at least not until you change your opinions on taxes and the housing markets! But thank you for being a good friend in and out of the office.
Laurens, I am happy that we have found each other in the same field again, and thank

you always for keeping me in the Dutch transport loop! I look forward to what collaborations the future will bring!
Jianning, Zian, and Gautam Rituraj somehow we always end up meeting in the coffee room! Thank you for all your uplifting conversations, and always being ready to listen and to share. I am always happier after having talked to you.
Aditya, we have been through so many ups and downs, but I am glad we came out of it better. I have seen you change and grow so much over the years, and your students are lucky to have you. (P.S: Nefeli says hi).

To the more recent and current crew. Marco, thank you for always playing the devil's advocate and for that limoncello workshop that never happened in the end. And thank you for bringing Vitoria into our lives to shut Pierpaolo up! (Thank you, Vitoria!)
Pierpaolo! Baberabuppi! In your short time here I think you have pissed more people off than made friends with your Italian opinions! I can't wait to see you in Rome in your natural habitat.
Thank you Wiljan for joining in on the fun moments and the frustrated complaints, and for tolerating me barging into your office every 10 minutes to talk to Franci. Siddesh, thank you also for tolerating that in your office!
Thank you Wenli for all the good times, and I am glad we will overlap at the office again and make up for the past years.
Thank you Robin for all our office conversations and complaints, and for editing my Dutch summary of the thesis. Thank you Sachin for being a great office mate and tolerating me not tolerating you haha.
Miad! Let me tell you something! Thank you for your energy and for making us laugh till we cry, but then again be the most serious person when needed. Thank you Farshid for being the opposite of that, hahah.
Thank you Calvin for being our Dutch encyclopedia at all times, our go-to person in every lunch discussion. Thank you, Faezeh, for always being there to roll your eyes at Miad's insanity, and thank you Carina for being there to do that to anyone when needed!
Yang, thanks for all the fun times, and I wish we had had our PEMC-moment years earlier! Rohan, thanks for being my UNO buddy! We still need to play a match with physical cards.
Lyu, thank you for being so amazing. Your friendship is one of the gems I take away from this journey.
István, I don't think I would have survived Franci leaving the office if not for your willingness -no, your desire- to sit down and nag for hours.
Leila, thank you for bulldozing your friendship into our group! I am glad we managed to form this friendship despite the short time we had to overlap. Manfredo, Felipe, and Julian: learn this lesson from her! I look forward to knowing you guys even more.
Yunhe, we've had such a long journey since our MSc days, and I am happy for every day of it.
E-Alvaro, thank you for tolerating me first of all and thank you for taking half of the load of Daro from our e-shoulders. You do it the hard way, by listening, not as Joel does in offering us chocolate to leave. But thank you, Joel, for keeping us all sugared and happy.
Reza, you are a saint for being in the same office as Sohrab. Sohrab, you have a kindness

and generosity that we do not understand. I am sorry if you don't see it received, and I hope it never changes. (But no, your movie and history views, have to change).
Alejandro, you will do great things, and you can bet I'll be there to watch.

I am also lucky to have had a wonderful support network of friends.
Dhanashree, Nikos, and Daro, I only think of you as friends and not colleagues.
Dhana, you are one of the sweetest people I have come to know, and I am amazed, however, at how much anger can come out of you suddenly! Haha. Thank you for making every day at the office a bit sweeter.
Nikos, it's easy not to think of you as a colleague because you are never at the office! I am still grateful for the few moments we have had sharing the same office, but the plenty of moments we had off-campus and abroad. I know we'd at least always have Athens!
Daro, by the time you arrived I had given up on making new friendships at the office and was already a foot and a half out the door. Thank you for proving me wrong, and for being a bitter, nagging person to put both me and István to shame. I am sure we'll be 50 and still find a Dutch or academic thing to nag about as passionately as day 1.

I am also grateful for those who made me call this place home with their friendship: Nourjane, Kim, Pia, Anthony, Sinin, Julian (woof!), Mike, Elias, Sweylim, Jessica, Giacomo, Anas, Tomek, and Jeroen.
Felix, thank you for being there at the start of the journey. I hope life gives you the happiness you deserve and had given me.
Julia, I am so grateful for my mistake and my dodged bullet of meeting you at the conservatory! All the turmoil and disappointment of those years were okay if it meant meeting you.
Anikaaaaaaaa, I wish the world would stop and we'd be stuck in one of our biking trips to Rotterdam. To think we had so much energy! Thank you for your friendship.
Jan, Nick, and Bobby, you three are the tripod of my sanity. An equally-fragile tripod, but still thank you for your friendship, and for always being there to listen or to call me a drama queen, as necessary.
Ali, it's funny that we had to cross continents to develop this friendship. We've had enough of the same journey and struggles that I trust no continent would break that again, no matter where we head. King el bro.
Siva, I owe you enough of my Delft years to say I owe you for life. You were there for me whether I knew I needed you or not. You're surely one of the blessings I count on one hand for being here.
Dario Garuti, I am happy that distance did not come in between this friendship. Berlin is always home with you there, and I hope we get closer in distance again soon.
Dearest Yalda, I owe you the precious gift of the mind an the body. I couldn't have gone through the years of lonely lockdowns and stressing research without your healing genius. I carry your lessons with me every day as dearly as I carry your friendship.
Christine, I would tear up if I have to go through thank you for all that I need to thank you for. Thank you for some of the best years of this life, and how sad that we did not know it back then. I think of you in every "ui" I pronounce, every He-Marieke moment I think of, and every fond memory I have of the regentessekwartier. Thank you, thank

you, thank you.
And to the other side of the coin that is my Dutch family, thank you Wouter for your unconditional friendship and always being there to nerd out on opera or languages or science. I hope the world always gives you the kindness you give it.

Sharmila, I did not even thank you in the part of colleagues or friends, because you are family. I know that I am here because of you pushing me (and for me) when it was necessary, and for telling me to *laat het met rust en als het komt, komt van zelf binnen*. You do so much to every one of us that we both feel special but also can't understand how you do it all. You are the angel we all needed. Thank you so, so much.

Franci and Lucia, you are as family as a family gets. Lucia, you bright up any room you walk into, and catch-up with any technical discussion you've been in for three minutes. I owe you some of my most valuable lessons in life and relationships and regret the lockdowns that robbed us of years of being in the same office. We have to make up for it ourselves, no?
Franci, I cannot even imagine a world without your friendship, and that world should not exist. I truly couldn't have gone through this PhD without you being every day there at the office and pushing me and yet never needing to be pushed. Thank you for bringing me into your life, home, and family, and coming into mine. Thank you for cheering me on in and outside of the office (and speaking Italian to me!), and for being through every high and low. I would say that I hope to repay it, but I don't even wish for you to ever need it. You are a gift to this world, and I'm lucky to be in the first row.

To my beautiful Greek family, Efcharistó. Thank you Marianthi, Syno, and Jimmy for giving me a place I call home. Thank you, Fadia, for filling it with joy.

To my brother, Hicham, my support net without knowing it. If only you knew how much of my motivation and sense of safety and belonging relied on your unconditional love. I really should say it more often. Adina, thank you for your warmth and for always making me feel at home; you are home and family. I wish Alex would give the world the love you give him.

Giovanni, if it were easy to say, I would have said it a thousand times already. Thank you for the late nights and the early mornings and the missed weekends. Thank you for calming me down and for picking me up. Thank you for always being ready to pick up the missing pieces and to keep me focused, loved, and supported. Thank you for putting me first more times than I deserved. Thank you for making me a better person every day, a person to deserve having been gifted you.
Gio, looking back, I surely couldn't have done it so smoothly without you. And looking forward, I am confident there is no joy or purpose in doing it without you. Maw maw.

And in the end, and above all, to Cleo. For how could any of it be done without your abundance of unconditional love? Without the making of the man, -the well-read, well-

behaved, well-critical man- before the making of this book? How would I have done any of it without you having offered me the world, the universe, and then some? Without all the calls, the talks, the skypes, and the pushing and tugging and cheering? Without the "Ela!" and the "Finish this and then you can go eat bonbons and paint your toenails!". The decades of your love and care and wisdom and advice are what brought me here, and what will bring me anywhere.
I give this all to Cleo, my wings, and the wind beneath them. The guardian angel, the guardian, the angel. The godmother, the god, the mother. The Everything.

CURRICULUM VITÆ

Ibrahim DIAB

Born in March 1991 in Beirut, Lebanon. He received his Bachelor of Engineering (BE) in Mechanical Engineering from the American University of Beirut (AUB) in 2012 (Dean's honor list 2012) and a minor in Creative Writing. He then worked as a Measurement-While-Drilling engineer with Schlumberger in Saudi Arabia until August 2014, and as a research assistant at the AUB fluid mechatronics lab on wave-energy powered reverse osmosis for a short period thereafter.

In 2015, he received the TU Delft "Delft Research Initiative - Energy" full scholarship and joined the Electrical Sustainable Energy department of the university as a master's student in the Sustainable Energy Technologies (SET) program. He graduated in 2017 with honors (minor in Control Theory and Vehicle Dynamics). He was the finalist representing TU Delft in the national ECHO award for academic and social excellence.

After graduating, he first worked briefly with Elemental Water Makers on solar-powered reverse osmosis projects and then started with the DCE&S group as a full-time teaching assistant on courses on AC and DC Microgrids and Electrical Power Conversion. He designed and managed the makeover of the System Integration project (SIP) from a one-Quarter elective to a three-Quarters core course for the SET Masters program. He then worked as a co-creator and course manager for the Professional Certificates online courses of the ESE department on Intelligent Electrical Power Grids (I and II), and on Electrical Power Conversion.

From July 2019 to June 2023, he joined the DCE&S group as a Ph.D. candidate researching the trolleybus grids as active, sustainable, multi-functional, and multi-stakeholder electric infrastructures.

Since September 2022 (full-time since August 2023), he is a Research Fellow at the AMS Institute in Amsterdam on transportation networks, working with GVB (municipal public transport operator for Amsterdam) on rethinking the tram/metro infrastructures of Amsterdam as sustainable and multi-functional grids by integrating electric bus chargers, solar panels, bidirectional substations, and energy storage into their DC infrastructures.

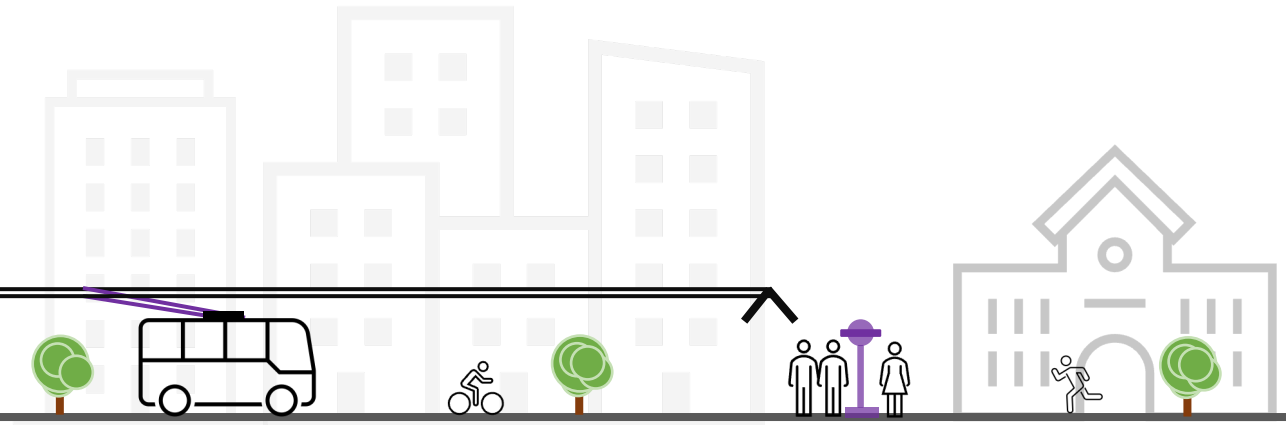

TU Delft Delft University of Technology